ASSESSING MODIS EVAPOTRANSPIRATION DATA FOR HYDROLOGICAL MODELLING IN SOUTH AFRICA

A thesis submitted in fulfilment of the

requirements for the degree of

MASTER OF SCIENCE

of

RHODES UNIVERSITY

Grahamstown

South Africa

by

SBONGISENI CHRISTIAN MAZIBUKO

Supervisor: Prof D.A Hughes

December 2016

ABSTRACT

Evapotranspiration as a major component of the water balance has been identified as a key factor in hydrological modelling. Water management can be improved by means of increased use of reliable methods for estimating evapotranspiration. The limited availability of measured climate and discharge data sets, particularly in the developing world, restricts the reliability of hydrological models in these regions. Furthermore, rapid changes in hydrological systems with increasing development mean uncertainties in water resource estimation are growing. These changes are related to the modification of catchment hydrological processes with increasing human activity. Dealing with data uncertainty and quantifying the impacts of catchment activities are significant challenges that scientists in the field of hydrology face today. Uncertainties in hydrometeorological data are associated with poor observation networks that provide data at point scales which are not adequately representative of the inherent heterogeneity within catchment processes. Using uncertain data in model applications reduces the predictive power of hydrological models as well as the ability to validate the model outcomes. This study examines the potential of using remote sensing-based evapotranspiration data to reduce uncertainty in the climatic forcing data and constraining the output of a rainfall-runoff hydrological model.

It is common to use fixed seasonally variable potential evapotranspiration (PET) instead of temporally varying PET data as inputs to standard rainfall-runoff models. Part of the reason is that there are relatively few stations available to measure a variety of meteorological input data needed to compute PET, as well as the apparent lack of sensitivity of rainfall-runoff models to different types of PET inputs. As hydrometeorological data become more readily available through the use of earth observation systems, it is important to determine whether rainfall-runoff models are sensitive to time-varying PET derived from these earth observations systems. Further potential includes the use of actual evapotranspiration (ETa) from this type of data to constrain model outputs and improve model realism. It is assumed that a better representation of evapotranspiration demands could improve the efficiency of models, and this study explores some of these issues. The study used evapotranspiration estimates (PET and ETa) from the MOD16 global product with one of the most widely used hydrological models in South Africa. The investigation included applying the Pitman model in a number of case study catchments located in different climatic regions of the country.

The main objectives of the study included (i) the establishment of behavioural model parameter sets that generate acceptable hydrological response under both naturalised and present-day conditions, (ii) the use of time-varying PET estimates derived from MOD16 data to force the model, and (iii) the use of MOD16 ETa estimates to constrain model-simulated ETa. Before examining the use of different PET forcing data in the model, a two-step modelling approached was employed both a single-run and an uncertainty version of the Pitman model. During the first step (using a single-run version), available information on catchment physical properties and regionalised groundwater recharge together with model calibration principles were used to develop model functionality understanding and establish initial parameter sets. The outcomes from the first step were used to define uncertain parameter ranges for the use in the uncertainty version of the Pitman model (second step). Further, catchment water uses were quantified to ensure comparability with present-day flow conditions represented by the stream flow records. The effects of forcing the Pitman model with MOD16-based time-varying PET data inputs were evaluated using static and dynamic sensitivity analysis approaches. In the static approach, parameter sets calibrated using fixed seasonal distributions of PET data remain unchanged when forcing the model with other forms of PET, whereas in the dynamic method, the model is re-calibrated with changing PET inputs. In both approaches, model sensitivity was assessed by comparing objective function statistics of reference flow simulations with those simulations incorporating changing PET data inputs. The use of the MOD16 ETa data to constrain model-simulated evapotranspiration losses was conducted by calibrating the parameters such that the simulated-ETa matched the evapotranspiration loss estimated from the MOD16 data.

Despite issues around model equifinality and significant uncertainty within water use information, the Pitman model simulations were generally satisfactory and compared with observed stream flow data where available. The use of time-varying PET data does not improve the efficiency of the model when both static and dynamic sensitivity approaches are used. This was highly expected with the static approach where fixed model parameter sets do not account for the changes in evapotranspiration demands. However, with the dynamic approach, it was difficult to conclude why the model efficiency did not improve given the flexibility of the model to achieve appropriate parameter sets to different forms of PET. The study noted that the insensitivity of the model to changes in PET demands could be due to uncertainties in the model structure and MOD16 data. Attempts to constrain the model-simulated actual evapotranspiration with MOD16 ETa estimates were hampered by large errors in the MOD16 data and resulted in the non-closure of the catchment annual water balance, even when likely errors in the other components of the water balance were accounted for.

There is still a great deal of work that needs to be done to reduce uncertainties associated with the use of earth observation data in hydrological modelling. This study has identified some of the specific gaps within the application of evapotranspiration data from earth observation information. While the MOD16 data applied with the Pitman model did not achieve improved simulations, the study has demonstrated the enormous potential of the data product in the future should the identified uncertainties be resolved. Lastly, the investigation highlighted some of the possible model structural uncertainties specifically associated with the simplified soil-moisture accounting routines within the model. It is possible that amending the model structure through investigating the dynamics of the relationship between soil moisture and evapotranspiration losses would assist in the improved utilisation of earth observation products related to the MOD16 ET data.

DEDICATION

This work is dedicated to all striving young water professionals in the developing world.

ACKNOWLEDGEMENTS

I am grateful to Prof Denis Hughes for opening his doors and offering me an opportunity to undertake this research under his supervision. Without your knowledgeable assistance in all aspects of the study and constructive critics, I would have not acquired the knowledge and skills from various tasks conducted in during the period of the study. I am grateful to the Carnegie Corporation of New York for funding this study through the Regional Initiative in Science and Education (RISE) Programme as well as the South African National Research Foundation (NRF).

I truly owe a great depth of gratitude to Dr. Jane Tanner and Dr. Sukhmani Mantel for proofreading my work. I also wish to acknowledge Mr David Forsyth of the Institute for Water Research for developing the MODIS extraction tool as well as the Council for Scientific and Industrial Research for providing insights on how to extract MOD16 data. The Western Cape Department of Agriculture is also acknowledged for providing the shapefiles and information on crops. Thanks to Umvoto Africa (Pty) Ltd. for their support in proofreading the thesis.

Special thanks also go to the stuff and fellow students of the institute for support throughout the period of the study. You will remain memorable in my mind.

Above all, I sincerely thank my family for their patience and their emotional support.

TABLE OF CONTENTS

LIST OF FIGURES

LIST OF TABLES

LIST OF APPENDICES

LIST OF ACRONYMS

AMSR-E:	Advanced Microwave Scanning Radiometer
ASCAT:	Advanced Scatterometer
AVHRR:	Advanced Very High Resolution Radiometer
CE:	Nash-Sutcliffe coefficient of efficiency
DWS:	Department of Water and Sanitation
EOS:	Earth Observing System
ETa:	Actual evapotranspiration
ET:	Evapotranspiration
FAO:	Food and Agriculture Organization
FPAR:	Fraction of Photosynthetically Active Radiation
GMAO:	Global Modelling and Assimilation Office
GIS:	Geographic Information System Office
GPCP:	Global Precipitation Climatology Project
GRACE:	Gravity Recovery and Climate Experiment
GUI:	Graphical User Interface
HDF:	Hierarchical Data Format
IAHS:	International Association of Hydrological Sciences
IGBP:	International Geosphere-Biosphere Program
LAI:	Leaf Area Index
LE:	Latent Heat Flux
MAE:	Mean Annual Evaporation
MAP:	Mean Annual Precipitation
mamsl:	Meters Above Mean Sea Level
MODIS:	MODerate Resolution Imaging Spectrometer
NASA:	National Aeronautics and Space Administration
NDVI:	Normalized Difference Vegetation Index
NTSG:	Numeric Terradynamic Simulation Group
PET:	Potential and evapotranspiration
PUB:	Prediction in Ungauged Basins

SAWS:	South African Weather Service
SEB:	Surface Energy Balance
SEBAL:	Surface Energy Balance Algorithm for Land
SEBI:	Surface Energy Balance Index
SEBS:	Surface Energy Balance System
SMOS:	Soil Moisture and Ocean Salinity
SPATSIM:	SPatial and Time Series Information Modelling
SVAT:	Soil Vegetation Atmosphere Transfer
TAMSAT:	Tropical Applications of Meteorology using SATellite
TMG:	Table Mountain Group
TRMM:	Tropical Rainfall Measurement Mission
WARMS:	Water Use Authorisation and Registration Management System
WMA:	Water Management Area
WRC:	Water Research Commission
WTW:	Water Treatment Works

CHAPTER ONE

1. INTRODUCTION

1.1. GENERAL BACKGROUND

There has been wide acknowledgement in many parts of the world that freshwater resources are becoming increasingly limited, in both quantity and quality (Sivapalan *et al.*, 2003). This is because of the ever-increasing water use and demand pressure that affect water availability, distribution and quality. The non-stationarity in the demand for water resources, climate, as well as in hydrological response, particularly in water scarce regions, is expected to worsen the situation of fresh water resources. Therefore, there is a need for appropriately formulated and reliable water resources assessment and management tools that are capable of dealing with different types of environmental changes. Hydrological models are used to simulate hydrological systems in order to understand hydrological processes and predict a system's response. Their simulation results provide useful information about complex and spatially distributed water movement processes in a hydrological system (Beven, 2012a). This information is vital for water resources planners and managers to make informed decisions about water resources (Hughes, 2010). Besides the role models play in decision-making, they have been widely used to evaluate scenarios to support the complex task of water resources operation and management, and as research tools for acquiring information about hydrological systems (Wagener and Gupta, 2005). However, their ability to reliably simulate hydrological processes and predict hydrological system responses depends significantly on the availability and quality of observed hydrometeorological measurement data to support their application (Hughes, 2006).

Good quality observed hydrometeorological data forms an integral part of modelling success (Kapangaziwiri and Hughes, 2008). Sustainable water resources management and development can only be achieved when a river basin's water balance components are adequately quantified and well understood in terms of their distribution in both space and time. However, in most river basins across the globe, especially in the developing regions, accomplishing good modelling results remains a challenge. This is because of the poor state of the hydrometeorological measurement networks, poor quality data, and the inability of measurement instruments to provide data at appropriate scales, which often result in the gaps of information about water balance components and subsequently, incomplete understanding of hydrological processes (Hughes, 2008). Overall, these inadequacies are constraining hydrological model applications,

especially for practical water resources planning and management (Oudin *et al.*, 2006). As a result, models may not reasonably simulate hydrological response and make adequate simulations because of the burden of uncertainties. Hence, in water-scarce regions of the developing world, where hydrological models are needed the most (Sivapalan, 2003), the optimum application of models is jeopardised and water resources related decisions are taken with high risks. In order to apply models optimally, to have confidence in their results and to plan and develop water resources sustainably, observation data and knowledge gap uncertainties need to be addressed and reduced. However, reducing these uncertainties requires reliable observation networks and adequate data acquisition methods to provide representative hydrometeorological data and other hydrological variables.

The evapotranspiration (ET) component of the water balance in dry and semi-arid regions is the second largest component after precipitation (Jewitt, 2006; Jarmain *et al.*, 2009a). ET plays a significant role in transferring latent heat energy and water vapour mass between the atmosphere and the land surface and provides the link between climatological, hydrological, and ecological systems. Most importantly, from a hydrological modelling point of view, ET dynamics regulate the availability of soil moisture, which has a significant influence on catchment hydrological processes and stream flow generation (Hughes, 2008). Multiple complex processes and their interactions drive ET dynamics within a hydrological system but most of these processes are inadequately quantified and understood, and are poorly represented in hydrological models (Jewitt, 2006). Improved understanding of ET dynamics could contribute to improvements is the prediction of drought events, managing water resources for agriculture, studying hydrological processes, and conducting water resources assessment and planning studies.

Traditional methods of studying hydrological processes need radical changes in order to improve process understanding and hydrological prediction (Thompson *et al.*, 2013). As a result, hydrological sciences today are shifting from understanding hydrological processes at point scales to understanding them across heterogeneous landscapes. The use of novel techniques that acquire hydrometeorological and hydrological data at large spatiotemporal scales could reduce input data uncertainties and the gap in understanding of hydrological processes, thereby reducing model uncertainties and increasing model confidence. In 2003, the International Association of Hydrological Sciences (IAHS) launched the decade on Prediction in Ungauged Basins (PUB: Sivapalan *et al.*, 2003). One of the major objectives of PUB was to assess the potential use of alternative sources of hydrological data, such as from satellite remote sensing, to improve hydrological processes understanding and prediction in ungauged basins (Hrachowitz *et al.*,

2013a). The new IAHS decade launched in 2013 continues to focus on many of the themes and includes a science into practice target (Montanari *et al.*, 2013).

1.2. REMOTE SENSING IN HYDROLOGY

The capability of remote sensing is unmatched by conventional ground-based (often at point scale) measurements that are generally unable to capture the variability across the landscape and are limited to accessible areas. Over the last decades, remote sensing techniques have proved to be capable of providing hydrometeorological measurements from small scales to global scales (Milzow *et al.*, 2011). However, the assumption that these techniques provide hydrological data products with sufficient accuracy to be useful for hydrological scientific studies, monitoring purposes and decision-making is open to question due to the methods used by remote sensing techniques. Generally, remote sensing techniques use satellite sensors to measure the emission and/or reflection of radiative energy of surface features from visible light to microwave frequencies of the electromagnetic spectrum. The measurements of variables, such as precipitation, vegetation-state and surface temperatures, are usually processed to estimate hydrological variables, such as soil moisture and evapotranspiration. However, these estimates are always subject to uncertainties.

Much effort that has been devoted to improving quantification of both potential and actual evapotranspiration (PET and ETa) using remote sensing techniques at various spatiotemporal scales (e.g. Su, 2002). However, adequate estimation of these variables at finer resolutions remains a challenge because of high heterogeneity of hydrological processes across the landscape within a catchment (Friedl, 2002). Nevertheless, various algorithms have been developed to consider heterogeneity when estimating PET and ETa using remote sensing data. With these remote sensing developments, Kongo *et al.* (2011) suggested and recommended using remotely sensed ET to quantify evaporative water from different land uses.

1.3. PROBLEM STATEMENT

In dry and semi-arid regions, evapotranspiration dynamics, (both PET and ETa) dominate hydrological processes and catchment water balances (Kongo *et al.*, 2011). Given the fact that some of these regions experience high climatic variability, ET dynamics can bring about differences in hydrological regimes. Inadequate quantification and the lack of understanding of ET dynamics at both spatial and temporal scales directly influence hydrological model applications and their results that could detrimentally affect the planning and management of

South Africa's scarce water resources. Rainfall-runoff hydrological models use PET estimates to represent the evapotranspirative water demands, but they are not directly measurable from the field, and are typically computed using a variety of methods that make use of meteorological observation data. Usually, these observation data are measured at point scales and it is impossible to establish a dense network of measuring stations in all catchments. Sparse observation networks do not account for spatial variability that occurs across the catchment landscape because of high meteorological heterogeneity (Jovanovic and Israel, 2012) and the computed PET estimates are highly uncertain.

Many hydrological models use long-term averages of PET estimates from point measurements instead of temporally varying PET from large spatial scale measurements (Oudin *et al.*, 2005b). The use of spatio-temporally varying PET input data should have a positive impact on water balance simulations and model efficiency. Similarly, spatio-temporally varying estimates of ETa could improve model calibration and model output constraints. ET dynamics are also anticipated to change in future (Shuttleworth *et al.*, 2009), and consequently, affect hydrological flow regimes. These changes are already evident in several parts of the world where PET shows increasing trends (e.g. Fu *et al.*, 2009) and where using long-term averages of PET estimates in modelling studies could result in biased model outputs.

Traditional approaches used to estimate PET could put water resources planning at risk. Similarly, the lack of measured ETa data that can be used to constrain model-simulated ETa could exacerbate this condition. While remote sensing techniques provide hydrologists with novel approaches to hydrological modelling, they have not received much attention for forcing, calibrating and constraining models used for practical water resources application. One of the reasons could be that remote sensing techniques do not measure hydrological state variables directly, but measure surface reflectance or surface-emitted energy signals (Jones *et al.*, 2011) and algorithms are required to generate the values of the hydrologic state variable of interest. As remote sensing data are becoming more widely and freely available, it is essential to assess their utility for hydrological modelling, particularly in data scarce areas. The question of how useful and reliable remote sensing data are, and their potential problems when applied in hydrological models, remains largely unanswered.

1.4. RATIONALE AND SIGNIFICANCE OF THE STUDY

Ever since the pioneering work of Engman (1993), the importance of improving hydrological observation data has been emphasised. The main focus has been on adequately quantifying

hydrological state variables for improving model applications by reducing input data uncertainty and reducing the gap in understanding of hydrological processes (for discussion see Sivapalan *et al.*, 2003). In recent decades, remote sensing satellite techniques have been deployed to quantify hydrometeorological state variables at large spatio-temporal scales, including from remote areas where it was impossible to conduct measurements (Liu *et al.*, 2012). These hydrological state variable measurements include rainfall, land cover, soil moisture, open water bodies, groundwater storage variations and evapotranspiration.

The acquisition of hydrologic state variables has been considered a major step in attempts to improve hydrological process understanding, and modelling results in particular (Hrachowitz *et al.*, 2013a). These data have been used to parameterise models, as well as to constrain model-simulated outputs. However, before these data can be used they often require processing and reformatting. For example, the data used to drive hydrological processes in a model (rainfall and potential evapotranspiration), model parametric data (water use, topography, etc.), and calibration data (observed stream flow) are prepared to be compatible with model requirements. This is true for the Pitman model, a monthly time-step rainfall-runoff model (Pitman, 1973), which has been developed with a data-efficient and user-friendly interface (Hughes, 2004). This model has proved to be a valuable tool for water resources assessment and development in South Africa (e.g. Middleton and Bailey, 2008) and for other hydrological investigations in large river basins of the southern African region (e.g. Hughes *et al.*, 2006; Tshimanga and Hughes, 2014).

The Pitman model was designed to use either long-term average or temporally varying PET estimates, but there have been no detailed investigations of exploiting spatio-temporally varying PET estimates. Despite the fact that some studies have applied temporally varying PET estimates, at different temporal resolutions (Hughes *et al.*, 2014a), there has been less focus on applying PET data with high spatial and temporal resolution and little use of remote sensing-based input data. There are reported studies (e.g. Andréassian, 2004; Oudin *et al.*, 2005a) that have applied temporally varying PET estimates derived from climatological data inputs to force other hydrological models. However, these estimates do not represent average PET across the catchment. Despite the possibility of hydrological models being insensitive to the temporally varying PET, as Oudin *et al.* (2006) concluded, there is still a gap in understanding the potential utility of exploiting satellite-derived PET estimates for model applications. Such data exploitation could prove useful in the improvement of model applications and the identification of possible uncertainties. From a water resources planning perspective within the South African context, testing of such data in a hydrological model such as the Pitman could prove to be useful.

The availability of the response data such as remote sensing-based ETa could also provide an opportunity to calibrate models and constrain model-simulated processes (e.g. Winsemius *et al.*, 2008; 2009; Hughes, 2013).

The limitations of obtaining temporally varying PET and ETa estimates from high spatial resolution measurements could be reduced using estimates from the MODerate Resolution Imaging Spectrometer (MODIS) global ET algorithm, which is referred to as the MOD16 ET product (Mu *et al.*, 2011). MOD16 ET provides spatially distributed PET and ETa estimates at a temporal resolution of 8-day, monthly, and annually and a spatial resolution of 1 km^2 (Mu *et al.*, 2011). MOD16 PET estimates can be used as an input to drive the Pitman model, whereas MOD16 ETa estimates can be used to constrain the Pitman model ETa simulations. Because MOD16 ET data has large spatio-temporal resolution, it is anticipated that they could provide adequate PET and ETa estimates that could improve our understanding of ET dynamics in relation to the hydrological heterogeneity and reduce PET data uncertainties in the modelling process. This study, therefore, aims to assess the potential use of remote sensing data for improving hydrological model applications with emphasis on the application of MOD16 ET data in the Pitman model.

In order to explore the potential that remote sensing data products have for hydrological modelling, this study will look at the following general aspects: (i) data needs to support the application of hydrological models, (ii) the prospective of remote sensing data products for hydrological sciences, (iii) the accessibility and compatibility of remote sensing data products (iv) the accuracy of remote sensing products, and (v) the ability of rainfall-runoff models to exploit spatio-temporally varying PET and their application. The following questions were identified at the start of the study:

- Is the improved version of the Pitman model (Hughes, 2004) capable of simulating the naturalised and present-day hydrological responses considering parameter uncertainty?
- Can remote sensing-based ET data be used to improve the application of hydrological models and assist in reducing uncertainties in the model input data?
- Are the MOD16 PET and ETa estimates adequate for use with hydrological models under different land cover and climate conditions?
- Can the MOD16 PET estimates be used to drive and calibrate the Pitman model with an aim of improving simulation efficiency as well as evaluating model sensitive to the use of different forms of PET estimates as compared to the long-term average estimates?

- Can the MOD16 ETa estimates be used to constrain the Pitman model simulated Eta as means of evaluating the model structure?

1.5. AIMS AND OBJECTIVES

This study aims to assess the potential use of remotely sensed evapotranspiration data products to improve modelling approaches, particularly addressing the issues of input data uncertainties. The emphasis of this study is on the potential use of MOD16 PET estimates for driving the Pitman model and MOD16 ETa estimates for constraining the model-simulated outputs.

To achieve the aims of this study, the following objectives have been established:

i. *To review the importance of hydrometeorological observation data in the application of hydrological models*. Models rely on hydrometeorological data in order to generate reliable hydrological information used in decision-making for water resources planning and management.

ii. *To critically review remote sensing technology, hydrometeorological data acquisition techniques and applications in hydrology*. Remote sensing technology provides innovative techniques for quantifying hydrometeorological data. However, the data are not always compatible with the models. Therefore, it is important to review the underlying technology, the data acquisition and processing methods and to develop a conceptual understanding of the techniques. This understanding will assist in the data-model compatibility assessments, proper formulation of data extraction tools, and in identifying potential sources of uncertainties in the processed data.

iii. *To identify catchment study areas from different climatic regions of South Africa that represent different hydrological regimes*. Different climate and land cover types play a vital role in determining the dominating hydrological processes.

iv. *To set up and calibrate the Pitman model (using both single-run and uncertainty versions) for the selected catchments using the conventional long-term averages of PET estimates and simulate both naturalised and present-day flows*. This objective is designed to establish a baseline of possible model results using conventional forcing data, against which the use of the MOD16 can be compared.

v. *To assess the Pitman model performance and sensitivity to the use of temporally varying MOD16 PET data*. This objective is designed to test the assumption that a more suitable

time series of evaporative demands should have a positive impact on water balance components simulations with the Pitman model and to identify the parameters that are most sensitive to changes in forcing data.

vi. *To test the use of MOD16 Eta data to constrain the Pitman model simulated ETa.*

1.6. STRUCTURE OF THE THESIS

Chapter 2 provides a general review of various aspects of hydrological modelling, the use of hydrological models in the South African context, the data requirement and measurements for model applications. A discussion of hydrological modelling concepts and their challenges particularly with uncertainties is provided. A review of remote sensing techniques, data acquisition, and their application in hydrology is given. Finally, a discussion of hydrological modelling practice concepts and their challenges is provided. **Chapter 3** briefly explains the methods used in this study and includes a description of the model and data used. **Chapter 4** gives a detailed explanation of the study area selection and focuses on the description of each catchment covering the hydrological, climatological, physiographic, and land use/land cover dynamics. **Chapter 5** provides a modelling approach that was used as well as providing a discussion of the model calibration results. This chapter also presents the results on the use of the MOD16 ET data product in the model. General discussion of the research results and summaries of the major conclusions as well as recommendations made from the study are outlined in **Chapter 6**.

CHAPTER TWO

2. LITERATURE REVIEW

2.1. INTRODUCTION

This chapter provides a review of hydrological models, the data used for modelling, and of the application of remote sensing in hydrology. The first subsection provides a general overview of the concept, development, types, and applications of hydrological models. This is followed by a discussion of data needed for hydrological models, modelling approaches, and the uncertainties in hydrological modelling. The chapter ends with a critical review of remote sensing techniques, remote sensing data acquisition, and applying remote sensing data in hydrology.

2.2. GENERAL ASPECTS OF HYDROLOGICAL MODELS

2.2.1. Hydrological Models

Hydrological models are tools that attempt to describe and represent complex hydrological processes and their interactions as simplified and conceptualized entities of a real hydrological system in mathematical terms (Beven, 2012b). Historically, conceptualisation of hydrological models simply tried to study the relationship between rainfall and runoff processes, mimicking hydrological system processes that transform precipitation inputs into stream flow. Currently, models are essential standard tools in scientific research and are relied upon to inform decision-making in operational hydrology. Models are continuously improved through testing new theories and hypotheses to increase the confidence in their results as well as their functionalities in solving water-related problems. Depending on what the modelling results are used for, hydrological models can either be complex in order to solve practical water problems, or simple for testing hypotheses (Beven, 2012a). However, because of the complexity of hydrological processes at the catchment scale, which are often poorly understood, and the lack of observation data that represent these processes, models often over-simplify the reality (Hughes, 2010). As a result, many hydrologists are seeking to improve their understanding and knowledge of hydrological processes (Montanari *et al.*, 2013) such that they simulate hydrological response in a more realistic way, which also improves confidence in the information they generate.

2.2.2. Hydrological Model Development

Generally, a comprehensive hydrological model should reliably simulate the hydrological system's response to data inputs with an acceptable error, and simultaneously reproduce contrasting signatures of the hydrological response with known scientific principles. The process of developing a model and applying it successfully depends on the adequate perception and understanding of hydrologic processes being modelled, the model developer's knowledge and experience, and the availability of adequate observation data and quantitative information to support the modelling process (Beven, 2012a). To date, inadequacies in observation data, lack of understanding of dominant hydrological processes, and the poor formulation of modelling objectives contribute to model development challenges. These challenges led Pechlivanidis *et al.* (2011) to formulate a list of considerations for model development: the purpose for the model (operational or investigative models), data availability (complex models require adequate observation data), and resource constraints (simpler models require a lower budget). Peel and Blöschl (2011) noted that, in most cases, hydrological interactions and system dynamics are not well described in models because of the complexities of scales at which they occur and due to the lack of observation data to quantify these dynamics. Given the scope that hydrological models have in confronting complex environmental, hydrological, and anthropogenic issues related to the sharing of water resources, Montanari *et al.* (2013) suggested that models should integrate all activities that interact with the hydrological cycle of the catchment. Given these challenges, it is easy to understand why developers of hydrological models face difficulties in trying to formulate models with sufficient representation of all interacting components that affect water resources within the catchments. For this reason, Beven (2002) stressed that instead of developing new models, the focus should be on improving the philosophy of modelling as a means to improve the existing models through understanding of hydrological processes and their interactions in detail.

2.2.3. Types of Hydrological Models

Many hydrological models have been developed to simulate rainfall-runoff processes (e.g. Pitman, 1973; Abbott *et al.*, 1986; Bergström, 1995) and are generally classified as *empirical, conceptual or physically-based*. Empirical models, also referred to as "black box models", regard a catchment as a dynamic system in which very few parameters, usually invariant across the catchment, are used to simulate stream flow (Beven, 2012a). They do not describe the internal catchment processes (Perrin *et al.*, 2010). Even though the use of "physically-based"

terminology is discouraged in the field of practice (Beven and Young, 2013), Beven (1989) described physically-based models as those based on the laws of thermodynamics, conservation of mass, momentum and energy as well as theoretical concepts that govern hydrological processes. The third type is conceptual models, which are formulated from an understanding of dominant hydrological processes either implicitly or explicitly. In conceptual modelling, the basin is perceived as consisting of elements such as linear or non-linear storages (expressed in mathematical terms) and channels that mimic the actual processes within a catchment in the generation of runoff (Beven, 2012a).

Rainfall-runoff models are generally regarded as deterministic because they produce outputs without evaluating the associated probabilities of their occurrence. Catchment processes are not lumped together by random unknown components, but rather by known system components with high temporal and spatial variability based on the understanding that known laws of conservation of mass and momentum govern the processes. Given that hydrological processes occur at different scales, Todini (1988) further classified rainfall-runoff models as either *lumped*, *distributed* or *semi-distributed*. Lumped models treat a catchment as a single modelling unit with a single set of parameter values that do not represent spatial and temporal variability in hydrological processes (Beven, 2012a). Distributed or semi-distributed models divide a catchment into grids, slope elements or sub-catchments, with the objective of incorporating a variety of spatially varying catchment characteristics (Shrestha *et al.*, 2006). The time-step used in the model structure and temporal scale of the input data are yet another basis of classifying models. The time-steps may range from sub-hourly to hourly for single event models and from daily to monthly for water resources models.

2.2.4. Application of Hydrological Models

Typical tasks for hydrological models include runoff estimation in gauged and ungauged catchments, prediction of the effects of the land use and climate change on catchment stream flow, generation of stream flow data for water resources evaluation, operational flood forecasting, design of irrigation schemes as well as reservoir design and operation (Wheater, 2008). Models are therefore the interface between hydrological data and decision-making, as they enable predictions about the current and future state of hydrological response as well as permitting the testing of different hypotheses (Clark *et al.*, 2011). Models are also used as learning tools in understanding catchment hydrological processes (e.g. McMillan *et al.*, 2011) and to evaluate the effects of integrating new datasets (e.g. Winsemius *et al.*, 2009). With the

continued exploitation of fresh water resources, as well as the alteration of natural hydrology, rainfall-runoff models have proved to be ideal tools to help solve a variety of water resources problems and are likely to continue to offer support for dealing with anticipated future problems that are threatening water resources (Montanari *et al.*, 2013).

2.3. HYDROLOGICAL MODELLING IN SOUTH AFRICA

2.3.1. Development and Application

Most of the applications of models include the estimation of water resources, assessing climate change scenarios, rainfall and flood estimation, land use change impacts on catchment hydrology, and estimating and determining environmental flows for rivers (Jewitt *et al.*, 2004; Hughes and Palmer, 2005). Amongst a number of hydrological models that have been developed for specific practical water resources problems and for research purposes in South Africa, the Pitman model (Pitman, 1973) is the most widely used. The Pitman model is a conceptual, semi-distributed rainfall-runoff model, which runs on a monthly time-step to simulate various components of a hydrological system. While a daily version of the model is available, the monthly version is used more frequently (Hughes, 2013). The Pitman model has effectively accomplished its fundamental development objectives since the original work by Pitman in 1973. Since then, it has received praise such as Hughes (2013) saying, "*There can be little doubt that the Pitman model has contributed enormously to the water resources assessment within southern Africa, and particularly within South Africa*". It is the most frequently used model for assessing, planning, and managing South African water resources (Middleton and Bailey, 2008).

2.4. DATA NEEDS FOR HYDROLOGICAL MODELS

Many researchers for example, Hughes, (2006, 2008), Wilk *et al.* (2006), and Mul *et al.* (2009) agree that one of the main hindrances to the appropriate application of hydrological models in the southern African region is the lack of adequate hydrometeorological and observed stream flow data to support the modelling process. Inadequate understanding of the complex underlying hydrological processes contributes to this challenge (Hughes, 2004). Despite the fact that there are well-established models that are used for practical water resources problems in many parts of the globe, it is clear that the lack of availability of hydrometeorological information continues to contribute to estimation uncertainty. Therefore, while there is a need for improved data, there is also a need to quantify the uncertainties associated with less than perfect data and with less than perfect models (Sawunyama and Hughes, 2008).

2.4.1. Model Input Data

In rainfall-runoff hydrological modelling, adequate and representative precipitation, potential evapotranspiration (PET), observed stream flow, and water resources development data play a vital role in the success of hydrological simulation. Precipitation data are used, mainly, as an input to drive hydrological processes whereas potential evapotranspiration data are used to represent catchment evaporation and transpiration demands. The process establishing representative model parameters make use of the observed stream flow data whereas water resources development data account for anthropogenic impact in the model simulations. A detailed description of these input components, their measurement and estimation methods are provided in the next subsections.

2.4.1.1. Precipitation data

Precipitation (rainfall) is the primary input flux for hydrologic models that activates flow and mass transport of water within hydrological systems. Because rainfall is naturally intermittent and highly variable in space and time, modelling a dynamic hydrologic system requires good quality rainfall data at the highest possible representative level (Faurès *et al.*, 1995). In many developing countries, including sub-Saharan Africa, the network density of ground-based rainfall measurement stations has always been relatively sparse and is declining dramatically (Hughes, 2006). Hughes (2008) noted that most of the available rainfall records do not provide detailed spatial characteristics of real rainfall because of difficulties in measurements. Wheater (2008) points out that these conditions pose a challenge for capturing representative rainfall particularly in arid and semi-arid areas where it is commonly characterised by large spatial and temporal variability. Hence, this variability affects the modelling process since rainfall accuracy is directly linked to successful stream flow simulations.

Rainfall is usually measured using rain gauges, which may be either non-recording or of recording type, or estimated by remote sensing systems (radar or satellite) (Thorne *et al.*, 2001; Grimes and Diop, 2003). While remote sensing systems provide estimates of rainfall in near-real time and at large spatial scales, rain gauges continue to be the primary source of rainfall data. However, given that ground-based gauging stations networks are on the decline, it is likely that remotely sensed rainfall data will be used more frequently in the future (Thorne *et al.*, 2001).

2.4.1.2. Evaporation and evapotranspiration data

In the hydrological cycle, water is lost to the atmosphere via two interlinked processes – evaporation (E) and evapotranspiration (ET) – and these are important components of the hydrological water balance, especially in arid and semi-arid regions (Allen *et al.*, 2011a). ET is sub-divided into two types, namely: potential evapotranspiration (PET) and actual evapotranspiration (ETa). PET defines the maximum possible amount of water transpired by a short vegetation canopy, completely shading the ground, of uniform height and with access to an unlimited supply of water from the soil profile (Burman, 2008). In other words, PET is equivalent to the evaporative demand for the atmosphere under given climatic conditions. This quantity is also referred to as reference evapotranspiration (ET_0) where a crop factor (K_c) is used to estimate PET for vegetation other than short vegetation. In this, study PET denotes potential evapotranspiration. ETa is defined as the sum of evaporative losses from the soil surface and interception storage combined with water that transpires from plants and which is limited by available water from the soil profile.

Accurate estimates of ET (both PET and ETa) over large areas are important for understanding land surface-atmosphere interactions and for closing catchment's water balance (Abtew and Melesse, 2012). These estimates can take any form i.e. long-term observation means or temporally varying time series data. Over the past few decades, it has been a challenge to estimate this important water balance component because it is not measured directly but estimated from equations that make use of meteorological data (Jewitt, 2006). The situation is worsened by the fact that the conventional methods used to measure detailed meteorological data such as relative humidity, air temperature, wind speed, and solar radiation, are always limited and not always available at the desired spatial and temporal scales (McMahon *et al.*, 2016).

Measurement and estimation methods of evaporation and evapotranspiration

Measurement of evaporation: The most common and probably the oldest evaporation measurement techniques used in different parts of the world are the American Class A-pan and the Symons pan. In most cases, a partial- or full-scale weather station may accompany pan evaporation station. These stations provide rain gauge measurements to account for the contributions of rainfall to the depth of water in the pan. The common sources of error in measurements of evaporation include environmental factors such as wind blow obstruction, advective losses, or losses in the pan-surrounding area, windblown sediment accumulation, and the measurement errors from the rain gauge (Abtew and Melesse, 2012).

The estimation of reference crop evapotranspiration (ET_{0c}) and open-water evaporation (ET_{oe}) using pan evaporation (E_{pan}) measurements are given by equation 2.1 and 2.2, respectively.

$$ET_{0c} = C_{et} * E_{pan} \quad (2.1)$$

$$ET_{oe} = K_{et} * E_{pan} \quad (2.2)$$

where C_{et} represent the crop coefficient and K_{et} is the pan coefficient (both between 0 and 1). The former is dependent on meteorological conditions (e.g. temperature, humidity, wind speed), whereas the latter is dependent on: (i) the type of pan used, (ii) the pan installation environment, and (iii) the climate: the humidity and wind speed. Usually, each country has its own published pan coefficients for different climatic regions (McMahon *et al.*, 2013).

Contrary to knowledge that global temperatures are increasing, a number of studies (e.g. Fu *et al.*, 2009; Abtew *et al.*, 2011), using pan measurements, have shown that evaporation has reduced in some parts of the world, including South Africa as reported by Hoffman *et al.* (2011). This evaporation paradox has been widely discussed by researchers including (e.g. Farah and Bastiaanssen, 2001; Donohue *et al.*, 2010a), and there are contrasting views based on the major findings. Measurement methods, catchment physiography, and changing meteorological conditions are the major influential factors.

Estimation of potential evapotranspiration: Being a function of solar radiation, temperature, wind speed, water vapour deficit, and atmospheric pressure, estimating evapotranspiration is always a challenging task (Allen *et al.*, 2011a). There is a variety of methods for estimating PET in the literature (see, e.g. Lu *et al.*, 2005), and they tend to provide inconsistent estimates due to their different assumptions, input data requirements, or because they were developed for specific climatic regions (Grismer *et al.*, 2002). Hence, the selection of the most appropriate method is often difficult and subjective because it is primarily dependent on the objectives of the study and the type of data available. These methods can be classified into: (i) combination, (ii) temperature-based, (iii) radiation and energy balance, and (iv) mass transfer balance. Verhoef and Campbell (2005) provide a summarised description of these techniques whereas Verstraeten *et al.* (2008) present a comprehensive scientific literature on methods for estimating PET. Table 2.1 lists the methods available for estimating potential evapotranspiration and discussion on categories is given in the below paragraphs. This table excludes satellite-based evaporation estimation methods, which are discussed in section 2.7.2.2 of this chapter.

Table 2.1: Classification of methods used to estimate potential evapotranspiration (adapted from Oudin *et al.* 2005b)

Classification	Common method name	Data needed
Combination	Penman	RH, T, U, D
	Penman–Monteith	RH, T, U, D
	Priestley–Taylor	T, D
	Kimberly–Penman	RH, T, U, D
	Thom–Oliver	RH, T, U, D
Temperature	Thornthwaite	T
	Blaney–Criddle	T, D
	Hamon	T, D
	Romanenko	RH, T
	Linacre	RH, T
Radiation	Turc	RH, T, D
	Jensen–Haise	T
	McGuinness–Bordne	T
	Hargreaves	T
	Doorenbos–Pruitt (FAO-24)	RH, T, U, D
	Abtew	RH, T, D
	Makkink	T

T–Temperature; ***U***–Wind Speed; ***D***–Radiation; ***RH***–Relative Humidity; R_e–Extra-terrestrial radiation

Among the available methods, under the combination approaches, the Penman-Monteith equation is presently considered as the state-of-the-art in the computation of PET. Monteith (1965) modified the Penman equation (Penman, 1948) to form a Penman-Monteith equation, which defines and accounts, explicitly, for mass, momentum, and energy transfer with internal and external resistance and conducted terms. This method (see Table 2.2 for the meaning of symbols) is given by equation 2.3 as:

$$PET = \frac{\Delta(R_n - G) + \rho_a C_p \left(\frac{e_s - e_a}{r_a}\right)}{\Delta + \gamma \left(1 \frac{r_s}{r_a}\right)} \qquad (2.3)$$

The input data required for the estimation of potential evapotranspiration of this method can be measured, derived, and estimated, as listed in Table 2.2, and the detailed procedures are given in the Food and Agriculture Organization (FAO) paper 56 (Allen *et al.*, 1998). After many evaluations (e.g. Xu and Singh, 2000) the Penman-Monteith approach has proved to be the most physically-robust for many applications (Shuttleworth, 1993; Allen *et al.*, 2011b; Beven, 2012).

Table 2.2: Input required for the Penman-Monteith method given in equation 2.3 (source: Abtew and Melesse 2012)

Measured	Derived	Estimated
T - air temperature	ρ_a -air density	g_s - stomata resistance
Rn - net solar radiation	r_c - canopy resistance	LAI - leaf area index
RH - relative humidity	$r_{s\&a}$ - aerodynamic resistance	h_c - height of cover
u - wind speed	e_s–e_a - vapour pressure deficit	d - displacement height
P - air pressure	Δ - saturation vapour pressure	z_o - aerodynamic roughness
	γ - psychometric constant	z_{om} - momentum roughness height
	G - heat storage	c_p - heat capacity
	λ - latent heat of vapour	

Measurement and estimation of actual evapotranspiration: Numerous methods have been developed and used to measure and estimate ETa and they vary in terms of complexity. Table 2.3 gives an overview of the various actual evapotranspiration estimation techniques that are frequently found in the literature. Generally, ETa measurement and estimation can be performed at the scale of plant leaf (perometer), an individual plant through sap-flow or lysimeter, at the field scale (using field water balance, Bowen ratio or scintillometer), and at the landscape scale (using eddy covariance and catchment water balance) (Abtew and Melesse, 2012). For regional to continental scales, the use of earth observation data or model assimilating remote sensing data are becoming widely used in the estimation process (Bastiaanssen *et al.*, 1998a). Estimation approaches developed and published in this respect are discussed in section 2.7.2.2.

Table 2.3: Different scales of observation to estimate evapotranspiration using a variety of techniques

Scale	Methods	Example	Description
Plant leaf and plant	Mass water balance	Perometer	Water loss from a leaf in a closed chamber is determined by measuring relative humidity and air temperature
		Lysimeter Water Balance	Measurement of water balance components such as rainfall under realistic environmental conditions
	Energy balance	Bowen ratio	Measurement of humidity and temperature at two heights to estimate the sensible heat flux and derive ET from the energy balance
		Scintillometer	Atmospheric turbulence and light propagation, a combination of the conservation of energy and mass principles
	Energy/Mass water balance	Sap-flow	Heat, air temperature, conservation of energy
		Penman-Monteith	Based on water pressure deficit where vegetation is modelled as a big leaf
		FAO-24, FAO-56	Based on Penman-Monteith for reference crop in water unlimited conditions combined with crop factors
Landscape & field	Energy balance	Eddy covariance	Covariance between with 3 dimensional wind speed and water vapour is determined as well as derivation of energy fluxes
	Mass water balance	Water balance	Rainfall, hydrographs, groundwater storage level, information on soil, vegetation, and elevation of terrain
Regional/ continental	Energy/mass water balance	SEBAL, MOD16	Include remote sensing data from optical and thermal satellite sensors as well as global meteorological data

Rana and Katerji (2000) categorised three main methods of ETa measurement as: (i) hydrological approaches, (ii) micrometeorological approaches and (iii) plant physiology approaches. Hydrological methods include lysimeter measurements and water balance. Micrometeorological approaches include Eddy Covariance, Bowen ratio energy balance, and scintillometer. Plant physiological method consists of sap flow measurements and chamber systems measurements using a perometer.

Table 2.4 lists the disadvantages and advantages of the ETa measurement and estimation methods that are widely used. Inherently, the measurements and estimates of ETa are prone to errors, which may be systematic, random, or human induced. Allen *et al.* (2011a, b) argue that some of the errors (10% - 30%) result from the fact that most estimation methods violate the law of conservation of energy that governs the ET processes. Kim *et al.* (2012) observed that the Bowen ratio, Eddy covariance and the weighing lysimeter methods provide the most reliable estimates of ET despite the fact that they may not provide estimates at large spatial and temporal scales due to the sparseness of the data points.

Table 2.4: Advantages and disadvantages summary of actual evapotranspiration computation methods (adopted from Nouri *et al.* 2013)

Methods	Advantages	Disadvantages
Lysimeter	Manual or automatic measurement	Point-based measurement
	High accuracy for undisturbed soil	Very sensitive to different vegetation conditions inside and outside lysimeter
	Easy inspection	Not practical for mixed vegetation types at large spacing
		Must consider plant root development and may have edge-flow effect
Eddy covariance	Direct method to study mixed vegetation over large areas	Expensive and need well-trained operators in electronics
	Feasible to predict evaporation and no need for specific evaporation equation for different plant species	Need monitoring tower above canopy and a uniform fetch
Bowen ration	Simple and cheap	Need uniform fetch for accurate measurement of net radiation and soil heat flux
	Can measure evaporation even from non-watered plantation surface	Need adequate elevation above the canopy to collect the required meteorological data
	Provided to be a robust method in many forested areas	Sensitive to the bias of instrument gradient and energy balance
Sap flow	Direct measurement of transpiration	Point-based measurement
	Cheap manual and automatic measurement	Only works for woody plant species
	Individual plant coefficient can be determined	The variable geometry of stems may result to some errors from the space between the probes
	Accurate technique to study ecophysiology and water use scheduling	Uncertainty in measuring soil evaporation

2.4.1.3. Observed stream flow data

Continuous, accurate and reliable measurements of stream flow are vital for many hydrological applications where they are used to calibrate hydrological models. Flow measurements integrate all generated runoff response for the whole catchment and can be determined at a specific location on a river channel. A significant amount of ungauged basins particularly in developing countries like South Africa means there is a significant amount of uncertainty regarding catchment discharge (Wessels and Rooseboom, 2009a).

Stream flow can be measured using either direct or indirect methods. Direct methods provide discharge values at an instant measurement, which could be from, for example, velocity-area method. Indirect methods make use of the surveyed cross-sectional area of a river-bed geometry and various gauging structures including weirs (e.g. broad-crested, sharp-crested, v-notch, ogee spillway etc.) to continuously measure river stage. Because continuous direct measurements of discharge are costly, time consuming and sometimes impractical during flooding events, indirect methods are the most widely used for continuous river discharge measurements (Westerberg *et al.*, 2011). Measurements of river stage are directly converted into river discharge by means of an established stage-discharge relationship (rating curve), which can take a form of a power function or a polynomial function. A rating curve is typically established through a series of simultaneous river stage and river discharge measurements, evaluated by using velocity-area method. Once the rating curve is established, the observed river discharge, at any given time, can be computed using river-stage measurement data and this approach can be considered adequate for all rivers with steady-flow and unsteady-flow conditions (Dottori *et al.*, 2009).

The accuracy of the rating curve of different types of weirs and rated sections differs across the range of flows that they measure, and their accuracy often decreases over time – due to non-stationary channel geometry – unless consistent calibrations are undertaken (Wessels and Rooseboom, 2009b). In South Africa for example, sharp-crested weirs are still predominant and they are relatively insensitive to the changes of weir pool depth during low flows due to problems of siltation. During flooding events, river stage is rarely measured and under unsteady-flow conditions, Dottori *et al.* (2009) noted there is no one-to-one relationship between the river stage and discharge. These conditions affect the proper computation of river discharge at the high flow end of the rating curve. As a result, the extension of the rating curve to the extreme high flow events, which is usually by extrapolation, could introduce errors in the computation of river discharge. The Department of Water and Sanitation (DWS) have accounted for this uncertainty by attaching data quality codes to daily and monthly stream flow data. It is clear that

observed stream flow data could be uncertain, which can affect the proper application of rainfall-runoff models and McMillan *et al.* (2010) have demonstrated this.

Relatively few guidelines exist in hydrological scientific literature on how long a stream flow record should be for effective model calibration (Seibert and Beven, 2009). Some authors have adopted the principle of the "*the longer, the better*" (e.g. Yapo *et al.*, 1996). However, a more relevant question is whether the data includes a good sample of hydrological states for the purpose of the model.

2.4.1.4. Water resources development data

The natural hydrological flow regimes of catchments are frequently impacted by upstream developments and they contribute to the non-stationarity by redistributing runoff over space and time in the present-day flow conditions (Milly *et al.*, 2007). These developments include the construction of dams (small dams and large reservoirs), run-of-river abstractions for irrigation and other uses (e.g. domestic and industrial), land use and land cover (LULC) changes, and diversion of river flow. Often is it straightforward to quantify the impacts of the last two; however, the effects of the first two are difficult to incorporate in the simulation models. The lack of quantitative data on historical water use patterns (e.g. irrigation and domestic), quantity and storage volume of small farm dams exacerbates this problem, particularly in the developing countries (Hughes and Mantel, 2010b). Given that catchment scale hydrological processes are complex and non-linear (McDonnell *et al.*, 2007), calibrating a model under co-evolving environments such as the changes in thresholds of different hydrological processes due to anthropogenic impacts becomes a challenge. For example, Schreider *et al.* (2002) demonstrated that increasing the capacity of small farm dams reduces mean annual flows. Adam *et al.* (2007) established that the long-term annual trends of stream flow change significantly because of the construction of the reservoir on the headwaters of a water-stressed catchment. It is, therefore, important to incorporate adequate representation of upstream water use patterns in order to obtain realistic hydrological simulations.

2.4.2. Model Calibration Data

In rainfall-runoff hydrological modelling, integrated hydrological system components and processes are represented by model parameters that are typically not directly linked to field-measurable quantities because of the limits of techniques able to provide measurements that are compatible with modelling scales. Because there is no unique hydrological equation that can

represent all catchments, models depend on site-specific hydrological system settings quantified through calibration (Bárdossy, 2007). These boundaries can take the form of any hydrological properties such as ETa, groundwater level, and soil moisture status. While these properties can change dramatically in both space and time, calibrating model parameters can significantly enhance the performance of rainfall-runoff models and help to identify stable model parameters. However, there is always the possibility that calibration data are inaccurate and that misleading results are produced (Kauffeldt *et al.*, 2013).

Traditionally, model calibration focused mainly on fitting simulated flow data to observed stream flow data. In ungauged catchments or catchments with poor quality data, this is not an option. Alternative strategies aimed at providing better insights into catchment runoff characteristics need to be considered. For that reason, it is often suggested that alternative sources of hydrological system response data can be used (Stisen *et al.*, 2011; Hrachowitz *et al.*, 2013a). The use of hydrological data from remote sensing products could prove to be useful in the provision of hydrological response data (Wagner *et al.*, 2009). The data could be a satellite image depicting the inundated areas after a flooding event, moisture changes in the soil profiles, estimation of actual evapotranspiration, groundwater recharge, and vegetation growth rate. Such data could be the used for further refinement of the model parameters during calibration process.

2.5. HYDROLOGICAL MODELLING APPROACHES

2.5.1. Assessing Model Performance

Hydrological model behaviour and performance are evaluated to ensure that a model is reliable and capable of producing acceptable simulation results. Such evaluations are important in any modelling study and in communicating the performance of modelling results to potential end-users (Pappenberger and Beven, 2006). In rainfall-runoff hydrological modelling, the comparisons of simulated and observed stream flow during the calibration step are conducted with the expectation that the model will reproduce flows that resemble the observed. Model performance assessment also provides the means to evaluate potential improvements to the model by adjusting model parameter values, modifying the structure of the model, and comparing current modelling efforts with previous studies (Kavetski *et al.*, 2011). In this process, the degree of correspondence between the simulated and observed flows during calibration steps can be achieved subjectively and/or objectively. However, as already noted, additional observed hydrological response data (e.g. evapotranspiration, soil moisture content, and groundwater recharge) can provide the basis for most robust calibrations.

Subjective approach: This approach uses visual judgment of the observed and simulated stream flow hydrographs to assess the model performance based on the behaviour of the model. Krause *et al.* (2005) described this approach as the most fundamental in evaluating different emphasis of the hydrograph. For example, a modeller can assess whether the model over- or under-simulates the systems response, identify the rising limb, falling limb, flood peaks, base flow, and determine variation of monthly and annual stream flow. Another feature of stream flow variability that is most used in practical water resources assessment and planning is the flow duration curve (FDC). An empirical FDC graphically represents the probability that a specific magnitude of stream flow has been equalled or exceeded over a historic period of time (Müller *et al.*, 2014). Despite losing information on the timing of the runoff response, representing the entire hydrograph time series in a form of the FDC makes the interpretation of runoff variability signatures easy (Castellarin *et al.*, 2013). These signatures are usually used to assess the performance of a model. The advantage of using visual judgment is that it is a simple way of integrating different signatures and allows the parameters that influence the different parts of system response to be identified. Boyle *et al.* (2000) have demonstrated the advantages of using subjective measures by closely visualising different aspects of hydrograph such as the rising and falling limb and base flow during model calibration. Currently, most hydrological models are integrated into user-friendly Graphical User Interfaces (GUIs) that allows modellers to observe, visually, the impact of parameter adjustments and the fit of observed and simulated stream flow hydrographs. While subjective measures can be helpful in manual calibration, they do not provide any efficiency measures of model behaviour.

Objective approach: In this approach, model performance assessment is conducted by using one of multiple statistical goodness-of-fit objective measures. Objective measures or objective functions are described as mathematical estimates of the error between the observed and simulated data (Beven, 2012b). Moriasi *et al.* (2007) and Wheater *et al.* (2008) describe various objective functions that can be used to assess model performance. Out of a large number of objective functions available, Moriasi *et al.* (2007) indicated it is difficult to justify the most appropriate indicator to use. Owing to the recommendations made by Biondi *et al.* (2012), proper evaluation of a model should include at least one dimensionless statistic, one absolute error of index, and a graphical representation of the relationship between model simulations and observations.

Over the years, several objective functions have been developed and used in hydrological modelling studies. Amongst those found in the literature (see e.g. McCuen *et al.*, 2006), the

commonly used objective function in assessing hydrological model performance, despite its deficiencies (Pechlivanidis *et al.*, 2011), is the Nash-Sutcliffe coefficient of efficiency (NSE), denoted as *CE* developed by Nash and Sutcliffe (1970). The Nash-Sutcliffe coefficient of efficiency is dimensionless and its value ranges between $-\infty$ and 1. The optimal value of *CE* is 1, indicates a perfect fit between the observed and simulated flows, while an efficiency value of 0 indicates that the model simulations are as accurate as the mean of the observed flows. When simulating stream flow, *CE* is generally not very sensitive to over- or under-simulation of low flows (Krause *et al.*, 2005) and additional logarithmic transformed (*CE {ln}*). Gupta *et al.* (2003) added that a further widely used objective function to reflect the deviations of the mean monthly volumes between the simulated and the observed flow data is the percent bias (*%BIAS*). Gupta *et al.*, (2009) refer to additional objective functions that can be used to effectively evaluate model performance.

Krause *et al.* (2005) pointed out that a choice of a single objective function could lead to bias in model performance evaluation because its performance criterion is sensitive only to certain characteristics of the hydrograph. To reduce this effect, Wagener (2003) proposed the use of multi-objective functions in the evaluation of model performance. This approach has enabled the implementation of multiple performance objectives such as the capturing of high flows, average flow, low flows, and other statistical aspects of hydrological variables (Tang *et al.*, 2006).

2.5.2. Model Calibration

The ultimate goal of model calibration is to establish 'behavioural' parameter values which represent physical processes and components such that the model produces acceptable hydrological system responses based on the set measures of model performance (Tada and Beven, 2012a). This is a crucial step in hydrological model application and it, therefore, requires measurements of catchment behaviour, usually in terms of the inputs to the system and the outputs as presented in a schematic diagram in Figure 2.1. For a model to be "well-calibrated", it is necessary that it has at least the following characteristics: (i) the input-state-output behaviour of the model is consistent with the observations of catchment behaviour, (ii) the model simulations have a negligible amount of bias and the predictive uncertainty is relatively small, and (iii) the model structure and simulations are consistent with a hydrologic understanding of reality (Gupta *et al,*. 2005). Pechlivanidis *et al.* (2011) regard this process as the most challenging aspect of rainfall-runoff hydrological modelling. However, its complexity is also dependent on the number of parameters of the model being calibrated. Usually, calibrations can be achieved more easily for a model with fewer parameters than that of a complex model, which

represents many processes. Generally, two calibration approaches are used in rainfall-runoff modelling, namely: manual and automatic calibration.

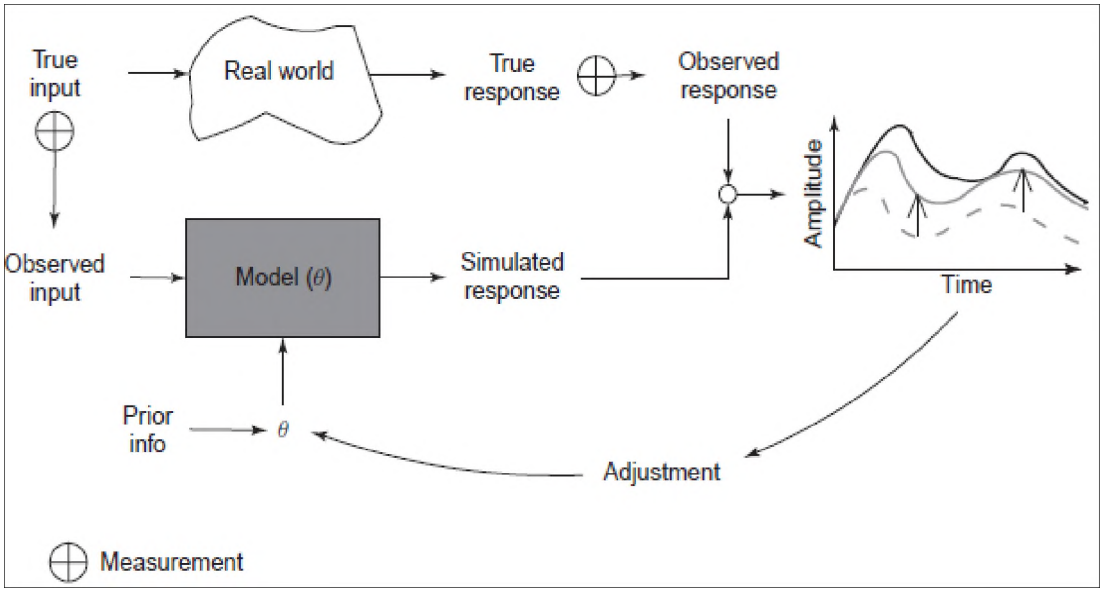

Figure 2.1: A schematic strategy for the calibration of a rainfall-runoff hydrological model. The model parameter set is represented by θ (source: Gupta *et al*., 2005).

Manual calibration: In this approach, the modeller manually adjusts parameter values consecutively in a trial-and-error mode, using visual judgements or objective functions to assess model performance so that the simulated outputs match the observed data with reasonably acceptable limits (Wheater *et al.*, 2008). Depending on the modeller's experience and understanding of dominant hydrological processes of the catchment being modelled, Ndiritu (2009) stressed that the manual approach is tedious and both time and labour intensive which is considered as its weakness (Gupta *et al.*, 2003). Another drawback of this approach is its subjectivity, making derived model parameter values prone to bias, especially when applied in heterogeneous river basins (Wheater *et al.*, 2008). However, Beven (2012) asserted that the advantage of this approach is that the selected model parameter values are hydrologically meaningful; therefore, a more experienced modeller usually needs less time than the inexperienced one to identify plausible parameter values.

Automatic calibration: This approach is formulated on the concept of optimization theory, where mathematical algorithms search the parameter space by performing multiple model runs to obtain the plausible parameter values that provide acceptable statistical measure of the difference between the simulated and observed data using specified objective functions (Pechlivanidis *et al.*, 2011). The drawbacks that are inherent in manual procedures motivated the establishment of

automatic methods where a modeller does not necessarily need to have considerable understanding and knowledge of the dominant hydrological processes, but a model determines plausible parameter values (Khu and Madsen, 2005). Recently, calibration procedures have allowed a detailed investigation of issues underlying the parameter space and search for global optimum parameter values that were not possible with manual calibration for models with many parameters (Madsen *et al.*, 2002). However, Beven and Freer (2001) indicated that obtaining unique optimal parameter sets that provide acceptable modelling results is highly unlikely, and this is a common challenge in model calibration regardless of the method used.

Equifinality problems: It might be expected that a calibration process is aimed at achieving a single and correct hydrologic process representation of reality (Beven, 2006), however, in reality, this is impossible because there are multiple behavioural models capable of simulating similar hydrological responses (Beven, 2012b). Beven (2006) described this modelling problem that is associated with parameter interaction, as *equifinality*. As hydrological models become more complex to increase their scope in testing different hypotheses, additional parameters might be incorporated into the model structure to enable the simulation of additional processes (Hughes, 2004). However, this can lead to over-parameterisation and increase problems of parameter interaction and equifinality (Wagener *et al.*, 2003). Beven and Freer (2001) drew attention to the fact that automatic approaches suffer more from equifinality problems because many parameter combinations provide similarly acceptable simulation results. To overcome some of the calibration problems, Boyle *et al.* (2000) considered that using a combination of manual and automatic approaches could result in a more robust calibration strategy.

2.5.3. Constraints in Hydrological Modelling

Realistic specification of parameter values that represent complex hydrological processes in a model for the simulation of catchment responses to climatic inputs remains the most challenging task (Gharari *et al.*, 2014). Hrachowitz *et al.* (2013a) have demonstrated that introducing expert knowledge and or additional data in specifying initial parameter ranges that define and constrain the prior parameter space improve model realism. The use of additional sources of information is aimed at reducing the degree of freedom of the model parameters to compensate for errors associated with the input data and model structure (Gupta *et al.*, 2008) as well as reducing equifinality problems which can substantially reduce model's predictive power. For example, Gao *et al.* (2014) demonstrated that a more complex, but simultaneously constrained, rainfall-runoff model provides improved simulations of hydrological flow regimes. Hrachowitz *et al.* (2014), who used 11 different model structures and 20 different signatures in a small-scale

catchment, reported similar results. The most noted and common consensus from these studies is that the introduction of vigorous constraints on the model parameters has the potential of improving model realism, better model performance, and for practical benefits (Martinez and Gupta, 2011). Furthermore, when discussing hydrological system behaviour, constraints are much easier to understand than parameters.

Gharari *et al.* (2014) classified model constraints into two categories: parameter and process constraints. The former are generally considered *a priori* because they are imposed on parameters without running the model whereas the latter, often called *a posteriori*, can only be carried out on model fluxes after a model is run with the 'best' parameter set. The use of parameter constraints provides information regarding the relationships between different parameters of the same hydrological processes that correspond to different spatial components of a model. In the data-scarce areas, prior information is incorporated into the models based on explicit hydrological reasoning and partly using quantitative expert knowledge (Hughes, 2013). Comparative information or data of the hydrological response from independent sources can be used as model flux constraint. Process constraints are used to ensure that the modelled outputs follow the modeller's perception of the hydrological system dynamics or match the observation data obtained from independent sources (Gharari *et al.*, 2014). With the availability of hydrological and hydrometeorological variable from remote sensing systems, both parameter and process constraints can be applied in the modelling practice as means of improving model efficiency, realism, and the understanding of hydrological processes at a catchment scale.

2.5.4. Model Sensitivity to Potential Evapotranspiration Inputs

In hydrological modelling, knowledge of the impact of input data errors in the calibration of rainfall-runoff models is crucial in understanding their effects on the performance of models as well as parameter estimation (Paturel *et al.*, 1995). These impacts are evaluated by conducting a sensitivity analysis that shows how the variation in the outputs of a model can be apportioned to different variation in the inputs (Sieber and Uhlenbrook, 2005). While sensitivity analysis has been conducted to evaluate the impacts of rainfall input errors, this study primarily looks at the sensitivity of rainfall-runoff models to the quality of available potential evapotranspiration inputs. The fact that hydrological models are insensitive to changes in the potential evapotranspiration inputs is not new but seems to be a neglected area of research (Oudin *et al.*, 2004; 2006). Oudin *et al.* (2006) indicated that this neglect has led to a lack of understanding of the impacts of input climatic data error on the calibrated parameter sets despite being viewed as one of the most fundamental component of modelling.

Parmele (1972) was one of the first authors to assess the sensitivity of a rainfall-runoff model to changing potential evapotranspiration inputs on model efficiency and parameter uncertainty. Using a sample of nine catchments, the author evaluated the impact of PET errors (random and bias) in three watershed models when simulating stream flow. The author noted that the impact of random PET errors on model performance was small when compared to PET with bias errors. The study also demonstrated that different parameter sets were able to compensate for biased PET estimates such that they presented model simulations considered acceptable. Nandakumar and Mein (1997) evaluated the impact of random and systematic PET errors on the efficiency of the Monash model (Porter and McMahon, 1976). They reported that random PET errors could result in poor runoff simulations while bias in PET had a linear relationship in the bias of the simulated stream flow. The authors further noted that the sensitivity of the model depends on the dominant hydrological processes in a catchment. The conclusion drawn from their results is that the impact of an under-estimated PET in model performance is greater than those that are over-estimated. Fowler (2002) investigated the validity of using fixed seasonal PET inputs and time-varying PET in a daily water balance hydrological model. The results indicated that, even for an extreme dry or wet year, there was no notable difference between the simulated flows using neither of the two PET inputs. Later on, Andréassian *et al.* (2004) used two rainfall-runoff models (GR4J and TOPMODEL) in a sample of 62 catchments to evaluate the impact of improved PET estimates on the simulated flows. The authors found that, in both models, fixed seasonal PET inputs for all catchments yield similar simulation results as a time-varying PET input. Their study demonstrated that the models used have high adaptive capacity to accommodate changing PET input and compensate for it. Contrary to the findings of Andréassian *et al.* (2004), Oudin *et al.* (2005a) concluded that rainfall-runoff models are insensitive to the time-varying PET inputs when compared with the use of fixed mean PET input in six hydrological models. Even though the authors conducted their study using only four different daily rainfall-rainfall models to simulate stream flow over a large sample of 308 catchments, questions on the methods used to estimate PET and the level of the adaptive capacity of the model structures to different forms of PET inputs are raised.

In the efforts of studying the most appropriate method used to estimate PET inputs to drive rainfall-runoff models, Oudin *et al.* (2005b) showed that a model run with temperature and radiation based PET estimates tend to provide better stream flow simulations compared to those run with Penman-Monteith based PET estimates. It therefore remains unclear if remote sensing-based PET inputs can improve the efficiency of rainfall-runoff models and be used to calibrate the model parameters, even though they are subjected to a great deal of ill-quantifiable

uncertainty (Winsemius *et al.*, 2008). There is also little clarity in the differences in sensitivity under energy or water-limited conditions.

2.6. UNCERTAINTY IN HYDROLOGICAL MODELLING

Given that the connections between the spatial and temporal patterns of hydrological processes are still poorly understood (Wagener *et al.*, 2013), it is clear that uncertainties in hydrological modelling are substantial. In a variety of modelling domains of earth sciences, uncertainties are unavoidable and inevitable. In recent years, hydrological uncertainties have enjoyed and still enjoy a considerable amount of attention in hydrology and has created a room for spirited debates amongst researchers (e.g. Montanari, 2007; Refsgaard and Hansen, 2010; Beven, 2016). Uncertainties are categorized as epistemic or aleatory (Montanari, 2007). The former arises when knowledge about a particular hydrological process is incomplete due to the lack of understanding about the system or because representative observations are missing (Beven and Westerberg, 2011). The latter arises because of the random natural variation of systems which results in unknown events that cannot be predicted or understood (Renard *et al.*, 2010). Beven (2012) argued that it is not easy to separate aleatory and epistemic sources of uncertainty in hydrological modelling. Di Baldassarre and Montanari (2009) summarise three common sources of uncertainty in the context of hydrological modelling: (i) model input data uncertainty, (ii) model parameter uncertainty, and (iii) model structural uncertainty.

Different sources of uncertainties do not have the same influence on the simulated hydrological response. Some might have a significant influence and others might have a relatively negligible impact. Climatological input data uncertainties affect the simulation results the most in comparison with model structure and parameter uncertainties (Montanari, 2007). Even though model structural and parameter uncertainties have the least impact on the simulation results, quantifying predictive uncertainty resulting from these sources is also important, and should be considered best practice in the post-PUB era (Hrachowitz *et al.*, 2013a; Montanari *et al.*, 2013).

Traditionally, the standard approach of uncertainty estimation in hydrology has been mainly via the propagation of error using two sets of methods. In the first approach, according to Gupta *et al.* (2013), uncertainties are initially quantified individually from their respective sources (i.e., input data uncertainty, model parameter uncertainty, and model structure uncertainty). In the second method, uncertainties are introduced through the model to estimate resulting prediction uncertainty. This method may include the assimilation of additional information such as that

which represents runoff signatures or system response to the model as means of reducing the predictive uncertainty (Wagener and Montanari, 2011).

2.6.1. Model Input Data Uncertainty

The major sources of input data uncertainties for hydrological modelling includes rainfall and potential evapotranspiration (Andréassian *et al.*, 2001). Other observational data of hydrological response that are used to calibrate hydrological models (groundwater recharge, stream flow and soil moisture status) and to account for water use, contribute to input data uncertainties (McMillan *et al.*, 2010). Inadequate spatial and temporal distribution representation, scale mismatch, data pre-processing, systematic and random errors in measurement and estimation in the variable data, and the lack of adequate water use data records are the main causes for the uncertainties that are introduced into the modelling process (Hughes and Mantel, 2010b). In data sparse regions, uncertainties associated with model input data will always be high (Sawunyama and Hughes, 2008).

Since model input data uncertainties are usually assumed the largest source of uncertainty in hydrological modelling (Di Baldassarre and Montanari, 2009), the focus of many modellers has been on improving the acquisition and the estimation of data on rainfall and evapotranspiration demands. Because point measurements do not capture information on spatial and temporal patterns, spatially distributed measurement data of high temporal resolution are desirable. Such data are useful in understanding the patterns of hydrological variables and could be used in attempts to improve model applications. These data can be acquired from earth observation systems that are now capable of capturing a variety of hydrological variables (see NASA, 2006). Hostache *et al.* (2010) have indicated that hydrological predictions can be improved using data assimilation techniques with the aim of reducing input data uncertainties.

Rainfall data: Numerous studies in the literature (e.g. Wotling *et al.*, 2000) have dealt with the sensitivity of hydrological models to uncertainties related to rainfall and have shown that the spatial distribution of rainfall should be accounted for, while others (e.g. Segond *et al.*, 2007) suggest that lumped rainfall inputs are often adequate. Andréassian *et al.* (2001) have demonstrated the importance of testing the sensitivity of rainfall-runoff model to different rainfall inputs as means of assessing their sensitivity and robustness. Arnaud *et al.* (2002) for example, showed that using mean areal rainfall instead of spatially distributed rainfall tends to underestimate the volumes and the peak flows. This underestimation was directly correlated with the spatial coefficient of variation of the rainfall.

Effects of rainfall uncertainty on hydrological modelling have been mainly studied by means of stochastic simulation or by incorporating rainfall error models in the total error models of uncertainty frameworks (Götzinger and Bárdossy, 2008). Gourley *et al.* (2011) assessed the performance of a distributed hydrological model using different sources of satellite-derived rainfall estimates. In their study, they discovered that rainfall data from different products resulted in differences in model performance. They argue that incompatible spatial resolution between rainfall products and the hydrological model used could increase uncertainties. In South Africa, Sawunyama and Hughes (2008) assessed the potential of using satellite-derived rainfall estimates with the aim of improving model simulations and addressing rainfall data uncertainties. The authors noted that satellite-based rainfall estimates need to be corrected before applying them to the model. They also reported that scale issues could increase uncertainties.

Evapotranspiration data: The common problem of PET estimates is that they are not truly representative of catchment evaporative demand fluxes (Oudin *et al.*, 2005b). This predominantly results in the use of point-based PET data in the models, which are mostly uncertain. Given the high degree of heterogeneity in catchments, point estimates are typically not capable of adequately representing these demands in the model. Therefore, the uncertainty in the estimates of PET can lead to the inadequate prediction of water balance, and thus jeopardising the practical application of hydrological models. The increase in the number of satellite-based products that provide PET data from remote sensing methods could prove vital in the application of hydrological models (Allen *et al.*, 2011a).

Winsemius *et al.* (2008) showed that evapotranspiration measurements from remote sensing products could improve the calibration of a rainfall-runoff model. Qin *et al.* (2008) compared physical-based distributed model-derived ETa to MODIS-retrieved, spatially-distributed evapotranspiration estimates. They reported that both ETa estimates resembled a good linear relationship although their spatial distribution depicted differences. Their overall study demonstrated that combining and integrating the capabilities of, and information from, model simulations and remote sensing techniques may provide plausible spatial and temporal characteristics of ETa across a catchment. The studies highlighted above demonstrate that there is great potential for using satellite-based rainfall and evapotranspiration estimates to improve hydrological modelling by reducing uncertainties. However, adequate data processing techniques and testing of the available data in different models and different parts of the world remain a task to explore.

Observed stream flow data: Stream flow is often regarded as a well-determined hydrological variable (Westerberg *et al.*, 2011). However, several studies (e.g. Di Baldassarre and Montanari, 2009; Wessels and Rooseboom, 2009b) have showed that stream flow data can have substantial uncertainties due to measurement inaccuracies, particularly during extreme high flows and low flows periods, poorly defined upstream developments, and in alluvial rivers with non-stationary river beds. Despite a number of methods that have been developed to estimate rating curve uncertainty, rating curves can be uncertain for a number of reasons, including (i) natural uncertainties, (ii) data uncertainties and (iii) knowledge uncertainty (Clarke *et al.*, 2000). Natural uncertainties include those generally caused by non-stationarity in the river cross-sections and flow that bypasses the gauging structure. They result from erosion, sedimentation, debris accumulation, variable backwater, vegetation growth, and other modifications in the channel. Data uncertainties are induced by measurement and data processing errors due to insufficient sampling of river cross-section geometry and inadequacies in velocity measurement. Knowledge uncertainty results from the lack of complete understanding of hydraulic processes used to formulate assumptions in the model of the rating curve.

To reduce the uncertainties that are associated with the rating curve, improvements in discharge measurements are required. Di Baldassarre and Montanari (2009) provide the guidelines that should be followed to reduce discharge measurements. Wessels and Rooseboom (2009b) recommended that a gauging structure should be calibrated, on average, every five years to account for the natural changes along the stream channel. Due to the lack of resources in South Africa for example, this is generally not done (Aldous *et al.*, 2014).

2.6.2. Model Parameter Uncertainty

Issues such as over-parameterisation of models and the lack of understanding regarding interrelationships between model parameters (Uhlenbrook and Sieber, 2005) are significant sources of uncertainties. Parameter uncertainty can be due to inaccurate input data with the result that calibration parameters are fitted to the errors and not the real hydrological response. As model parameters are frequently not measurable in the field, this results in the inability of models to converge on a parameter set that provides an acceptable simulation of system response (Wagener and Gupta, 2005); the equifinality problem (Beven, 2006). These uncertainties affect the simulation results for periods outside the calibration period or when models are applied to ungauged catchments. The lack of accurate input data, such as catchment property, stream flow, or other sources of hydrological system response used to calibrate a model directly hinders the estimation of reliable model parameters.

Winsemius *et al.* (2008) stressed that modellers are forced to look beyond the classical approach of hydrograph-fitting and come up with innovative alternative approaches to finding behavioural parameters or use other data sources to constrain parameter ranges during model calibration. Fenicia *et al.* (2008) added that approaches such as the incorporation of soft data and remote sensing data in model calibration could help in constraining model parameters. The study by Gharari *et al.* (2013a) indicates that sub-period calibration could be used for model parameter identification. Winsemius *et al.* (2008) used evaporation estimates from MODIS images, extracted using the SEBAL algorithm, to constrain model parameters of modelling units with similar land cover. Their work revealed that model parameters of modelling units with similar land cover could be identified as they were clustered in similar patterns. However, Seibert and McDonnell (2002) noted that remote sensing data are subject to a great deal of noise that could result in substantial and non-quantifiable uncertainties. They recommend that these data can be applied as soft data to update *a priori* knowledge of initial model parameters.

2.6.3. Model Structure Uncertainty

Because rainfall-runoff hydrological models are simplifications and interpretations of a real hydrological system in nature, they are usually expressed as a set of mathematical equations based on model designers' understanding of the hydrological processes (Refsgaard *et al.*, 2006). In general practice, a modeller's perception, imagination, and hydrologic understanding of the processes of a hydrological system are used to derive the model structure (Gupta *et al.*, 2005). This has been pointed out by Beven (2012) who reiterates that model structural uncertainties are introduced into the model because of the lack of understanding of hydrological processes in catchments, wrong perceptions about dominant hydrological processes, the oversimplification of the reality of hydrological processes, and unrealistic expressions of hydrological variables and fluxes in both space and time.

From the literature, structural uncertainty in rainfall-runoff models have not been adequately dealt with despite continuous efforts aimed at helping to improve our understanding and knowledge about dominant processes as well as means of address this source of uncertainty. One of the widely acknowledged reasons is that it is often much difficult to quantify these uncertainties compared to those from other sources (Warmink *et al.*, 2010). Nevertheless, several strategies have been developed to deal with model structural uncertainties. These include the use of multiple conceptual rainfall-runoff methods (Refsgaard *et al.*, 2007), and the use of statistical probability methods to isolate structural uncertainties from the total model predictive uncertainty (Renard *et al.*, 2010). The development of these strategies have to keep pace with the non-

stationarity of hydrological system processes, thus, extensive gathering and monitoring of hydrological variables and a detailed understanding of their dynamics could help in modifying the model structure to cater for these evolving processes (Butts *et al.*, 2004). In this context, for example, the availability of remotely sensed hydrological, environmental, and geological data can help to improve model conceptualisation and reduce uncertainties that are associated with improper formulation of model structure.

2.7. EARTH OBSERVATION DATA IN HYDROLOGY

2.7.1. Remote Sensing Techniques

Remote sensing is becoming an increasingly valuable technique for providing landscape characteristics data on a large-scale and can replace the time-consuming and expensive process of taking ground measurements. Engman (1993) defined remote sensing techniques as the science and art of remotely obtaining information or measurements of the object's properties on the earth's surface through the analyses of reflected or emitted data acquired by sensors on-board satellites and aircraft. The measured electromagnetic radiation and thermal emissions are interpreted using formulated algorithms in order to extract surface feature signatures of interest (NASA, 2006).

2.7.2. Application of Remote Sensing in Hydrology

The concept of integrating remote sensing data into hydrologic studies is relatively old, dating back to the work of Schultz (1988) and Engman (1993, 1996). A large number of diverse useful examples of the application of remote sensing in hydrological modelling can be found in Schultz and Engman (2000). Over the last decade, the number of remote sensing products has made tremendous contributions to hydrological sciences (see Lettenmaier *et al.*, 2015 and McCabe *et al.*, 2017 for discussion) and the number of products continues to increase.

2.7.2.1. General model calibration

Remote sensing data are often treated as "soft data" in hydrological modelling as it provides only qualitative hydrological information. Seibert and McDonnell (2002) demonstrated that "soft data" could potentially improve calibration procedures, particularly in data scarce areas. Wagener *et al.* (2013) also drew conclusions that soft data helps in obtaining educated estimates on the magnitude of model parameters, and can improve the overall modelling approaches used in rainfall-runoff modelling. For this particular study, the focus is on PET and ETa; however, a

brief review of other important hydrologic aspects such as precipitation, soil moisture, groundwater, LULC, open water bodies, and vegetation cover are given.

2.7.2.2. Evapotranspiration estimation

Evapotranspiration fluxes are highly variable over space and time due to differences in topography, vegetation cover, soil properties, climate, and other heterogeneities. Conventional point-based ET estimation methods are incapable of capturing this large spatial scale variability, while remote sensing based methods have the capability to estimate spatial and temporal variation of ET from catchment to global scales (Ruhoff *et al.*, 2013). Over the past few decades, there have been numerous efforts aimed at developing and refining remote sensing-based products that provide ET estimates at these scales (e.g. Kalma *et al.*, 2008). Kustas and Anderson (2009) categorised remote sensing based ET estimation approaches into two types: (i) an aerodynamic resistant-land Surface Energy Balance method (SEB) and (ii) a reference-surface ET method. The former uses surface reflectance from visible and near infrared bands as well as land surface temperature from thermal band of the satellite image. In the latter, remote sensing-based vegetation cover data are used to estimate canopy conductance. In the literature, both approaches have been extensively reviewed (e.g. Su, 2002; Allen *et al.*, 2011c).

The energy balance approaches were established in the early 1990s to estimate ET from large areas. The pioneering work by Menenti and Choudhury (1993) formulated and developed a Surface Energy Balance Index (SEBI) algorithm. The SEBI algorithm introduced the fundamental concept of applying the energy balance concept using remote sensing data for ET estimation. Following the work of Menenti and Choudhury (1993), a number of studies, including Cleugh *et al.* (2007) have used this concept in the estimation of ET.

Cleugh *et al.* (2007), for example, compared ETa estimates obtained using both the energy balance and reference approaches at monthly temporal scales and continental spatial scales. The authors asserted that the energy balance methods did not provide reliable ETa estimates due to difficulties in sensible heat flux estimation by radiative surfaces. Kustas and Anderson (2009) drew a similar conclusion in their simulation study, which used a Soil-Vegetation-Atmosphere Transfer (SVAT) scheme, over a range of heterogeneous hydrometeorological and vegetative conditions. The conclusions of Cleugh *et al.* (2007) may emanate from a typical assumption that radiative surface temperatures are equal to aerodynamic surface temperature. However, this assumption may not be appropriate according to Kustas *et al.* (2007). This is simply because the relationship between radioactive surface temperature and aerodynamic surface temperature

depends mainly on the extent of vegetation cover and canopy structure (Su *et al.*, 2001). Hellegers *et al.* (2009) also used the energy balance approach to quantify and map ETa variations in basins with different vegetation cover as well as to identify catchments that are experiencing water deficit. From a hydrological modelling perspective, Winsemius *et al.* (2008) used ETa estimates derived from this approach to calibrate and constrain different parts of a simplified version of the 1-dimensional HBV hydrological model (Lindström *et al.*, 1997) for the Luangwa River basin in Zambia.

A number of algorithms have been developed and validated for estimating ETa at a local and regional scale (Allen *et al.*, 2011a). These include the Surface Energy Balance Algorithm for Land (SEBAL: Bastiaanssen *et al.*, 1998a, b) and the Surface Energy Balance System (SEBS: Su, 2002). SEBAL is conceptualized from both the empirical relationships and physical parameterisation of energy balance components and uses the Normalized Difference Vegetation Index (NDVI), albedo maps, air temperature and wind speed to estimate ETa at a catchment to regional scale. It has been used in different applications in water resources planning and management disciplines (Zwart and Bastiaanssen, 2007). In South Africa, Hellegers *et al.* (2009) used SEBAL to improve decision-making about water resources management by assessing the status of water use within catchments. Gibson *et al.* (2010) applied SEBAL to assess the state of legal water use compliance in the Western Cape Province of South Africa. At the start of this study, in South Africa, there were no studies reported that have attempted to use SEBAL-derived ETa estimates in the application of a rainfall-runoff model. Initially, this study intended to use SEBAL to extract ETa for constraining model outputs; however, because of its intellectual property rights held by WaterWatch, the computational algorithm was not available for public use (Kongo, 2011). Bastiaanssen *et al.* (1998a, b) provide detailed explanations of the SEBAL computational algorithms, whereas a broad review of SEBAL operational applications across different parts of the world is given by WaterWatch (2011).

SEBS is formulated based on the determination of (i) land surface physical parameters, (ii) the roughness length of heat transfer, and (iii) the evaporative fraction on the basis of the energy balance approach (Su, 2000). The first set consists of remote sensing-based data that are used to derive land surface physical parameters such as emissivity, land surface albedo, temperature, leaf area index (LAI), NDVI, fractional vegetation coverage, and the height of the vegetation. The second dataset comprises wind speed at a reference height, air pressure, temperature, and humidity, which can be measured or estimated by a large-scale meteorological model. The last set consists of the measured or simulated incoming solar and long-wave radiation. Su, (2002)

provides a description of the computation of ETa using the SEBS algorithms. While SEBS has been used in various studies for the estimation of ETa and has proved to produce reliable estimates in southern Africa (e.g. Jarmain *et al.*, 2009b; Gibson *et al.*, 2011; Rwasoka *et al.*, 2011), the amount of observation data it requires renders it inapplicable in most parts of South Africa.

Apart from using the energy balance methods, combinations of empirical approaches with remote sensing data are used to estimate ETa as well as PET. Mu *et al.* (2011) applied this combination methodology in the estimation of spatial and temporal patterns of global PET and ETa that are included in the MOD16 ET product. The use of the MOD16 ET product data has not attracted much attention from hydrological perspective in South Africa, but has been explored internationally (e.g. Hamel and Guswa, 2015). A study by Műnch *et al.* (2013) used MOD16 ETa data to quantify groundwater recharge in the Western Cape Province of region of South Africa as well as quantifying ET signatures from a model and from MOD16 ET product. When comparing MOD16 ETa with the model simulated ETa data, the authors show that these data had similar response in years with normal rainfall compared to the wet seasons. This indicated that the MOD16 ET product requires further validation as a means of reducing the uncertainties associated with the data. The use of MOD16 estimates in hydrological modelling for constraining model outputs (ETa), or calibrating model parameters (PET) that affect evapotranspiration processes, remains an area of research still to be explored in South Africa.

2.7.2.3. Precipitation estimation

Conventional methods used to measure rainfall provide only point measurements; consequently, in remote areas with complicated topography (e.g. mountainous), these measurements are impossible or very difficult to obtain (Thorne *et al.*, 2001). The inability of point-scale measurements to represent catchment average rainfall raises concerns in its application to hydrological models. Despite the efforts made in developing interpolation techniques used to generate catchment average rainfall, Habib and Krajewski (2002) reported that interpolated rainfall records could not represent the nature of a catchment's rainfall variability. Therefore, new techniques must be used to provide adequate rainfall estimates and remote sensing has been one of them. Various research institutes have embarked on estimating rainfall and most of them have made their data products available for public use. These projects include the version-2 of Global Precipitation Climatology Project (GPCP: Adler *et al.*, 2003), Tropical Applications of Meteorology using SATellite (TAMSAT: Thorne *et al.*, 2001) and the National Aeronautics and Space Administration's (NASA) Tropical Rainfall Measurement Mission (TRMM: Huffman *et*

al., 2007). However, several studies have reported setbacks with satellite-derived rainfall data because of the lack of ground-based validation data and scale limitations (e.g. Hossain and Huffman, 2008).

2.7.2.4. Soil moisture estimation

Soil is an influential storage of water in the hydrological cycle. It plays a major role in partitioning rainfall into runoff, as an infiltration medium, partitioning of mass and energy fluxes between the hydrosphere, the biosphere and the atmosphere, and effectively governing complex hydrological processes through the control of evapotranspiration fluxes. Conventional methods used to measure soil moisture are adequate to allow meaningful interpretation at the point scale. However, it is more difficult to measure at large spatial scales (Parajka *et al.,* 2006). The use of remote sensing techniques is promising in providing spatially distributed estimates of soil moisture over large areas, but with a low temporal resolution. Microwave remote sensing instruments such as the Advanced Microwave Scanning Radiometer (AMSR-E), Advanced Scatterometer (ASCAT) as well as the Soil Moisture and Ocean Salinity (SMOS) are employed to estimate and provide soil moisture data products over large areas (Njoku *et al.*, 2003). Some of these products have been locally validated with in-situ soil moisture in-situ data in different parts of the world (e.g. Scipal *et al.*, 2005). These data products have helped in not only improving the fundamental understanding of unsaturated zone processes but also in describing the spatial and temporal dynamics of precipitation, evaporation and temperature of the soil profile. However, despite the potential of these data products, there are still many challenges in reliably obtaining soil moisture estimates, especially in the areas with radio-frequency interference such as in densely inhabited areas (Albergel *et al.*, 2012).

Hydrologically related studies, using soil moisture data derived from remote sensing, have been conducted in the past. These include (but are not limited to) the establishment of moisture-runoff relationship in different catchments, data assimilation for improving runoff prediction in both gauged and ungauged catchments, and for comparison with model-simulated soil moisture (Brocca *et al.*, 2010; Chen *et al.*, 2011). Western *et al.* (2004) hinted that satellite-derived estimates of soil moisture would be an obvious choice for explicit soil moisture accounting in a hydrological model. However, the inability of satellite systems to retrieve deep soil moisture in depths that are equivalent to plant root depth is a limiting factor. The reason is that rainfall-runoff models normally represent soil moisture storage at the depths equivalent to plant roots, while satellite data do not. The majority of the above-cited studies have indicated major setbacks to the application of soil moisture estimates derived from remote sensing techniques – scale

limitations and the inability to represent the full soil moisture column. These limitations were major determining factors to the changes of one of the objectives of this study. Initially, this study aimed at applying soil moisture estimates derived from AMSR-E to constrain model simulated soil moisture. However, due to spatial scale limitations (43 km x 75 km to 8 km x 14 km), it was impossible to apply the data at the catchment scales used in this study.

2.7.2.5. Groundwater estimation

In groundwater studies, the application of remote sensing has been useful in detecting lineaments and identifying faults and dykes that normally designate signs of faults and fractures, which usually indicate aquifers with potential sources of groundwater (e.g. Meijerink *et al.*, 2007). Acquiring such information plays a major role in the conceptualisation of groundwater models, informing surface hydrological models about the dynamics of groundwater recharge Brunner *et al.* (2007). Milzow *et al.* (2011) calibrated and constrained groundwater storage parameters of a rainfall-runoff model in the poorly gauged Okavango River basin, using GRACE data. However, the GRACE data should be downscaled to finer scales that are suitable for hydrological models used for practical water resources assessments. It must be noted, however, that the application of GRACE data in small catchments has been regarded as impractical if the data are not downscaled (Becker, 2006). The spatial resolution range of GRACE data is from 400 km to 4 000 km (Tapley *et al.*, 2004). Given the potential that GRACE data have on the improvement of hydrological models, this study intended to apply the data in constraining model-simulated soil moisture to catchments with an area of up-to 2 400 km^2 but it was deemed impossible, as the surface areas of the selected catchments were relatively small.

2.7.2.6. Vegetation cover and land use

The use of MODIS, Advanced Very High Resolution Radiometer (AVHRR), and Landsat satellites have attracted attention in the acquisition of up-to-date global land cover data at high temporal and spectral resolutions ranging from daily to 8-day and 2.5 m to 1000 m (Foody, 2002). Data of such resolution are ideal for detecting change and can provide useful information concerning the state of vegetation growth, which can be useful in the calibration of rainfall-runoff models for ungauged catchments. A number of hydrological studies have used these data for hydrological assessments. For example, Kim *et al.* (2005) employed land use dataset derived from Landsat Thematic Mapper (TM) to investigate the impacts of land use changes on hydrological response to an urbanising catchment. Landsat TM data proved to be useful in quantifying the changes at a small scale. Öztürk *et al.* (2013) used satellite maps of the land use

in addition to meteorological and daily stream flow data to calibrate a hydrological model to evaluate the impacts of land use change on hydrology. Donohue *et al.* (2010b) demonstrated the potential use of remotely sensed vegetation cover data to improve Budyko's hydrological model calibration as they discovered that stream flow simulations were improved when using data with finer spatial resolution. Despite the promising trials, it is worth noting that land use and vegetation cover data from satellites are subject to quality distortions because of cloud cover, and this problem is the main hindrance in the acquisition of the data (Ferguson and Wood, 2010). Nevertheless, the evidence from studies on the use these data seems to suggest that there is great potential to improve hydrological modelling and other aspects of catchment hydrology such as studying the impact of open water bodies on hydrological flow regimes.

2.8. KEY SUMMARY

This chapter presented a review of the literature, which is relevant to the broad concepts and application of hydrological modelling with emphasis on the use of data from earth observations systems. Since South Africa experiences high climatic variability at different temporal and spatial scales, a variety of hydrological models have been developed to help in the assessment of water resources and other related aspects. However, the widely noted hindrance is the scarcity of observation data to support the modelling processes. Modelling under such conditions contributes further to the modelling uncertainties – a major challenge to the proper application of models. Traditional methods used to measure and estimate hydrometeorological variables to support model applications are typically not capable of providing representative data at adequate scales, and remote sensing could be used an alternative to this challenge. This study therefore attempts to explore the potential of remote sensing in the provision of both potential and actual evapotranspiration estimates for the use in attempts to improve model simulations, and the following chapter provides the methods that were used in this study.

CHAPTER THREE

3. DATASETS AND METHODS

This chapter provides a description of the model input dataset, the Pitman model, the MOD16 ET product, and various modelling methods that were used. Various rainfall-runoff hydrological models have been developed and applied to assess water resources, but the Pitman model is arguably the most widely used model in southern Africa (Hughes, 2013). However, the incorporation of remote sensing based evapotranspiration data such as the MOD16 ET product has not received much attention in hydrological model applications in southern Africa. For this reason, PET and ETa data from the MOD16 ET product were applied in the Pitman model to assess potential improvements of model efficiency and to evaluate the sensitivity of the model parameters. To achieve the objectives outlined above, the following procedures were undertaken:

- Initial setups and calibrations of the Pitman model under natural conditions were undertaken using both single-run and the uncertainty version.
- The MOD16 ET product data were acquired, extracted, and processed for model use.
- The uncertainty version of the Pitman model was applied by using fixed seasonal distributions of pan-based PET data to simulate hydrological response for present-day conditions and to obtain the 'best' parameter sets to be used in the evaluation of the impacts of using changing PET data inputs in the model.
- The uncertainty version of the model was also applied using MOD16 PET time series data to re-calibrate the model as mean of evaluating the sensitivity of the model parameters.

The MOD16 ETa time series data were applied to constrain model-simulated ETa.

3.1. SUMMARY OF THE DATASETS

Preparing model-supporting data for forcing a hydrological model is an essential first step in the modelling of hydrological systems. Most importantly, without adequate model input data it is difficult to generate sensible simulations. The adequacy of model forcing data depends on the quality of the data and their spatial representativeness. Hence, it is important to identify and address data uncertainties before undertaking hydrological modelling. The datasets used in this study are catchment average rainfall, potential and actual evapotranspiration, stream flow

(observed and naturalised), groundwater recharge, and water resources development data (see Table 3.1).

Table 3.1: The summary of the datasets used in the study

Dataset	Temporal resolution	Spatial resolution	Source	Length	Reference
Rainfall	Monthly	Quaternary	WR2012	1920 - 2010	Bailey and Pitman (2015)
PET	Monthly means	Quaternary	WR2005	-	Middleton and Bailey (2008)
MOD16 PET & ETa	Monthly	1 km^2	NTSG	2000 - 2010	Mu *et al.* (2011)
Naturalised flow	Monthly	Quaternary	WR2005	1920 - 2005	Middleton and Bailey (2008)
Observed flow	Monthly	Various	DWS	see Table 3.2	www.dwa.gov.za/hydrology
Water use	Varies	Various	various	-	see text below
Groundwater recharge	Annual means	Quaternary	DWAF	-	DWAF (2005b)

- ***Rainfall data*** are based on spatial interpolation of gauged rainfall data and are expressed as a monthly percentage of the mean annual precipitation (MAP) value for each quaternary catchment. The quality of the rainfall data is dependent on a number of factors for individual catchments. These include a lack of adequate density of rainfall gauging stations, gaps in the records of individual gauging stations, steep rainfall gradients and spatial variability of rainfall within a catchment.
- ***Potential evapotranspiration data*** (PEVAP) are based on regionally fixed mean monthly evaporation distributions available from the WR2005 reports (Middleton and Bailey, 2008) and mean annual evaporation (MAE) values from a limited number of A-pan or S-pan measurements. These data do not represent the spatial variability of potential evapotranspiration fluxes across the catchment landscape. As an alternative, remote sensing-based estimates of PET (MOD16) could be used to define the monthly variations in PET using either pan-based annual PET values or remote sensing-based annual PET. An alternative is to use remotely-sensed actual evapotranspiration (ETa) time series to constrain model-simulated total ETa values that include interception loss and soil evapotranspiration in the model. A short description of the methods used to process remotely sensed PET and ETa data is given in section 3.4.4 whereas the detailed MOD16 processing steps are provided in Appendix 1.
- ***Naturalised flows:*** Inadequate and discontinuous records of stream flow are common problems in many catchments and these affect the application of hydrological models (section 2.6.1). These problems make the observed stream flow data uncertain with respect to their representation of natural flow regimes and introduce uncertainty into the calibration of hydrological models. Under these conditions, it was appropriate to

use the naturalised stream flow records from the WR2005 database (Middleton and Bailey, 2008) for the initial calibration (natural conditions) of the Pitman model. These data are based on calculations that remove all upstream water resource developments that affect the natural hydrology of a catchment.

- ***Observed flow data*** were used to simulate the present-day flow hydrological conditions as they include the upstream impacts. It is important to recognise that these impacts are likely to be non-stationary over extended periods of observation and results in the inconsistencies in the observed hydrological response. Qualitative and quantitative measures were used to evaluate the inconsistencies and stationarity of the observed stream flow records. Qualitative methods for evaluating inconsistencies included plotting stream flow data to identify gaps and outliers in the data. Data values that were indicated to be "above rating" were removed from the records (i.e. treated as missing values) because they could have an impact on the model simulations of high flows. A quantitative method applied to evaluate data stationarity was trend analysis using the Mann-Kendall non-parametric test (Mann, 1945; Kendall, 1975). The other non-parametric test developed by Pettitt (1979) widely used to determine the occurrence of a significant change point in the mean of the time series point was applied in this study. Table 3.2 lists the gauging stations used in this study, and the periods for which data were available, as well as the summary information on data quality.
- ***Water resources development*** data used in this study included dams and run-of-river abstraction volumes for irrigation and domestic use, as well as their respective seasonal water demand patterns. The data and information on water abstractions for industrial and domestic use as well as crop water use were obtained from various sources. These include consultancy reports (e.g. DWA, 2010a; Taylor and Gush, 2014; Hortgro, 2015), web-based CapeFarmMapper application (WCDA, 2015), SAPWAT software (van Heerden *et al.*, 2009) and the DWS Water Use Authorisation and Registration Management System (WARMS) database (DWS, 2014a). It is worth noting that the temporal patterns of water use data and other qualitative information are frequently incomplete and these add uncertainty into the modelling process (Hughes and Mantel, 2010b). To account for anthropogenic impacts of small dams on stream flow, the surface area and capacities of all the small farm dams in each sub-catchment were combined to form one 'dummy' dam that was then modelled per sub-catchment (Hughes and Mantel, 2010a, b). Due to the lack of ground survey data for

area and volume of the dams, Google Earth (2013) images (e.g. Rodrigues *et al.*, 2012) were used to determine the surface area of the farm dams for estimating their storage capacity. These images were used to digitise polygons of small farm dams and irrigated areas assumed to be supplied by water from rivers and farm dams, both as circles, rectangles, triangles, and trapezoids. These polygons were used to determine the surface area for individual farm dams by measuring their geometric parameters (width, length, and radius) and applying Earth Point – a web-based tool available from http://www.earthpoint.us. A robust regression relationship between full supply area and volume of dams was used to estimate the storage capacity. Meigh (1995) defined this method as given by regression equation 3.1:

$$V = a * (A^2)^b \qquad (3.1)$$

where V ($m^3 * 10^6$) and A (km^2) represent storage capacity of the dam and surface area, respectively, whereas a and b are regional constants.

Table 3.2: Stream flow data attributes for the selected catchments (see Chapter 4)

Station No.	River	Area (km^2)	Latitude	Longitude	Data period	Missing data (%)
T1H001	Xhora	978	31°40′12.81″	28°06′41.97″	31-12-1998 – 30-09-2010	0
G1H008	Klein Berg	393	33°18′50.55″	19°04′29.16″	01-05-1954 – 30-09-2010	2.7
K4H003	Diep	72	33°54′45.00″	22°42′28.09″	30-06-1961 – 30-09-2010	1.2
R2H005	Buffalo	411	32°52′31.37″	27°22′57.90″	01-10-1947 – 30-09-2010	20.1
Q6H003	Baviaans	814	32°36′21.34″	25°53′04.85″	08-09-1980 – 30-09-2010	1.1
X2H001	Noordkaap	126	25°36′39.86″	30°52′29.22″	11-02-1948 – 30-09-2010	1.9

3.2. THE PITMAN MODEL

The model used in this study is a modification of the original Pitman (Pitman, 1973) monthly time-step rainfall-runoff model that has been widely used for research and practical water resources assessments in South Africa for many years (Hughes, 2013). The model is primarily a conceptual, semi-distributed model with parameters representing the main hydrological processes such as storages (interception, soil moisture and groundwater) and fluxes (infiltration, groundwater flow, saturation excess flow, and direct overland flow) that constitute the natural water balance of river basins (Hughes, 2013). The original version of this model was based on the understanding of dominant climatic and hydrological conditions of South Africa (Pitman, 1973). Although its basic structure has been preserved, it has undergone several modifications to incorporate important components of the water balance that are necessary in addressing a variety of water resources management challenges in the southern African region. The main

modification of the model, the GW-PITMAN version (Hughes, 2004), focusses primarily on improving the links between surface water and groundwater (e.g. Hughes, 1995). Hughes (2013) provides a full description of the development and the application of this model.

3.2.1. Modelling Platforms of the Pitman Model

Various modelling platforms of the Pitman model are available and they exist in a number of different forms. In the present study, the GW-PITMAN model used for modelling the selected catchments was applied within the SPATSIM (SPatial and Time Series Information Modelling) platform. Hughes and Forsyth (2006) developed the SPATSIM integrated modelling software package with ESRI MapObjects to link several data types (input, output, and parameters) for hydrological modelling. The platform provides generic data input, processing, analysis and display procedures. The advantage of this software is that it uses a Geographic Information System (GIS) user-friendly interface and shapefiles to display spatial data types such as points (e.g. streamflow gauge and rainfall gauge), lines and polygons (e.g. rivers and catchment boundaries), and link these with a database of multiple types of data (e.g. rainfall, stream flow, parameters). The software enables the graphical display of time series data, flow duration curves, monthly distributions, as well as statistical analysis of the objective functions used to evaluate the performance of the model. A more detailed description of the software can be found in Hughes and Forsyth (2006), and Kapangaziwiri (2010).

3.2.2. The Components and Parameters of the Pitman Model

Figure 3.1 illustrates the conceptual structure of the GW-PITMAN model used in this study. Table 3.3 lists the GW-PITMAN parameters in the model, while brief descriptions of some of the parameter functions, excluding the wetland component (see Hughes *et al.*, 2014b for more details) which was not used in the study, are given below. Some of the parameters of the model (RDF, TL and CL) were set to default values for this study and are not described in detail as they do not affect the modelling results.

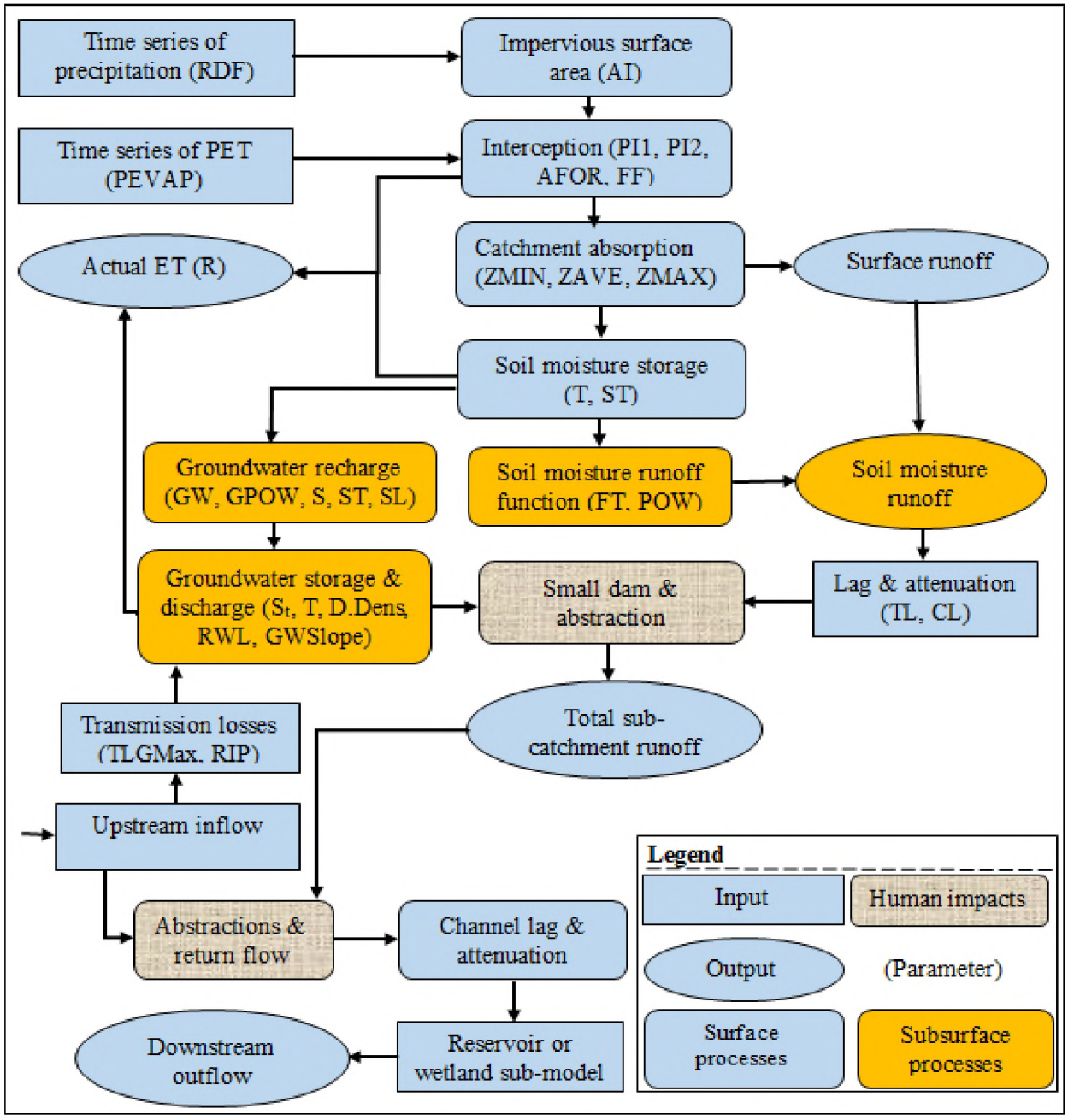

Figure 3.1: Flow diagram of the GW-PITMAN model's main structure and relevant parameters (modified from Kapangaziriwi, 2010 and Hughes, 2013).

Table 3.3: List of the parameters of the GW-PITMAN model representing hydrological processes including those of water uses (source: Hughes *et al.* 2006)

Model component	Model parameter	Parameter description	Units
Surface processes			
Precipitation	RDF	Rainfall distribution factor (default to 1.28)	[-]
Impervious area	AI	Catchment fractional area that is impervious (not used)	%
Interception	PI1 and PI2 (s and w)	Summer (s) and winter (w) interception storage for vegetation type 1 and type 2	mm
	AFOR	Catchment proportional area covered by vegetation type 2	%
	FF	The ratio of PET rate for vegetation type 2 relative to type 1	[-]
Potential ET	PEVAP	Annual catchment potential evapotranspiration	mm
Actual ET	R	Evapotranspiration-moisture storage relationship parameter	[-]
Catchment absorption	ZMIN, ZMIN and ZMAX	Minimum, mean and maximum sub-catchment absorption rate	mm month^{-1}
Sub-surface processes			
Soil moisture storage	S, ST	Relative soil moisture, maximum moisture storage capacity	mm
Soil moisture runoff	POW	Power of the moisture storage equation	[-]
	FT	Runoff from moisture storage at full capacity	mm month^{-1}
GW recharge	GW	Maximum groundwater recharge at full capacity (ST)	mm month^{-1}
	SL	Soil moisture storage below which there is no GW recharge	mm
	GPOW	Power of moisture storage-groundwater recharge equation	[-]
GW storage & discharge	T	Groundwater transmissivity	m^2 d^{-1}
	D.Dens	Drainage density of the catchment	km km^{-2}
	RWL	Groundwater rest water level	m
	GWSlope, RIP	Regional groundwater gradient, riparian strip factor	%
	S_t	Groundwater storativity	[-]
	TLGMax	Maximum channel losses to groundwater	mm month^{-1}
Flow routing and water use			
Channel routing	TL and CL	Lag of surface and soil moisture runoff and routing coefficient (TL default of 0.25 and CL not used)	months
Water use	AIRR, IRRIG	Run-of-river irrigation area, irrigation area from small dams	km^2
	EFFECT, IWR, *A & B*	Effective rainfall fraction, irrigation water return flow fraction, and parameters in non-linear dam area-volume relationship	[-]
	RUSE	Non-irrigation demand from the river	Ml year^{-1}
	DSTORE	Maximum storage capacity for all small dams in the sub-catchment	Ml
	DAREA	Proportion of catchment above dam	%
	GWA (U & L slopes)	Groundwater abstraction far from the channel (U) and near to the channel (L)	Ml year^{-1}
	CAP	Reservoir storage capacity	m^3 * 10^6
	INIT, DEAD	Reservoir magnitude at the beginning of simulation period, dead storage of the reservoir	%
	RES 1-5	5 levels of operating rules used to reduce abstraction of reduced storage	%
	ABS, COMP	Annual demand from the reservoir, annual environmental compensation flow released into the river	m^3 * 10^6

Rainfall Interception (PI1, PI2, and AFOR): The interception storage parameter (PI in mm) and the total monthly rainfall determine the depth of rainfall intercepted for a month. PI varies seasonally and accounts for two different vegetation types: dominant vegetation (PI1: type 1) and secondary vegetation (PI2: type 2) (Hughes, 2004). De Groen (2002) considers a range of 1–7 mm day^{-1} for South African conditions, when litter interception is included; however, Pitman (1973) asserts that this parameter can range between 0 and 8 mm day^{-1} in southern Africa. In practice, Hughes (2013) points out that the values for PI parameter range between 3 and 5 for a forest (type 2) while 1.5 is the approximate value for grassland (type 1). Parameter AFOR (%) represents the proportion of the catchment covered by the secondary vegetation types and is frequently used in catchments that have plantation forestry.

Evapotranspiration (PEVAP, R, and FF): The annual potential evapotranspiration (PEVAP) in the GW-PITMAN model is distributed into 12 fixed monthly mean values or time series of variations in the mean values. The actual evapotranspiration (ETa) is calculated from an assumed linear relationship (Figure 3.2) between the current monthly potential evapotranspiration value relative to the maximum monthly value.

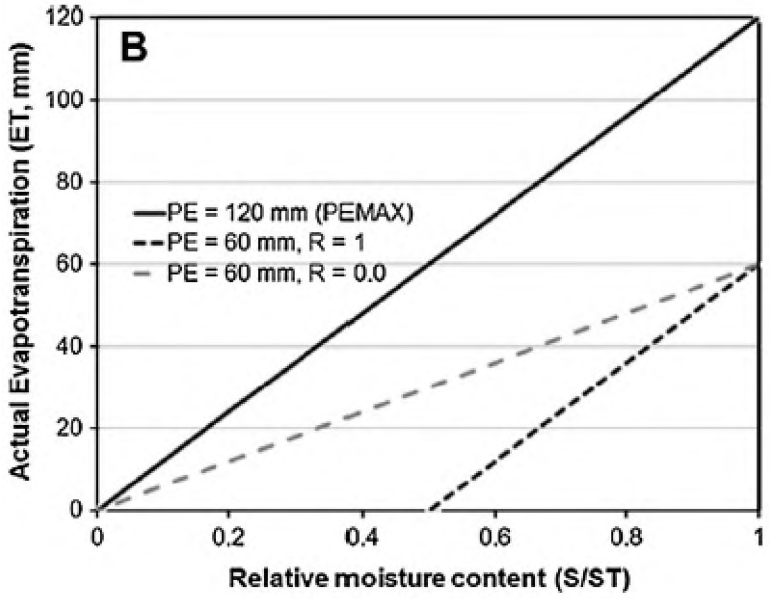

Figure 3.2: Relationship between catchment actual evapotranspiration (ETa) and relative soil moisture content (S/ST) (source: Hughes, 2013).

The model uses parameter R to define the relationship between relative soil moisture storage (S/ST), PET for the month, and the actual evapotranspiration (ETa). Parameter R ranges from 0 to 1, where a value towards 0 reflects higher ETa losses at low moisture storages, and a value towards 1 reflects generally lower ETa losses. The dominant vegetation type is a major determining factor for the value of R. R values are expected to be low for deep-rooted vegetation

and high for shallow-rooted vegetation. The model uses parameter FF as an evapotranspiration scaling factor to increase the amount of evapotranspiration for the secondary vegetation type relative to the primary vegetation type. The value of FF typically ranges between 1.0 and 1.4 where greater values imply higher evapotranspiration.

Catchment Absorption and Surface Runoff Generation (AI, ZMIN, ZAVE, and ZMAX): Catchment characteristics such as the topographical and geological setting, land cover, and soil properties (e.g. porosity, structure, and texture) determine the spatial and temporal infiltration dynamics as well as the generation of surface runoff. Surface runoff in the GW-PITMAN model is conceived as being generated from three possible functions representing hydrological processes, namely: (i) impermeable area overland flow, (ii) infiltration excess flow, and (iii) saturation-excess overland flow (Hughes, 2013). In the first process, the AI parameter represents the total impermeable area of the catchment so that all rainfall becomes runoff. This process is only applicable in predominantly urban areas or in very rocky catchments. In the second, any rainfall amount that is greater than the catchment absorption rate will contribute to surface runoff and this process is conceptualized from the *Hortonian* runoff. The catchment absorption rate is based on an asymmetric triangular distribution (Figure 3.3.A), which is defined by the ZMIN, ZAVE, and ZMAX parameters (all in mm month^{-1}), respectively. The distribution determines the frequency of the amount of rainfall that can be absorbed at different rates. The surface runoff rate (mm month^{-1}) is determined by the area under the cumulative rainfall input rate curve for each model iteration (Figure 3.3.B). The third process is discussed in the next paragraph.

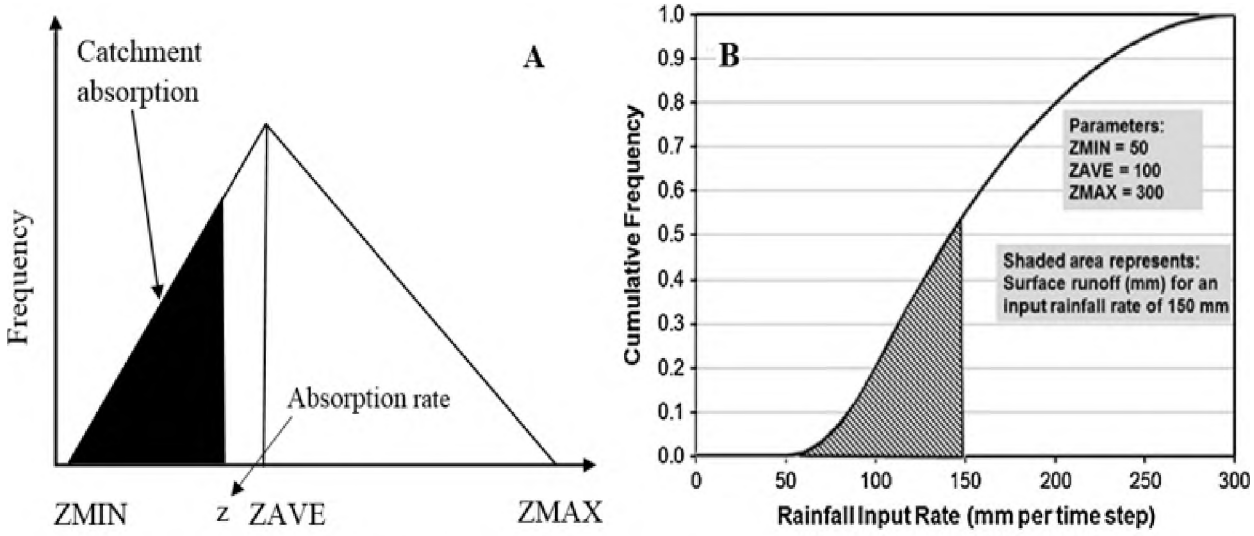

Figure 3.3: **A**: Frequency distribution of the catchment absorption rate z in mm month^{-1} (adopted from Hughes, 2004) and **B**: cumulative frequency curve of the surface runoff generation (source: Hughes, 2013).

Catchment Subsurface Storage and Runoff (FT, POW, S, and ST): In the GW-PITMAN model, infiltrating water accumulates soil moisture storage (S in mm) which is limited to a maximum value of parameter ST (mm). Evapotranspiration losses, groundwater recharge, and unsaturated zone runoff deplete the soil moisture storage. This conceptual approach is based on the assumption that infiltrating water from the unsaturated zone directly contributes to groundwater storage as recharge, some parts evaporate, and other parts generate runoff through the interflow component. If the soil moisture level (S) exceeds ST, the excess becomes saturation-excess overland flow. The FT parameter, expressed in mm month^{-1}, defines the maximum interflow runoff rate at maximum soil storage (ST) and is influenced by soil properties as well as topography (Kapangaziwiri, 2010). The depth of runoff from the soil moisture storage is determined by a non-linear relationship (Figure 3.4) between maximum interflow runoff (FT) and the current level of soil moisture storage (S). Parameter POW defines the power of this relationship.

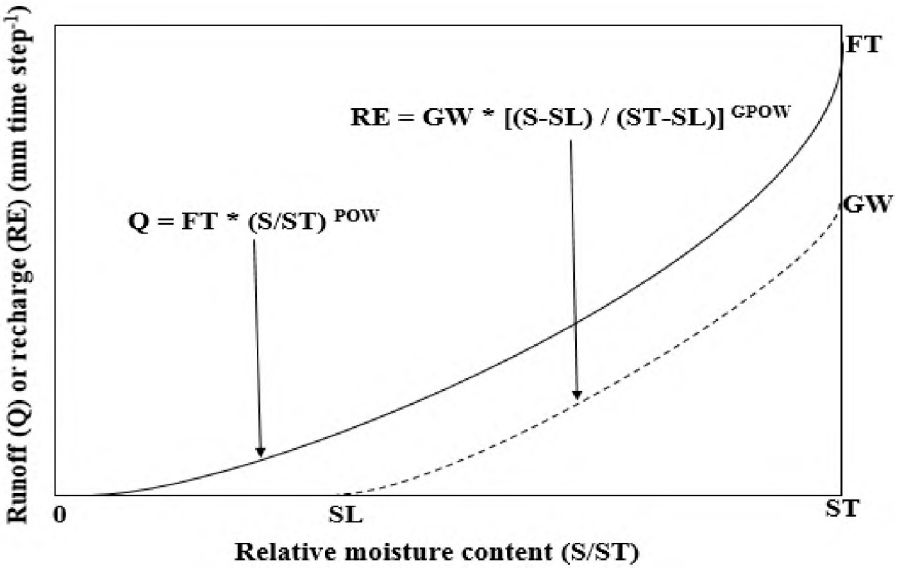

Figure 3.4: The GW-PITMAN model conceptual runoff reduction rate from soil moisture storage (modified after Hughes, 2004).

Groundwater Recharge (GPOW, GW, and SL): Hughes (2004) explicitly describes groundwater storage and discharge to the river. The GW-PITMAN model estimates groundwater recharge to the groundwater store based on the maximum monthly recharge rate, the status of the unsaturated soil moisture storage and a non-linear power function (Hughes *et al.*, 2010b). The groundwater recharge function (Figure 3.4) uses a similar non-linear relationship as the soil moisture runoff function, with GW (mm month^{-1}) representing the maximum monthly recharge rate at maximum storage (ST), SL (mm) is the soil moisture storage level at which recharge

ceases, and GPOW is the power of the relationship. SL is normally set to 0 as its influence on the simulation results is negligible (Hughes, 2004). GPOW is very similar to POW and is expected to reflect similar physical relationships. High values for GPOW (±4) would increase the non-linearity in the relationship between recharge and soil moisture storage.

Groundwater Storage and Discharge (D.Dens, GWSlope, RIP, RWL, S_t, T, and TLGMax): Topographic and geologic conditions together with land cover and soil characteristics all determine the groundwater storage fluxes and drainage properties of the catchment. The GW-PITMAN model applies a simple geometry (Figure 3.5), defined by Hughes (2004), to determine groundwater storage and discharge to the river channel. Groundwater storage is assumed to lose water through three processes, namely: (i) evapotranspiration from the channel riparian zones, (ii) discharge to the river channels, and (iii) groundwater flow to downstream catchments (see Hughes *et al.*, 2010b for more details).

The first process is based on a parameter RIP (%) which specifies the proportion of the channel riparian zones that are assumed to lose groundwater through evapotranspiration from riparian vegetation and monthly PET inputs. The second is based on the estimation of the following parameters: *transmissivity* and *storativity*, *regional groundwater drainage slope*, *rest water level*, and the *drainage density*. In the model, groundwater gradients are simulated based on the catchment water balance. *Transmissivity* (T in m^2d^{-1}), which is the product of the permeability and saturated aquifer thickness, reflects the hydraulic characteristics of geological settings, while *storativity* (S_t) is the measure of the capacity of the aquifer to store water. The *drainage density* (D.Dens. in km km^{-2}) is expressed as the ratio of the total channel length expected to receive groundwater inputs to the catchment area. This parameter can be roughly inferred from maps, satellite imagery and an appropriate understanding of the catchment characteristics. Lower drainage densities result in fewer slope elements and therefore lower rates of groundwater discharge per month. Lower values also result in smaller total sub-catchment outflow widths and therefore lower rates of downstream groundwater drainage. *Rest water level* (RWL in m) and TLGMax (mm $month^{-1}$) parameters refer to the depth of the aquifer below the channel at which groundwater ceases to flow and catchment's maximum channel losses, respectively. In the third process, the *regional groundwater gradient* parameter (GWSlope in %) refers to the gradient appropriate for estimating outflows from one sub-catchment to the next downstream. The model simulates the changes in lateral gradient with a representative hillslope (Figure 3.5), such as a positive gradient indicates drainage to the river channel whereas a negative gradient implies that water can flow from the channel to the groundwater body (Tanner and Hughes, 2013).

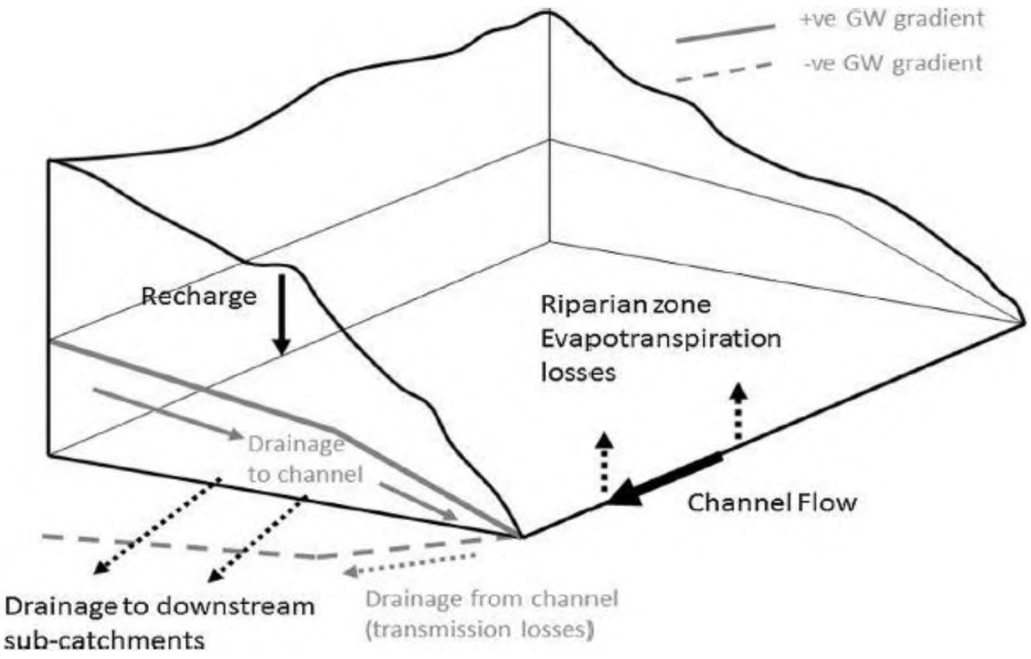

Figure 3.5: Diagrammatic geometry of the groundwater components of the GW-PITMAN model (source: Hughes, 2013).

Water Use Parameters (AIRR, DAREA, DSTORE, EFFECT, GWA, IWR, RUSE, IRRIG, *A*, and *B*): The GW-PITMAN model includes routines to represent anthropogenic impacts that influence the natural hydrology such as surface water use (run-of-river abstractions for irrigation, domestic and industrial purposes) and dams (abstractions from small farm dams and large dams), which are considered important when evaluating water resources. These routines have been applied successfully in various studies with different climatic conditions (e.g. Hughes and Mantel, 2010a, b).

Small farm dams and large dams are accounted for in the GW-PITMAN model with surface storage (and abstraction) of runoff generated within a sub-catchment and reservoir water balance routines (e.g. Hughes, 1992). Parameters DAREA (%) and DSTORE (Ml) represent the proportion of a sub-catchment contributing runoff to the dams and the combined maximum storage capacity for all the small dams within a sub-catchment, respectively. While the model has an option to include in-channel dams in the modelling application, stream flow in the main channel from upstream sub-catchments is assumed to have no contribution to the small farm dam storage (Hughes and Mantel, 2010b). The simulated runoff from the DAREA proportion is assumed to contribute to the dam storage (Hughes and Mantel, 2010a). For large reservoirs, water inflow to the storage includes simulated flows generated from all upstream sub-catchments and within the sub-catchment. The model routines use a number of abstractions and release operation rules based on current storage levels in the dam. Water losses from both small and

large dams are assumed to occur mainly through evaporation since the model does not account for seepage losses (Hughes and Mantel, 2010b). Evaporation losses are calculated at the potential rate using the water surface area of the aggregated dams derived on the bases of a non-linear power relationship (equation 3.2) of the current stored volume and surface area between the iterations of the model.

$$Surface\ Area\ (m^2) = A * volume\ (m^3)^B \quad (3.2)$$

Parameters A and B are regional constants that represent surface area-volume relationship of the dam. Parameters AIRR and IRRIG, both in km^2, together with RUSE and GWA (U and L), also in Ml $year^{-1}$, represent the total irrigation area irrigated from run-of-river abstractions, small farm dam's abstraction, and the annual volume of non-irrigation demand from the river, groundwater abstraction far from the channels (U) and near to the channel (L), respectively. All these parameters are applied with a table of fixed monthly distribution of demands that are quantified to match the known or the assumed patterns of abstraction from dams, streams or boreholes (Hughes and Mantel, 2010b). The effective rainfall parameter (EFFECT), expressed as a fraction, refers to the proportion of monthly rainfall which satisfies irrigation demand, whereas parameter IWR (fraction) represents irrigation water return flow.

3.2.3. Data Requirements for the Pitman Model

Three categories of data are required for the Pitman model: (i) model input data, (ii) catchment parameter data, and (iii) model calibration data. In this study, the model input data include rainfall and potential evapotranspiration (PET). The model uses a time series of catchment average rainfall and PET data to force the hydrological processes represented in the model. The PET data can take two forms in the model: (a) fixed mean monthly evaporation distributions of mean annual evaporation (MAE), or (b) time series of fractions that modify the monthly average values for each month of the simulated time series. In a semi-distributed modelling approach, catchment-modelling units are delineated so that the model can simulate hydrological processes in one catchment at a time. For model calibration, time series data of observed stream flow are normally used. Furthermore, if hydrological response data from other sources are available (e.g. soil moisture, groundwater recharge or actual evapotranspiration), they can be used to calibrate the other parts of the model.

3.2.4. Versions of the Pitman Model

There are several versions of the Pitman model. These range from the original model (Pitman, 1973) to later versions (Hughes, 2004; Hughes *et al.*, 2013, 2014a), which have incorporated several components and parameters to improve the functionality of the model. This study applied the GW-PITMAN model (Hughes, 2004) which has several versions within the SPATSIM framework: a single-run version and the uncertainty versions.

Single-run Version

In this version, a single parameter set for each sub-catchment is manually calibrated using the guidelines provided by Hughes *et al.* (2006) and Kapangaziwiri (2010). After populating the model parameters, the model is run and various subjective and objective measures can be used to evaluate the performance of the model. If the simulation results are not satisfactory, the parameters are adjusted and the model is re-run. This process is repeated until the model performance measures are considered satisfactory from a modeller's perspective and modelling objectives. Although this process is somewhat subjective, it is much more effective in exploring and accounting for the equifinality problems during calibration (Tshimanga and Hughes, 2014).

The initial and final modelling step of this study applied the single-run version of the Pitman model to quantify parameter sets that can sensibly represent the hydrological behaviour of the selected catchments. A detailed explanation of the calibration of individual parameters for different modelling steps is given in section 3.4.1.

Uncertainty Versions

The uncertainty versions of the Pitman model (Hughes, 2013; Hughes *et al.*, 2014a) use a simple independent Monte Carlo sampling of the *a priori* parameter space to generate (typically 10 000) ensembles of model parameter sets and simulation results. The inputs of the uncertainty version include the values of the mean (μ), standard deviation (σ), dependency index, minimum and maximum, as well as the assumed uncertainty distribution type for all uncertain parameters. For each run of the model, a parameter set is sampled from the uncertain parameter space that can be defined by normal, log-normal or uniform distributions (Figure 3.6). The dependency index value is used to assign a group of sub-catchments that are assumed to have both similar hydrological responses and direction of uncertainty.

When applying the uncertainty version of the GW-PITMAN model, the generated ensembles of simulated flows are saved as time series in the SPATSIM database, whereas additional model outputs are saved to two separate text files with extensions of .un1 and .un2. The former consists of (for each of the ensembles) the list of sampled parameter values, the simulated monthly flow volume, the simulated mean monthly groundwater recharge, the slope of the FDCs, the 10^{th}, 50^{th} and 90^{th} percentiles of the annual FDCs, and five objective functions based on comparison between the simulated flows and the observed flows or reference time series data. The latter contains the 5^{th}, 50^{th} and 90^{th} percentiles of the simulated monthly flows for each month, and the time series of the observed stream flow data or reference data for the simulation period (Hughes *et al.*, 2010a). The calculated percentiles are simply the bounds around the ensemble outputs and determine the range of output uncertainty.

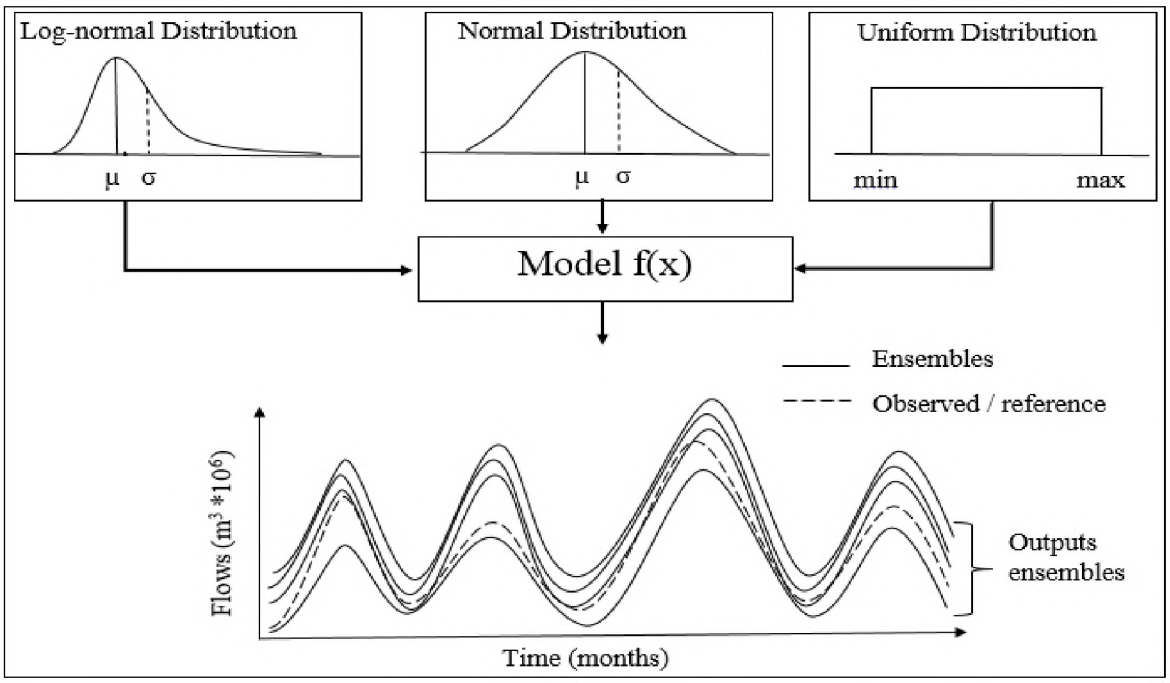

Figure 3.6: Schematic diagram of the uncertainty version of the GW-PITMAN model (modified after Kapangaziwiri, 2010).

This study applied the structured uncertainty version of the GW-PITMAN model, which was developed to ensure that independent sampling of the value for each parameter, and each sub-catchment does not cancel out the variability in the downstream ensemble simulations. After generating the ensembles of model results, a post-processing filtering is applied to select the ensembles that are capable of representing the known hydrological response regimes of the catchment being modelled, using subjectively defined thresholds of the calculated objective functions (Kapangaziwiri *et al.*, 2012). The thresholds that determine which ensembles can be

considered behavioural are based on the set of defined objective functions that are also used to evaluate the performance of the model (Beven, 2006). If the values of the objective functions for a particular ensemble exceed (or are less than) defined thresholds, they are considered non-behavioural (Uhlenbrook and Sieber, 2005).

The criteria used to select behavioural ensembles included the use of four objective functions based on their acceptable ranges. These objective functions are the Nash-Sutcliffe coefficient of efficiency (*CE*) and the relative percent bias of mean monthly flows (*%BIAS)*, both based on untransformed and natural log-transformed values (*CE {ln}* and *%BIAS {ln}*). Moriasi *et al.* (2007) recommended the use of these objective functions as they are easy to understand and powerful in many hydrological applications.

While it is possible to analyse the contents of the uncertainty simulations (.un1 file) in the GW-PITMAN model using the regional sensitivity analysis software or in an excel spreadsheet, the latter approach, which is similar to that used by Hughes (2015), is as follows:

(i) Sort the ensembles based on *%BIAS* and select those less than ±10%.

(ii) Sort the previously selected ensembles using *%BIAS {ln}* and select those less than ±10%.

(iii) Sort the previously selected ensembles using the *CE* value and identify the best ensemble using all four objective functions. In the cases where the model performance did not meet the desired threshold (*CE* and *CE {ln}* > 0.5), behavioural ensembles were selected based on the 'best" combination using the four objective functions.

(iv) Select all behavioural ensembles based on all four objective functions identified from (i) to (iii).

To combine the effects of all four objective functions a best-fit index (equation 3.3) was used to identify the behavioural ensembles based on the best combination of the objective functions. Higher values of this index relates to the best combination of the objective functions used. The 'best' ensembles can be further assessed by comparing them with observed data using flow duration curves, monthly distributions, and time series.

$$Best\ Fit\ Index = (CE + CE\ (ln)) + \left[\frac{1}{\{Abs(\%bias) + Abs(\%bias\ \{ln\})\}}\right] \quad (3.3)$$

3.2.5. Setting up the Pitman Model

The GW-PITMAN model for the selected catchments (see Chapter 4) was set up in the SPATSIM software, and the steps that were followed include the creation of necessary features by loading shapefiles of all catchment polygons, rain and stream flow gauging station points, and river polylines. Table 3.4 lists the attribute data that were used in setting up both the single-run version and the uncertainty version of the model.

Table 3.4: List of attribute data required for setting up of the GW-PITMAN in the SPATSIM interface

Attribute type	Attribute name	Description
Text	Catchment ID	Identifies quaternary catchment number
	Downstream area	Identifies the links of the quaternary catchments
Single real number	Catchment area	Quantifies the catchment area [1]
	Catchment accumulated area	Catchment cumulative area [1]
1-D Array	Model parameters	Represents parameters of the single-run GW-PITMAN model [2]
	WR2005 mean monthly evaporation	Represents mean monthly distribution percentage of potential evapotranspiration data based on WR2005 pan data [-]
	MOD16 mean monthly evapotranspiration	Represents mean monthly distribution percentage of potential evapotranspiration data based on MOD16 PET [-]
	Reservoir model parameters	Represents the parameters of the reservoir model [2]
2-D Array	Uncertainty parameters	Represents uncertain parameters of the GW-PITMAN model [2]
	Monthly water use distributions	Represents monthly distribution percentage of water use [-]
	Reservoir monthly distributions	Represents monthly reservoir water use data [-]
Time series	Catchment average rainfall	Represents the catchment average rainfall [3]
	Observed monthly flow	Represents stream flow volume at the catchment outlet [4]
	Simulated flow	Represents simulated stream flow volume [4]
	MOD16 PET	Represents a time series of PET fractions [-]
	MODIS simulated	Represents simulated stream flow using MODIS PET data [4]
	Ensembles outputs	Represents the simulated ensembles of the model [-]
	MODIS monthly ETa data	Represents MODIS ETa estimates

Key: 1 – km^2; **2** – units in Table 3.3; **3** – mm; **4** – ($m^3 * 10^6$)

3.3. MODIS SATELLITE DATA

3.3.1. Description of MODIS Satellite

The MODerate Resolution Imaging Spectrometer (MODIS) is a passive imaging spectrometer carrying 490 sensors that are arranged in 36 spectral bands, which cover the visible and the infrared bands of the electromagnetic spectrum (Parkinson and Greenstone, 2000). These sensors operate on board the NASA Earth Observing System (EOS) platforms, the Terra and Aqua

satellites that have been orbiting around the Earth since their launch in December 1999 and May 2002, respectively (NASA, 2006). These satellites orbit the earth diagonally in the opposite direction: the Terra satellite orbits from north to south and crosses the equator in the morning, whereas the Aqua satellite orbits from south to north, crossing the equator in the afternoon. The original objectives of MODIS were to capture and provide a comprehensive series of global observations of terrestrial data (Terra satellite) and ocean data (Aqua satellite). These sensors provide data at three different spatial resolutions: 250 m (band 1, 2), 500 m (bands 3 – 7) and 1 000 m (bands 8 – 36), covering a swath dimension of 2 330 km (cross track) x 10° of latitude (along the track) (Barnes *et al.*, 1998). The provision of large spatial and temporal resolution data is an improvement of the MODIS' predecessor, the AVHRR, and it surpasses its orbital neighbour Landsat 7 (MRT, 2011). MODIS observations are important for studies on climate, vegetation, earth sciences, and many other environmental related disciplines. Parkinson and Greenstone (2000) provide detailed technical specifications of the MODIS satellites and for other EOS data. For this particular study, MOD16 PET and ETa were used.

3.3.2. Description of the MOD16 Algorithm

The MODIS global ET algorithm (MOD16) is one of NASA's EOS projects that is hosted by the Numeric Terradynamic Simulation Group (NTSG) aimed at estimating global ETa, PET, latent heat flux (LE), and potential latent heat flux (LET), using remote sensing data from MODIS and meteorological data for hydrological and ecological applications. Mu *et al.* (2011) undertook the MOD16 project as an updated version of the old algorithm conceptualized by Mu *et al.* (2007a) and developed by Cleugh *et al.* (2007). The MOD16 algorithm is based on the Penman-Monteith approach (Monteith, 1965, 1981) and is defined by equation 2.3 given in section 2.4.1.2. Allen *et al.* (2011b) have recommended the Penman-Monteith equation for its reliability in the estimation of evapotranspiration. Figure 3.7 provides a flowchart of the data used to develop the MOD16 algorithm. A detailed description of the algorithm's development is not provided in the present study but is given by Mu *et al.* (2007a, 2011). This study provides only a description of the remote sensing data and meteorological input data used in the MOD16 algorithm development.

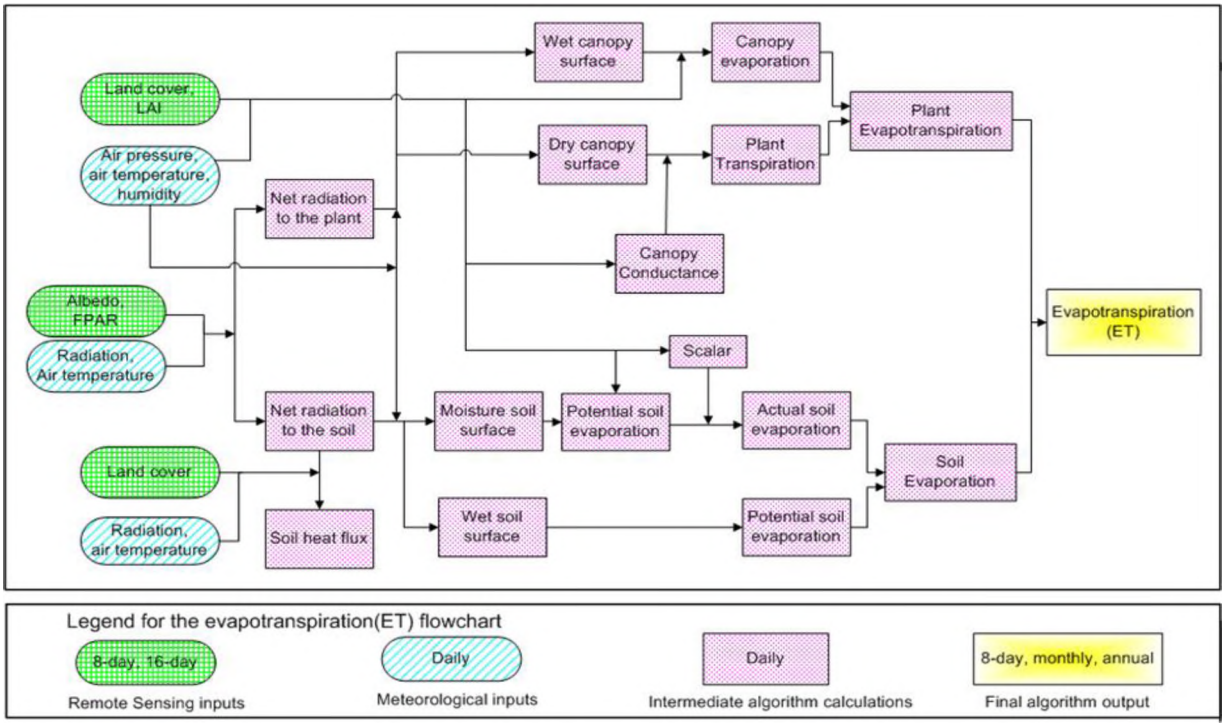

Figure 3.7: Data flowchart used in the development of the improved MOD16 algorithm (source: Mu *et al.*, 2011).

Remote Sensing Input Data

The MOD16 ET product uses remotely sensed land surface data inputs derived from three MODIS products at a spatial resolution of 500–1 000 m. These products are:

(i) Land use and land cover classification data (MOD12Q1 Collection 4) processed by Friedl *et al.* (2002).

(ii) Leaf Area index (LAI) and Fraction of Photosynthetically Active Radiation absorbed by vegetation (FPAR) referred to as MOD15A2 Collection 5 product processed by Myneni *et al.* (2002).

(iii) Surface Albedo (MCD43B2/B3 Collection 5), which was initially processed by Lucht *et al.* (2000) and was further improved by Schaaf *et al.* (2002).

The Mu et al. (2011) version has incorporated the following components: (i) revised land use and land cover data, (ii) estimating LE as the sum of day-time and night-time components, (iii) improving the calculation of aerodynamics, boundary-layer and canopy resistance, (iv) estimating the soil heat flux using available energy and simplified NDVI, (v) dividing the vegetation canopy into wet and dry components, and (vi) separating moist soil surfaces from saturated wet ones.

Meteorological Input Data

The Global Modelling and Assimilation Office (GMAO) processes global meteorological data at a global scale that are made available to the public. The MOD16 ET data products created using the GMAO data consist of daily incoming radiation, day-time and night-time air temperature, daily average temperature, daily minimum and maximum air temperature, and vapour pressure (GMAO, 2004). All these variables were used in the development of the MOD16 ET product. It must be noted that these data are at a spatial resolution of 1.00° x 1.25° and they were interpolated to 1 km^2 spatial resolution to fit the spectral scale of the MODIS products' pixels. Prior to the publication of the MOD16 ET product, GMAO (2004) indicated that the spectral differences between GMAO meteorological data and that of MODIS pixels are likely to introduce inconsistencies in the scales used. Furthermore, the GMAO stressed that cloud cover contaminated the FPAR and LAI data during the data acquisition periods and they concluded that this condition could introduce considerable errors into the other products derived from these data, such as the MOD16 ET product.

The availability of the observation data, at local scales, of the above-listed variables could be used to improve the potential errors that result from scale issues. In South Africa for example, Jovanovic *et al.* (2012) used historical *in situ* ETa measurement data from Eddy covariance, Bowen ratio, and Scintillometer equipment in attempts to evaluate the MOD16 ETa data. In their study, they discovered that, in most catchments, MOD16 ETa data were under-estimated. However, similarities were observed when measured ET values are low. The authors concluded that these differences could have resulted from the uncertainties in the algorithms, assumptions, procedures, input data, measurement techniques, different sampling areas, and scaling. Ramoelo *et al.* (2014) attempted to validate the 1 km^2 pixel of the 8-day MOD16 ETa data using the ETa estimates derived from Eddy covariance towers over two areas covered with Savannah and woodland biome. They found that there were discrepancies between MOD16 ETa and flux tower ETa, which could have resulted from flux tower measurement-errors, input data to the Penman-Monteith equation and the fact that the input data to the MOD16 ET product are not validated in semi-arid conditions like South Africa, which are likely to generate significant estimation errors. Therefore, the use of available land cover, LAI and NDVI data, at large spatial scales, could be used to further improve the MOD16 ETa algorithm particularly in semi-arid regions where ET are vital in water resources evaluation.

3.3.3. Description of the MOD16 ET Product

The MOD16 ET products are archived and distributed in Hierarchical Data Format for Earth Observing System (HDF-EOS), tiled in grids of 10° x 10° and are computed at temporal resolutions of 8-days, monthly, and annually. The MOD16 tiles are labelled horizontally from left to right and vertically from top to bottom, starting at position 00. The MOD16 tile data are represented by horizontal (h) and vertical (v) position of the Sinusoidal projection grids. They range from position h00 to h35 (horizontally) and v00 to v17 (vertically) respectively. The selected MOD16 tiles are mapped on a Sinusoidal projection system and each tile has 1 200 horizontal and 1 200 vertical pixels fitted in one grid as shown in Figure 3.8. These pixels store the actual values of average ETa, PET, LE, and PEL that represent an area equivalent to 1 km^2 (NASA, 2012).

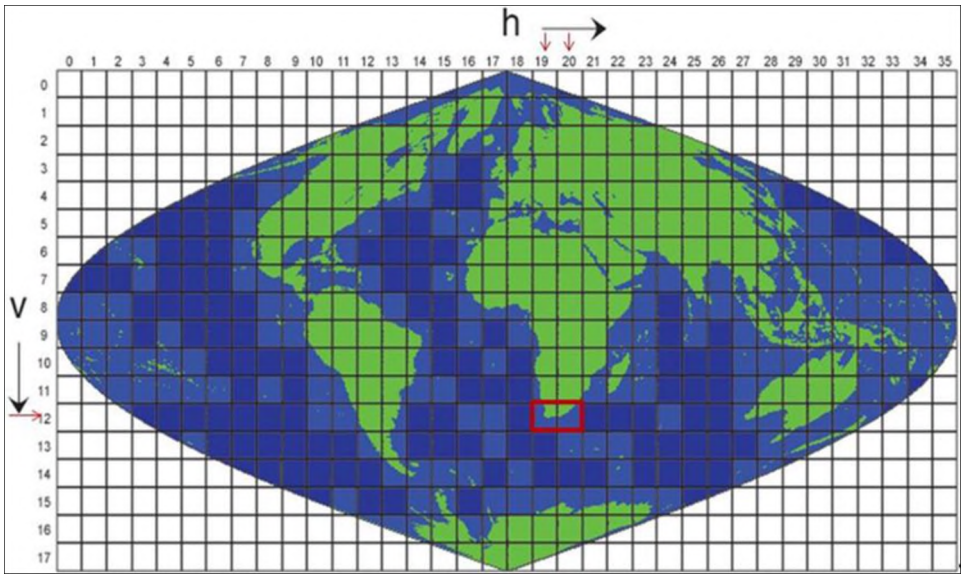

Figure 3.8: MOD16 selected tiles mapped in the Sinusoidal grid (source: MRT, 2011).

NASA formulated the naming standards for their products to simplify the retrieval and identification of tile data files. File naming consists of fields specifying the product name, acquisition date, a position of the tile, data product collection, production date, and file type. Hence, the MOD16 ET products follow a naming convention that provides useful information regarding the specific product, and this naming convention played an important role in the pre-processing of the data used in this study. An example of the MOD16 tile file is given below:

MOD16 8-day tile:

A generic file name is given as MOD16A1.A2000001.h19v12.005.2006012234657.hdf

where: *MOD16A1 - Product short name.
*A2000001 - Julian date of acquisition (A-YYYYDDD).
*h19v12 - Tile location on the Sinusoidal grid.
*005 - Collection version.
*2000012234567 - Julian date of production (YYYYDDDHHMMSS).
*hdf - Data format file extension (HDF-EOS).

MOD16 monthly tile:

A generic file name is given as MOD16A2.A2010M01.h19v12.105.2011050081458.hdf

where: *MOD16A1 - Product short name.
*A2010M01 - Julian date of acquisition (A-YYYYMM).
*h19v12 - Tile location on the Sinusoidal grid.
*105 - Collection version.
*2011050081458 - Julian date of production (YYYYDDDHHMMSS).
*hdf - Data format file extension (HDF-EOS).

3.3.4. The Acquisition and Preparation of the MOD16 ET Product

The Numeric Terradynamic Simulation Group (NTSG) at the University of Montana hosts MOD16 ET data, which are freely accessible and downloadable from http://www.ntsg.umt.edu/project/mod16#data-product. The study used the monthly MOD16 data. The MOD16 monthly tile data were downloaded for a period of 11 years, starting from 2000. Five hundred and six (506) tiles, in *hdf format, were downloaded and saved for further processing.

The HDFView version 2.8, a free-source Java-based software, developed by the HDF Group was downloaded from http://www.hdfgroup.org/downloads/index.html to transform MOD16 ET data to ESRI GIS interpretable format and convert the data from *hdf format to *txt file format. Appendix 1 provides a detailed step-by-step method used to (i) import MOD16 into HDFView, (ii) selection of pixels of interest within the selected catchments, (iii) the determination of pixel position in relation to the MOD16 tile, and (iv) the compilation of a text file required in the application of the software. Additional software was developed by David Forsyth at the Institute for Water Research (IWR) to facilitate the generation of single pixel or catchment average data into a data format suitable for use with the Pitman model. The software is also capable of excluding non-vegetated pixels, mainly corresponding to open water-bodies, permanent wetland, and urban areas. Since one of the focus areas of this study is on using time series deviations from the mean based on MOD16 data rather than the actual values of potential evapotranspiration, the MOD16 PET data were processed further to derive the time series of deviations. Evapotranspiration demand time series in the Pitman model are based on fractional deviations from the long-term monthly means.

3.4. GENERAL MODELLING METHODOLOGIES OF THE STUDY

The main objectives of this study were to reduce input data uncertainty from evapotranspiration demands and to constrain model parameters with remote sensing (ETa) data in a South African context. The modelling procedures followed in this study are presented in a schematic flowchart shown in Figure 3.9 and are outlined below whereas detailed explanations of these procedures are given in the next subsection.

(i) Initial calibration of the GW-PITMAN model under natural hydrological conditions involved trial runs of the single-run version to establish the 'mean' of parameter values considered likely to represent hydrological response for each sub-catchment, using the pan-based mean monthly evapotranspiration estimates. The calibrated parameters were validated using a split sample test, which were all evaluated with naturalised flow data.

(ii) Further investigate appropriate parameter sets with the uncertainty version of the GW-PITMAN model under natural conditions to establish behavioural parameter sets. The mean, minimum and maximum values of the uncertain parameter distributions will be informed by the initial calibration in step (i).

(iii) Use the behavioural parameters from step (ii) to simulate present-day hydrological conditions using the uncertainty version of the Pitman model and further evaluate the model performance using observed flow data. The present-day simulations include the impacts of water uses.

(iv) Applying time series variations of monthly mean derived from MOD16 PET data to distribute pan-based PEVAP and MOD16-based mean annual PEVAP to drive the Pitman model processes. Evaluate the performance of the model by comparing these simulations to those obtained from step (iii) as well as an analysis of parameter sensibility.

(v) Apply time series based on the mean annual of MOD16 PET data to re-calibrate model parameters and evaluate the performance using the uncertainty of the model.

(vi) Constrain the model-simulated ETa using MOD16 ETa time series in the single-run version, using the best ensemble obtained in step (iv) and evaluate the performance of the model as well as identifying sensitive model parameters. This step also included the evaluation of the potential sources of input data uncertainties from MOD16 ETa data through the computation of the annual water balance of the selected catchments.

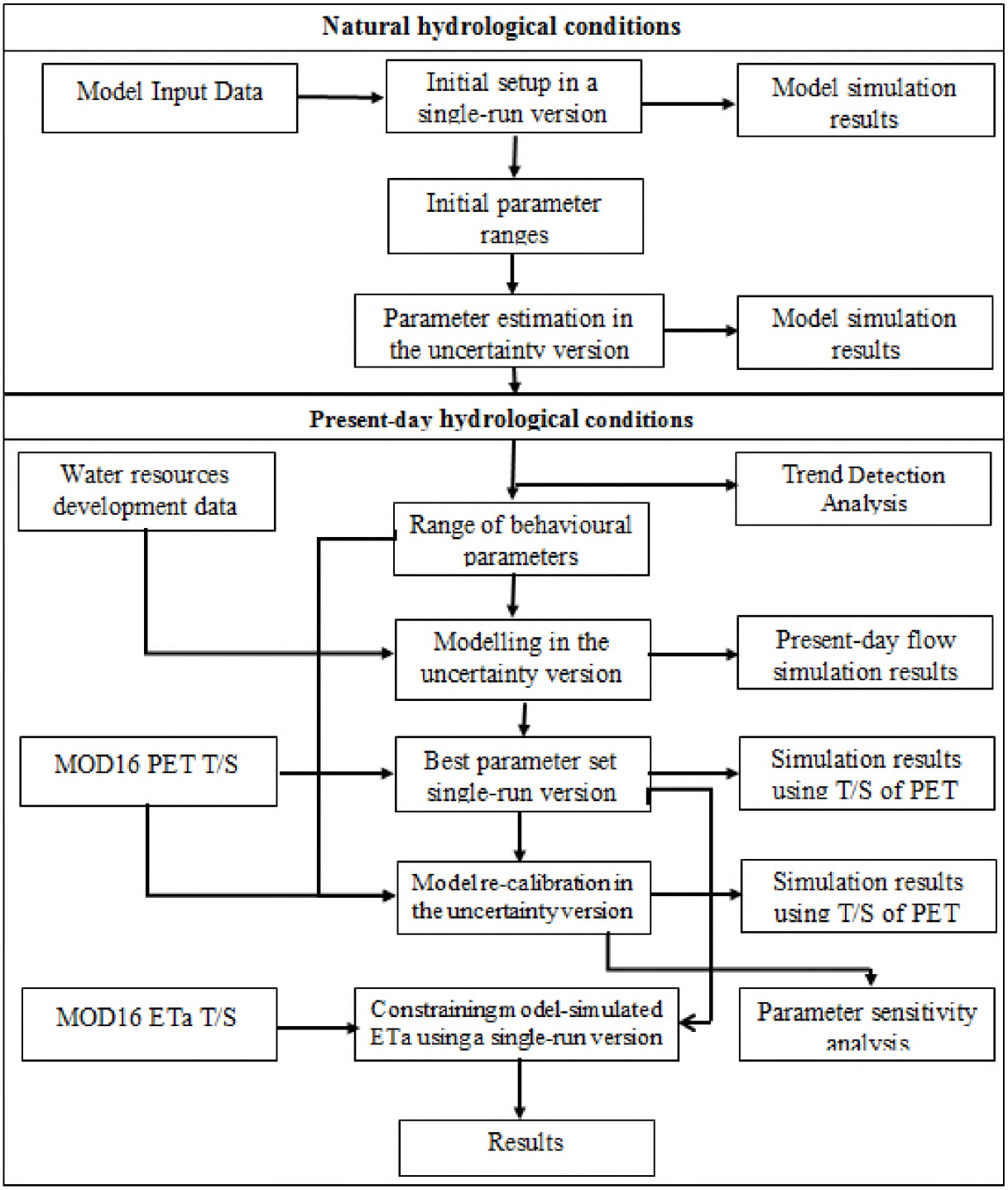

Figure 3.9: Schematic flowchart showing the modelling procedures followed in the study.

3.4.1. Initial Calibration of the Pitman Model

Because some of the model parameters were regionally established from the WR2005 study, excluding groundwater parameters of the uncertainty version, the initial focus was on the development of a conceptual understanding of the dominant hydrological processes, as recommended by Hughes *et al.* (2010a). Model parameters representing evapotranspiration

losses (R, RIP), interflow runoff (FT and POW), surface runoff (ZMIN, ZAVE and ZMAX), unsaturated soil moisture storage (ST), and groundwater recharge and losses to ground water (GW and GPOW: TLGMax) processes were calibrated against naturalised flows. The values of the parameters that influence groundwater storage and discharge (D.Dens, GWSlope, RWL, S_t, and T) were not calibrated, but estimated from available information from the GRAII database (DWAF, 2005b). The other parameters (AFOR, AI, FF, PI1, PI2, TC, TL, and RDF) remained fixed to specific values throughout this calibration step because they were considered less uncertain. The physical interpretations of the Pitman model parameters listed in Table 3.5 were used to guide the calibration process. The table identifies how hydrological process understanding and the calibration of model parameters are linked in relation to simulating a system's response.

The calibration of model parameters started in the headwater sub-catchments and progressed downstream. This calibration step was aimed at establishing feasible model parameters suitable for simulating the natural hydrological response, i.e. calibration against the naturalised flows of individual sub-catchments. The physical interpretations of the Pitman model parameters listed in Table 3.5 were used to guide the calibration process.

Table 3.5: Catchment physical interpretations that guide the calibration of the main model parameters

Parameters	Parameter Range	Influences	Description
ZMIN	Large differences	Soil properties variations	Large variation in soil properties
ZMAX	High values	Soil types, vegetation and geology	Coarse textured soils
	Low values		Fine textured soils and arid catchments
POW	High values	Soil moisture storage	Dry to ephemeral basins with little or no interflow
	Low values		Wet mountainous basins dominated by interflow
GPOW	High values	Groundwater recharge	Semi-arid regions with episodic recharge
	Low values		Wet basins with recharge throughout the year
ST	High values	Soil moisture holding capacity	Deep and well-drained soils
	Low values		Thin soils
FT	High values	Catchment slopes and soil properties	Wet basins with steeper gradients where base flow is generated from high relief areas
	Low values		Semi-arid regions with gentle gradients where there is no interflow
GW	High values	Underlying aquifer, soil moisture	Well fractured, coarse textured soils
	Low values		Fine textured soils
R	High values	Evapotranspiration	Sparse vegetation with show roots
	Low values		Dense vegetation with deep roots

3.4.2. Calibration Under Natural Conditions Using the Uncertain Conditions

The established parameters from the single-runs (section 3.5.1) were used to define the 'acceptable' parameter sampling space (based on quantifying the minimum and maximum values of a uniform sampling distribution) in the uncertainty version of the GW-PITMAN. In this modelling step, parameters considered uncertain were restricted to FT, GW, GPOW, POW, RIP, ST, ZMIN, and ZMAX, whereas FF, PI1, PI2, RDF, and groundwater flow parameters were fixed at specific values throughout the calibration step. The uncertainty version of the model was run to simulate the incremental flows for individual sub-catchments and to identify behavioural parameter sets from the 10 000 ensembles using Monte Carlo sampling approach explained in section 3.2.4.

3.4.3. Present-day Flow Simulations

This modelling step involved the running of the uncertainty model with the inclusion of water use impacts (small and large dams, run-of-river abstractions, forest plantations) and the same natural flow parameter bounds as used in the previous step. However, for the catchments that were considered to have negligible impacts, upstream water uses were not included. Their degree of uncertainty was subjectively determined by the confidence in the sources of water use data and their estimation methods. Stream flow simulations were compared with the observed data and the model results were evaluated together with the analysis of the calibrated parameters. Furthermore, the behavioural ensembles together with the 'best' parameter sets were identified using the methods provided in section 3.2.4.

3.4.4. Evaluating the Impact of using MOD16 Potential Evapotranspiration

As already noted, the Pitman model uses fixed seasonal distributions of long-term monthly mean, which are expressed as a percentage of mean annual evapotranspiration or monthly time series of evapotranspiration estimates, expressed as fractions (deviations) of the mean monthly values. The time series deviations were based on MOD16 PET estimates. Figure 3.10 shows a typical example of the variations in PET data resulting from fixed seasonal distributions and MOD16 time series.

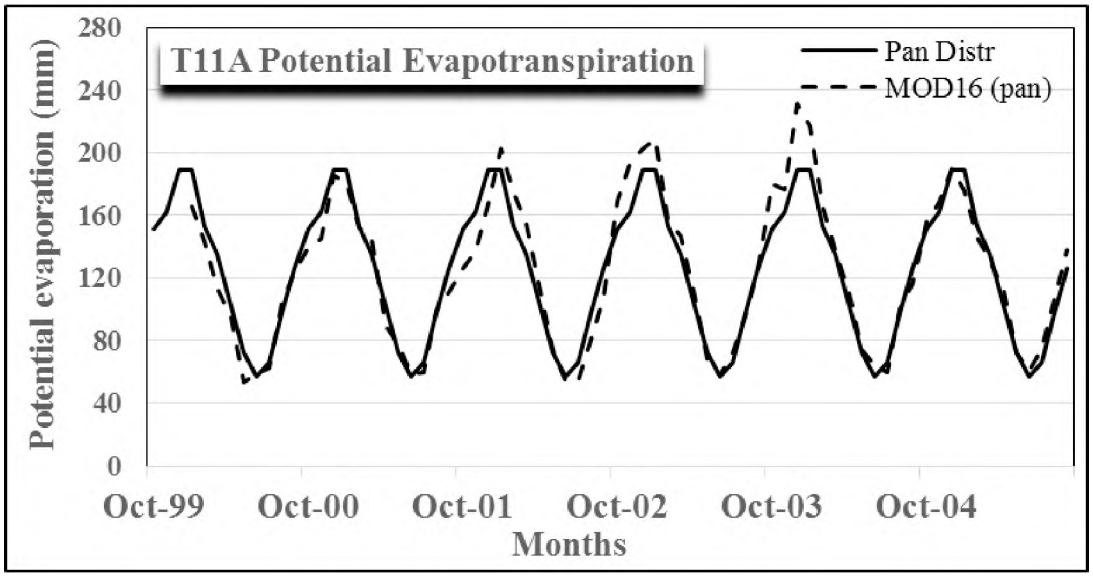

Figure 3.10: Monthly potential evapotranspiration demands derived from using fixed monthly distributions for T11A sub-catchment.

The sensitivity of the model to the use of different forms of potential evapotranspiration inputs was evaluated based on the approach defined by Andréassian *et al.* (2004) which has two modelling steps: static and dynamic.

Static Sensitivity Analysis: The 'best' model parameter sets from the calibration step (section 3.5.2) were used to evaluate model sensitivity to MOD16-based PET inputs without any further re-calibration. Sensitivity analysis was assessed by comparing model performance of the flows simulated with the reference PET (expressed as Mean {Pan}) with those simulated with different forms of PET inputs. The procedure involved expressing the monthly MOD16 PET values as deviations of long-term mean monthly values from both A-pan and MOD16 data for each calendar year. The modelling procedures were applied as follows:

(i) Apply time series deviations to distribute mean annual PEVAP referred to as T/S (Pan), and

(ii) Apply time series deviations to distribute MOD16-based mean annual potential evapotranspiration derived from the data covering the period 2000 - 2010. These data are referred to as T/S (MOD16).

Model simulations obtained with the use of Mean (Pan) data were used as the basis for comparison.

Dynamic Sensitivity Analysis: Model sensitivity was evaluated in a similar manner to that of the static analysis, however, with the re-calibrated set of parameters. Because of the adaptive capacity of the models, the re-calibration of the parameters allows the model to be influenced by the change of climatic inputs particularly for the parameters affected by the evapotranspiration demands (Vázquez and Feyen, 2003). In this study, this approach was used to evaluate the effects of calibrating the Pitman model using both T/S (Pan and MOD16) inputs compared to the traditional Mean (Pan), using the uncertainty version. The modelling involved the selection of the 'best' parameter sets (for both T/S {Pan} and T/S {MOD16} simulations), comparing their model performance statistics as well as evaluating the variation in the behavioural parameter sets, particularly those affecting evapotranspiration losses in the model.

3.4.5. Constraining Model Simulated Actual Evapotranspiration Procedure

Multi-calibration methods or multiple system responses for calibration methods are effective in constraining model parameters to produce more realistic parameter sets when observations of at least one hydrologic variable other than stream flow are available (Gharari *et al.*, 2013b; Gao *et al.*, 2014). These methods have also shown that the parameter sets from constrained calibration achieve improved simulation of the systems response for the right reasons. Imposing constraints on model parameters ensures that that the internal dynamics of the model are realistic and that the approximation of the feasible parameter space is improved (Hrachowitz *et al.*, 2013b; van Emmerik *et al.*, 2015). Because of the lack of information regarding the relationship between parameters of a hydrological system process that correspond to the actual heterogeneous process in the catchment, process constraints could also provide insights into how the real system can be expected to behave (Gharari *et al.*, 2014).

One of the objectives of this study was to identify parameter sets that simultaneously produce reasonable system response when constraining model-simulated ETa with MOD16-based ETa estimates. The modelling conducted in this step involved the use of the 'best' parameter set (from section 3.5.2), in the single-run version of the Pitman model, to simulate flows and simultaneously get the 'best-fit' between the MOD16 ETa time series data and model-simulated ETa. The number of parameters that had to be calibrated in this modelling step was intentionally decreased to minimise equifinality (Savenije, 2001) and the focus was mainly on those that impact on changes in actual evapotranspiration. The model was calibrated such that the simulated ETa was within the MOD16 ETa range as well as making sure that the simulated stream flows remain sensible.

3.5. CONCLUSION

This chapter has provided a summary of the modelling data and various methods used in the hydrological modelling conducted in this study. Model data preparation encompasses preparation of rainfall time-series data, provision of the description of MODIS satellite, the development of the MOD16 ET data extraction algorithm and the processing of MOD16 ET data as well as the estimation of water resource developments. A brief description of the Pitman model was given together with the various key hydrological modelling approaches used, as well as the model performance measures. The following chapter provides and explains the criteria used to select the catchment areas and briefly describes the locality, hydrological, climatological and geological setting of the catchments as well as other LULC features that influence hydrological processes understanding used in the parameter estimation.

CHAPTER FOUR

4. STUDY AREA

4.1. INTRODUCTION

This chapter presents a summarised description of the selected catchments in relation to a hydrological understanding of these areas. South Africa is a relatively dry country that experiences substantial inter- and intra-annual climate variability in different parts of the country (Dye and Croke, 2003). Evapotranspiration and rainfall are among the notable climatological variables that have relatively large variability. The dry parts of the country experience high evapotranspiration as compared to the wet parts. This is also the case for rainfall spatial and temporal distribution where different parts of the country receive rainfall in different seasons of the year (Schulze and Maharaj, 2004). Most of the eastern parts of the country experience summer rainfall, while the western parts, especially the coastal areas, are winter rainfall areas. The southern parts of the Eastern Cape are located in a transitional zone and experience rainfall throughout the year (Schulze, 1997). Given this rainfall variability and the different inter-climatic conditions, the dynamics of hydrological process differ from one climatic region to another and could result in differences in the performances of rainfall-runoff models. The catchment locality and physiographic setting determine the hydrological characteristics that are responsible for the dominant hydrometeorological events that drive the processes of a hydrological system. Therefore, the selection criteria for this study have included catchments in: (i) the different rainfall regions of South Africa, (ii) areas with different climatic conditions, and (iii) with different vegetation cover.

Within South Africa, water resources assessments are typically conducted in water management units called quaternary catchments. In South Africa and the trans-boundary countries of Lesotho and Swaziland, Midgley *et al.* (1994) demarcated 1 946 quaternary catchment management units that are nested within primary, secondary, and tertiary drainage basins. Using the selection criteria listed above, headwater quaternary catchments were selected. Figure 4.1 and 4.2 shows the geographic and climatic zone location of the selected catchments. Figure 4.3 shows average monthly rainfall and potential evapotranspiration for the selected catchments used in this study. A general overview of catchment locality, climatological and physiographic conditions, generalised geology, vegetation cover and soil types, as well as land use and water use activities are summarised below.

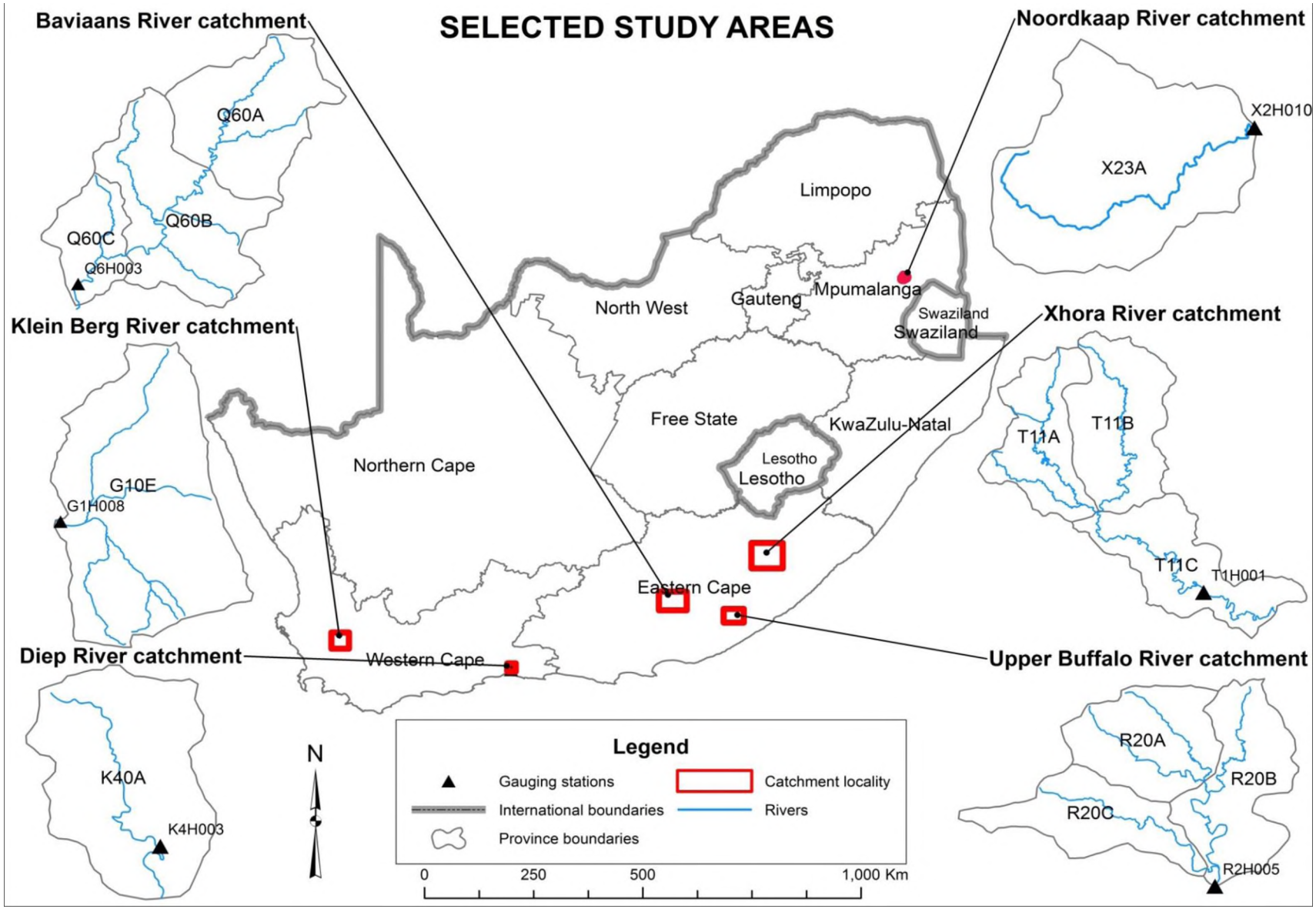

Figure 4.1: Map showing selected sub-catchments locality relative to the country (modified after Middleton and Bailey, 2008).

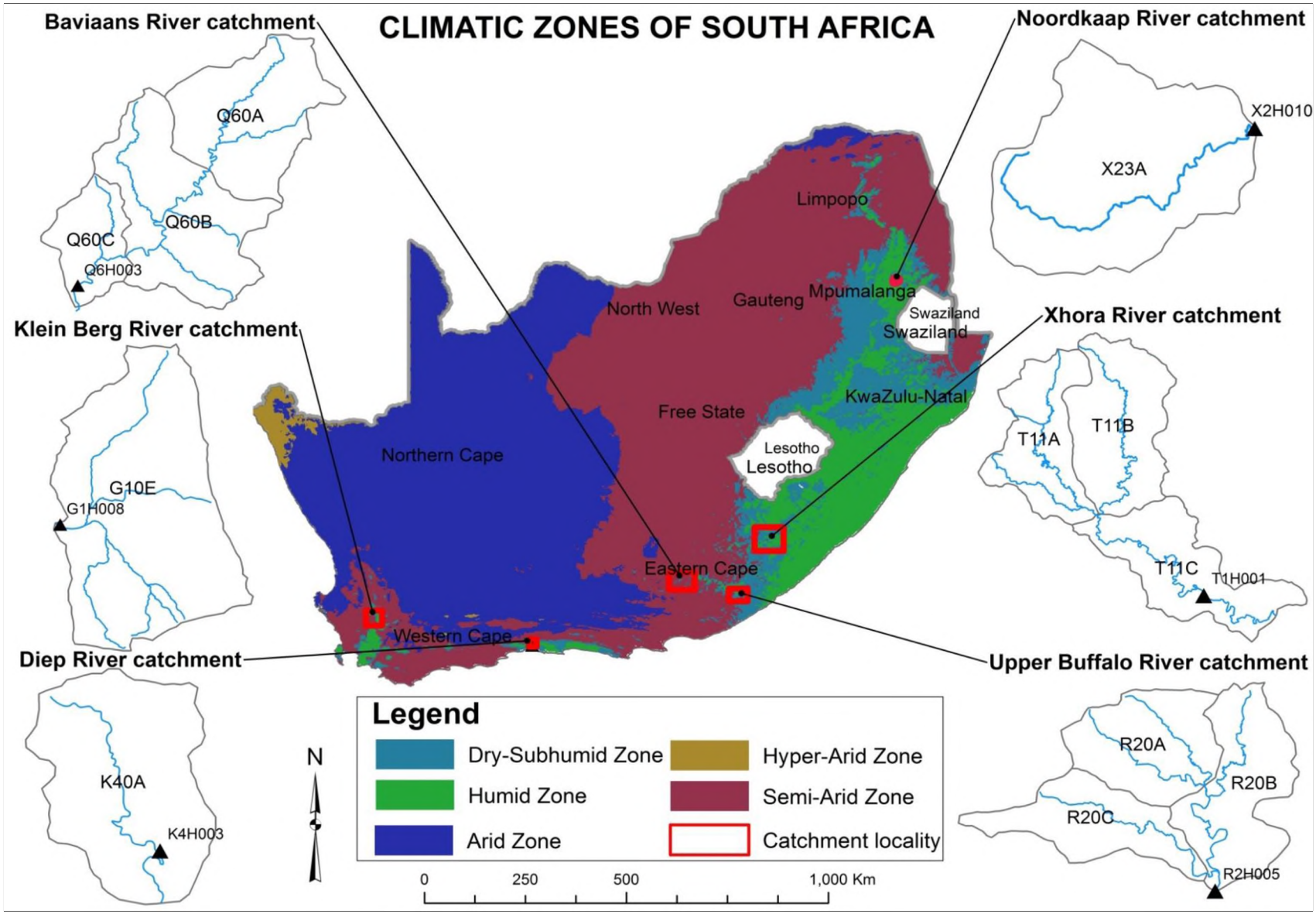

Figure 4.2: Map showing selected catchment localities with their relative climatic zones (modified from Middleton and Bailey, 2008).

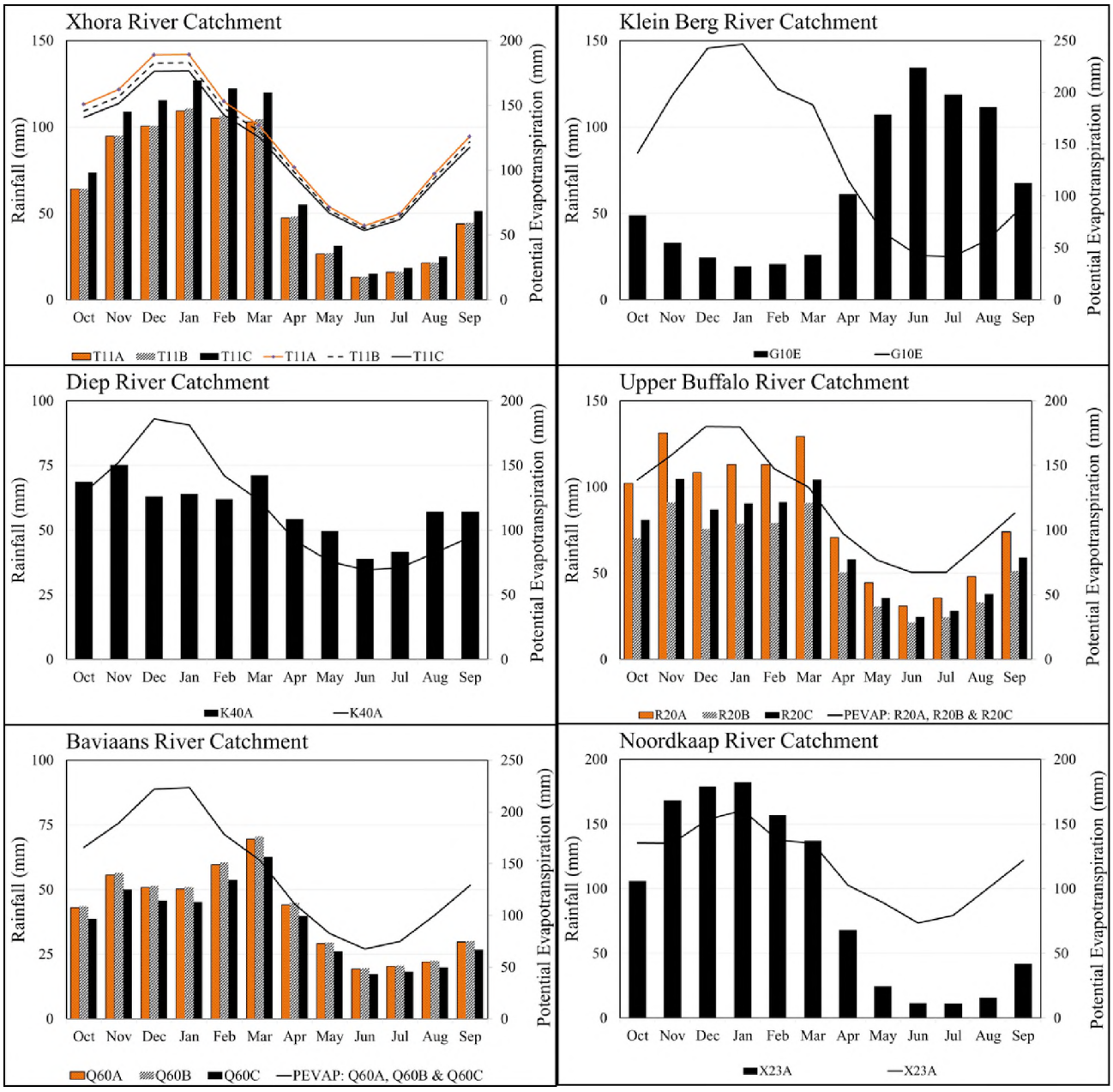

Figure 4.3: Average monthly rainfall and potential evapotranspiration for the selected study areas. The solid lines represent potential evapotranspiration and rainfall is bar chats.

4.2. THE XHORA RIVER CATCHMENT

The Xhora River originates in the southern Drakensberg Mountains at an altitude of about 2 198 meters above mean sea level (mamsl), draining a total area of 978 km^2 (Figure 4.4.a). The river flows southeast through deeply incised topography, roughly 75 km northwest of Mthatha, in the Eastern Cape Province. The Xhora River catchment (T11A to T11C) is located in a predominantly dry to sub-humid climatic zone (Figure 4.2) which experiences hot weather conditions, with most rainfall occurring during the summer months (Schulze, 1997). The overall catchment experiences a mean annual precipitation (MAP) of 800 mm (Figure 4.4.b) and a mean annual potential evaporation (MAE) of 1 450 mm (Middleton and Bailey, 2008).

Geologically, the northern part of the catchment predominantly lies on the Molteno, Elliot, and Clarens Formations of the Stormberg Subgroup, whereas the southern parts are underlain by the Katberg Formation of the Tarkastad Subgroup (see Figure 4.4.c and their description in Table 4.1) (AGIS, 2013). These rocks have a relatively low porosity (DWA, 2010b) and result in smaller groundwater recharge and yield (< 1 l^{-1}: DWS, 2015). Soils in this catchment are moderately deep clay loam in the river valleys, shallow in the high ridges and result in a relatively small soil moisture holding capacity as shown in Figure 4.4.d (Madi, 2010). The most recent Google Earth (2013) images show that a majority of the cultivated land is abandoned due to overgrazing and degradation of the land through soil erosion. Rill and gully dongas are manifest in the valley reaches of the catchment. Dongas modify hydrological response regimes and increase sedimentation to the downstream areas due to excessive overland flow. The natural vegetation found in the catchment (Figure 4.4.e) comprises of temperate and transitional forest on the river valleys and predominantly False Karoo grassveld in the low-lying areas of the catchment (DWAF, 2005c). A small proportion of the catchment has Eucalyptus (0.9 km^2) and Pine plantations (30.3 km^2), as well as alien invasive plants (0.9 km^2), mainly along the river channel (Middleton and Bailey, 2008).

Table 4.1: The summarized description of the geological setting of the Xhora River catchment

Formation	Description	Reference
Molteno	Medium- to coarse-grained sandstone, shale and grey mudstone	Dondo *et al.* (2010)
Elliot	Alternating sequence of maroon and greyish-red mudstone, with subordinate fine- to medium-grained sandstone	Woodford and Chevallier (2002)
Clarens	Fine-grained sandstone and homogenous siltstone	
Katberg	Multi-stored, fine- to medium-grained sandstones and laminated to massive mudstones	

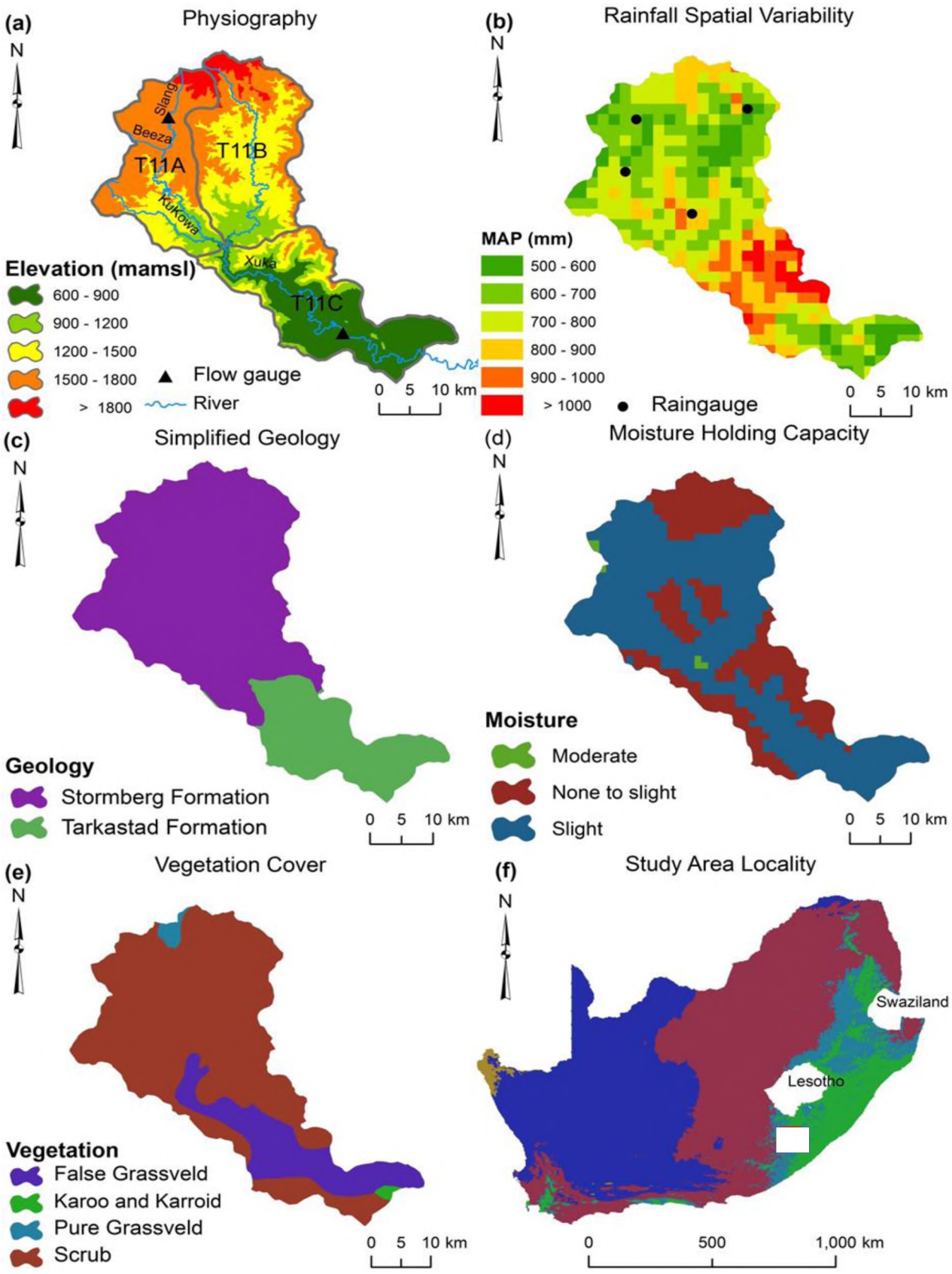

Figure 4.4: Map showing physiography (a), rainfall spatial variability (b), simplified geology (c), soil moisture holding capacity, (d) vegetation types (e), and locality of the Xhora River catchment (f) (modified after Middleton and Bailey, 2008).

4.3. THE KLEIN BERG RIVER CATCHMENT

The Great Winterhoek Mountains, Witzenberg Mountains, Waterval Mountains, and the Obiekwa-Voelvlei Mountains are the sources of the Klein Berg River. The river rises at an altitude of roughly 1 340 mamsl (Figure 4.5.a), within the vicinity of the town of Tulbagh, 120 km northeast of Cape Town in the Western Cape Province. The river flows perennially through regular plains with low hills before the confluence of the greater Berg River system in the Berg-Olifants Water Management Area (WMA). The Klein Berg River catchment (G10E) drains a total area of 394 km^2 and consists of flat valley floors and steep mountain slopes, forming the catchment boundary in the southern, eastern, and northern reaches. Located in the winter rainfall area (Figure 4.2), which is subject to cold, wet winters and hot, dry summers, typical of the Mediterranean climate, this catchment receives rainfall in the cooler months of April to October (Schulze, 1997). Rainstorms tend to be of low intensity for long duration associated with the passage of cyclonic cold fronts. Figure 4.5.b shows that the catchment experiences large spatial variability in MAP. Because of an orographic influence of the mountains, the mountainous areas receive significantly higher rainfall that the lower lying areas. Middleton and Bailey (2008) indicate that the catchment MAP is 764 mm and has a MAE of 1 635 mm.

Figure 4.5.c shows a simplified geological map of the catchment. The mountain tops consist of quarzitic sandstone of the Table Mountain Group (TMG), whereas the overall catchment valleys consist of sedimentary rocks dominated by consolidated sands, gravel, and boulders derived from the shales of the Porterville Formation of the Malmesbury Group (Görgens and De Clercq, 2006). The steep slopes of the catchment consist of shallow sandy loam soils formed out of weathered rocks while the valleys have deep sandy clay loam (Middleton and Bailey, 2008). WCDA (2015) indicates that the catchment has soil depths ranging from 450 mm to 750 mm which results in differences in water holding capacity (Figure 4.5.d). The natural vegetation of the catchment (Figure 4.5.e) is Shrubland fynbos in the mountainous reaches, whereas Pine (17.2 km^2) and Eucalyptus (2.5 km^2) plantations as wells as invasive alien vegetation (8.3 km^2) that occur in the valleys form a proportion of the secondary vegetation (River Health Programme, 2004). While the catchment has water shortfalls because of increased water demands (DWA, 2011a), a relatively large part of the catchment of approximately 36 km^2 (DWAF, 2004a) is extensively used for deciduous fruit farming which is supplied by water from the surrounding 323 small farm dams (Figure 4.5.a) and tributaries of the catchment. These abstractions affect the low flow regimes of the catchment during dry season.

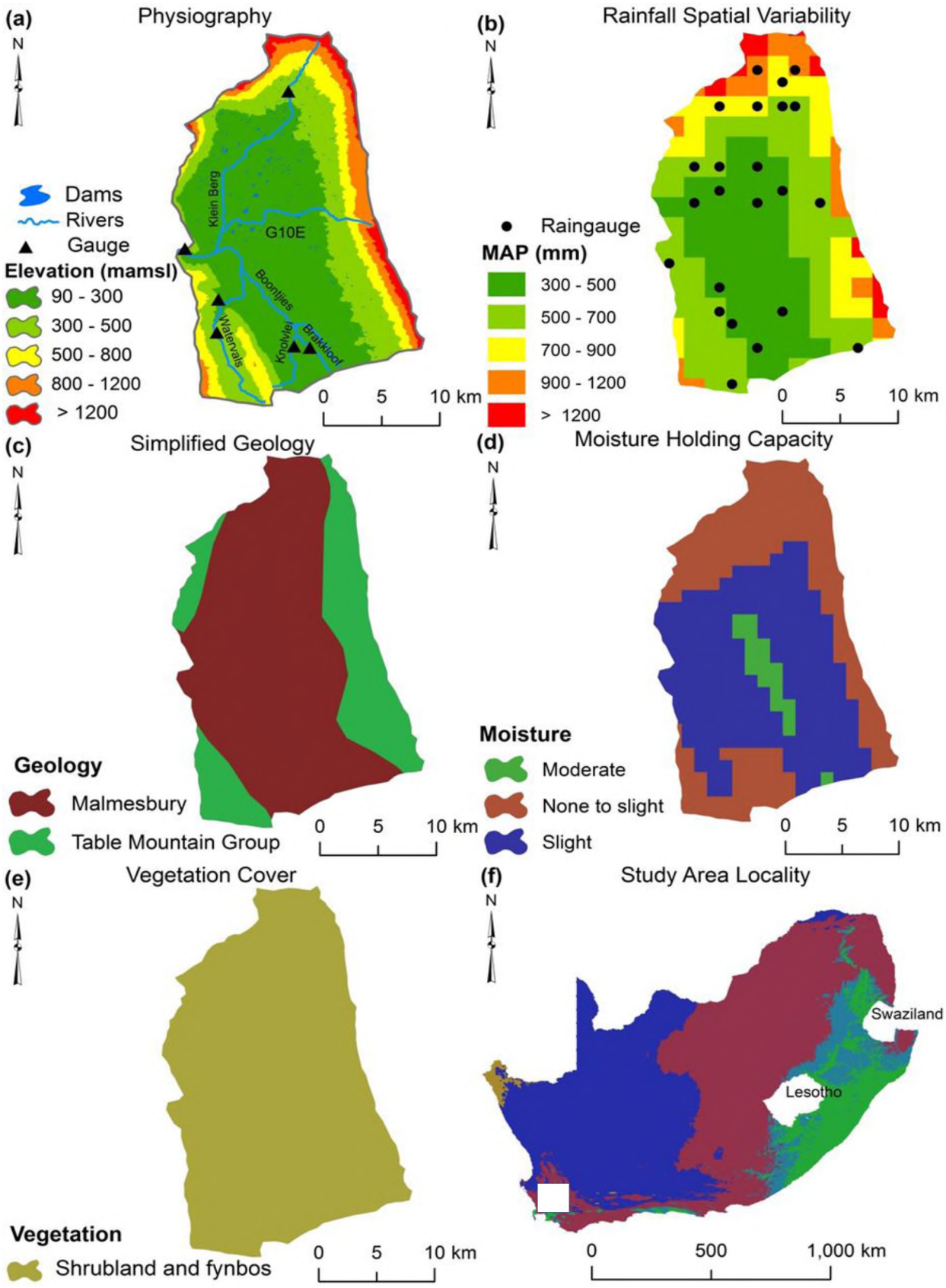

Figure 4.5: Map showing physiography (a), rainfall spatial variability (b), simplified geology (c), soil moisture holding capacity, (d) vegetation types (e), and locality of the Klein Berg River catchment (f) (modified after Middleton and Bailey, 2008).

4.4. THE DIEP RIVER CATCHMENT

The Diep River catchment (K40A) has a catchment area of 87 km^2 and drains the steep and hilly Outeniqua Mountains roughly 21 km inland from the Indian Ocean seaboard (Figure 4.1). This catchment forms part of the Swartvlei river system located between Knysna and Wilderness in the Western Cape Province, within the Breede-Gouritz WMA. The catchment (Figure 4.6.f) has a short river with high elevation variations ranging from 179 mamsl (catchment outlet) to 1 050 mamsl (catchment headwaters), and an average slope of 13.6%. Figure 4.6.f shows that this catchment is located in a transition zone between warm coastal temperate to dry sub-humid climatic regions of South Africa and is typically characterised by uniform rainfall throughout the season (Schulze, 1997). Figure 4.6.b shows that rainfall spatial distribution within this catchment varies because of altitude differences, which result in the mountains experiencing higher orographic rainfall. Middleton and Bailey (2008) indicated that this catchment has a MAP and a MAE of 706 mm and 1 400 mm, respectively. Steeper slopes are also expected to increase the interflow whereas the valley floors are expected to have groundwater seepage.

The geology of the region has a significant influence on the physiographical orientation, hydrology and the soil formation for this catchment. Figure 4.6.c shows that a relatively large proportion of this catchment consists primarily of compact arenaceous strata of the Nardouw Formation, which is sandwiched between the Peninsula Formation that is part of the long Cape Fold Belt. Lubke and De Moor (1998) described these rocks as fractured quartzite sandstones and subordinate shale, which are dominant in the mountain tops and are assumed to have high porosity which increases groundwater recharge and discharge. These rocks produce thin podzolic soils which are sandy, leached and with subsurface accumulation of organic matter in the mountainous areas, whereas in the catchment foothills, they form deep and well drained sandy clays with high water holding capacity. The natural vegetation of the catchment is characterised by small patches of open to medium dense coastal tropical forest and South Outeniqua Sandstone Fynbos occurring on the steep mountain tops, deciduous forest and Granite Fynbos in the low-lying areas of the catchment (Mucina and Rutherford, 2006; Hughes, 2013) as shown in Figure 4.6.e. The canopy density of these vegetation types increases the interception storage as well as the absorption capacity of the catchment while Pine plantations area (42.7 km^2), along the low lying areas modifies the hydrological flow regime of the catchment.

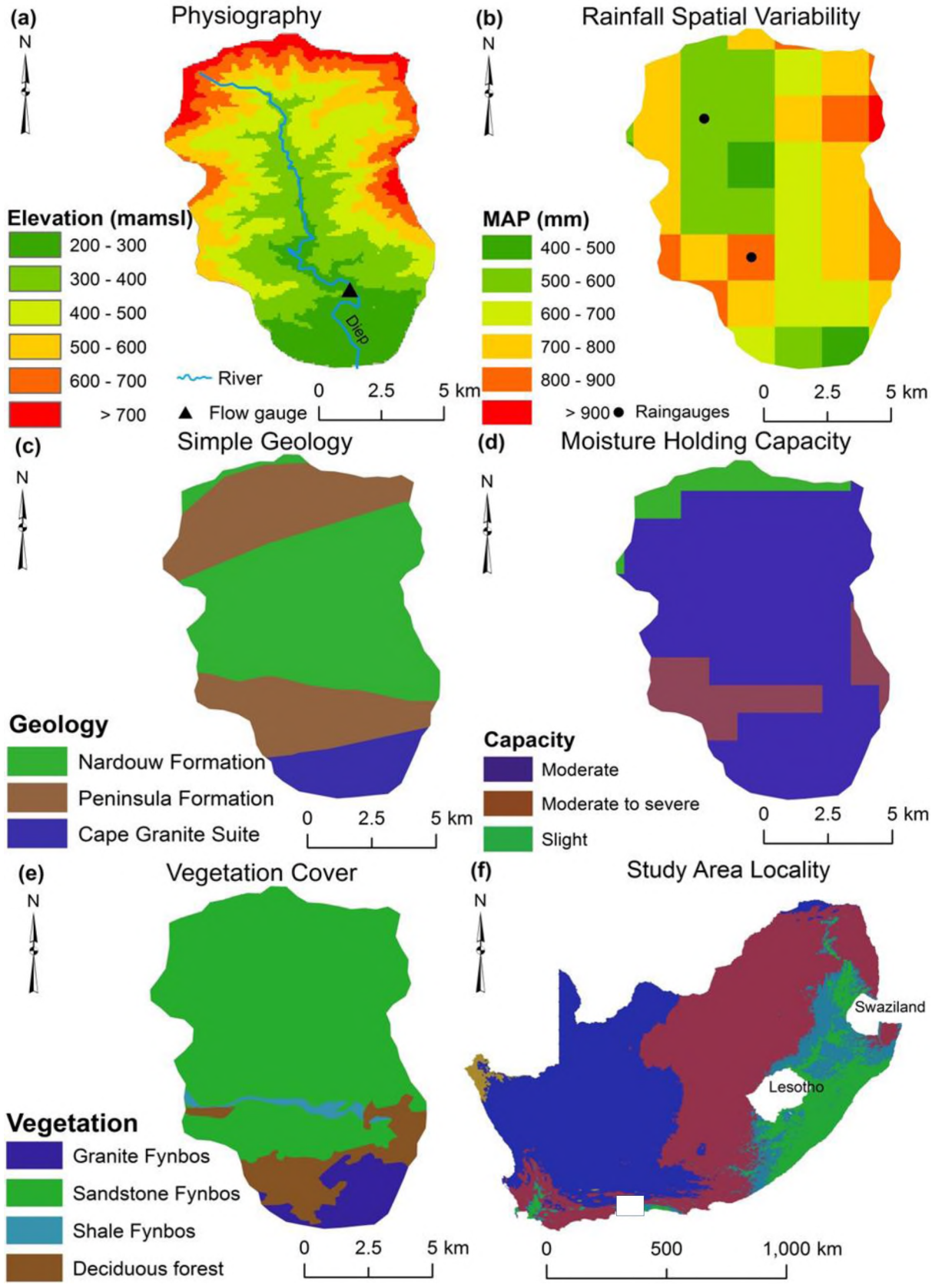

Figure 4.6: Map showing physiography (a), rainfall spatial variability (b), simplified geology (c), soil moisture holding capacity, (d) vegetation types (e), and locality of the Diep River catchment (f) (modified after Middleton and Bailey, 2008).

4.5. THE UPPER BUFFALO RIVER CATCHMENT

The Upper Buffalo River catchment (R20A to R20C) has its source in the steep and forested Amatola Mountains at an altitude of 1 300 mamsl between King Williams Town and Stutterheim in the Eastern Cape Province. The catchment drains an area of 411 km^2 with a deeply-incised channel that runs through undulating plains (Figure 4.7.a). Figure 4.7.f shows that the catchment is located in a semi-arid to temperate climatic zone of the summer rainfall region of South Africa that receives maximum rainfall from spring to autumn (Schulze, 1997). There is high rainfall variability within this catchment as shown in Figure 4.7.b, where the mountainous reaches, on average, receive 890 to 1 850 mm y^{-1} compared to the low-lying areas, which receive between 310 to 890 mm y^{-1} (van Ginkel *et al.*, 1993). The overall catchment MAP and MAE are 700 mm and 1 450 mm, respectively (Schulze, 1997).

The catchment lies predominantly on the Adelaide Subgroup whereas a small proportion lies in the Tarkastad Subgroup (Figure 4.7.c) The Adelaide Subgroup comprises of grey and brownish-red mudstones and fine to medium-grained sandstones that generally constitute 20 - 30% of the total thickness. The Tarkastad Subgroup consists of a lower sandstone-rich Katberg Formation and an upper mudstone-rich Burgersdorp Formation (Chevallier *et al.*, 2004). The intergranular pore spaces of the Sandstone aquifers enhance its transmissivity and therefore the movement of water to recharge the groundwater store and discharge to sustain the base flow. Van Ginkel *et al.* (1993) describe the weathering processes of the Tarkastad and Adelaide subgroup rocks form shallow sandy loam soils with minimal development in the mountain tops (Tarkastad), and well-drained moderately deep clayey loams in the valleys of the catchment (Adelaide). According to AGIS (2013), soils found in the mountainous reaches have a relatively small water holding capacity compared to those in the foothills (see Figure 4.7.d), which are prone to erosion because of reduced vegetation cover (DWAF, 2004b) thus modifying the runoff-generating processes. Coastal tropical and transitional forest types in the mountain tops, arid savannah grasslands, and thornveld in the catchment valleys are the dominant natural vegetation of the catchment (O'Keeffe *et al.*, 1996) (see Figure 4.7.e). Pine and Eucalyptus plantations that are found in the higher rainfall areas of the Amatola Mountains cover an area of approximately 30.1 km^2 and 3.2 km^2, respectively, while exotic weeds are invading most of the riparian zones (AGIS, 2013). The natural flow regimes of the catchment, which are currently water stressed (BCMM, 2014), are modified by two impoundments namely the Maden Dam and the Rooikrantz Dam located in sub-catchment R20A.

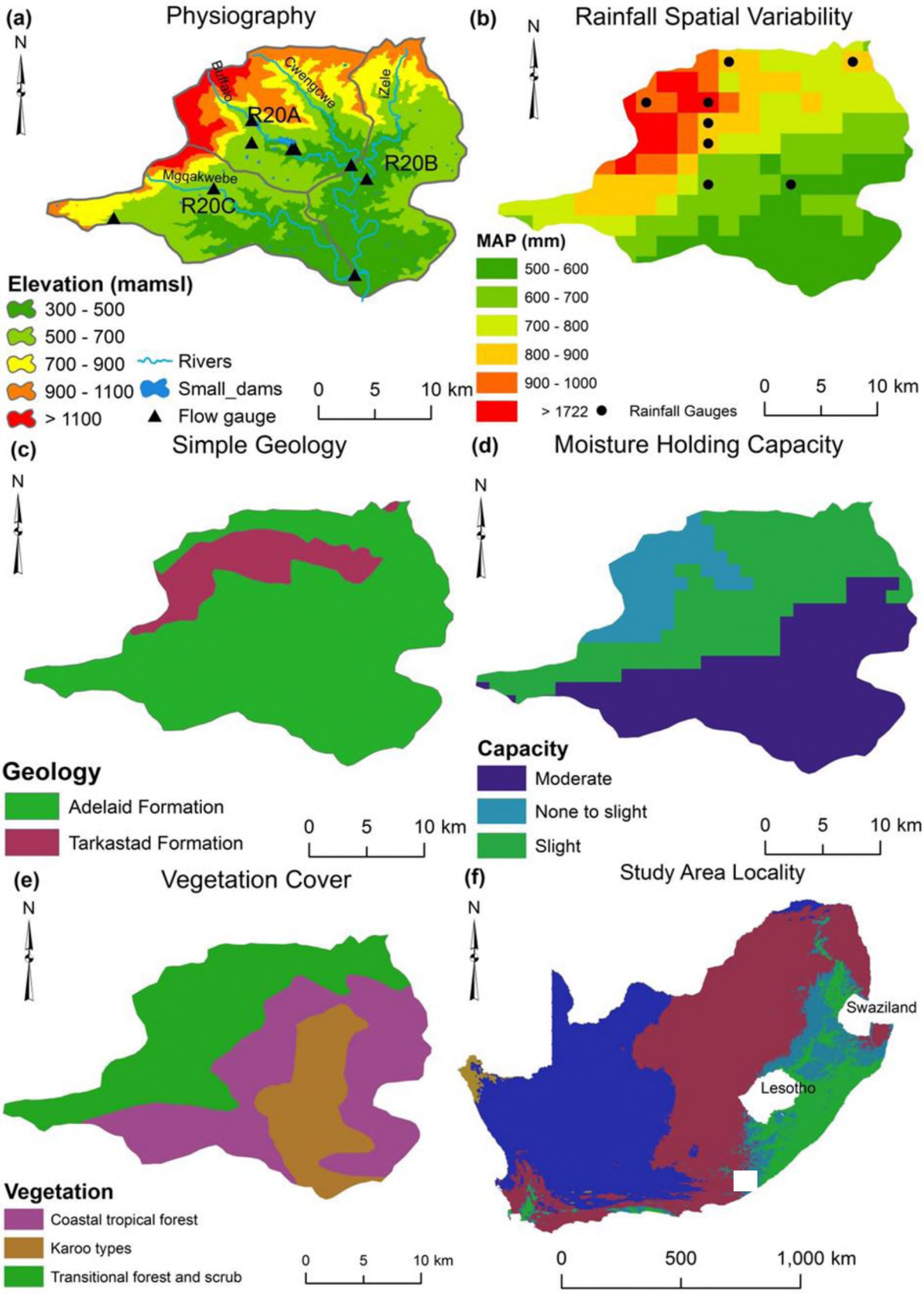

Figure 4.7: Map showing physiography (a), rainfall spatial variability (b), simplified geology (c), soil moisture holding capacity, (d) vegetation types (e), and locality of the Upper Buffalo River catchment (f) (modified after Middleton and Bailey, 2008).

4.6. THE BAVIAANS RIVER CATCHMENT

The tributaries of the Baviaans River originate from the steep Camdeboo-Winterberg Mountain escarpment at an altitude of about 1 700 mamsl, roughly 70 km northeast of the town of Somerset East in the Eastern Cape Province (Figure 4.1). With a total area of 814 km^2, this catchment (Q60A to Q60C) has numerous small, and usually dry, tributaries that rise from the edge of the escarpment and flow through deeply incised hilly terrain to join the lower reaches of the Fish River Valley (Figure 4.8.a). This catchment (Figure 4.8.f) is located in a semi-arid climatic zone of South Africa that experiences cool, dry winters and hot summers, with rain accompanied by frost occurring during the winter months (Schulze, 1997). Summer rainfalls are dominant in this area and vary slightly within the catchment as shown in Figure 4.8.b. This catchment is relatively dry with an MAP of up to 600 mm y^{-1} and the MAE is 1 700 mm y^{-1} (Middleton and Bailey, 2008).

The sedimentary rocks, mudstones, and sandstones of the Adelaide and Tarkastad Subgroup within the Beaufort Group, as shown in Figure 4.8.c, lie beneath the Baviaans River catchment. These rocks form shallow inter-granular, weathered, and fractured aquifers (Hancox and Rubidge, 2001). Due to the underlying geology, the catchment has an undulating landscape that results in the instability of soil formation. Hence, moderately shallow sandy loam soils are found in the till-tops of the catchment (DWAF, 2005a) and have a relatively small water holding capacity (Figure 4.8.d). The catchment has a combination of different arid vegetation types such as the false bushveld, false Karoo and pure grassveld that are distributed across the catchment as shown in Figure 4.8.e. According to the visual assessment conducted using Google Earth (2013) images and WARMS database (DWS, 2014a), there are small-scale crop farming activities along the river banks and predominantly towards the catchment outlet. Irrigation water for these crops is abstracted from a limited number of small farm dams, run-of-river, and boreholes. Attempts to estimate small dam surface area using Google Earth images were hindered by the fact that most of these dams are relatively small and they were dry during the satellite overpass. However, the volume of water from run-of-river abstraction was from the approximated WARMS database.

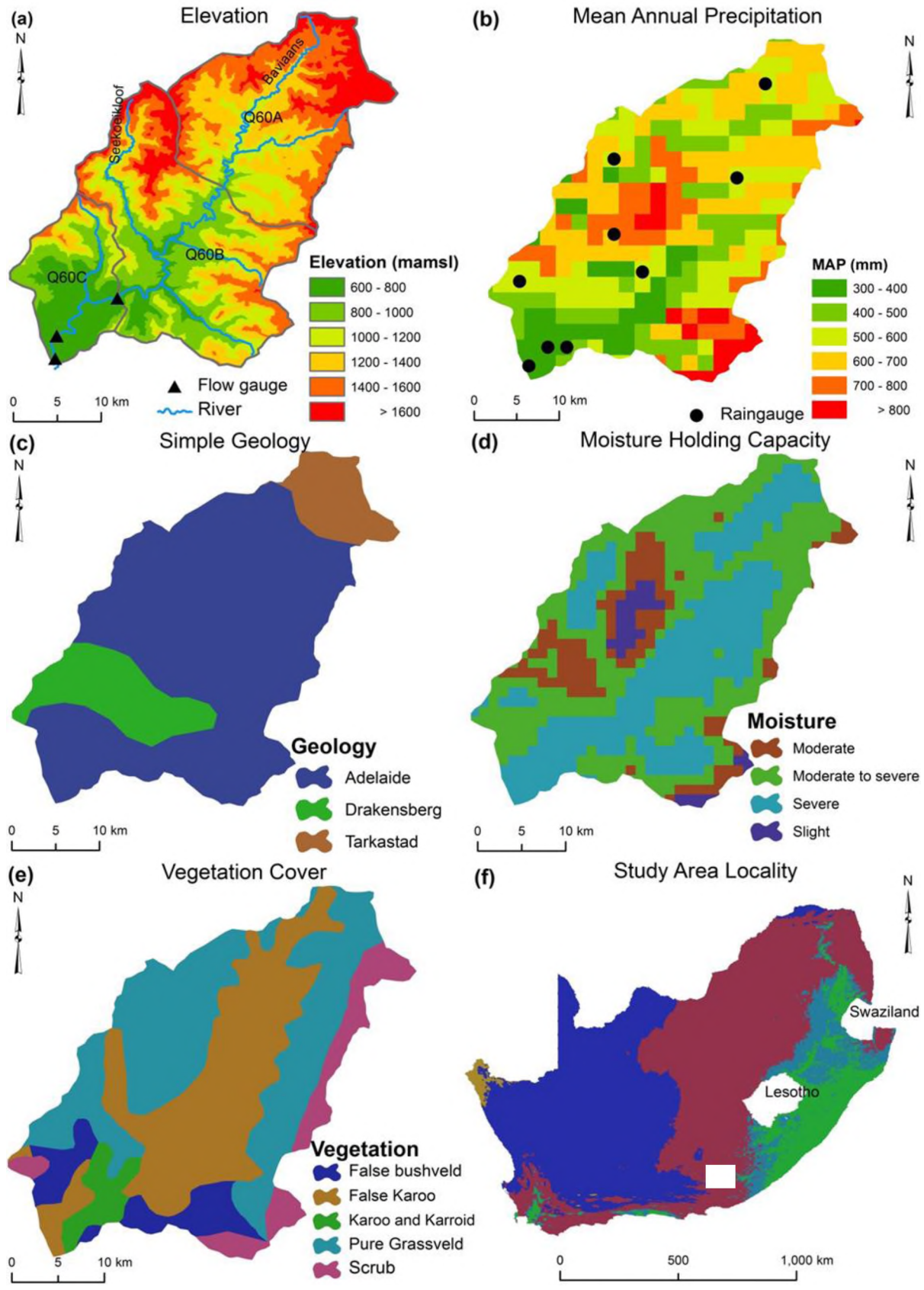

Figure 4.8: Map showing physiography (a), rainfall spatial variability (b), simplified geology (c), soil moisture holding capacity, (d) vegetation types (e), and locality of the Baviaans River catchment (f) (modified after Middleton and Bailey, 2008).

4.7. THE NOORDKAAP RIVER CATCHMENT

The Noordkaap River catchment (X23A) is located roughly 20 km southwest of Nelspruit in Mpumalanga Province within the Inkomati-Usuthu WMA and forms part of the Crocodile River system (Figure 4.1). The catchment area has an area of 126 km^2, and its elevation ranges between 850 and 1 700 mamsl, with steeper slopes in the headwater parts of the catchment and gentle slopes in the downstream areas (Figure 4.9.a). The catchment is characterised by a humid climate (Figure 4.9.f) with more than 80% of the annual rainfall received between November and March in the form of tropical storms (Mussá *et al.*, 2015). While there is high rainfall variability within the catchment (with mountainous areas receiving more than the downstream areas: Figure 4.9.b), the overall MAP in the area is 1 110 mm and MAE is 1 425 mm (Middleton and Bailey, 2008). Steeper slopes in the mountainous areas are assumed to enhance the interflow processes which could be a dominant runoff generating process in the catchment whereas groundwater seepage from the low-lying areas is expected to sustain the base flow during the dry season.

The geology (Figure 4.9.c) is characterised mainly by granitic rocks of the Kaap Valley which produce reddish-brown to red shallow soils on deep saprolite with a hard rock base that exhibits banded gneiss. The weathering of the granite rocks form deep sandy clay to sandy clay loam soils which enhance the absorption capacity of the catchment (Figure 4.9.d). The soil conditions make the area favourable for commercial forest plantations (Pine and Eucalyptus trees), which is the dominant land use as it accounts for more than 70% of the catchment area (Aird *et al.*, 2014) as shown in Figure 4.9.e. The manifestation of forest plantations indicates that the catchment has adequate soil-moisture storage capacity (Figure 4.9.d) to supply trees with moisture for a long period. Afforestation has been on the rise since the 1950s and has been reported to have a significant impact on the flow regimes not only in the Noordkaapp River but in the overall Crocodile River basin (Saraiva-Okello *et al.*, 2015). The downstream areas of the catchment have small patches of cultivated land (1.5 km^2 according to Bailey and Pitman, 2015). Google Earth images (September 2004 and 2010) depicts that irrigated areas are supplied by water from a number of small farm dams. These images show that the riparian areas in the mountainous reaches had invasive alien plant and their occurrence has also been reported by Aird *et al.* (2014). These plants are expected to have a significant impact on the natural flow regime of the catchment.

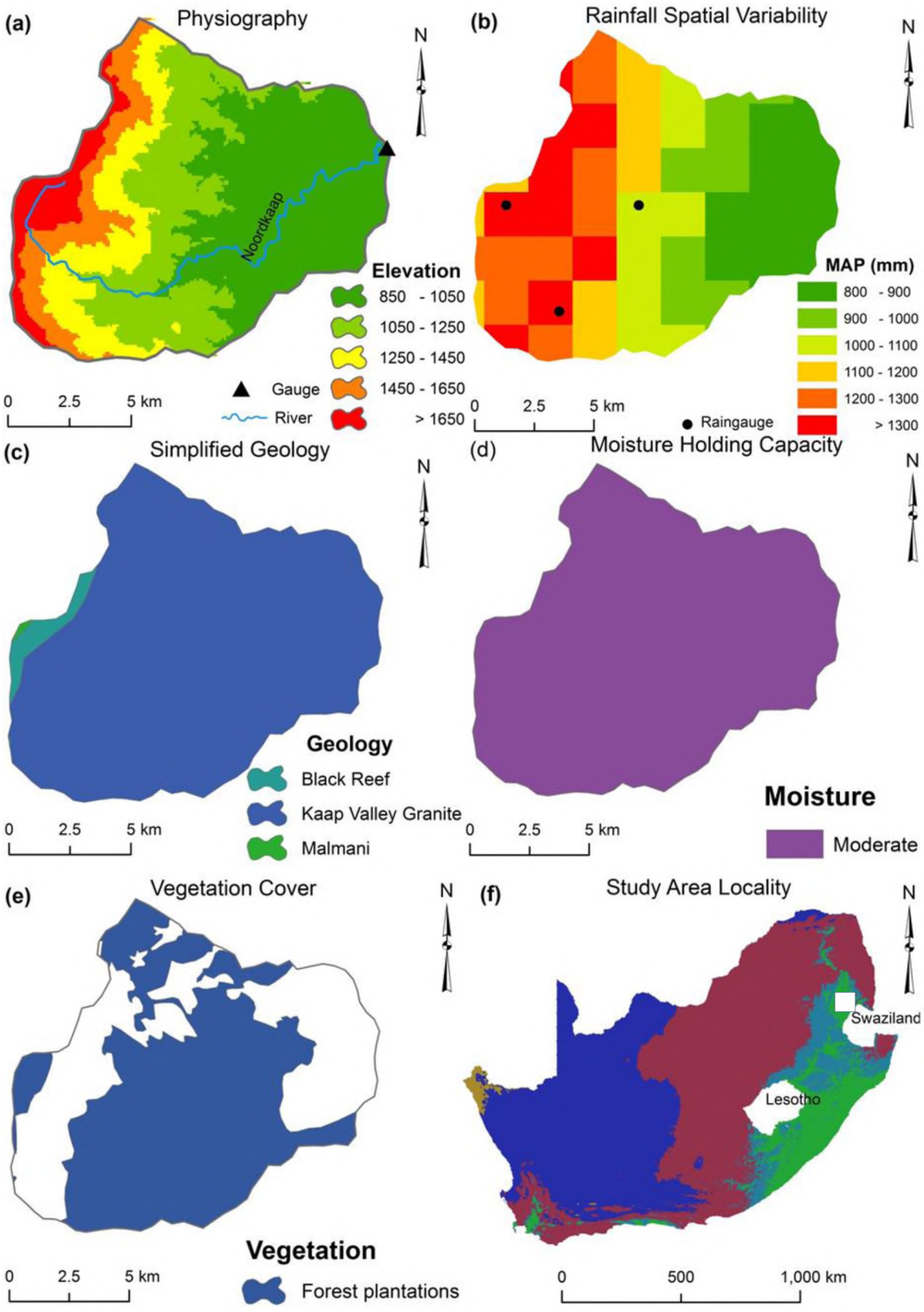

Figure 4.9: Map showing (a) physiography, (b) rainfall spatial variability, (c) simplified geology, (d) soil moisture holding capacity, (e) vegetation types, and (f) locality of the Noorkaap River catchment relative to the aridity zones (modified from Middleton and Bailey, 2008).

4.8. ADDITIONAL CATCHMENTS

Several additional catchments were used to further evaluate the use of MOD16 ETa data in the areas where detailed rainfall-runoff modelling has been conducted with the Pitman model during previous studies. These areas are the Manubi forest, Kosi Bay, and Lake Sibaya. The objective of selecting the Manubi forest was to compare the model-simulated total evapotranspiration with ETa data from short-term observations and MOD16. The Kosi Bay and Lake Sibaya areas were also selected to conduct a comparison between the model-simulated total ETa and MOD16 ETa data of a forested and grassland area for both sites. ETa data were obtained from Hughes *et al.* (2014a) for Manubi forest and Tanner (2015) for Kosi Bay and Lake Sibaya.

4.8.1. The Manubi Forest

The Manubi forest is located along the coastal region of the Eastern Cape Province of South Africa (Figure 4.10) about 90 km northeast of East London. The forest consists of mixed-species, mixed-age evergreen indigenous forest that covers an area of 7 km^2. The geology of the catchment comprises of mudstones of the Adelaide Formation, which is dominant in the area, and fine-grained doleritic rocks that are in the high-lying areas (AGIS, 2013). The rocks form deep well drained doleritic soils which provide adequate soil moisture for the forest. The climatic conditions of the surrounding area are characterised by humid conditions with an MAP and MAE of 1 070 mm and 1 250 mm, respectively (Schulze and Maharaj, 2006).

4.8.2. Kosi Bay and Lake Sibaya

The selected areas are within W70A quaternary catchment that forms part of the Pongola-Mtamvuna WMA. The coastal areas of the catchment are characterised by interconnected lakes and wetlands. The Kosi Bay site (Figure 4.10) is located about 1 km south-west of the Mozambique boarder gate while the Lake Sibaya site is on the northern shores of lake. These sites are located in a relatively flat floodplain that experiences a humid subtropical climate and has a MAP of 769 mm and MAE of 1 500 mm (Middleton and Bailey, 2008). The geology of the selected areas consists of the loosely fine-grained to, coarse sandy clay material of the Holocene sediments of the Sibayi Formation forming the cover sands and active dunes (Porat and Botha, 2008). The natural vegetation of the catchment is dominated by swamp forest, coastal thicket, and grassland whereas managed forest plantations dominate the secondary vegetation (Mucina and Rutherford, 2006).

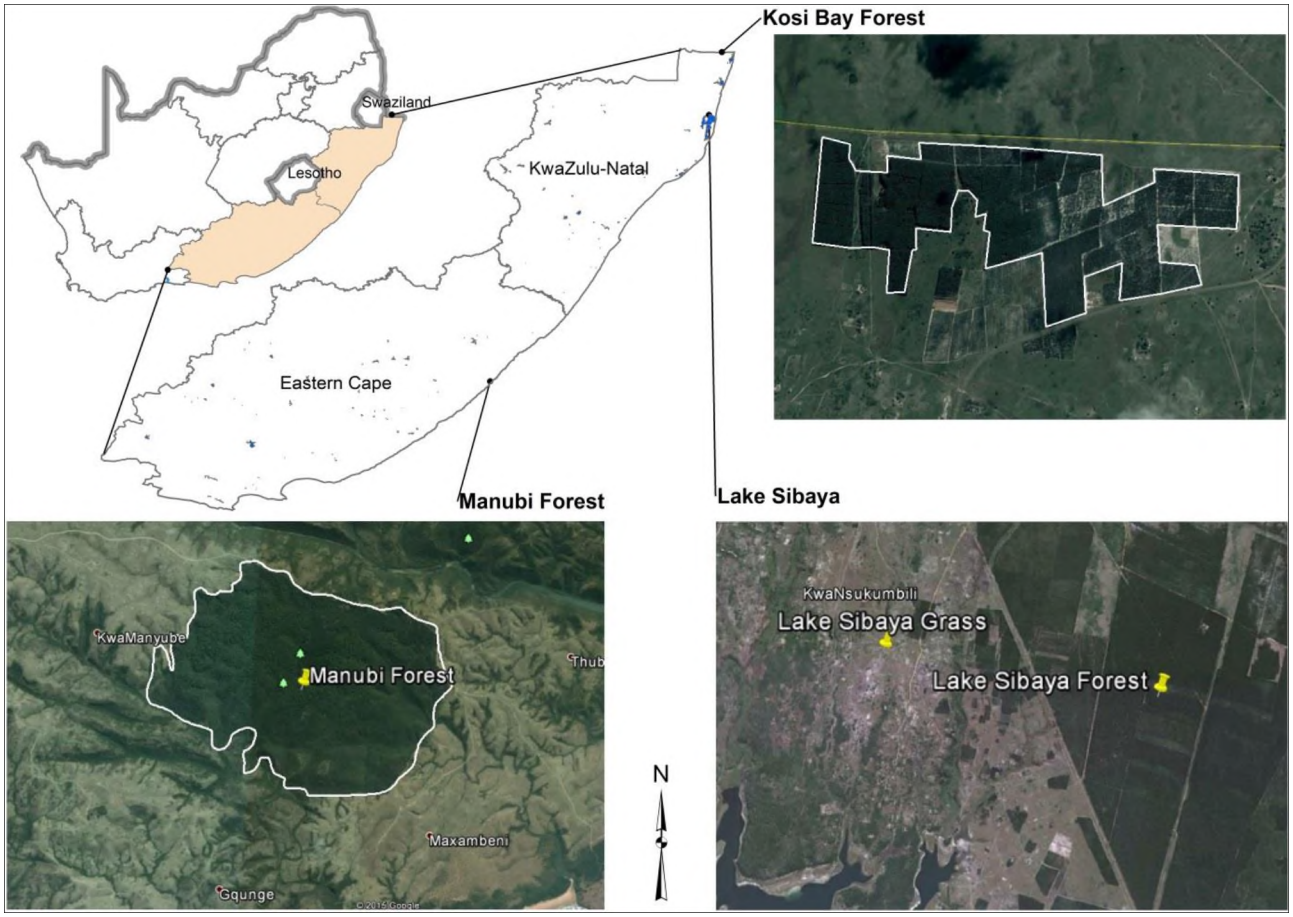

Figure 4.10: Google Earth images showing the location of the selected sites. The top right image shows the forested area near the Kosi Bay. The bottom right image shows two place marks that represent a forested area and grassland area near Lake Sibaya, and the bottom left shows an aerial extent of the Manubi Forest.

4.9. SUMMARY

This chapter has provided an overview of the hydrometeorological, physiographical, geological, and land cover setting of the selected catchments. The settings play a vital role in hydrological studies as they guide the setting up of hydrologic system understanding used in hydrological modelling. Overall, rainfall data records from the WR2005 indicated the known hydrometeorological patterns for the selected catchments. The rainfall data records for individual quaternary catchments with mountainous areas showed high spatial variability different from those with uniform landscape. This phenomenon has been demonstrated in the catchments' MAP maps provided in Chapter 4. Orographic rainfall effects could be attributed to this variability and are often neglected in the modelling process, as they are hard to model on their own (Hughes, 2008).

CHAPTER FIVE

5. HYDROLOGICAL MODEL CALIBRATION AND RESULTS

5.1. INTRODUCTION

This chapter reports on various activities carried out to achieve modelling results for the study areas under investigation. The modelling results outlined in this chapter are divided into five sections:

(i) The first two sections (5.2 and 5.3) provide the initial calibration results of the Pitman model under natural conditions together with the model parameter uncertainty. The modelling exercises were conducted using both a single-run version (section 5.2) and the uncertainty version of the model (section 5.3).

(ii) The third section (5.4) presents the trend tests analysis of the observed flow records, quantification of water uses and the simulation results of the present-day conditions with uncertainty version of the model.

(iii) The simulation outcomes of use of the MOD16 PET data as input into the model are presented in section 5.5. The simulation results are based on a single-run version of the model.

(iv) The last section (5.6) presents the results of the simulations based on calibration of the model with MOD16 ETa data used to constrain model-simulated ETa in a single-run version of the model.

5.2. INITIAL CALIBRATION OF THE PITMAN MODEL

A single-run version of the GW-PITMAN model was set-up using the guidelines discussed in section 3.2.5 to calibrate the model against the simulated naturalised flows obtained from the WR2005 study (Middleton and Bailey, 2008) with a different version of the Pitman model. The aim was to apply the IWR version of the model and calibrate other parameters not used in the WR2005 study. The majority of the calibration results are generally satisfactory as the model was successfully able to capture the magnitude and temporal variations of the naturalised stream flows. Visual comparisons between the hydrographs of the naturalised and simulated flows were in agreement with each other. Model performance assessed using objective functions (described in section 2.5.1) resulted in values of both the untransformed and log-transformed data greater than 0.7 for *CE* and

within the range of ±10% for the *%BIAS*. Figure 5.1 shows a summary graph of the performance of the model for the selected sub-catchments using the four objective functions. The results presented do not include the Noordkaap River catchment because Hughes (2015) already established appropriate model parameters.

While it is acknowledged that these are comparisons of two sets of model simulations, it is important to establish parameter sets of the updated version of the model (Hughes, 2004) that generate results that are consistent with the version of the model used with the WR2005 study. It is assumed that the WR2005 simulated naturalised flows were based on the best available calibration against naturalised observed flows.

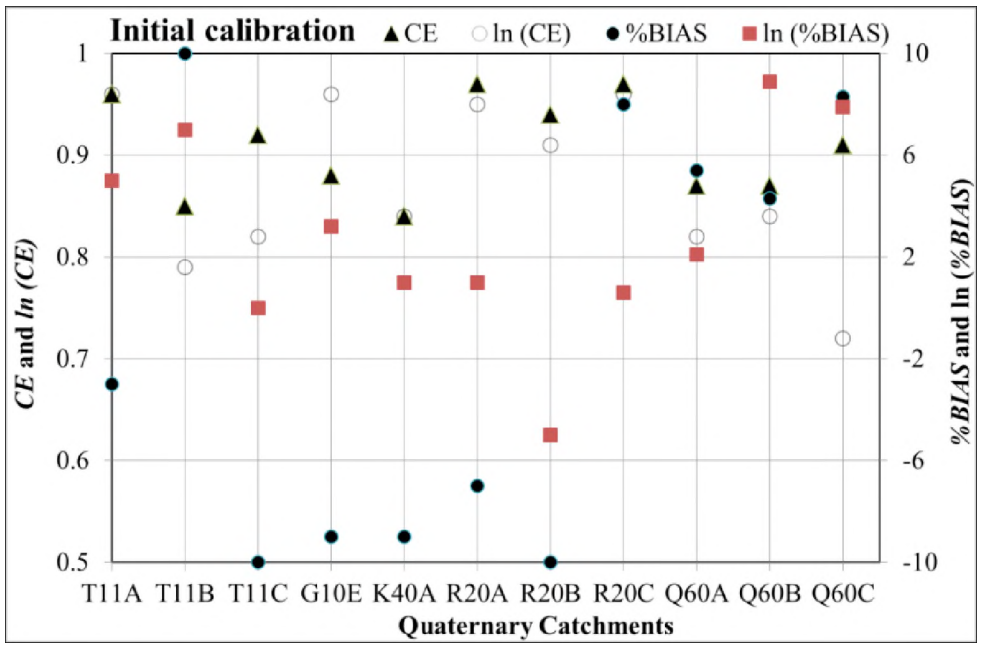

Figure 5.1: The summarised performance measure statistics for the initial calibration of the Pitman model for the selected sub-catchments under natural conditions. *CE*, *CE (ln)*, *%BIAS*, and *%BIAS (ln)* are the objective functions used for the model evaluation. The scale for *CE* and *%BIAS* (both untransformed and log-transformed data) ranges from 0.5 to 1 and -10% to 10%, respectively.

The sub-sections below present a summarised discussion of the calibrated model parameters (Table 5.1), hydrographs, the flow duration curves (FDCs), and the objective function statistics for the selected catchments simulated under natural conditions. The various simulation periods for each

catchment were selected to ensure that they include a range of hydrological regimes (wet and dry hydrological years).

Table 5.1: The initial values of the calibrated parameters of the GW-PITMAN model and the four objective functions for the selected sub-catchments (see Table 3.3 for units). The values of the fixed parameters are given in the footnote

Parameter	Sub-catchments										
	T11A	T11B	T11C	G10	K40A	R20A	R20B	R20C	Q60A	Q60B	Q60C
ZMIN	10	69	20	70	11	48	20	249	15		
ZAVE	154	259	162	230	208	326	132	605	240		
ZMAX	264	494	301	400	280	227	302	1198	650	625	650
ST	40	203	400	420	40	143	150	312	150	150	180
POW	3	3.5	2.8	3.45	3.0	3.5	2	3.8	3.4		
FT	10.0	19.0	7.0	34.0	18.0	57.0	35.0	65.0	0.8	0.0	0.0
GW	0.0	1.8	2.0	4.1	5.6	5.6	3.0	3.6	0.01		
R	0.5	0.5	0.4	0.5	0.5	0.5	0.5	0.5	0.5		
GPOW	0.45	0.61	2.80	3.50	2.80	3.50	2.80	3.80	3.00		
TLGMax	0.1	1.5	2.0	2.5	0.0	0.15	1.5	6.0	0.3		
D.Dens*	0.12	0.21	0.19	0.19	0.19	0.19	0.23	0.25	0.16	0.19	0.19
T*	9.4	14.9	13.9	10.0	25.0	10.0	10.0	10.0	15.0		
S_t *	0.004	0.004	0.004	0.001	0.002	0.027	0.027	0.027	0.001		
GWSlope*	0.011	0.011	0.011	0.011	0.050	0.01	0.01	0.01	0.01		
RWL*	10	25	15	15	10	12	12	15	25		
RIP	0.1	0.1	0.05	0.2	0	0.15	0.15	3.0	0.21	0.21	0.2
Model performance											
CE	0.96	0.85	0.92	0.88	0.80	0.99	0.93	0.63	0.87	0.87	0.91
CE (ln)	0.96	0.79	0.82	0.96	0.80	0.98	0.94	0.74	0.82	0.84	0.72
%BIAS	-3.0	10.0	-10.0	-9.0	-9.9	-7.0	-10.0	8.0	5.4	4.3	8.3
%BIAS (ln)	5.0	7.0	0.0	3.2	-9.4	1.0	-5.0	0.6	2.1	8.9	7.9

Note: '*'–*fixed to various values;* ***RDF****–1.28;* ***AI****–0;* ***PI1****–1.4;* ***PI2****–4;* ***FF****–1;* ***SL****–0;* ***CL****–0; and* ***TL****–0.25.*

5.2.1. The Xhora River Catchment

Table 5.1 (column T11A to T11C) lists the calibrated model parameters for the Xhora River catchment while Figure 5.2 illustrates the resulting simulation for the period October 1970 - September 1990. Figure 5.2 compares the hydrograph time series of the WR2005 flows (referred to as the naturalised) and simulated flows together with their FDCs for the three sub-catchments of the Xhora River. The results from the figure illustrate that the model was capable of simulating the naturalised flow volumes throughout the range of flows for sub-catchments T11A and T11C but not for sub-catchment T11B, where the high flows were over-simulated between the period 1978 - 1984. For all three sub-catchments, an acceptable comparison between the naturalised and simulated flows was obtained with values of *CE* greater than 0.79, regardless of whether untransformed or log-transformed data were used. The percentage bias in the mean of the simulated high flows *(%BIAS)* and low flows (*%BIAS {ln}*) were within ±10% of the naturalised flow data. The over-simulation of

high flows in sub-catchment T11B could result from a slightly different calibration approach used within this study compared to the WR2005 study.

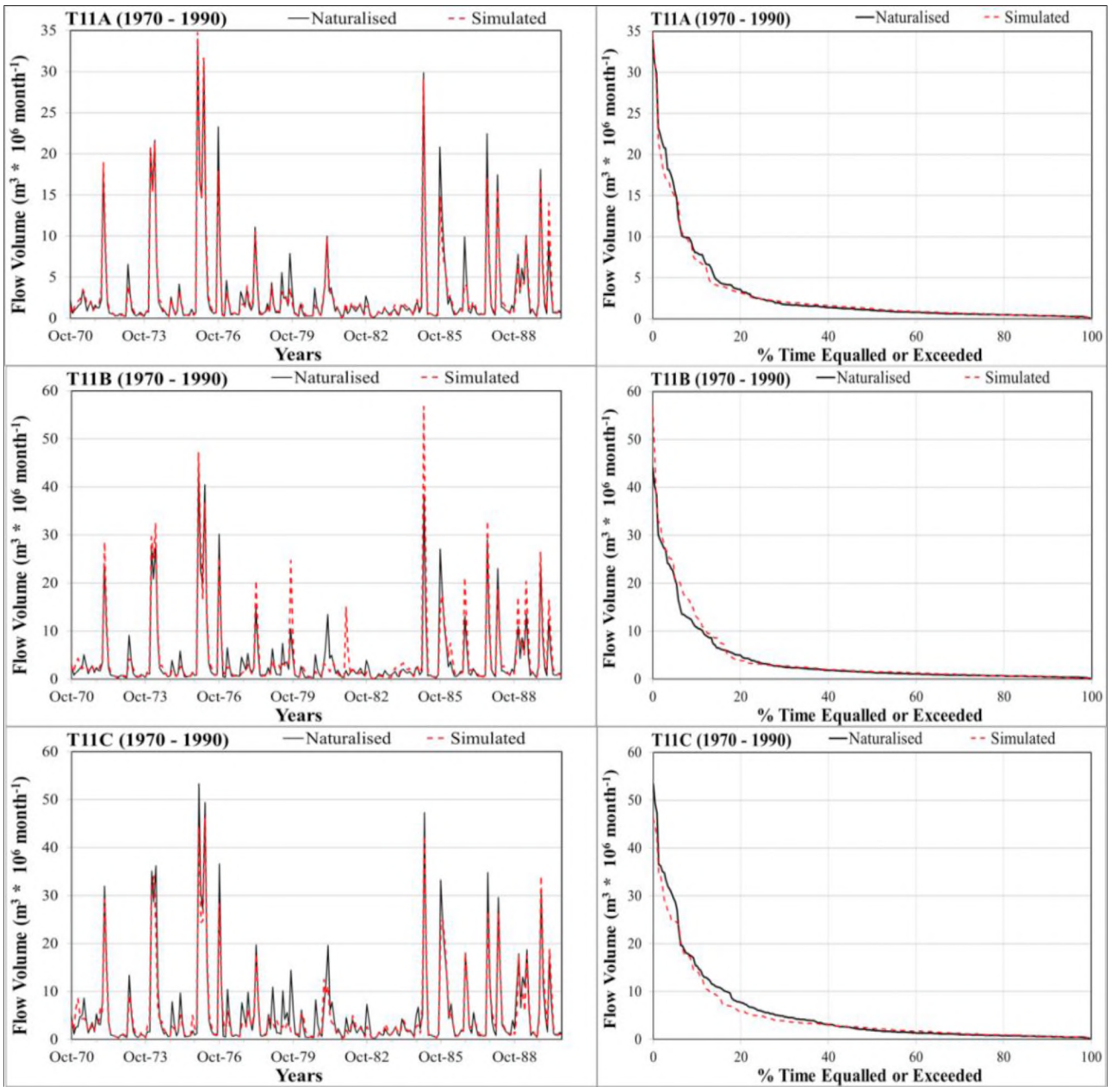

Figure 5.2: Hydrographs (left) and the flow duration curves (right) comparison of the WR2005 naturalised flows with the simulated monthly flows for the Xhora River catchment.

5.2.2. The Klein Berg River Catchment

The calibration of the model for the Klein Berg River was conducted for the period October 1965 - September 1985 in order to cover both dry and the wet periods. The hydrograph comparison between the simulated and naturalised flows together with their respective FDCs are presented in Figure 5.3, and the simulation results were obtained using the model parameters listed in Table 5.1 (the G10E column). Figure 5.3 illustrates that the calibrated parameters are a satisfactory representation of the timing and magnitude of both high and low naturalised flows from the WR2005 database. Overall, the calibrated parameters resulted in acceptable model performance, as the values of *CE* and *CE (ln)* were 0.83 and 0.95, respectively. The values of the *%BIAS* and *%BIAS (ln)* indicate a variability of mean of both high and the low flows as they ranged between ±9%.

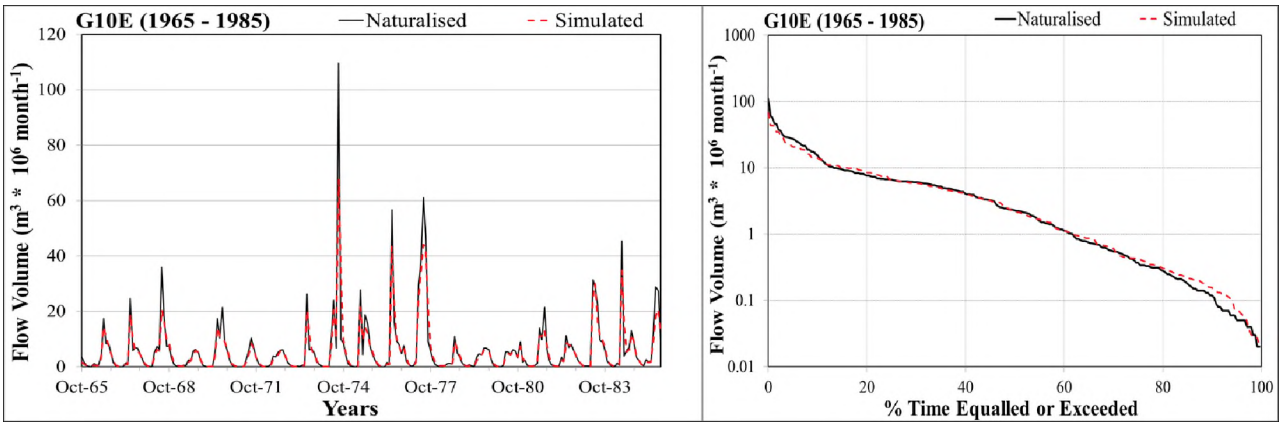

Figure 5.3: Hydrographs and the FDCs comparison of the WR2005 naturalised flow with the simulated monthly flow for the Klein Berg River catchment.

5.2.3. The Diep River Catchment

Figure 5.4 shows the hydrograph and the FDCs resulting from the calibration of the model for the period October 1960 - September 1980. The simulation results in the figure generally show good agreement between the simulated and naturalised monthly flow volumes for both high and low flow regimes. Table 5.1 (the K40A column) lists the calibrated model parameters and the results of the four objective functions used. The values of the objective functions are within the set threshold and the calibrated model parameters were considered acceptable. However, it should be noted that the simulated flows under-estimated the high flows during the wet years. The FDC demonstrates that the high flows are under-simulated around 5% of the time.

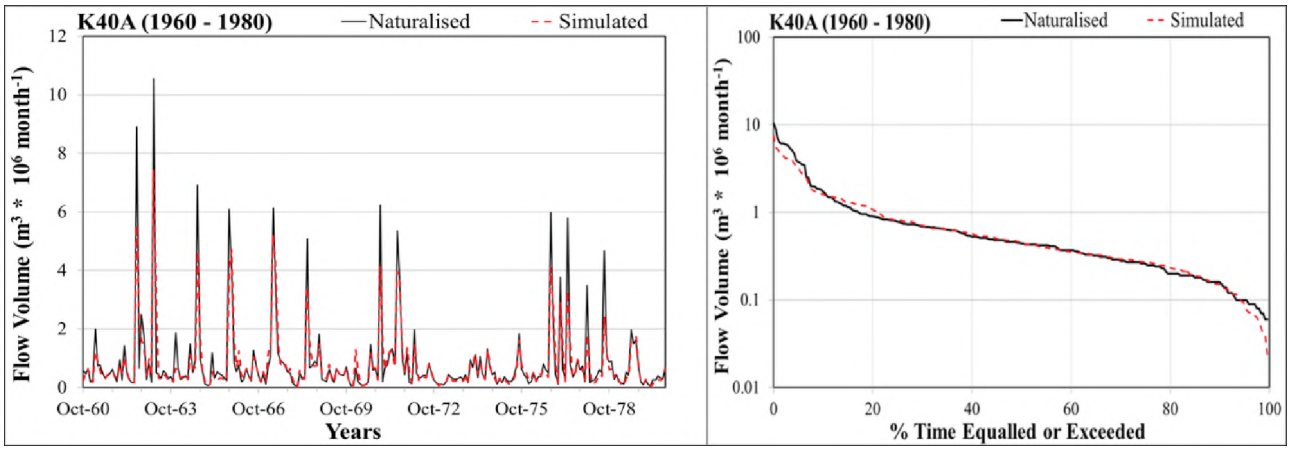

Figure 5.4: Hydrographs and the FDCs comparison of the WR2005 naturalised flow with the simulated monthly flow for the Diep River catchment.

5.2.4. The Upper Buffalo River Catchment

Figure 5.5 illustrates the comparisons between the simulated and naturalised flow data for the Upper Buffalo River catchment, calibrated for the period October 1950 - September 1970. Calibration results presented in Table 5.1 (columns R20A to R20C) show that the model was capable of successfully simulating the natural hydrological response assumed by the WR2005 study. The magnitude of both high and low flows are within an acceptable range based on the four objective functions used. While the hydrographs of R20A and R20B show a good-fit, the hydrograph for the R20C sub-catchment indicates an over-simulation during the summer months of 1962, 1966, and 1969. This is further supported by the fact that the model did not over-simulate the flows of the other two sub-catchments for the similar periods. The *CE* and *%BIAS* values of the untransformed and log-transformed data were within the predefined threshold of acceptable model performance.

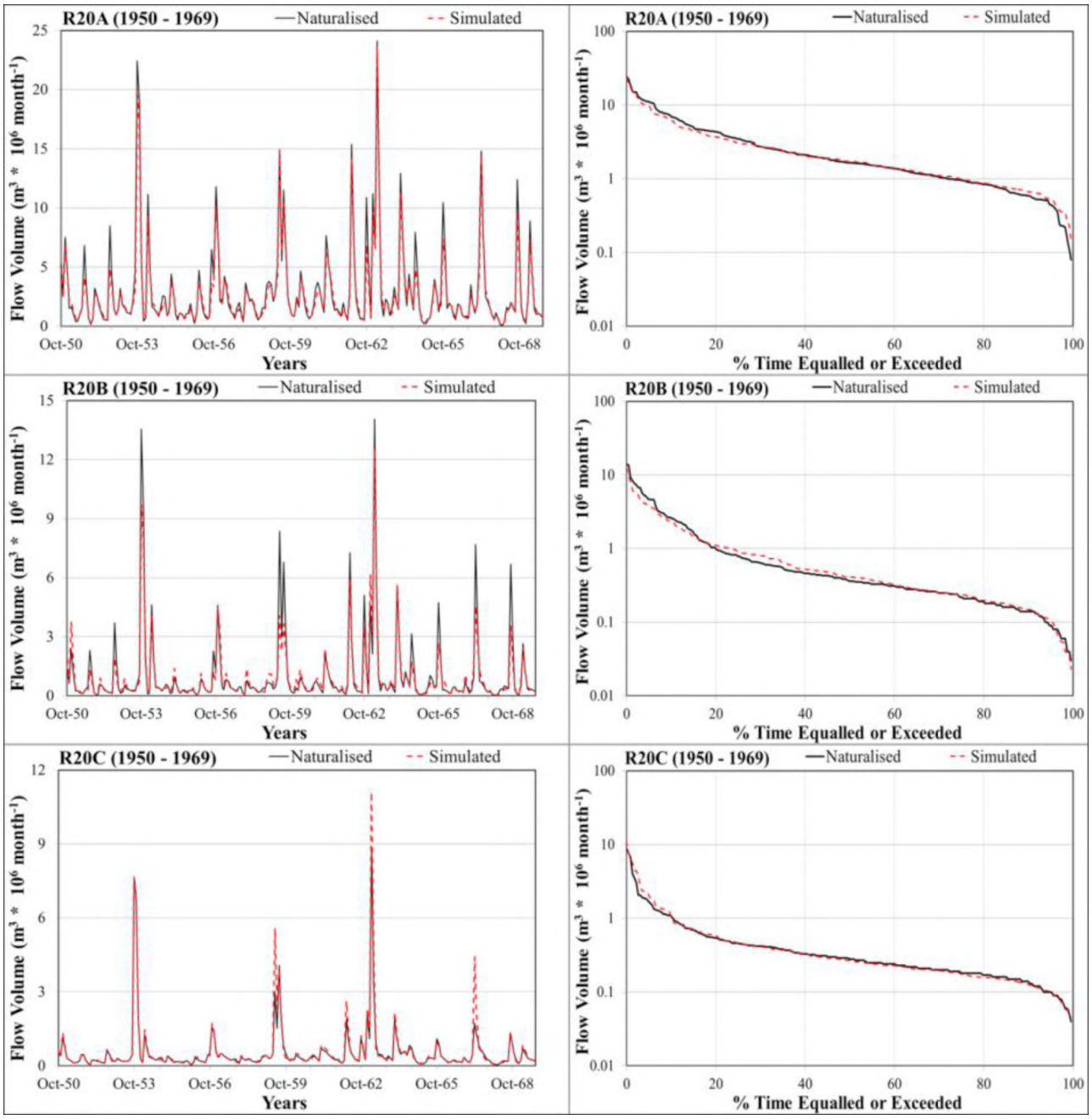

Figure 5.5: Hydrographs and the FDCs comparisons of the WR2005 naturalised flows with the simulated monthly flows for the Upper Buffalo River catchment.

5.2.5. The Baviaans River Catchment

Figure 5.6 presents the hydrograph comparison between the simulated and naturalised flows together with the FDCs for the Baviaans River while the calibrated parameters and statistics of the four objective functions are listed in Table 5.1 (column Q60A to Q60C). The hydrographs indicate

that the flows are over-simulated for the majority of the wetter periods for all three sub-catchments, but the low flows were captured successfully. The FDCs demonstrate that over-simulation of the naturalised flows occurs less than 40% of the time. Calibration results, for the period October 1954-September 1975, were within the acceptable threshold of the four objective functions used.

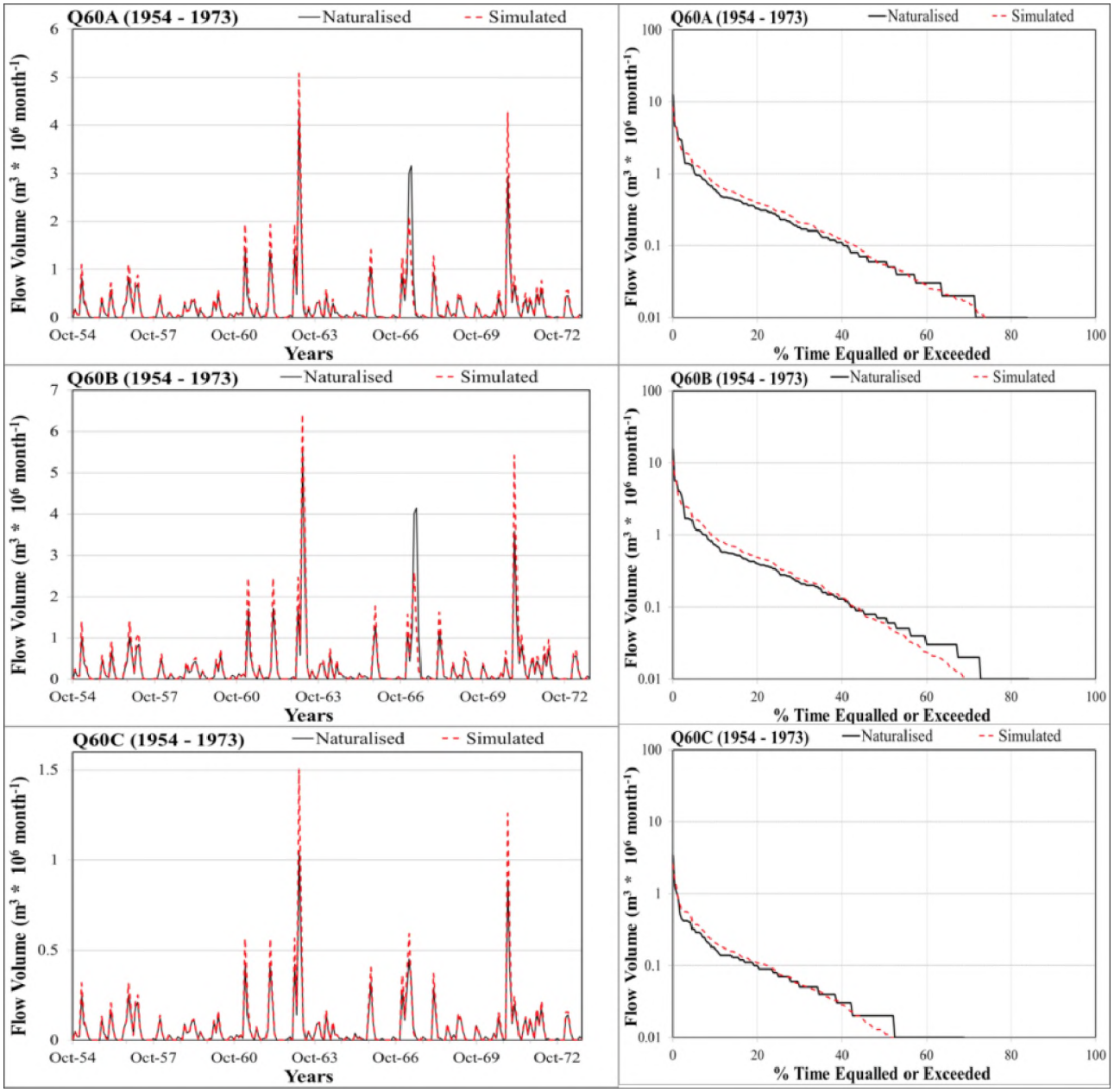

Figure 5.6: Hydrographs and FDCs comparisons of the WR2005 naturalised flows with the simulated monthly flows for the Baviaans River catchment.

5.3. ASSIGNING THE INITIAL PARAMETER UNCERTAINTY RANGES

The model calibration results obtained from the first part of the modelling process (section 5.2) were aimed at establishing the 'mean values' of the uncertain parameter bounds (minimum and maximum) that are likely to generate an acceptable natural hydrological response. The conceptual understanding of the Pitman model parameters (Kapangaziwiri and Hughes, 2008) and calibration principles (Hughes, 2013, 2014a) together with a qualitative interpretation of the physical catchment characteristics (Kapangaziwiri *et al.*, 2012) were used to assign and constrain the initial ranges of possible uncertain parameter values for each sub-catchment. This was done as a means of overcoming the parameter identifiability and equifinality problems of the Pitman model that have been noted in previous studies as well as to overcome the limitation of a manual calibration approach (Hughes *et al.*, 2010a). The structured uncertainty version of the model, which employs a simple Monte-Carlo sampling technique to explore the parameter space of 10 000 ensembles, was used to establish uncertain parameter sets that could simulate the naturalised flows. This modelling step involved the grouping of sub-catchments assumed to have similar hydrological response characteristics into clusters that have more or less similar model parameter ranges. The model was set-up to simulate the naturalised incremental flow contribution of each sub-catchment (without routing the flow downstream) and comparing it to the WR2005 naturalised flows. Attempts to formulate individual constraints for the model parameters were jeopardised by the fact that there are relatively few gauged sub-catchments, especially in the mountainous headwater areas, where the observed stream flow data or other measured physical characteristic information could be used. Therefore, an ensemble was considered behavioural if its resulting simulation comparison with the WR2005 naturalised flow was within the set threshold (see section 3.2.4) of the four objective functions used.

The initial uncertainty ranges of the model parameters representing dominant hydrologic processes in a catchment were subjectively set to be quite large to account for many possible parameter combinations. The parameters included were only those affecting the main runoff generation, soil moisture and groundwater accounting part of the model. The following assumptions were used to set the ranges:

- Catchment absorption parameters (ZMIN and ZMAX) were generally set mostly to low values for the steeper areas and higher values for the downstream sub-catchments with

relatively flat landscapes. This was important for conditioning the model to generate more infiltration excess surface runoff in the steeper areas than in the low-lying flat areas.

- The maximum unsaturated storage parameter (ST) had its uncertainty ranges set to lower values in the steep headwater sub-catchments to account for small moisture storage capacity and to higher values for the downstream flat areas where soils are assumed to be deeper on average.
- The uncertainty ranges of the maximum monthly interflow (FT) and groundwater recharge (GW) parameters were set to higher values for the wetter areas with steeper slopes and to lower values for semi-arid areas. The two lower estimates of recharge given in the GRAII database (DWAF, 2005b) were used to constrain the uncertainty ranges of the GW parameter, an approach suggested by Kapangaziwiri *et al.* (2012).
- The ranges of the nonlinear power functions of the two equations that control the interflow and groundwater recharge estimations (POW and GPOW) were set to different values for different sub-catchments depending on the understanding of the dominant hydrological processes. Lower values of POW and GPOW account for less variable amounts of interflow and groundwater recharge, whereas higher values reflect more volumes of these fluxes.
- The riparian evapotranspiration parameter (RIP) was set to lower values for the steep headwater areas than for the relatively flatter downstream sub-catchments.

Based on previous experience of applying the model (e.g. Kapangaziwiri *et al.*, 2012; Tumbo and Hughes, 2015) the values of the rainfall distribution factor (RDF), impervious area (AI), interception (PI1 and PI2), groundwater geometry (D.Dens, S_t, T, GWSlope, and RWL), flow attenuation (CL and TL), and the evapotranspiration factor (FF) parameters were not set as uncertain but fixed to the values given in Table 5.1. While it is noted that these parameters will have an impact on the catchment absorption capacity and the timing and distribution of flow (low flows particularly), their impacts are lower compared to the other parameters.

Since the focus of this study was on evapotranspiration processes represented by the Pitman model, parameter R was initially set with large ranges as a means of understanding the effects of the variations in the values of this parameter. These ranges were then narrowed using information on the physical characteristics of the catchments. The ranges with lower values (close to 0) indicate that the catchment has deep-rooted vegetation, which relies on large unsaturated soil moisture storage while

higher values (close to 1) represent shallow-rooted vegetation with limited soil moisture storage. Due to the heterogeneity of the unsaturated soil storage across the catchment, parameter R was assumed to be highly uncertain and therefore assigning the values of the ranges was somewhat subjective.

Modelling experience and conceptual understanding of the Pitman model (e.g. Hughes *et al.*, 2010a; Tumbo and Hughes, 2015) suggest that the low flows can be generated from both interflow (FT) and groundwater (GW) with many combinations (e.g. low FT/high GW and higher FT/low GW) which can produce the same simulation results in terms of low flows. The wide range in FT and GW makes it difficult to identify and separate individual contributions for each of these parameters. This equifinality problem is further exacerbated by additional power parameters (POW and GPOW) which also influence the simulated volumes of low flows. Multiple combinations of these four parameters represent a significant source of equifinality in the Pitman model. It is therefore difficult to resolve this equifinality without additional physical characteristic data to suggest whether interflow processes dominate over groundwater drainage or vice versa (see Tanner and Hughes, 2015). The use of the combination of FT, POW, GW, and GPOW parameters has the potential to narrow the range of behavioural combinations than the full range based on initial values. The combination can be based on the model's ability to generate moderate flows (FT/POW), low flows (GW/GPOW), or an index which is a combination of all four parameters and is defined as FT/POW + GW/GPOW.

Table 5.2 presents the initial ranges of the uncertain parameters that were assumed to produce a variety of acceptable hydrological responses. Table 5.3 gives the minimum and maximum values of the uncertain, but behavioural, parameters that were considered an acceptable representation of the naturalised flows for the selected catchments based on the selection criteria described in section 3.3.4. Under model performance in Table 5.3, model performance statistics of some of the behavioural ensembles are given. The thresholds set to select the behavioural ensembles were 0.80 for both *CE* and *CE (ln)* and within the ±10 for *%BIAS* and *%BIAS (ln)*.

Table 5.2: Initial ranges of the uncertain parameters for the selected sub-catchments

Parameter	Sub-catchments																					
	T11A		T11B		T11C		G10E		K40A		R20A		R20B		R20C		Q60A		Q60B		Q60C	
	Min	Max	Min	Max	Min	Max	Min	Max	Min	Max	Min	Max	Min	Max	Min	Max	Min	Max	Min	Max	Min	Max
ZMIN	10	120	20	130	10	150	10	150	5	20	10	120	20	180	50	180	10	90	10	90	10	90
ZAVE	150	450	250	550	200	600	250	950	50	350	180	405	180	310	225	610	150	350	150	280	130	280
ZMAX	350	800	500	900	400	1100	300	1100	100	450	350	700	300	850	400	950	250	800	250	800	250	700
ST	90	180	90	280	50	300	180	650	30	200	70	220	50	350	100	310	120	250	100	280	100	280
POW	3.0	3.5	3.0	3.5	3.0	3.5	2.0	3.8	1.5	3.0	1.5	3.5	2.0	3.8	2.0	3.8	3.0	3.5	3.0	3.5	3.0	3.5
FT	5.0	30.0	5.0	30.0	5.0	20.0	10.0	60.0	10.0	40.0	20.0	65.0	3.0	25.0	5.0	25.0	0.0	2.0	0.0	2.0	0.0	2.0
GW	1.4	4.0	1.2	3.8	2.6	5.0	1.8	3.7	1.7	3.8	2.7	5.6	0.9	3.0	1.2	3.6	0.3	1.5	0.8	2.4	0.4	1.7
R	0.3	0.7	0.3	0.7	0.3	0.7	0.3	0.7	0.3	0.6	0.0	0.5	0.0	0.6	0.0	0.5	0.3	0.7	0.3	0.7	0.3	0.7
GPOW	2.8	3.5	2.8	3.5	2.8	3.5	2.0	3.6	2.0	3.0	3.0	3.8	3.0	3.5	3.0	3.8	2.0	3.5	2.0	3.5	2.0	3.5
FT/POW	1.7	8.6	1.7	8.6	1.7	5.7	5.0	15.8	6.7	13.3	13.3	18.6	1.5	6.6	2.5	6.6	0.0	0.6	0.0	0.6	0.0	0.6
GW/GPOW	0.5	1.1	0.5	1.1	0.9	1.4	0.9	1.0	0.9	1.3	0.9	1.5	0.3	0.9	0.4	0.9	0.2	0.4	0.4	0.7	0.2	0.5
FT/POW+ GW/GPOW	2.2	9.7	2.2	9.7	2.6	7.1	5.6	16.8	7.6	14.6	14.2	20.1	1.8	7.5	2.9	7.5	0.2	1.0	0.4	1.3	0.2	1.3
RIP	0.1	0.2	0.1	0.2	0.1	0.3	0.1	0.3	0.0	0.2	0.1	0.4	0.0	0.25	0.1	0.3	0.10	0.30	0.10	0.30	0.10	0.30

Table 5.3: Final input parameter ranges (minimum and maximum) and the objective functions results for the selected sub-catchments

Parameter	Sub-catchments																					
	T11A		T11B		T11C		G10E		K40A		R20A		R20B		R20C		Q60A		Q60B		Q60C	
	Min	Max	Min	Max	Min	Max	Min	Max	Min	Max	Min	Max	Min	Max	Min	Max	Min	Max	Min	Max	Min	Max
ZMIN	10	120	21	130	10	149	11	146	5	20	10	120	21	109	50	180	10	24	10	33	10	29
ZAVE	192	381	275	508	209	568	260	567	141	350	175	360	126	300	256	477	267	330	222	274	224	257
ZMAX	351	788	500	899	400	1095	300	657	172	438	350	700	303	848	407	950	503	634	562	713	593	689
ST	90	180	90	275	50	113	239	479	31	200	70	220	51	349	150	310	122	241	112	274	100	266
FT/POW	1.7	9.4	1.9	5.8	1.8	5.7	3.4	17.1	5.1	14.4	10.7	30.1	2.3	10.1	2.9	9.1	0.0	0.6	0.1	0.5	0.0	0.6
GW/GPOW	0.4	1.2	0.4	1.3	0.0	1.0	0.6	1.5	0.6	1.8	0.7	1.8	0.3	1.0	0.2	1.0	0.1	0.7	0.0	0.6	0.0	0.7
FT/POW+ GW/GPOW	2.8	10.3	3.0	6.8	1.8	6.7	4.5	18.0	6.0	16.2	12.2	31.6	3.4	11.4	3.4	9.6	0.2	1.1	0.2	1.0	0.2	1.0
R	0.3	0.6	0.3	0.7	0.4	0.7	0.3	0.7	0.3	0.6	0.	0.5	0.0	0.6	0.0	0.5	0.3	0.7	0.3	0.7	0.3	0.7
RIP	0.1	0.2	0.1	0.2	0.0	0.3	0.1	0.3	0.0	0.2	0.1	0.4	0.2	0.4	0.1	0.3	0.1	0.3	0.1	0.3	0.1	0.3
Model performance																						
Ensembles	290		518		131		77		184		974		220		705		53		28		38	
CE	0.87	0.97	0.80	0.84	0.90	0.93	0.80	0.93	0.80	0.87	0.91	0.99	0.88	0.98	0.89	0.99	0.87	0.99	0.85	0.99	0.83	0.99
CE (ln)	0.80	0.94	0.80	0.86	0.80	0.85	0.84	0.98	0.80	0.86	0.84	0.96	0.80	0.94	0.81	0.96	0.80	0.94	0.80	0.92	0.80	0.94
%BIAS	-9.9	9.8	-9.9	9.9	-9.9	2.3	-9.9	9.5	-9.9	1.4	-9.9	9.6	-9.8	9.9	-9.9	9.8	-9.8	9.9	-9.4	8.8	-9.5	9.2
%BIAS (ln)	-9.9	9.9	-9.9	9.9	-9.9	9.7	-9.9	9.8	-9.9	8.6	-9.9	9.9	-9.8	9.9	-9.9	9.9	-9.9	9.1	-8.0	8.6	-7.9	9.1

5.3.1. The Xhora River Catchment

Out of the 10 000 generated ensemble outputs for each sub-catchment, 230 (T11A), 45 (T11B), and 578 (T11C) behavioural ensembles were capable of representing acceptable naturalised flows. The results in Table 5.3 show the *CE* and *%BIAS* values for both untransformed and log-transformed data are above 0.8 and are within the ±10% set threshold, respectively. Figure 5.7 illustrates the upper and lower uncertainty bounds of the FDCs for the simulated and naturalised flows.

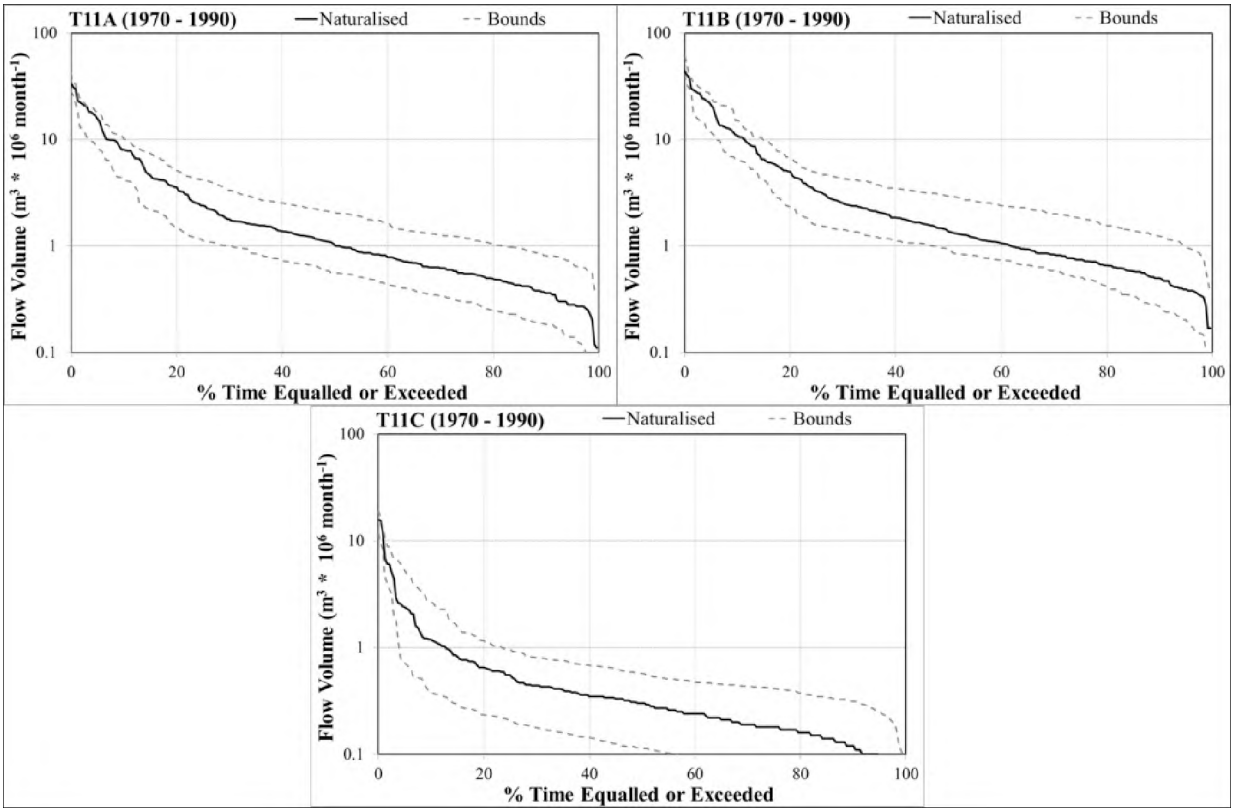

Figure 5.7: Flow duration curves of the WR2005 naturalised flows and the uncertainty bounds of the full range of the ensembles for three sub-catchments of the Xhora River.

The predominant dry conditions of the area, particularly in the lower sub-catchment T11C, and moderately wetter steep headwater areas (T11A and T11B) constitute varying catchment absorption dynamics across the area. The steep mountainous areas, with grassland vegetation, are expected to have lower absorption rates than the flatter areas with small patches of natural forest. However, the presence of eroded soils in the low-lying areas (T11C) – from Google Earth (2013) imagery analysis – could be an indication that more surface runoff is generated in the low-lying valleys. The uncertain but behavioural parameters given in Table 5.3 suggest that the values of the catchment absorption

parameters (ZMIN and ZMAX) could be considered acceptable to represent the dynamics of catchment absorption that generate surface runoff. A wide range of maximum moisture storage capacity (ST) values reflects shallow to moderately deep-clay loam soil characteristics across the catchment. POW values were considered representative of the expected interflow processes in the catchment since the steeper areas are expected to have higher rates of water losses from the unsaturated storage zones (low values of POW) than the relatively flat areas (high values of POW). The values of the FT parameter reflected a variation in topographic slope as well as a high drainage density. The low flow regime of the catchment is thought to be sustained by relatively small volumes of groundwater, which sustains the base flows. The values for the GW parameter were relatively small and had a range, which reflect the assumed differences in recharge rate across the catchment. As expected, the values of the GPOW parameter were high, representing highly variable (in time) rates of groundwater recharge. High values of the RIP parameter reflect higher losses in the downstream areas due to wider riparian margins than the steep areas with narrow channels and assumed narrow riparian zone. The behavioural values representing all the above-mentioned processes were assumed to be acceptable as the naturalised flows fall within the uncertainty bounds of the low flow component of the FDCs. The presence of the dominant grassland vegetation in the catchment signifies that evapotranspiration losses are smaller than in the mountainous areas where there are small clusters of natural forest with deep roots. The resulting uncertain range of the parameter R indicates that there is large uncertainty in in the range of ET expected in the catchment.

5.3.2. The Klein Berg River Catchment

The simulations of the naturalised flows for the Klein Berg River were obtained from the behavioural ensembles listed in Table 5.3 (the G10E column) based on the defined objective functions in the 'model performance' row. Only 136 ensembles out of the 10 000 generated were considered as acceptable to present the naturalised flow of the catchment for the period October 1920 - September 1985. The resulting uncertainty bounds of the FDC between the simulated and naturalised flow are illustrated in Figure 5.8.

The Klein Berg River is characterised by relatively steep terrain and flat valleys with deep and well-drained soils. The topographic nature of the catchment suggests that the steep areas have low infiltration capacity compared to the relatively flat valley floors. This is reflected in the small to moderate ZMIN and ZMAX values where valley floors would have higher absorption capacity (251

– 694 mm month^{-1}) than the steep areas (30 mm – 138 mm month^{-1}). Figure 5.8 illustrates that the upper band of the high flow regime is close to the naturalised flows and this may be attributed to the uncertainties in the rainfall inputs which may not adequately represent catchment average rainfall in the steeper parts of the catchment. The dominant soil characteristics are linked to the high absorption capacity and are reflected with high values of the ST parameter. Interflow was expected to be relatively high in the steep areas with low unsaturated soil moisture storage and gradually reduce with lower slopes of the flat valleys. The resulting behavioural values of the FT component ranged from 10–58 mm month^{-1}. As the catchment falls within the TMG region, it is expected to have high groundwater recharge that sustains the low flows during the dry season. The values of the GW parameter were set to fall within the estimates suggested by the GRAII database and show a wide band of the low flow regime (see Figure 5.8). Evapotranspiration losses are assumed to be small since the catchment does not have deep-rooted natural vegetation. However, RIP values were assumed to account for relatively high losses because the catchment tributaries have substantial riparian vegetation margins.

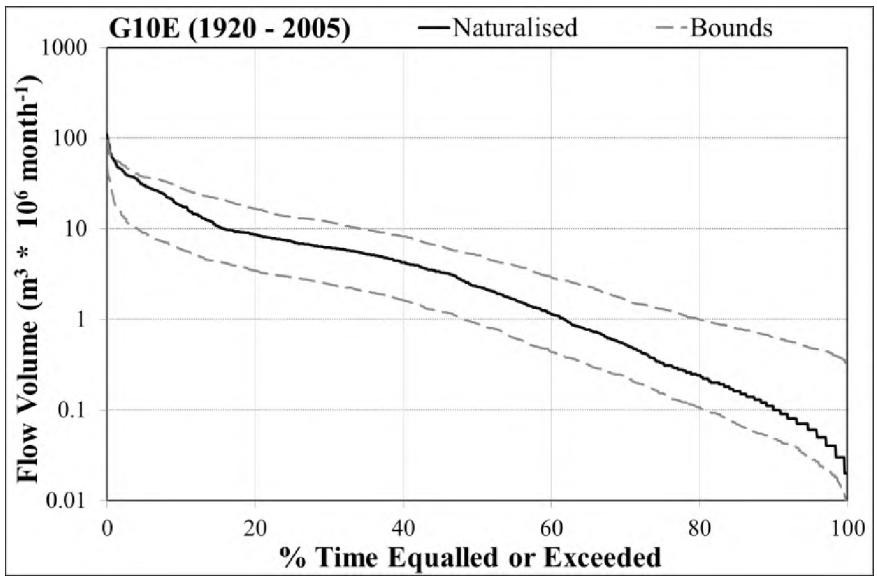

Figure 5.8: Flow duration curves of the WR2005 naturalised flow and the uncertainty bounds of the full range of the ensembles for the Klein Berg River catchment.

5.3.3. The Diep River Catchment

The simulation results presented in Figure 5.9 are for the period October 1960 - September 1980 and were obtained with the initial ranges of uncertain parameters given in Table 5.2 (the K40A column).

Table 5.3 (the K40A column) shows the uncertain behavioural parameters that were obtained with the use of the defined threshold based on the four objective functions. Figure 5.9 shows that the uncertain parameters were capable of representing acceptable bounds of the moderate to low flow regime but that the high flow regime were not represented well.

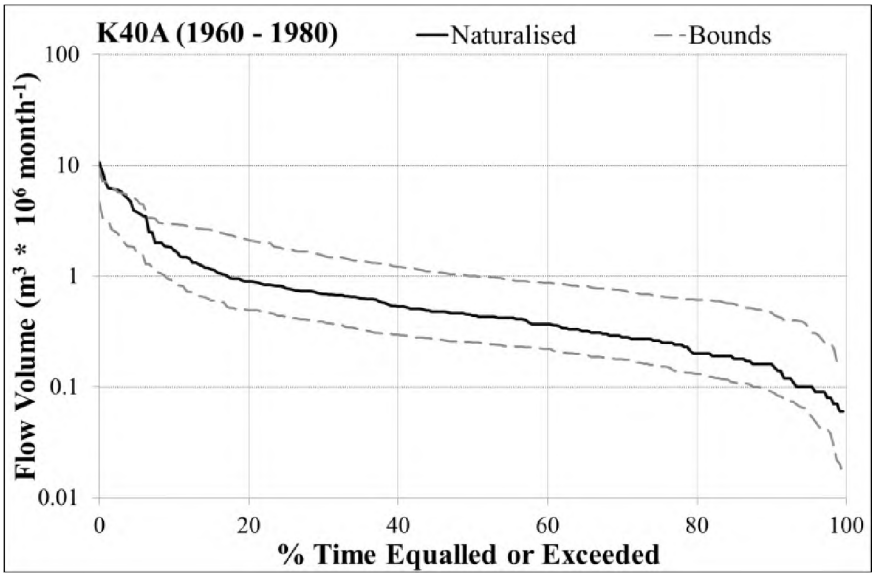

Figure 5.9: Flow duration curves of the WR2005 naturalised flow and the uncertainty bounds of the full range of the ensembles for the Diep River catchment.

The Diep River catchment is characterised by fynbos vegetation on steep slopes with shallow soils. There is, however, dense indigenous forest in the lower parts of the catchment, situated on deep well-drained soils which suggest high soil-moisture storage capacity. The ranges of the ZMIN and ZMAX parameter values reflect a low to moderately high absorptive capacity of the catchment, expected because of the differences in topography and soils. Similarly, patterns of the interflow and groundwater recharge are expected to vary with higher values expected in the steep slopes than in the downstream areas. The wide range of uncertain values of parameter POW reflect the expected differences in the interflow process across the catchment. The GPOW values were low, which indicated increased groundwater recharge in the area. While there are small patches of indigenous forest, the range of the values of parameter R indicates that acceptable simulations of the natural hydrology could be obtained with different values (low and high) of evapotranspiration in the model.

5.3.4. The Upper Buffalo Catchment

This catchment presents heterogeneous hydrological characteristics, which includes the natural forest in the high-rainfall mountainous areas, and a relatively dry and flat grassland area with erodible soils. The resulting behavioural parameters were obtained by simulating the naturalised flows for the period October 1975 - September 1995. Table 5.3 (column R20A to R20C) lists the ranges of the uncertain model parameters and the objective functions obtained from 1192, 333, and 790 behavioural ensembles for R20A, R20B, and R20C, respectively. Figure 5.10 presents the simulated bounds of the full range of uncertainty together with the FDC of the naturalised flows. The figure shows a well-enveloped simulation of the moderate to low flows for the all the sub-catchments.

The catchment is characterised by mountain reaches which have small absorptive capacities compared to the low-lying areas which have well-drained clayey loams. The values of the ZMIN and ZMAX parameters reflect these dynamics where higher values are expected for the low-lying areas than the mountainous areas. The visual inspection of the vegetation cover from Google Earth (2013) imagery suggests that the unsaturated soil moisture storage (ST) is highly variable across the catchment. The steep slopes of the mountaintops are expected to have lower ST values than the plateau and further downstream. However, the presence of some patches of the dense natural forest in the mountain escarpment could be an indicator of the unsaturated moisture store variability because soils are expected to be deeper in an area with such vegetation. The resulting ST values have a range that was considered representative of the variability where deep soils (higher values) are expected in the low-lying areas of the catchment than the in the mountain tops (lower values). The wide ranges of the FT and POW parameter values could represent a dominant interflow process in the steeper areas. The uncertainty ranges of the GW and GPOW parameters suggest that groundwater contributes small volumes that sustain the base flow during the dry season. The presence of indigenous forest in the mountainous areas of the headwater sub-catchments indicates higher evapotranspiration losses than the low-lying areas that have savanah vegetation. The uncertain values of parameter R were assumed to account for these differences as they cover the range of evapotranspiration dynamics that are expected from this catchment. Riparian channel losses to evapotranspiration were expected because of the aridity of the lower parts of the catchment reflected in the RIP values.

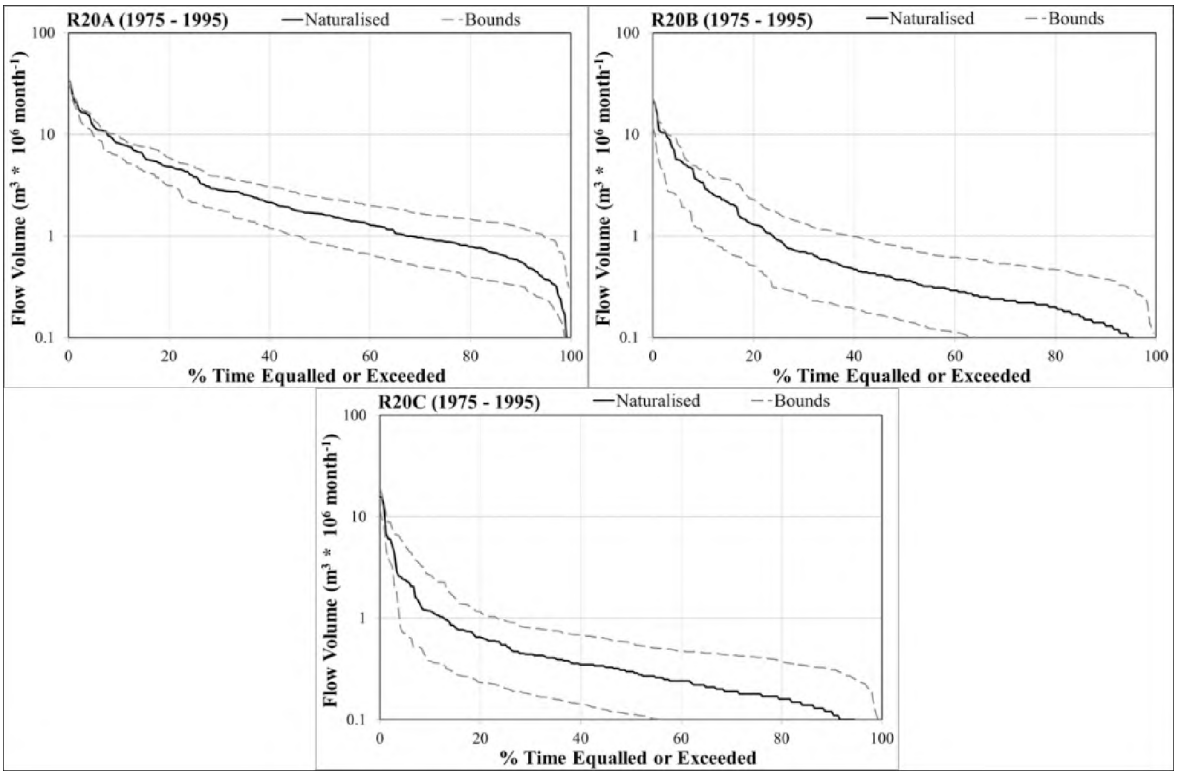

Figure 5.10: Flow duration curves of the WR2005 naturalised flow and the uncertainty bounds of the full range of the ensembles for the Upper Buffalo River catchment.

5.3.5. The Baviaans River Catchment

The model was set up to simulate the naturalised flows for the period October 1955 - September 1975. The resulting behavioural ensembles are listed in Table 5.3 (column Q60A to Q60C) together with the ranges of the four objective functions. Figure 5.11 illustrates the full uncertainty bounds together with the FDCs of the simulated and naturalised flows. The number of the behavioural ensembles varied significantly between sub-catchments (Table 5.3). Nevertheless, the values of the four objective functions indicate that the behavioural ensembles successfully represent the natural hydrology of the catchment.

The Baviaans River catchment is located in a relatively dry area which is dominated by arid vegetation underlain by shallow and poorly-drained sandy loam soils. The values of the ZMIN and ZMAX parameters reflect that small amounts of rainfall generate surface runoff and they signify the flashy nature of the catchment. Steep slopes in the high-lying areas have thin soils compared to those in the river valleys and the values of the ST parameter reflect these characteristics. The interflow process does not play a significant role in the generation of runoff from the unsaturated

storage because of the limitation in unsaturated soil moisture storage. This led to the conclusion that a significant proportion of the stream flow is generated from the infrequent infiltration excess surface runoff. The intermittent nature of the tributaries of the catchment is a clear indicator that groundwater makes a relatively small contribution to sustaining the low flows during the dry season. Hence, the values of GW parameter were small. High potential evapotranspiration in the area suggests that water from thin unsaturated soil storage is lost through evapotranspiration and the wide range of the values of parameter R were considered to represent this process despite the fact that water losses are through the shallow-rooted vegetation.

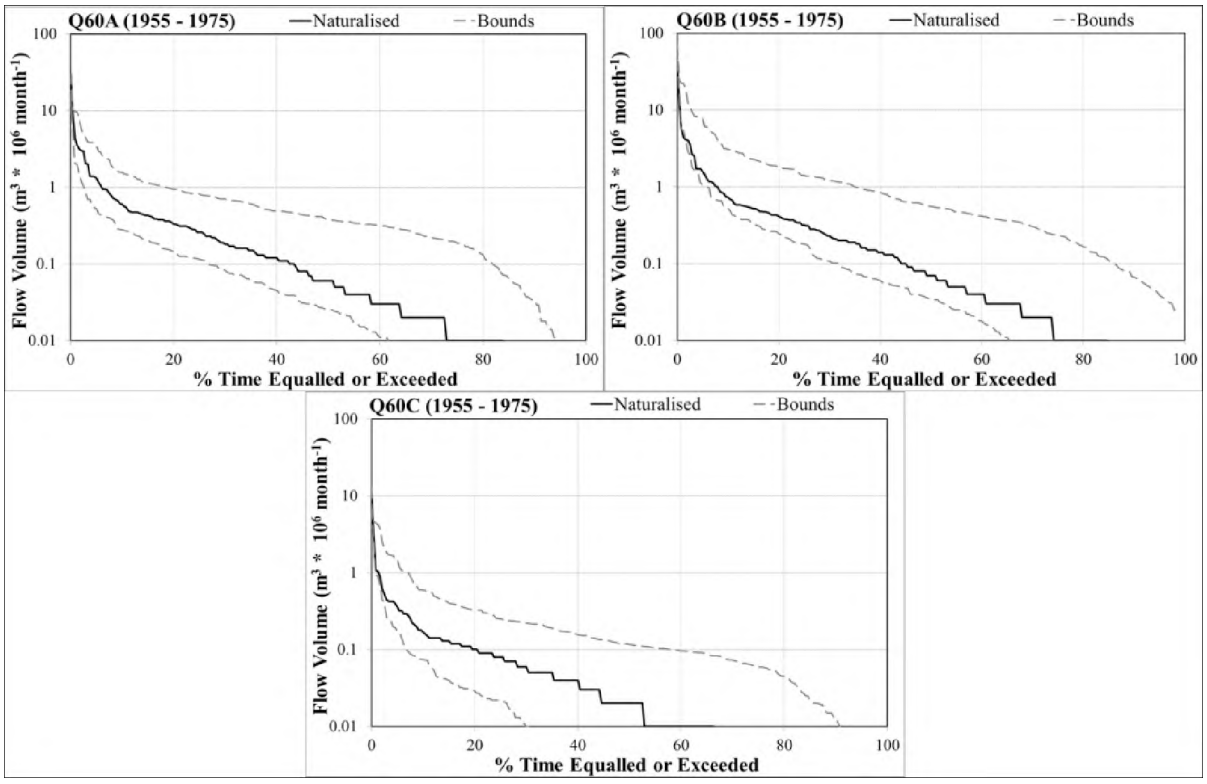

Figure 5.11: Flow duration curves of the WR2005 naturalised flow and the uncertainty bounds of the full range of the ensembles for the Baviaans River catchment.

5.3.6. Parameter Uncertainties

The model parameters listed in Table 5.2 were used to define the parameter space capable of representing parameter combinations that can simulate an acceptable hydrological response. This sub-section presents the comparisons of uncertain, but behavioural, parameters (in Table 5.3) with the input parameter ranges. This was done as means of demonstrating three attributes: (i) the

behavioural parameters occupy the full range of defined uncertainty, (ii) the equifinality problem, and (iii) parameter identifiability issues in the model.

Figure 5.12 illustrates the ranges of the surface runoff generating parameters (ZMIN and ZMAX), unsaturated soil moisture storage (ST), maximum monthly interflow (FT), groundwater recharge (GW), and the combined effect of the medium to low flow generating parameters (FT, POW, GW and GPOW). The equifinality and identifiability of the model parameters are summarised as follows:

- The behavioural values of the ZMIN and ZMAX parameters were within the defined constraints. For the Baviaans River catchment and sub-catchment R20B of the Upper Buffalo, the ZMIN values occupy the lower end of the range. The behavioural values of ZMAX indicate a wider range in sub-catchment G10E and Xhora River catchment.
- For parameter ST, most sub-catchments occupied the full initial range except for sub-catchment T11C and G10E where the behavioural values of this parameter are biased towards lower end of the range.
- The behavioural values of the maximum interflow (FT) and groundwater recharge (GW) parameters suggest that these parameters are not easily identifiable when considered separately as it is not straightforward to identify whether groundwater or interflow is dominating the generation of medium to low flows. This results from the interactions of these parameters and the effect of the POW and GPOW functions in the generation of the flow volumes. However, because GW parameters were constrained with data from GRAII database, they suggest that a majority of the catchments had values biased towards the upper end of the initial range.
- The combination effect of interflow (FT/POW) and groundwater recharge (GW/GPOW) parameters illustrates that the range of behavioural combinations is within the range of the defined inputs for almost all sub-catchments. The exception is noted in sub-catchment R20A where high initial values of the FT parameter in combination with a low POW value resulted in upper end values of the FT, POW, GW, and GPOW combinations exceeding the initial range.

The availability of additional information could improve equifinality issues associated with many parameters of the Pitman model detailed in this sub-section.

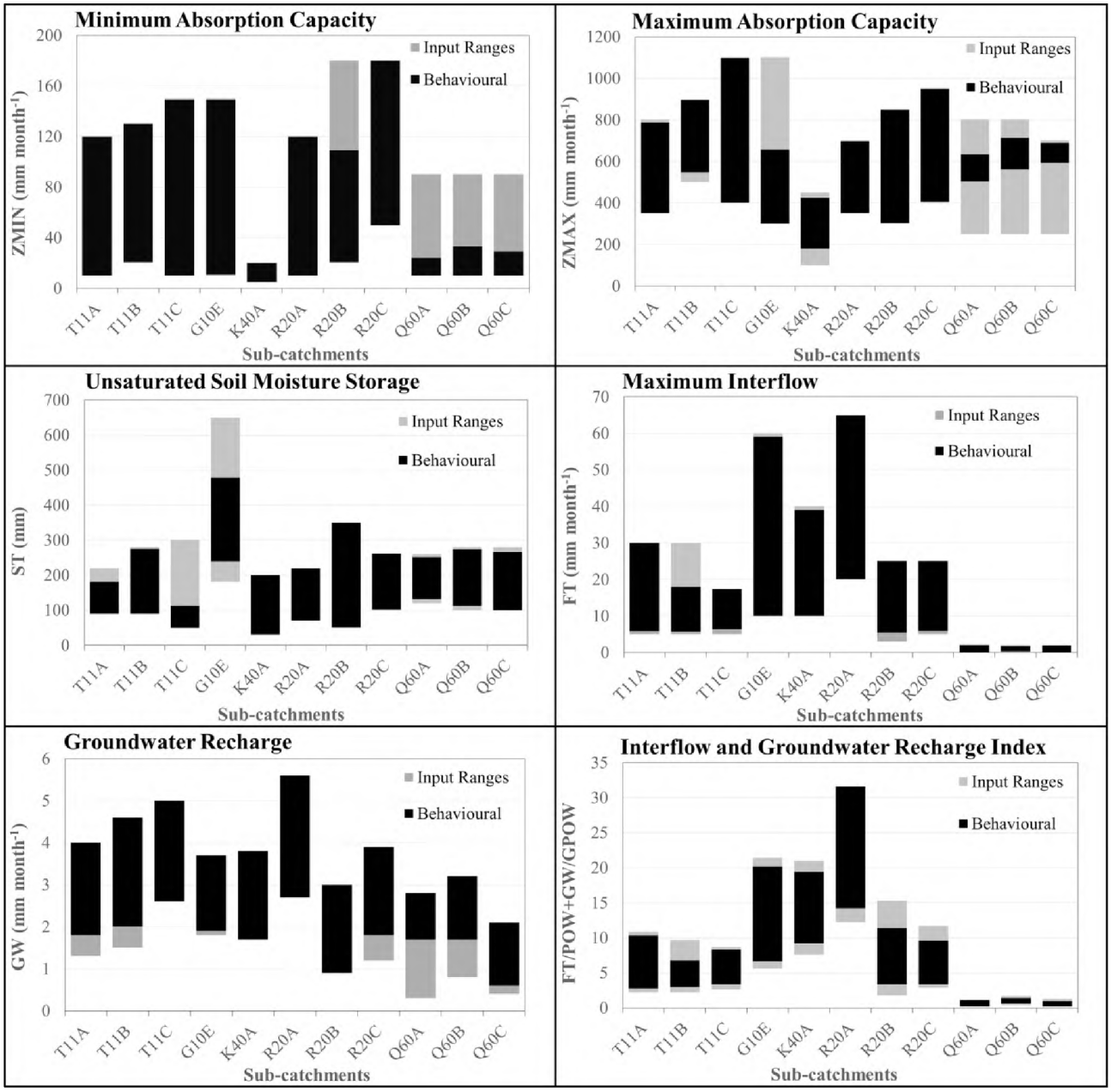

Figure 5.12: Uncertainty ranges of parameter ZMIN (minimum absorption capacity), ZMAX (maximum absorption capacity), ST (unsaturated soil moisture storage), FT (maximum interflow), GW (groundwater recharge), and range of input and output values for an index of model's potential to generate medium to low flows using the summation of FT/POW and GW/POW. The grey blocks represent the full input range whereas black blocks quantify the behavioural ensembles for all the selected sub-catchments used in this study.

5.4. MODELLING UNDER PRESENT-DAY CONDITIONS

While water resource assessments were previously based on assumptions of stationarity of hydrological processes, many authors (e.g. Milly, *et al.*, 2007) including the new IAHS scientific decade, 'Panta Rhei' (Montanari, 2013), have recognised that this assumption is no longer valid and that the modelling of hydrological processes for water assessments should account for non-stationarity. Hughes (2015) argues that non-stationarity in the model calibration can be considered if known information about changes in water resource development is available. This is valid for most of the selected catchments used in this study as they have water resource developments that have changed their flow regimes over time. Therefore, the modelling of present-day conditions incorporated the effects of the water resource development. The structured uncertainty version of the Pitman model was set-up to include all sub-catchments, and generated cumulative monthly streamflow volumes using the established 'behavioural' model parameters which were compared with the observation records.

Before commencing with the simulation of the present-day flows, trend analysis was conducted to evaluate the stationarity in the time series data of the observed flow records. It was noted earlier that a number of water resource developments affect the present-day flows in most of the selected catchments. The most common are (i) the construction of small farm dams for irrigation, (ii) run-off-river abstractions for irrigation and domestic use, (iii) managed forest plantations, and (iv) large reservoir storage. These water uses have to be quantified before comparing simulated flows with observed flow records and were included in the modelling process as follows:

(i) To account for ***farm dams***, the capacity of the small farm dams (DSTORE) was estimated using the method described in section 3.2.4 which is based on the assumption that the dams are at full capacity. Due to the uncertainty in the values of the total farm dam volume resulting from the difficulties in aggregating all dams into a single storage (Hughes and Mantel, 2010b), a uniform uncertainty distribution was used to specify the minimum and maximum values in the model. The estimates of the percentage of the catchment area contributing runoff to the farm dams (DAREA) were estimated based on an analysis of Google Earth (2013) imagery through the delineation of a polygon and calculating its area. In some cases, it was difficult to determine this value because of the spatial distribution of the dams across the catchment and the values were set as uncertain

in the model using a uniform distribution. The distinction between the ***irrigated areas supplied by farm dams*** (IRRIG) and from ***run-off-river abstractions*** (AIRR) were drawn from a subjective approach which involved the identification of parcels of land that appeared to be under irrigation closer to the farm dams and those that are allocated along the riverbanks, through Google Earth (2013) imagery visual inspection. It must be noted that there were difficulties in differentiating whether the irrigated areas are supplied by run-off-river abstractions or from small farm dams. Information from the WARMS database (DWS, 20014a) was also used to substantiate the source of irrigation water. It is also worth noting that the WARMS database has some discrepancies regarding registered water use, water entitlement, and actual water use, which together, could result in erroneous estimates.

(ii) The water abstractions for ***non-irrigation demand*** (RUSE) were accounted for using the information on population and assumed seasonal patterns of abstraction obtained from various sources such as DWA (2010b) and DWA (2011b). The annual values of non-irrigation water were fixed.

(iii) The areal extents of ***managed forest plantation*** (AFOR) were obtained from the WR2005 database whereas the information on large ***reservoir storage capacity*** (CAP), ***annual abstraction demand*** (ABS), and ***water release operation rules*** (RES1-5) were based on the WR2005 database and other various reports (e.g. DWA, 2011b).

The present-day flows were simulated with the use of existing regional information (Bailey and Middleton, 2008b) to define both the annual PET and fixed seasonal distributions and the resulting range of the behavioural parameter sets applying the uncertainty version of the model. The 'best' ensemble for each catchment (gauged) was selected using the best-fit-index and the simulated results are referred as Mean (Pan). The simulation period for the present-day flows was October 2000 - September 2010 except for the Noordkaap River catchment, which ends in September 2005.

5.4.1. Trend Detection Analysis

The time series of the observed stream flow records was tested for trends in monthly variability and the resulting analysis is presented in Table 5.4 as well as graphically in Figure 5.13. The table shows that all selected catchments indicate a decrease in monthly flow trend. Figure 5.13 illustrates the time series of the observed flow records which has significantly reduced mean monthly flows.

Analysis of the means and standard deviations of the monthly stream flow in the pre-change and post-change point change periods were beyond the scope of this study. While the impact of water resources developments on the present-day flows are observed, in most catchments, during the periods prior to the availability of the MOD16 data, sub-catchments T11C and Q60C are the ones that experienced changes during the period which was used to evaluate the MOD16 data.

Table 5.4: Trend test results for the monthly-observed stream flow records. Positive and negative signs of Z indicate increasing and decreasing monthly trend, respectively

Quaternary	Variable	Period	Test Z	*S*	*ρ*-value	Error (%)	Point change	P-value	Trend
T11C	Monthly	1998 - 2010	-1458	yes	$\alpha > 0.010$	1.02	Mar 2007	0.04	Downward
G10E	Monthly	1954 - 2010	-9303	yes	$\alpha < 0.099$	9.94	Sept 1997	0.08	Downward
K40A	Monthly	1961 - 2010	-6044	yes	$\alpha < 0.201$	20.15	Nov 1968	0.001	Downward
R20B	Monthly	1947 - 2010	-1783	yes	$\alpha > 000$	0.03	Apr 1990	0.0001	Downward
Q60C	Monthly	1980 - 2010	-3688	yes	$\alpha < 0.100$	10.02	May 2002	0.008	Downward
X23A	Monthly	1948 - 2010	-1064	yes	$\alpha > 0.0001$	0.01	July 1976	0.0001	Downward

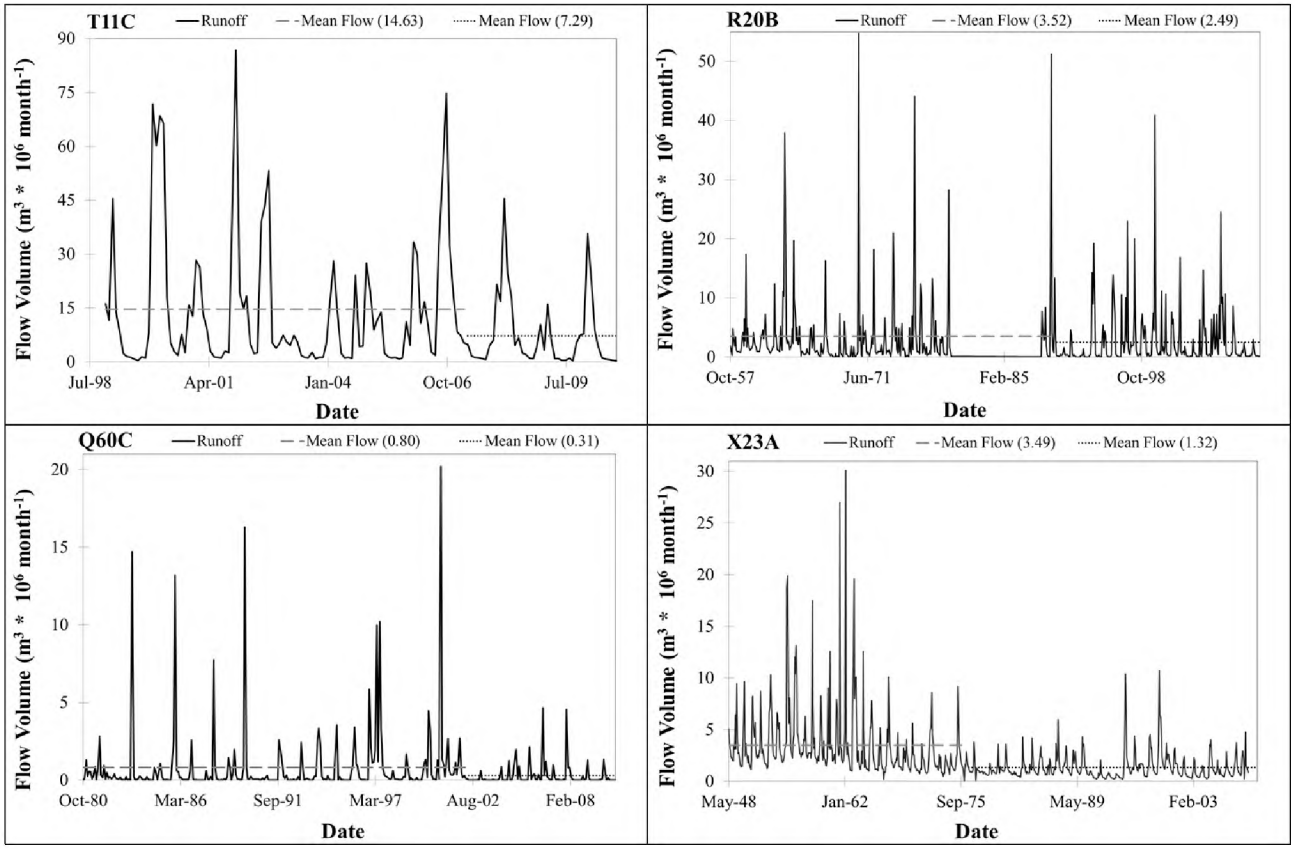

Figure 5.13: Monthly time series and long-term mean before (grey dash) and after (black dots) changes in the observed stream flow records for the T11C, R20B, Q60C and X23A.

5.4.2. Quantifying the Water Use

Xhora River Catchment

The Xhora River is the main source of domestic and municipal water for the town of Elliot and the surrounding rural areas. The town is supplied with water from the Thomson Dam located on a tributary of sub-catchment T11A. The dam has an estimated capacity of 0.45 $m^3 * 10^6$, of which 0.31 $m^3 * 10^6$ is allocated to meet the annual water requirements for the town (DWA, 2010b; DWS 2014b). The seasonal distributions of water requirements in Table 5.5 were derived from the average annual daily requirements provided in DWA (2010b). Water abstractions for irrigation are assumed to be relatively small as the majority of the cultivated land (1.2 km^2) seems (from Google Earth image visual analysis) to be irrigated from a small number of farm dams which can only be seasonally utilised during the wet season when they are filled from local runoff. Therefore, the simulation of the present-day flow did not include an irrigation component as it was assumed to have a relatively small impact on the simulated flow. The managed forest plantations (parameter AFOR) cover 7% of the total catchment area (T11A: 16%, T11B: 5%, T11C: 2%).

Table 5.5: Seasonal distributions (fractions of the annual value) of non-irrigation water demands from the Xhora River catchment

Oct	Nov	Dec	Jan	Feb	Mar	Apr	May	Jun	Jul	Aug	Sep
0.073	0.043	0.063	0.010	0.072	0.160	0.140	0.083	0.083	0.083	0.091	0.099

Klein Berg River Catchment

The tributaries of the Klein Berg River catchment supply the surrounding farms and the town of Tulbagh with water for irrigation, domestic, and municipal use. The annual water requirements for domestic and municipal use for the town (RUSE parameter) are estimated to be 0.78 $m^3 * 10^6$ (DWA, 2010a) and were distributed in the model such that the early summer months used larger quantities than winter months (see the water use row in Table 5.6). This is mainly because summer months have higher water requirements due increased tourism activities in the area (DWA, 2010a).

Of the 116 km^2 cultivated land in the catchment, only 32 km^2 is irrigated (WCDA, 2015). Table 5.6 lists the monthly irrigation water demands for the cultivated crops and their respective cultivated area. The data on irrigation water demands for individual crops were obtained from the SAPWAT software (van Heerden *et al.*, 2009). While it was difficult to determine the exact source of irrigation

water for a majority of the cultivated land, Google Earth (2013) visual assessments suggest that the majority of irrigation water is abstracted from about 323 small farm dams. These dams are distributed across the catchment, particularly in the northern parts, whereas other farms are supplied directly from rivers. Figure 5.14 shows the areal extent of the cultivated (irrigated and non-irrigated) land and the distribution of the small farm dams across the catchment, not located on the main river channel but on small drainage valleys.

Table 5.6: Irrigation water demands (mm) and total irrigated areas (km^2) for cultivated crops together with seasonal distributions of scaled irrigation demands (mm) and non-irrigation water demand (fractions of annual values) in the Klein Berg River catchment

Crops	Oct	Nov	Dec	Jan	Feb	Mar	Apr	May	Jun	Jul	Aug	Sep	Area
Apples	85	204	258	264	178	115	38	0	0	0	0	23	0.24
Apricots	160	201	220	214	149	101	37	0	0	0	0	52	0.55
Peaches	168	204	224	227	168	125	55	13	0	0	34	92	5.08
Grapes	85	116	135	151	120	89	31	0	0	0	0	23	9.93
Pears	120	211	257	279	194	123	40	0	0	0	0	27	4.86
Plums	122	179	264	274	193	124	46	0	0	0	0	23	5.66
Butternut	117	89	0	0	0	0	0	0	0	0	8	57	0.16
Lucerne	105	140	215	235	194	153	77	7	0	0	4	43	0.21
Necturines	132	171	234	226	163	109	43	0	0	0	0	37	2.32
Olives	98	170	252	273	226	140	0	0	0	0	0	25	2.79
Wheat	127	0	0	0	0	0	0	0	0	0	22	83	0.18
Irrigation	116	166	209	221	164	112	37	2	0	0	6	37	31.98
Water use	0.049	0.065	0.160	0.201	0.220	0.215	0.021	0.002	0.00	0.00	0.032	0.035	-

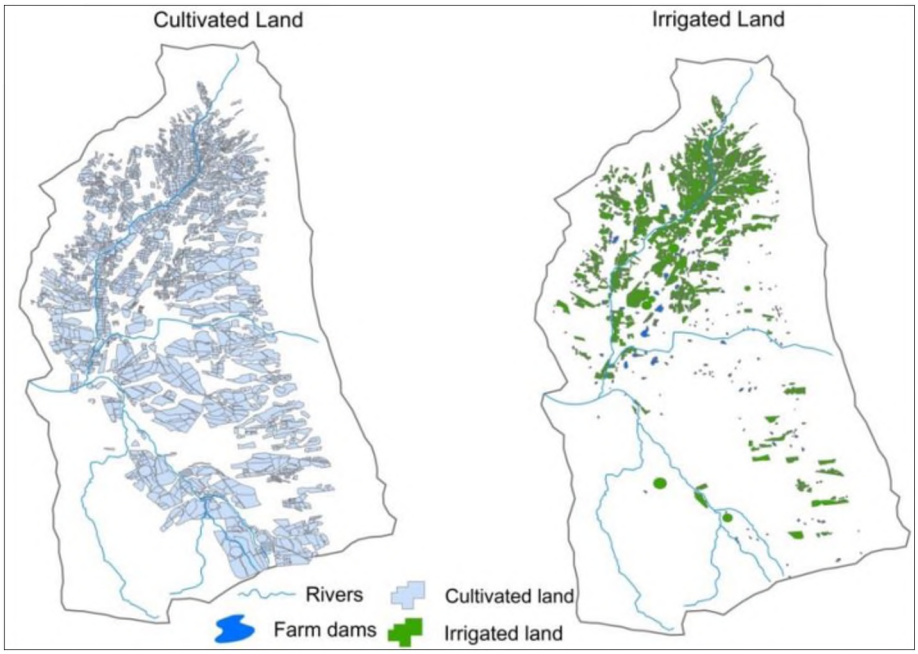

Figure 5.14: Cultivated and irrigated area together with the distribution of the small farm dams in the Klein Berg River catchment (modified after WCDA, 2015).

Irrigation return flow (IWR) and effective rainfall factor (EFFECT) were set to 0.1 and 0, respectively. The IWR value accounts for a moderately flat terrain whereas the EFFECT value represent no contribution of rainfall to irrigation during the wet season because there are relatively few cultivated crops between the month June and August. The constants (a = 4.41 and b = 0.8) from an adjacent study area (Hughes and Mantel, 2010b) and a total surface area of farm dams (47 km^2: Middleton and Bailey, 2008) were used to determine the uncertain aggregated total volume of all dams which was estimated to range between 9 to 11 $m^3 * 10^6$. The small farm dams were assumed to drain water from between 25% to 40% of the catchment area.

Diep River Catchment

Water resource developments within the Diep River catchment are dominated mainly by managed forest plantations and small patches of agricultural land which are assumed to have a relatively small impact on the flows. Figure 5.15 illustrates the land cover map for the year 2000. The model parameter accounting for evapotranspiration from secondary vegetation (AFOR) was set to 60% and the evapotranspiration-scaling factor (FF) set to 1.5. Given that the land cover features change with

time, the availability of the recent land cover (e.g. NLC, 2014) could have improved the quantification of water use in the model application.

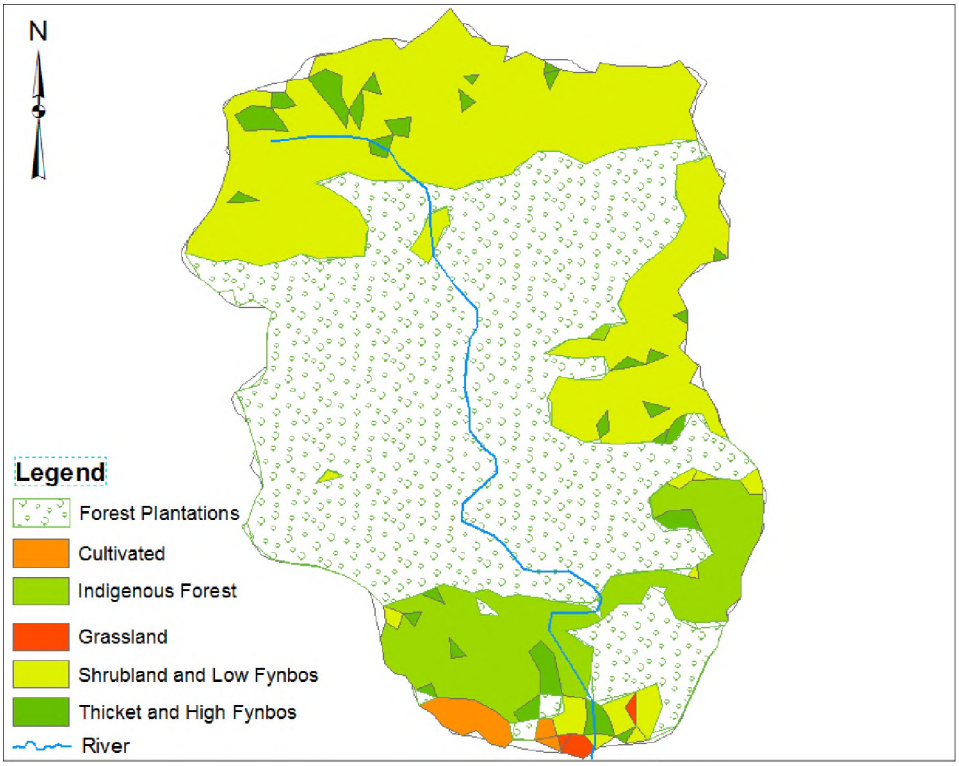

Figure 5.15: Land cover in the Diep River catchment (modified after van den Berg *et al.*, 2008).

The trend detection results presented in Table 5.4 indicate that the hydrological responses for the catchment have reduced from November 1968. Although the results do not show changes between year 2000 and 2010, changes in hydrological response could have happened due to the forest plantation cycle of clearing and re-planting. The changes in the areal extent of the forest cover for the period 2000 – 2010 were not accounted for in the model due to the lack of information related to planting and forest harvesting cycles. Simulating a hydrological response without considering non-stationarity could result in poor simulations.

Upper Buffalo River Catchment

The Upper Buffalo River supplies King Williams Town and the surrounding rural villages with water for domestic and industrial use through the Maden and Rooikrantz Dam (Figure 5.16). The two dams are located in the headwaters of R20A and have a full storage capacity (parameter CAP) of 0.33 and 4.9 $m^3 * 10^6$, respectively (DWA, 2010c).

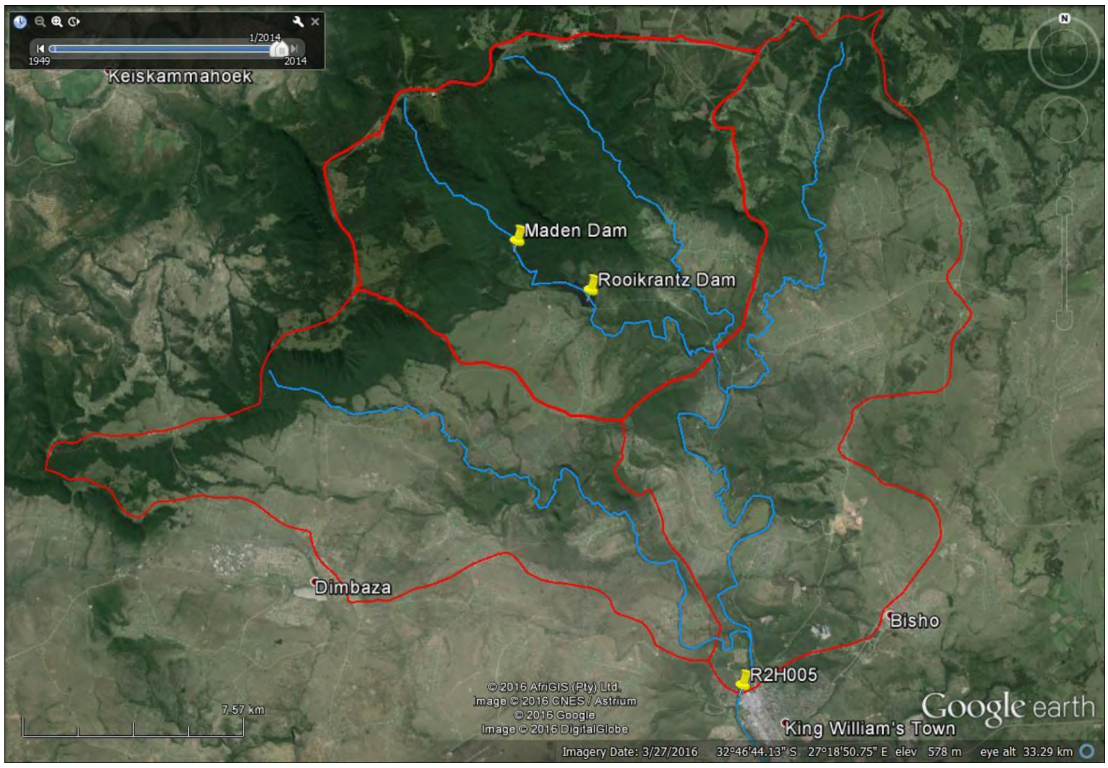

Figure 5.16: The Maden and the Rooikrantz Dams and stream flow gauging station (R2H005) in the Upper Buffalo River catchment. The red lines represent the catchment boundaries and the blue lines are the tributaries found in the catchment.

Water abstractions from the dam (Rooikrantz) are done via three separate offtakes: Da Gama textile industries, Rooikrantz and King Williams Town Water Treatment Works (WTW). The estimated annual water requirements from the Rooikrantz Dam experienced an increase from 2.8 $m^3 * 10^6$ in 2003 to 5.5 $m^3 * 10^6$ in year 2010 (Morrison *et al.*, 2001). The annual water abstractions given in Table 5.7 indicate an increase in the demand of water and the actual patterns of water. For this study, an average of 4.5 $m^3 * 10^6$ (DWA, 2011b) was used for the annual abstraction volume parameter (ABS) in the model.

Table 5.7: Domestic and industrial water abstracted from the Rooikrantz Dam (source: DWA, 2011b)

Year	2005/06	2006/07	2007/08	2008/09	2009/10
Total consumption (m^3*10^6)	4.12	4.86	4.86	4.55	5.00

The operation rules used for the Rooikrantz Dam were suggested by DWAF (2006) and decisions to reduce water releases are made on an ad hoc basis by the Amatole Works Committee of the Permanent Water Commission (DWA, 2011b). The operation rules are summarised as follows:

(i) when the dam storage is above 80% of full capacity, 4.9 $m^3 * 10^6$ $year^{-1}$ of water is released to all offtakes,

(ii) if the water storage falls from 80% to 60% and 60% to 40% of full capacity, the dam releases are reduced to 3.5 $m^3 * 10^6$ $year^{-1}$ and 2.5 $m^3 * 10^6$ $year^{-1}$, respectively,

(iii) the water volume drop between 40% and 25% of full supply capacity, 1.9 $m^3 * 10^6$ $year^{-1}$ of water is supplied only to the Rooikrantz WTW and Da Gama textile, and

(iv) if water in the dam is less than 25% of full supply capacity, a draft with 0.6 $m^3 * 10^6$ $year^{-1}$ is used.

Managed forest plantations are estimated to cover 2% in sub-catchments R20A and R20B, and 3% in R20C.

The Baviaans River Catchment

The main water resource development in the Baviaans River catchment is the farming of groundnuts and lucerne in a 3.9 km^2 area located along the river valley. Table 5.8 lists the seasonal distributions of irrigation water requirements for the cultivated crops in the catchment (Midgley *et al.*, 1994). The WARMS database (DWS, 2014a) suggests that a majority of irrigation water is abstracted directly from the tributaries of the catchment (see Table 5.9). However, the small farm dams listed in Table 5.10, with a total capacity of 0.25 $m^3 * 10^6$, are also used as a source of irrigation water (Midgley *et al.*, 1994). In sub-catchment Q60C, the Baviaans River has two water-diverting canals (see Figure 5.17) that feed two small dams: one along the riverbank and the other in the downstream sub-catchment Q70A. The unquantified volume of water from the diversion canal means that quantifying the present-day hydrological regime of the Baviaans River catchment is difficult.

Table 5.8: Seasonal distribution of irrigation water requirements (mm) for groundnuts and Lucerne in the Baviaans River Catchment (source: Midgley *et al.*, 1994)

Oct	Nov	Dec	Jan	Feb	Mar	Apr	May	Jun	Jul	Aug	Sep
85	204	258	264	178	115	38	0	0	0	0	23

Table 5.9: Active registered water users for irrigation in the Baviaans River catchment (source: DWS, 2014a)

Sub-catchment	Start Date	WU Sector	Resource Name	Volume (m^3*10^6/a)
Q60A	01/02/1983	Irrigation	Baviaans River tributary	0.068
	01/01/1994		Baviaans River	0.057
	01/03/2005		Upper Baviaans River	0.067
	01/08/1990		Baviaans River	0.018
Q60B	01/03/2000		Bosfontein River	0.004
	01/10/1998		Baviaans River	0.044
	01/01/1969		Daggaboerloop River	0.003
	01/10/1993		Baviaans River	0.120
	01/01/1969		Baviaans River	0.007
Q60C	01/10/1998		Baviaans River	0.044
	01/01/1969		Daggaboerloop River	0.003
	01/10/1993		Baviaans River	0.120
	01/01/1969		Baviaans River	0.007

Table 5.10: Registered small farm dams in sub-catchment Q60A of the Baviaans River (source: Midgley *et al.*, 1994)

Drainage	Dam name	Construction year	Capacity (m^3*10^6)	Surface area (km^2)
Q60A	Waterkloof No.1	1968	0.100	0.04
	Waterkloof No.2	1987	0.075	0.04
	Geit-hoek	1950	0.072	0.01

Figure 5.17: Google Earth image showing water diversion canal and cultivated areas in the Baviaans River. The red place mark represents cultivated land whereas blue line is the river diversion canal.

Noordkaap River Catchment

Figure 5.18 illustrates the land cover and the land use of the Noordkaap River catchment based on Google Earth image. The figure shows that managed forest plantations and a relatively small area under irrigation dominate the catchment water uses. While these water use activities affect the flow patterns and hydrological regime of the catchment, irrigation was assumed to have a relatively small impact and was ignored for the simulation of the present-day flows. The afforested area (AFOR parameter) was populated to represent 70% of the catchment area. FF and PI2 parameters were set with uncertain values, which range from 1 to 1.4 and 4 to 10 mm, respectively, to account for increased evapotranspiration and large interception storage from densely deep-rooted forest plantations.

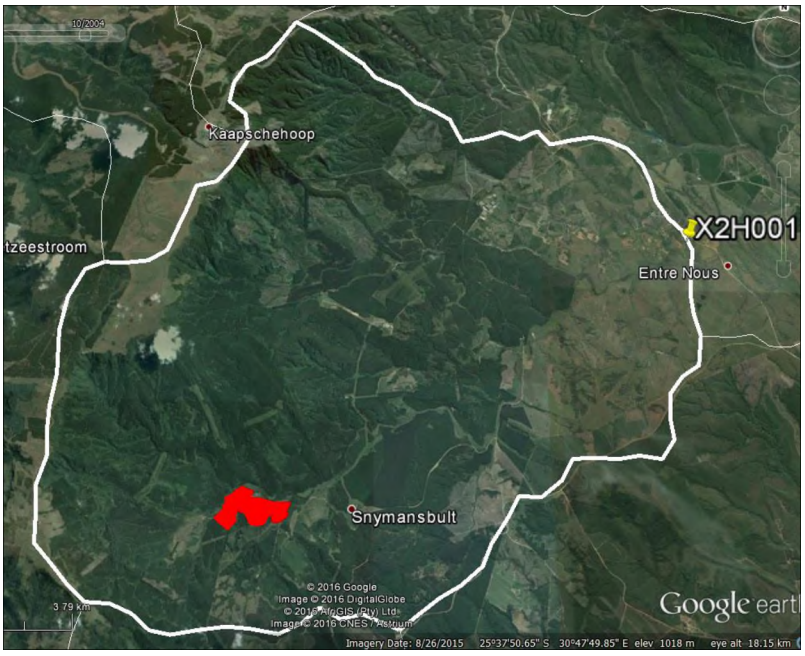

Figure 5.18: Google Earth image showing the areal extent of the managed forest plantations and cultivated land (red) in the Noordkaap River catchment. The white colour represents the catchment boundary.

The water use data from various sources have high degree of uncertainties, which affects the modelling results. In this study, some of the water use data were fixed to estimated values while others were treated with a high degree of uncertainty. Table 5.11 lists the minimum and maximum values of some of the water use parameters, which were used in the simulation of the present-day flow conditions, while the other water use parameter data are included in the text.

Table 5.11: The uncertainty bounds of the water use data for some of the sub-catchments used in the study

Sub-catchment		***Maximum dam storage ($m^3 * 10^6$)***		***Non-irrigation water ($m^3 * 10^6$ $year^{-1}$)***		***% of area above dams***		***Irrigated area (km^2)***	
		Min	*Max*	*Min*	*Max*	*Min*	*Max*	*Min*	*Max*
Xhora River	T11A	-	-	0.28	0.35	-	-	-	-
Klein Berg River	G10E	8.00	10.00	0.65	0.95	20	30	25	40
Baviaans River	Q60C	0.09	0.11	-	-	10	20	0.5	0.9

5.4.3. Quantification of Uncertainties in the Simulated Present-day Flows

This sub-section presents the full range of uncertainty of the simulated flows with water use data. Table 5.12 lists the minimum and maximum values of the four objective functions (*CE, CE {ln}*,

%BIAS and *%BIAS {ln}*) for gauged sub-catchment and their respective number of behavioural ensembles. While all the sub-catchment had acceptable *%BIAS* values (untransformed and log-transformed data), some had *CE* and *CE (ln)* values below 0.5 and are highlighted in grey.

Table 5.12: The range of performance measure statistics for the present-day simulations and the number of acceptable ensemble outputs for the gauged sub-catchments

Catchment	*CE*	*CE (ln)*	*%BIAS*	*%BIAS (ln)*	No. of Ensembles
Xhora (T11C)	0.43 : 0.53	0.74 : 0.82	-9.81 : 2.52	-6.32 : 9.90	77
Klein Berg (G10E)	0.20 : 0.32	0.51 : 0.69	-9.80 : 6.53	-9.90 : 9.94	57
Diep (K40A)	0.83 : 0.89	0.50 : 0.65	-9.98 : 9.95	-9.98 : 9.98	569
Upper Buffalo (R20B)	0.50 : 0.55	0.66 : 0.60	-9.53 : -1.04	-9.77 : 4.09	11
Baviaans (Q60C)	0.66 : 0.78	0.20 : 0.32	-8.28 : 8.68	-9.58 : 1.16	9
Noordkaap (X23A)	0.50 : 0.61	0.56 : 0.68	-8.52 : 4.20	-7.90 : 8.64	14

Figure 5.19 illustrates the flow duration curves (FDC) of the simulated uncertainty bands and the observed flow records whereas Figure 5.20 presents the best-fit-index of the 10 000 ensembles for the gauged sub-catchments using the Mean (Pan) input data to drive the model for the period 2000 – 2010. The simulation results under uncertainty conditions for the selected catchments are summarised below.

In the **Xhora River catchment (T11C)** the present-day flows are well simulated, although some of the values of the model performance measures did not reach the set threshold values. Figure 5.19 illustrates that the uncertainty bounds bracket the majority of the observed high flows but the lower uncertainty bands tend to over-simulate the medium to low flow regime. Part of the over-estimation could perhaps be related to the misrepresentation of water abstractions during the dry season. The best-fit-index illustrated in Figure 5.20 illustrates that the majority of different parameter combinations result in variable acceptable model performance. In addition, the higher values of *%BIAS* (untransformed and log-transformed data) are associated with lower *CE* and *CE (ln)* values. However, the majority of the combinations of the four objective functions with an index between 1 and 2, dominate the behavioural model parameter sets.

The FDCs of the **Klein Berg River catchment (G10E)** in Figure 5.19 show that the upper and lower uncertainty bounds mostly bracket the observed flow except for the low flows (85% exceedance). However, while acceptable values of the low flow regime (*CE {ln}*) for the 57 behavioural ensembles were obtained, the simulations had poor *CE* values. Non-stationarity conditions due to varying water use over the simulation period, together with inappropriate rainfall

inputs, (highly variable rainfall, see section 4.2), could possibly account for the poor simulation of the high flows. The values of the *%BIAS* in Figure 5.20 suggest that there are hydrological years where the model acceptably simulates the high flow regime. Figure 5.20 indicates that different *CE* and *CE (ln)* values with an index value below 0.5 correlate with predominantly acceptable values of *%BIAS* and *%BIAS (ln)* and the acceptable parameter combinations have an index value greater than 1.

The uncertainty bounds for the **Diep River catchment (K40A)** illustrated in Figure 5.19 shows bias towards under-simulation of the low flows. This is further confirmed by the value of the objective functions, which indicate that high flows were better simulated than the low flow regime. This could be linked to inadequate representation of the effects of the forest plantations together with the inability of the gauging station to measure very low flows. The best-fit-index of sub-catchment K40A in Figure 5.20 shows that, the majority of the 10 000 parameter sets represent the high flow regime well better than the low-flows.

In the **Upper Buffalo River catchment (R20B)**, the FDCs in Figure 5.19 show an inadequate representation of the medium to low flow hydrological response when compared to the high flows. A limited number of behavioural ensembles (11) however, represented the medium to low flows with an acceptable level of model confidence. Part of these inconsistencies could be related to incorrect quantification of water resource developments, probably due to errors in the estimation of water abstractions from the reservoir. This assumption is because the catchment is water-stressed and during the dry season, water abstraction patterns are subject to changing decisions. The abstractions patterns are not recorded, hence, they could not be accounted for in the model. While the majority of the combinations of the four objective functions using the best-fit-index (Figure 5.20) indicate poor results, index values greater than 1.4 resulted in acceptable simulation results.

Figure 5.19 illustrates that the upper and lower uncertainty bounds for the **Baviaans River catchment (Q60C)** bracket the frequency characteristics of the observed flow record. However, a small number of the behavioural ensembles, shown in Table 5.12 indicate the complexity of the processes involved and that highlights the model parameters were not adequately constrained. This is due to ungauged upstream sub-catchments, resulting in an unresolved amount of uncertainty especially regarding the low flows. The estimation of water use data from unreliable sources together with the inability of the flow gauge to measure low flows could be some of the reasons why

the low flows were poorly simulated. While the low values of the best-fit-index (<1 in Figure 5.20) result in unacceptable simulations, the *CE* values (both natural and log-transformed data) with index values between -1 and 1 are considered acceptable although, their relative *%BIAS* values are not.

The **Noordkaap River catchment (X23A)** is a catchment with approximately 70% coverage with managed forest plantations. Figure 5.19 shows that the full uncertainties of the simulated flows are evenly distributed from high to low flows. The number of behavioural ensembles (14) could be a result of the changes in land cover – through felling of trees – during the selected simulation period. This could make the generated flows inconsistent with the observed flows. This is particularly true for the medium to low flow simulations. The analysis of Figure 5.20 shows that while the majority of the full ensemble outputs have a relatively large number of acceptable *CE* and *%BIAS* values, the low flow measures are poor below an index value of 2. The uncertainty in the low flow regime could be attributed to the fact that the different stages of forest plantations were not accounted for adequately in the model or perhaps due to the rating curve of the flow gauging station, which may not represent the very low flows adequately.

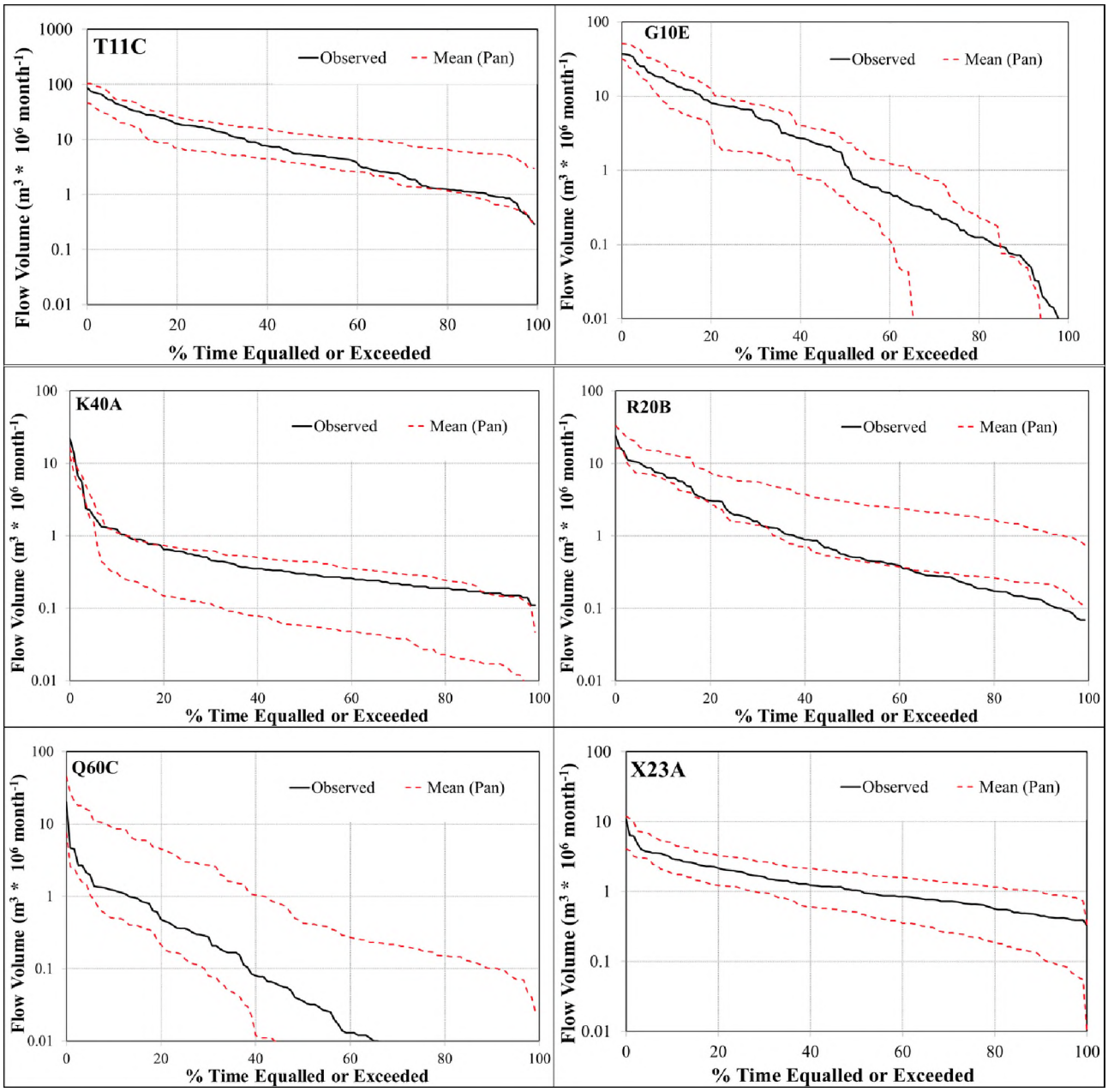

Figure 5.19: Flow duration curves of simulated upper and lower bound uncertainty (red dotted lines) compared with the observed flow data, under present day conditions, for the gauged sub-catchments.

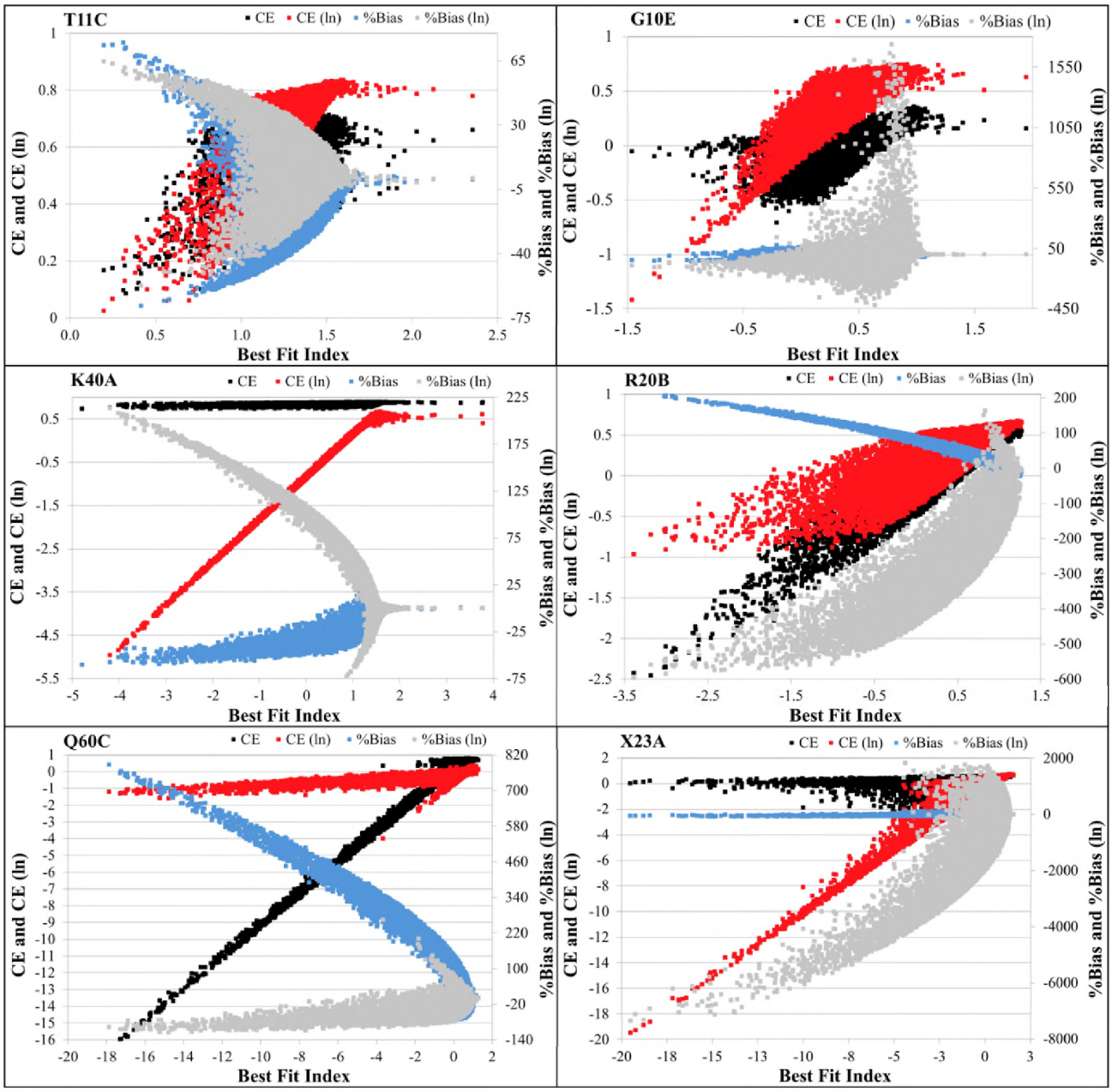

Figure 5.20: The best-fit-index versus the four objective functions for the 10 000 generated ensemble outputs for the gauged sub-catchments used in this study.

It is very difficult to use the best-fit-index diagrams (Figure 5.20) to reduce the number of poor simulation results by reducing the ranges of individual parameters. This is largely due to the fact that most of the poor simulation results are associated with inappropriate combinations of the values of two or more parameters.

5.5. UNCERTAINTY IN POTENTIAL EVAPOTRANSPIRATION INPUTS AND IMPACTS ON SIMULATED FLOWS

This section presents the resulting variations in PET demands and model efficiency when Mean (Pan), T/S (Pan), and T/S (MOD16) data are used in the model. Table 5.13 lists the mean annual PET values based on pan measurements and MOD16 estimates. The comparisons of the three PET datasets illustrated in Figure 5.21 indicate that the T/S (Pan) data have a relatively small variation from Mean (Pan) compared to T/S (MOD16). The time series in Figure 5.21 show averaged PET data for the selected areas with more than one sub-catchment. The differences in T/S (MOD16) data result for the general over-estimation of the mean annual PET as listed in Table 5.13.

Table 5.13: MAE (mm) based on long-term pan-measurements and the MOD16 PET data

PET Data	Sub-catchments											
	T11A	**T11B**	**T11C**	**G10E**	**K40A**	**R20A**	**R20B**	**R20C**	**Q60A**	**Q60B**	**Q60C**	**X23A**
Mean (Pan)	1 500	1 450	1 400	1 635	1 400	1 450	1 450	1 450	1 700	1 700	1 700	1 425
MOD16	2 380	2 380	2 287	2 697	2 140	1 642	2 017	2 016	2 942	2 889	2 842	1 923

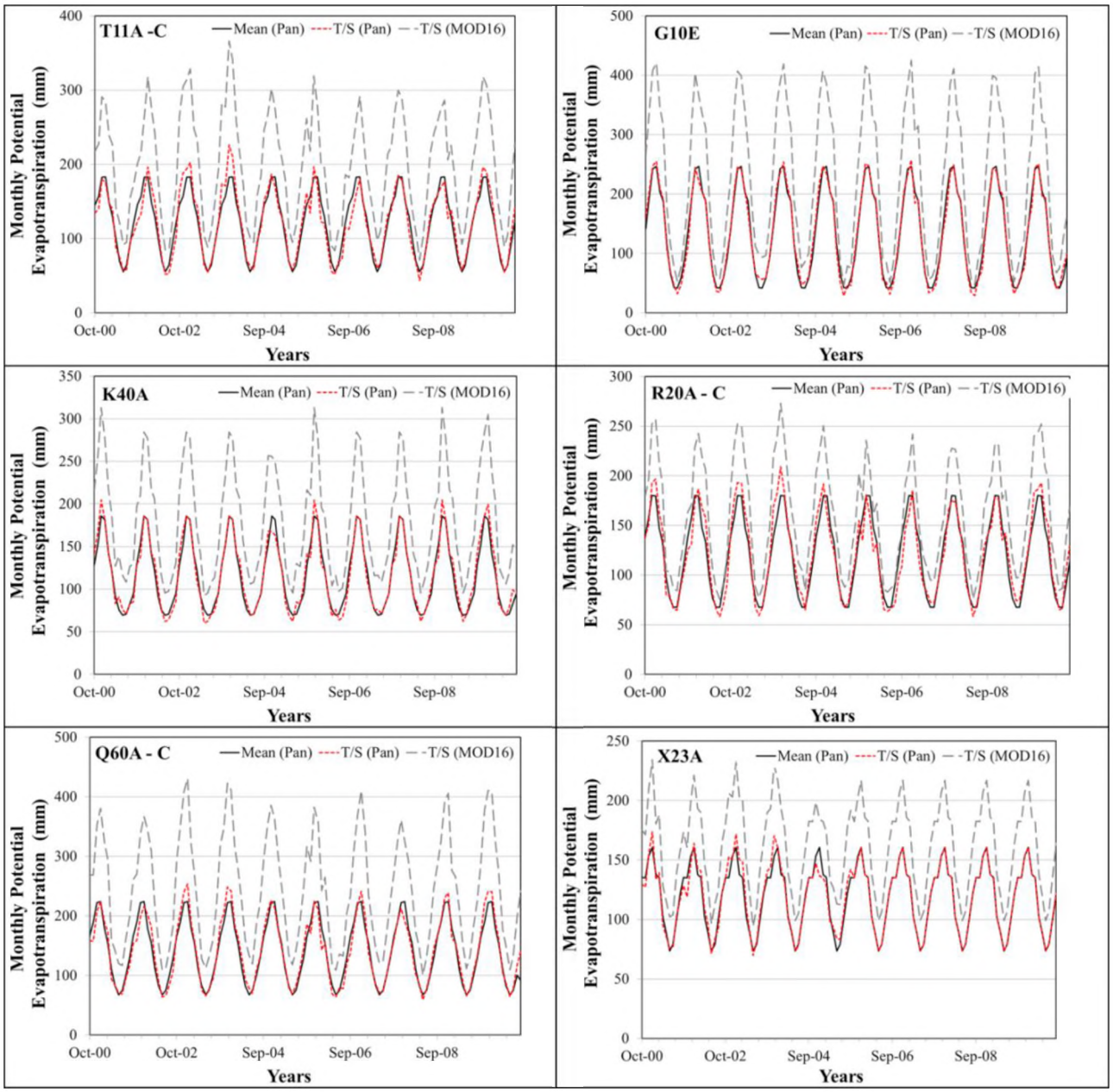

Figure 5.21: Comparison of monthly PET derived using fixed mean monthly and time series estimates perturbed based on both mean-Pan and MOD16 data.

The results of the use of the Pitman model with different forms of potential evapotranspiration data input are divided into two sub-sections: static and dynamic sensitivity analysis. The results given in the first sub-section are presented as summary statistics and graphically using monthly hydrographs and the flow duration curve comparisons. Dynamic analysis results are given in summary statistics and graphically comparing the variations of the objective functions with different values of the

parameters resulting from model re-calibration with changing potential evapotranspiration data inputs.

5.5.1. Static Sensitivity Analysis

The model efficiency results are based on the simulations of a single-run version of the model using the best ensemble parameter set selected based on the four objective functions (*CE*, *CE {ln}*, *%BIAS* and *%BIAS {ln}*), explained in section 3.2.4. The final 'best' parameter sets for each sub-catchment, obtained from the previous modelling step, are given in Appendix 2. It should be noted that during the modelling step reported in this section, there was no further form of model calibration and changing water use data, but only changing PET inputs. The simulation results for the period 2000 – 2010 are presented both in the form of graphics and objective function statistics. Table 5.14 lists the model performance statistics of using the two PET time series variations compared to the reference simulation results using Mean (Pan) data for all gauged sub-catchments. Figure 5.22 and 5.23 illustrate the monthly stream flow hydrographs and FDC curve comparisons of the observed and simulated flows using different forms of PET data in the model.

Poor simulation results for the sub-catchments with *CE* and *%BIAS* (regardless of the data transformation) values below 0.5 and out of ±10% range, respectively, are highlighted in grey colour in Table 5.14. The results indicate that in some catchments, the 'best' parameter sets using Mean (Pan) data produced poor high flow simulations. Nevertheless, the results generally show that there are no substantial positive differences in the model simulation statistics for most catchments when using the two time series data (T/S {Pan} and T/S {MOD16}) compared to using Mean (Pan) data. The insignificant differences in the simulations resulting from using T/S (Pan) data are evident in the monthly hydrographs and the FDCs illustrated in Figure 5.22 and 5.23. The larger differences when using T/S (MOD16) in the model manifest in most FDCs of the selected catchments.

Table 5.14: Statistical measures of the model performance for monthly flows simulations using different forms of PET time series data in the model for the gauged sub-catchment

Catchment	PET Data Type	Period	Untransformed		Log-transformed	
			CE	*%BIAS*	*CE*	*%BIAS*
Xhora (T11C)	Mean (Pan)	2000 - 2010	0.44	-3.33	0.80	-1.12
	T/S (Pan)		0.47	6.21	0.82	5.81
	T/S (MOD16)		0.30	6.32	0.78	-3.76
Klein Berg (G10E)	Mean (Pan)		0.25	-0.61	0.63	-0.30
	T/S (Pan)		0.28	3.17	0.66	35.0
	T/S (MOD16)		0.37	-23.1	0.33	-45.3
Diep (K40A)	Mean (Pan)		0.87	-0.15	0.58	-0.01
	T/S (Pan)		0.87	2.27	0.60	-3.90
	T/S (MOD16)		0.87	-11.30	0.41	30.86
Upper Buffalo (R20B)	Mean (Pan)		0.57	-8.20	0.66	-5.70
	T/S (Pan)		0.57	4.81	0.66	-24.05
	T/S (MOD16)		0.59	-21.00	0.44	154.90
Baviaans (Q60C)	Mean (Pan)		0.73	8.68	0.32	-1.41
	T/S (Pan)		0.73	10.41	0.21	-6.39
	T/S (MOD16)		0.73	2.51	-0.07	2.31
Noordkaap (X23A)	Mean (Pan)		0.58	0.1	0.64	0.15
	T/S (Pan)		0.58	5.8	0.63	-127.3
	T/S (MOD16)		0.30	-37.3	-0.01	1123.2

The T/S (Pan) Results

The resulting model simulation statistics given in Table 5.14 illustrate that, when using the T/S (Pan) data, there are relatively small changes in *CE* and *CE (ln)* values for most catchments except for sub-catchment Q60C and X23A. These model performance indicators suggest that T/S (Pan) inputs do not have any significant impacts on the generated runoff, particularly the high flows. This is evident in sub-catchment K40A, R20B, Q60C and X23A that had similar *CE* values when compared with Mean (Pan) simulations. Concerning the deviations of the simulated mean monthly flows, the bias of the high flows increased towards under-estimation of the observed record, but with an acceptable range of *%BIAS* values for all catchments. While the mean of the low flow regime simulations *(%BIAS {ln})* for sub-catchment T11C and G10E were biased towards an under-estimation of the observed record, sub-catchments K40A and Q60C were biased towards an over-estimation. Systematic errors in the mean of the low flow simulations are evident in sub-catchments X23A and R20B, however, those of the latter could be considered less because they are within ±25%, which is considered acceptable in the application of the hydrological model. It is worth noting that if the mean of the ln values of observed flow is close to 0, *%BIAS (ln)* value becomes a poor indicator of model performance because it is very sensitive to small changes (the denominator in the equation is close to zero).

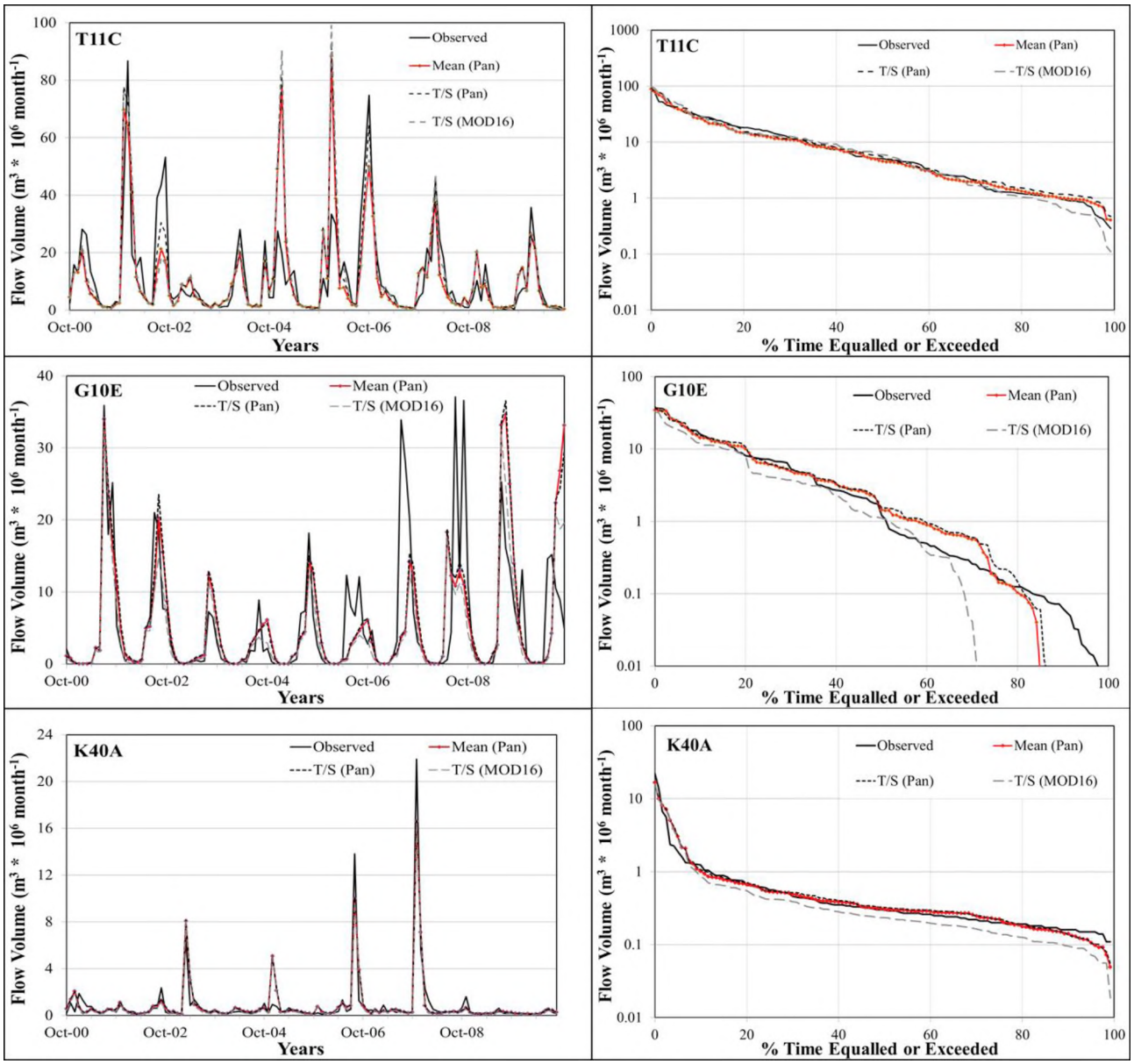

Figure 5.22: Hydrographs and the FDC comparisons of the observed and simulated monthly flows using different forms of potential evapotranspiration at the gauging sites of the Xhora (T11C), Klein Berg (G10E), and Diep River (K40A) catchments.

The T/S (MOD16) Results

The majority of the results show no significant improvements of model efficiency in the simulation of the present-day flows when using T/S (MOD16) data. Small or no differences in the high flow simulations are indicated from the *CE* values for the majority of the catchments except sub-catchment X23A. The indicators of the low flow regime (*CE {ln}* and *%BIAS {ln}*) clearly show that

T/S (MOD16) data inputs results in poor simulations. This is also evident in the hydrographs and the FDC comparisons illustrated in Figure 5.22 and 5.23. Part of the poor simulations of the low flows could be due to very high PET demands that intensify moisture losses. The use of the T/S (MOD16) data of the simulated flows relative to the observed flows had varying differences when different forms of PET data are used in the model. The values for the majority of the selected catchments indicate that changing PET inputs in the model is sensitive to the mean of the simulated flows.

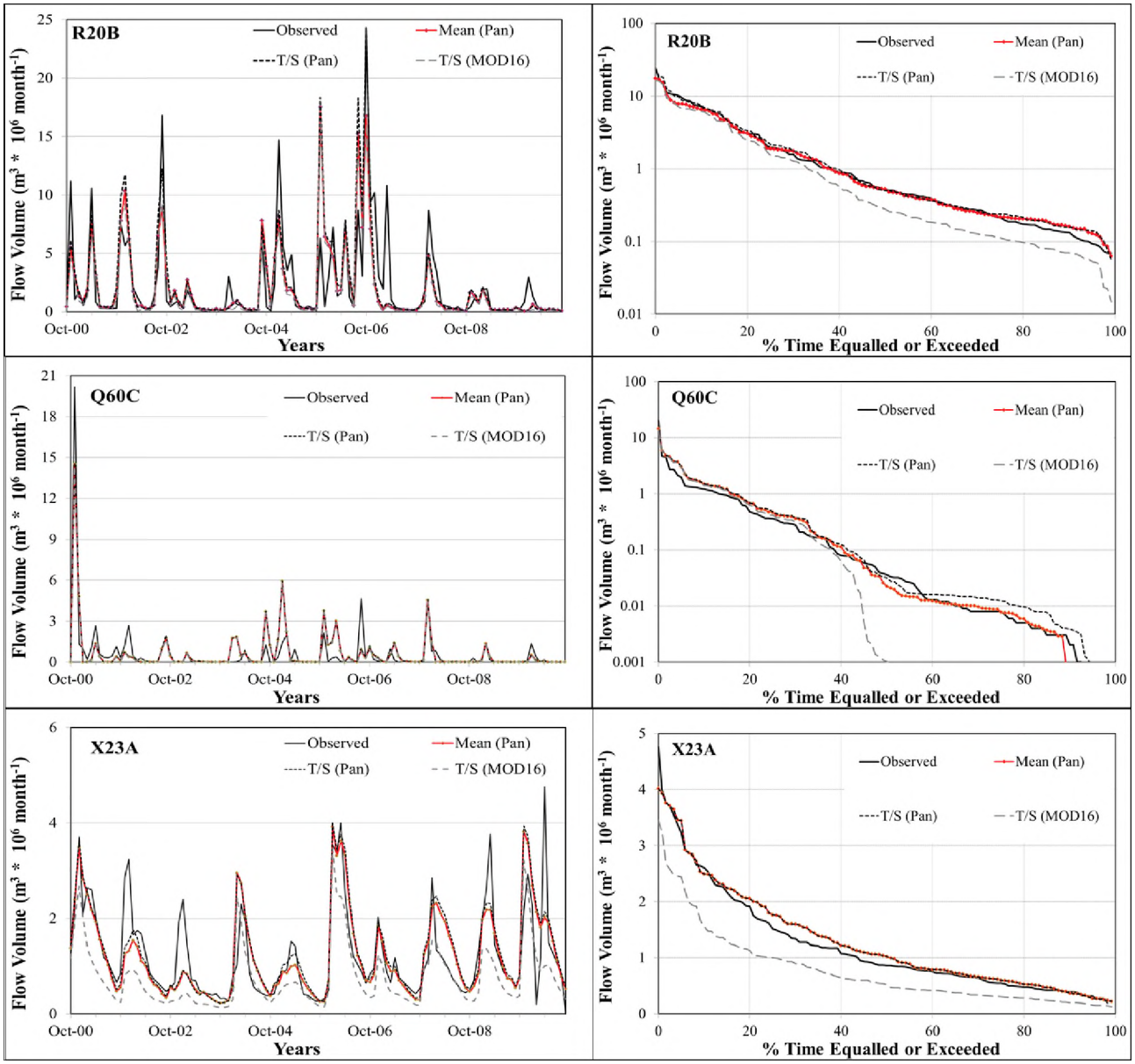

Figure 5.23: Hydrographs and the FDCs comparisons observed and simulated monthly flows using different forms of potential evapotranspiration at the gauging sites of the Upper Buffalo (R20B), Baviaans (Q60C), and Noordkaap River (X23A) catchments.

5.5.2. Dynamic Sensitivity Analysis

The previous sub-section presented the simulation results of applying different forms of potential evapotranspiration inputs into the model using a fixed parameter set. There was no noticeable difference in the model performance between model-run with Mean (Pan) inputs and T/S (Pan) however, in some sub-catchments, the use of T/S (MOD16) resulted in poor simulations considered unacceptable. The results presented in this sub-section illustrate the impact of re-calibrating the model with T/S (Pan) and T/S (MOD16) PET inputs on the model efficiency and parameters. The uncertainty version of the Pitman model was applied with parameter ranges listed in Table 5.3 however, increasing the range of parameter R (from 0 to 1). The behavioural and the 'best' parameter sets, for both calibration sets, were selected based on the criterion and the best-fit-index, respectively, detailed in section 3.3.4. Table 5.15 lists the minimum and maximum values of the four objective functions and their relative number of behavioural ensembles for model simulations obtained when calibrating the model with different forms of PET inputs. Reduced model performance in the high flow simulations (*CE* values), compared with the Mean (Pan) calibrations, are highlighted in dark grey colour whereas light grey designates an increase in the number of behavioural ensembles.

Table 5.15: The range of the four objective functions and the number of acceptable ensembles resulting from model re-calibration using different forms of PET inputs

Catchment	PET Input Type	*CE*	*CE (ln)*	*%BIAS*	*%BIAS (ln)*	Behavioural Ensembles
Xhora (T11C)	Mean (Pan)	0.43 : 0.53	0.74 : 0.82	-9.81 : 2.52	-6.32 : 9.90	77
	T/S (Pan)	0.50 : 0.63	0.56 : 0.84	-9.90 : 8.06	-9.90 : 9.97	***474***
	T/S (MOD16)	0.40 : 0.53	0.71 : 0.80	-9.77 : 6.15	-9.43 : 9.82	32
Klein Berg (G10E)	Mean (Pan)	0.08 : 0.30	0.52 : 0.71	-9.78 : 9.92	-8.95 : 9.55	36
	T/S (Pan)	0.08 : 0.29	0.53 : 0.76	-7.98 : -0.19	-9.96 : 8.56	***48***
	T/S (MOD16)	0.21 : 0.44	0.50 : 0.71	-9.94 : 9.83	-9.86 : 9.95	***92***
Diep (K40A)	Mean (Pan)	0.85 : 0.89	0.50 : 0.66	-9.95 : 9.87	-9.97 : 9.99	332
	T/S (Pan)	0.84 : 0.90	0.50 : 0.67	-9.92 : 9.73	-9.99 : 9.95	***500***
	T/S (MOD16)	0.85 : 0.88	0.50 : 0.65	-9.90 : 9.64	-9.93 : 9.96	221
Upper Buffalo (R20B)	Mean (Pan)	0.42 : 0.56	0.61 : 0.66	-9.21 :7.74	-9.20 :6.04	13
	T/S (Pan)	0.52 : 0.61	0.57 : 0.67	-8.67 : 7.23	-9.27 : 9.92	***15***
	T/S (MOD16)	0.50 : 0.59	0.50 : 0.68	-9.67 :9.61	-9.85 : 9.92	***41***
Baviaans (Q60C)	Mean (Pan)	0.64 : 0.78	0.10 : 0.32	-9.82 : 9.83	-9.15 : 8.25	35
	T/S (Pan)	0.64 : 0.85	0.10 : 0.28	-9.90 : 9.82	-9.95 : 9.00	***40***
	T/S (MOD16)	0.65 : 0.77	0.10 : 0.31	-9.95 : 9.75	-9.92 : 9.98	***61***
Noordkaap (X23A)	Mean (Pan)	0.50 : 0.61	0.56 : 0.67	-9.31 : 3.72	-9.36 : 9.58	23
	T/S (Pan)	0.50 : 0.61	0.63 : 0.67	-8.51 : 0.97	-9.81 : 9.93	11
	T/S (MOD16)	0.51 : 0.52	0.61 : 0.65	-6.91 :-0.95	-2.73 : 9.68	3

The following analysis compares the variations in the model efficiency of the best parameter sets when different forms of PET inputs are used simulate the present-day flows. Table 5.16 lists the summary of the four objective function statistics of the best ensembles from the three sets of model calibrations. Improved model efficiency statistics in the table are in bold/italics format whereas reduced model performance measures are highlighted in grey colour. The results presented in Table 5.16 illustrate that, in some catchments, there appears to be some insignificant benefits of calibrating the Pitman model with time series variations of potential evapotranspiration estimates. For example, when calibrating the model with T/S (Pan) inputs, both high and low flow simulations had insignificant changes in *CE* and *CE (ln)* values. With the exception of sub-catchment G10E, the results show that T/S (MOD16) calibrations have some impacts on the simulated low flows, which are predominantly under-simulated (low *CE* values). This implies that increasing PET demands results in more ET losses that may be depleting soil moisture more rapidly. Bearing in mind that model calibration is often affected by equifinality where changes in the input data can be compensated for by changes in parameter values, it is necessary to re-calibrate the model when different PET inputs are used.

Table 5.16: Statistical measures of the model performance for monthly flows simulations using different forms of potential evapotranspiration time series data in the model for the gauged sub-catchment.

Catchment	PET Input Type	Period	Untransformed		Log-transformed	
			CE	*%BIAS*	*CE*	*%BIAS*
Xhora (T11C)	Mean (Pan)	2000 - 2010	0.44	-3.33	0.80	-1.12
	T/S (Pan)		***0.52***	***0.57***	***0.82***	***0.19***
	T/S (MOD16)		***0.50***	***0.41***	0.79	7.18
Klein Berg (G10E)	Mean (Pan)		0.16	0.13	0.70	-1.59
	T/S (Pan)		***0.29***	1.27	0.57	***-0.67***
	T/S (MOD16)		***0.38***	-0.13	0.64	-1.58
Diep (K40A)	Mean (Pan)		0.87	-0.51	0.58	-0.10
	T/S (Pan)		***0.88***	***0.20***	0.52	-0.10
	T/S (MOD16)		***0.88***	-1.40	***0.59***	0.01
Upper Buffalo (R20B)	Mean (Pan)		0.50	-1.96	0.65	0.42
	T/S (Pan)		***0.56***	***0.90***	0.61	***0.53***
	T/S (MOD16)		***0.54***	***0.15***	***0.66***	1.05
Baviaans (Q60C)	Mean (Pan)		0.77	-5.39	0.28	9.72
	T/S (Pan)		0.67	***-0.10***	0.12	***0.05***
	T/S (MOD16)		0.73	***-0.14***	0.16	***2.53***
Noordkaap (X23A)	Mean (Pan)		0.54	-0.32	0.62	2.28
	T/S (Pan)		***0.57***	***0.09***	0.60	1.01
	T/S (MOD16)		0.52	-0.95	0.61	-2.73

Note: *Bold values indicate improvements after re-calibration using either T/S (Pan) and/or T/S (MOD16) estimates.*

The parameter sensitivity analysis to model re-calibration using different forms of PET inputs (T/S {Pan} and T/S {MOD16}) focussed only on the parameters affecting evapotranspiration losses i.e. ST and R. The Mean (Pan) calibrations were used as the baseline for comparisons. The results of the model re-calibration are presented in the form of scatterplots of the variations of the objective function values of both untransformed (*CE*) and log-transformed (*CE {ln}*) flows with the classified ensemble values of R and ST parameter. The ensembles are classified into: i) *all* ensembles symbolized with green round dots, ii) *behavioural* with white squares, iii) best *25%* of the behavioural denoted as black triangles, and iv) the *best* parameter set represented by a grey circle.

Figure 5.24 to Figure 5.27 show the comparisons of the variations of *CE* and *CE (ln)* values with ensemble values of the evapotranspiration parameter R for different model calibrations of two exemplary catchments: Xhora and Klein Berg. The T/S (Pan) calibration results of the Xhora River catchment, from Figure 5.24, illustrate that both lower and higher values of R generate a large number of acceptable stream flow simulations (474 ensembles) on the basis of the two objective functions compared to Mean (Pan) calibrations. The best 25% of the behavioural ensembles, based on the best-fit-index, suggest that increasing evapotranspiration losses from the unsaturated soil moisture storage (ST) similarly generate acceptable simulations of both high and low flows. On the other hand, the T/S (MOD16) calibration indicates that, generally, lower values of R (<0.4) result in poor simulations (low *CE* and *CE {ln}* values) and the behavioural ensembles have predominantly R values greater than 0.5. This suggests that the use of T/S (MOD16) inputs are over-estimating PET demands which forces the model to compensate by reducing evapotranspiration losses. The results of the Klein Berg River catchment (Figure 5.25) illustrate that the 'best' parameter set from both T/S (Pan) and T/S (MOD16) calibration is obtained with relatively low rates of evapotranspiration losses ($R \geq 0.9$) compared to those of the Mean (Pan) calibration ($R = 0.4$). Regardless of PET inputs used, a wide range of the values of R similarly generate acceptable simulations, however, the model tends to under-simulate the low flows with R values closer to 1.

Similar patterns of model calibration results were observed in the other catchments used in this study and their graphic plots are given in Appendix 3. While the optimum parameter sets for forested catchments were obtained with the lower values of R (e.g. K40A and X23A), there were no clear identifiable patterns of the values that generate better simulation in all catchments. Further, the efficiency of the model did not show any improvements.

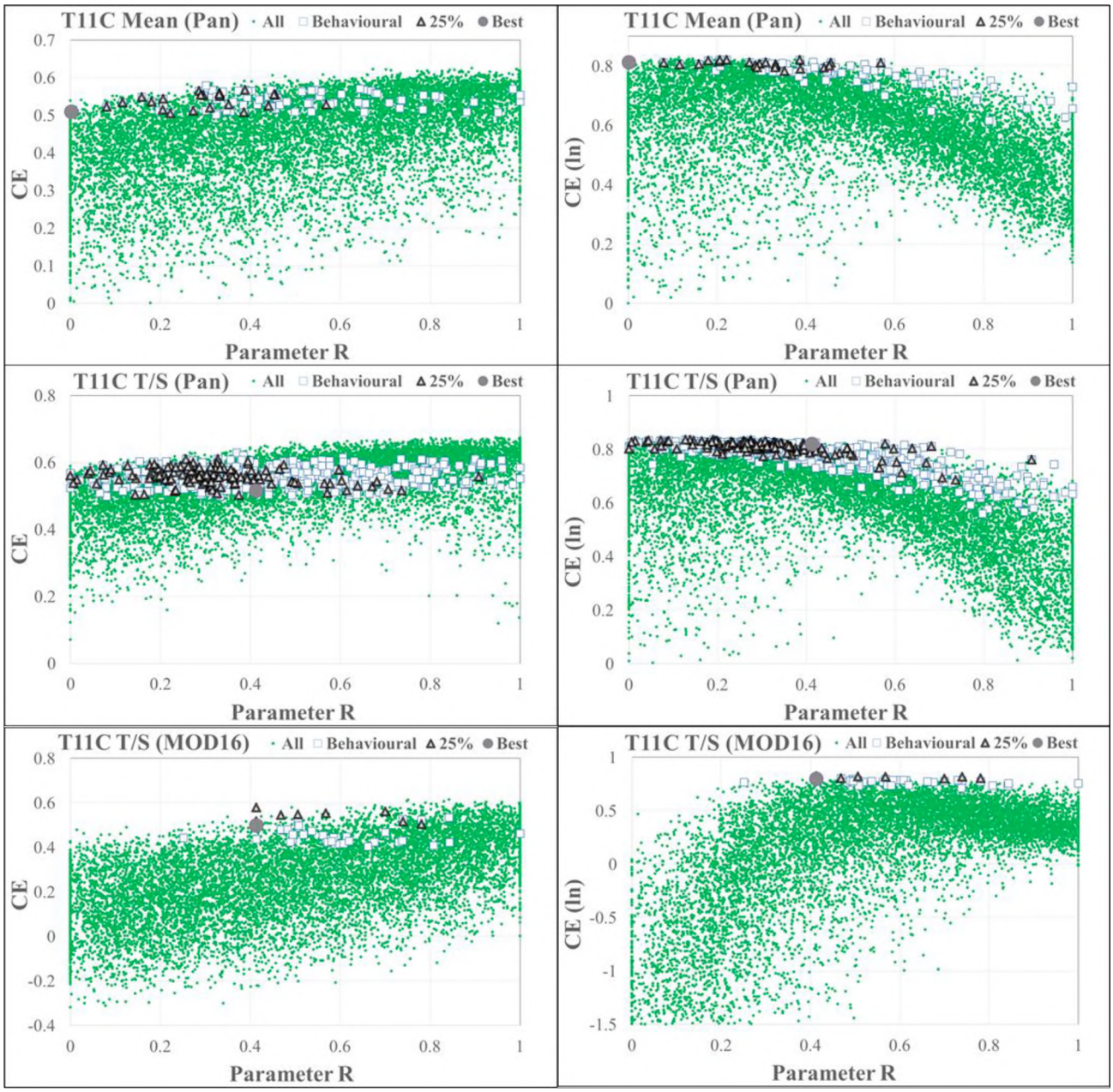

Figure 5.24: Scatterplots of the variations of the coefficients of efficiency based on untransformed (*CE*) and log-transformed (*CE {ln}*) flows with ensemble values of parameter R for the Xhora River catchment.

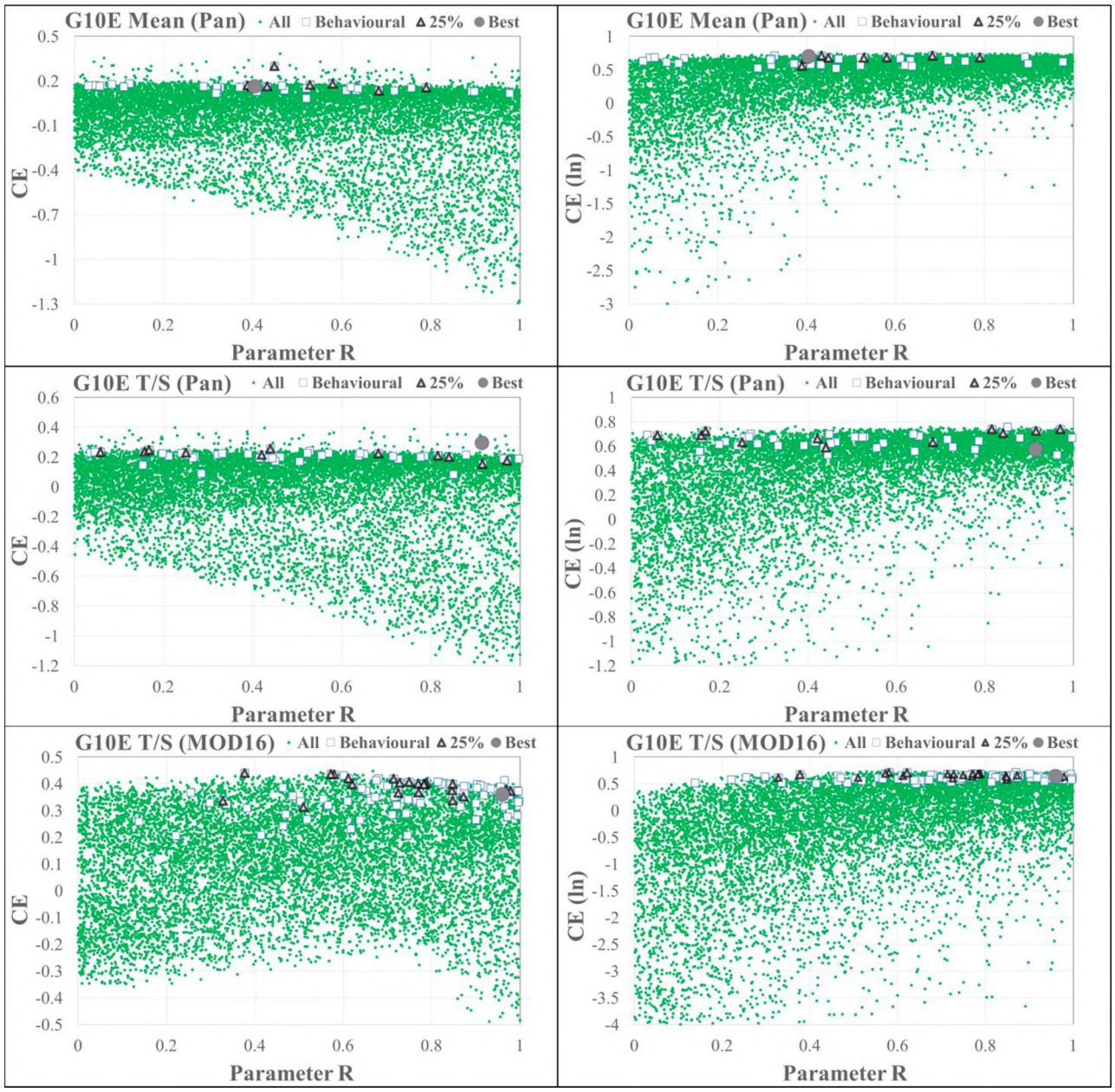

Figure 5.25: Scatterplots of the variations of the coefficients of efficiency based on untransformed (*CE*) and log-transformed (*CE {ln}*) flows with ensemble values of parameter R for the Klein Berg River catchment.

The analysis of the effects of changing PET inputs on ST parameter for the two exemplary catchments are graphically presented in Figure 5.26 and 5.27. Figure 5.26 shows that while a wider range of ST values for all calibrations generate acceptable medium to low flow simulations of the Xhora River catchment, ST values resulting from T/S (Pan) calibration have different patterns to that of the other calibrations. The trend from Mean (Pan) and T/S (MOD16) calibrations shows that

lower soil moisture storage (SR< 180 mm) tend to generate acceptable high flow simulations. However, T/S (Pan) calibration suggests that higher ST is associated with better values of *CE* despite the fact that those that the majority of those considered behavioural had lower values. The comparison of model performance to uncertain parameter R values in Figure 5.24 suggest that increasing evapotranspiration losses to moderately higher values (R < 0.5) compensate the runoff generation at the end of the rainy season. These results show that there is equifinality problem in ST values relative to low flows for this catchment.

Figure 5.27 illustrates that, regardless of the form of PET inputs used to calibrate the model, the values of ST parameter capable of generation better high flow simulations are fairly identifiable for the Klein Berg River catchment. All ensembles with ST > 300 mm, from T/S (Pan) calibration, generate better simulations. The T/S (MOD16) calibration results suggest that the model is sensitive to 300 mm < ST > 450 mm range as they generate poor simulations of the high flows. This further suggests that increasing evapotranspiration demands in reduces the available water that can contribute to runoff. Nevertheless, the majority of the behavioural ensembles were within somewhat similar range, of course, with different optimum value of this parameter. ST values that generate of moderate to low flow simulations using different PET inputs show a high degree of equifinality. Figure 5.27 also illustrates that acceptable *CE (ln)* values can be obtained with a large variation of soil moisture storage depths, which further suggest a high degree of equifinality in this parameter.

While the results of Pitman model calibration with different forms of PET inputs for the two catchments reported above show that there is large equifinality and a lack of clear parameter identifiability of R and ST, similar cases were observed also in the other catchments used. The graphic presentations of the other catchments are given in Appendix 3. The general picture that can be drawn from the results is that in some cases, when using T/S (Pan) inputs to calibrate the model, the number of acceptable simulation improves compared to T/S (MOD16) calibrations.

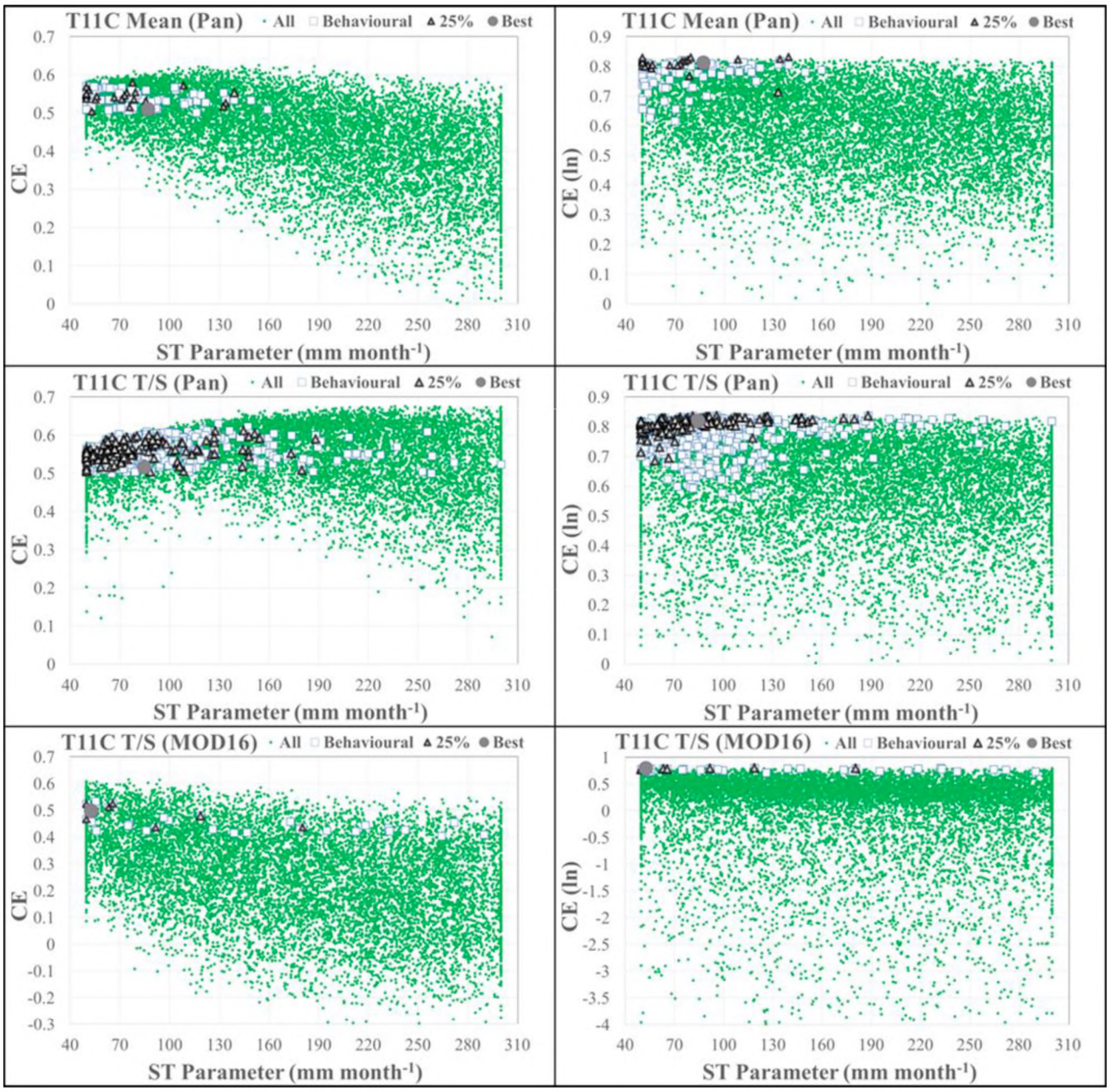

Figure 5.26: Scatterplots of the variations of the coefficients of efficiency based on untransformed (*CE*) and log-transformed (*CE {ln}*) flows with ensemble values of ST parameter for the Xhora River catchment.

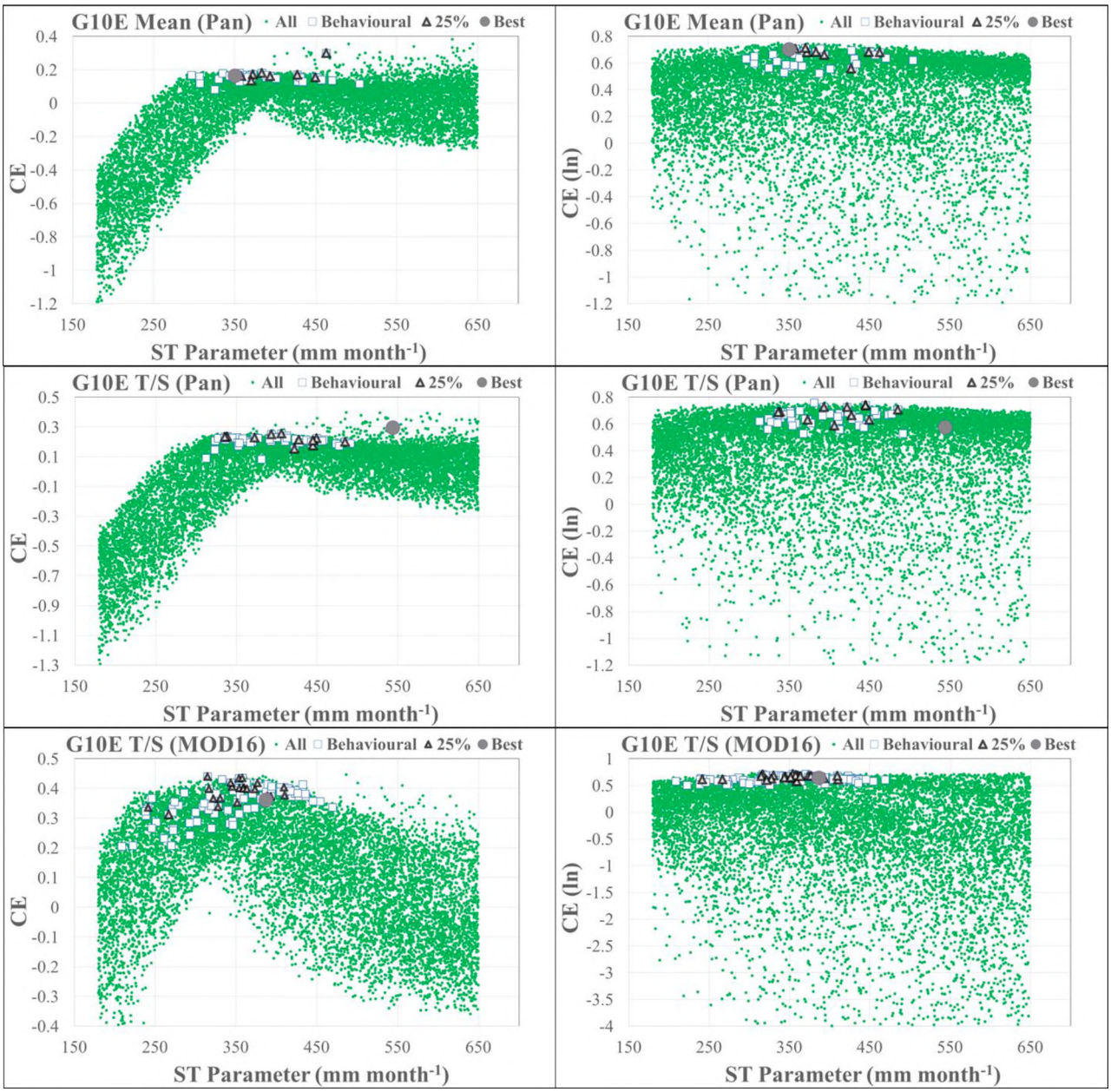

Figure 5.27: Scatterplots of the variations of the coefficients of efficiency based on untransformed (*CE*) and log-transformed (*CE {ln}*) flows with ensemble values of ST parameter for the Klein Berg River catchment.

While the sensitivity was limited to only two parameters (ST and R), the calibration results suggest that the model has the flexibility capacity to compensate for the changes in PET demands in generating acceptable simulations. In some catchments, the increase in the number of behavioural ensembles, particularly when the model is calibrated with T/S (Pan) inputs, also demonstrate this. In the same way to the static analysis results presented in the previous sub-section, the T/S (Pan)

calibrations result in insignificant differences in model efficiency when compared to Mean (Pan) simulations. While calibrations with T/S (MOD16) inputs had no noticeable improvements on model efficiency in all catchments, the results presented in Figure 5.24 to Figure 5.27 illustrated that, however, there are some differences in the analysed parameters. The overall results also indicated that, regardless of the PET inputs used in the calibration process, the Pitman model suffers from parameter identifiability problems. These problems make it difficult to conclude that calibrating the model with potential evapotranspiration time series is more pleasing than using Mean (Pan) inputs.

5.6. CONTRAINING MODEL-SIMULATED ACTUAL EVAPOTRANSPIRATION WITH MODIS DATA

Realistic internal dynamics of a hydrological model could be better understood if different fluxes of a hydrological system, represented in a model, are constrained with complementary or soft data after a model is run with optimum parameter set (Gharari *et al.*, 2014). Complementary data can take a form of information or short-term estimates of various hydrological response fluxes. The use of MOD16 data has been explored internationally to provide additional information used in different aspects of hydrological modelling. However, in South Africa the use of the MOD16 data in attempts to improve model application and process understanding has not attracted a huge interest in practicing hydrologists. The post-PUB era (Hrachowitz *et al.*, 2013a) created a consensus about the use of parameter and processes constraints in improving the predictive power of complex models (e.g. Gao *et al.*, 2014). This nexus motivated this study to use the MOD16 ETa data in attempts to constrain the model-simulated actual evapotranspiration. The results from the study of Műnch *et al.* (2013) and Hughes *et al.* (2014a) have demonstrated that the MOD16 ETa data are promising to improve model-simulations and model structure when used as reference data despite the noted uncertainties in the data (Hughes, 2013).

This section of this study, therefore, presents the results of the application of the MOD16 ETa data in the Pitman model. The first part presents the analysis of the previous studies where the MOD16 ETa data are compared with actual evapotranspiration estimates derived from field measurements and those simulated by the Pitman model. Findings from these studies could suggest the potential of constraining the model-simulated ETa with the MOD16 estimates. Therefore, the results of the

model application using MOD16 ETa data as constraint of the model-simulated ETa are given in the last sub-section.

5.6.1. Previous Studies

The Manubi Forest Area

One of the objectives of Hughes *et al.* (2014a) study, at the Manubi Forest site (see section 4.8.1) was to compare the actual evapotranspiration from the extrapolated Eddy Covariance and MOD16 data which is presented as a time series in Figure 5.28. The authors extracted the 8-day MOD16 ETa data for 6 grid (1 km^2) transacts adjacent to the forested (4 grids) and a grassland area (2 grids) for 2011 hydrological year and compared them with ETa estimates extrapolated from two short periods of Eddy Covariance observations. ETa estimates from Eddy Covariance were based on continuous measurements of soil moisture and other climatic variables. It is apparent from Figure 5.28 that during the start and towards the end of the observation record, MOD16 data for the forested area reflects higher evapotranspiration losses values than the field data. There is reasonable match between the two forest datasets between February and July. Differences in the ETa dynamics from the two land cover types (high in the forest and low in grassland) are also evident in the time series. A possible explanation is that the MOD16 data do not adequately reflect differences in the catchment wetness, and therefore moisture availability, which are reflected in the field estimates. This could be one of the shortcomings of the MOD16 data in representing the total evapotranspiration depth relative to the availability of the stored soil moisture.

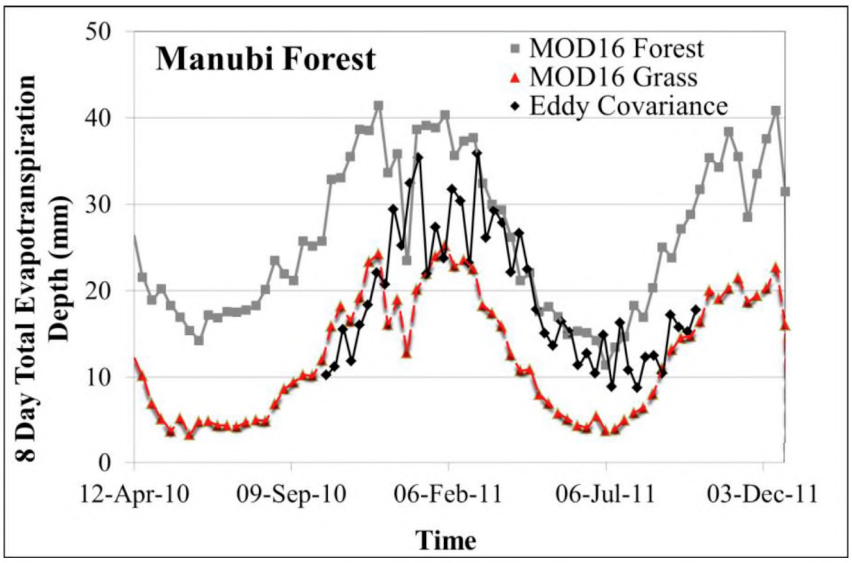

Figure 5.28: Time series comparison of actual evapotranspiration based on field measurements and 8-day MOD16 ETa data across the forest (4 grids) and grassland area (2 grids) for the Manubi Forest site.

The Kosi Bay and Lake Sibaya Areas

For both sites, the Pitman model was set up for two nodes: one within the forest plantations and the other in a grassland area. The model-simulated ETa, for the forested sites, included evapotranspiration from the groundwater, which occurs through deep-rooted plants. The monthly MOD16 ETa data, for the period 2000 – 2005, were extracted from 1 grid covering both land cover types for the two sites. This was aimed at comparing monthly actual evapotranspiration from both MOD16 data and the model. The comparisons are presented in Figure 5.29 and 5.30, which also include monthly average rainfall for the area that was obtained from the WR2005 database (Middleton and Bailey, 2008).

Actual evapotranspiration comparison for the Kosi Bay site (Figure 5.29) shows that the start of the simulation period (year 2000 to 2001) was particularly wet and this is reflected in the response of the evapotranspiration losses from the model. While the model-simulated ETa estimates reflect high levels of available soil moisture in the storage, the MOD16 data does not capture the variations in soil moisture for this wet period in both land cover types. However, post-2001 period, ETa from the two sources do not have large differences. Part of this could perhaps be attributed to the cutting of the forest plantation, which inevitably results in the reduction of the evapotranspiration losses. The global forest change database (Hansen *et al.*, 2013) indicates that between year 2000 and 2003, there

was a reduction in the forest cover in the area around the Kosi Bay site. These changes could be explaining the declining trend of evapotranspiration losses. With this analysis, it is worth mentioning that the MOD16 data has a potential in providing ETa estimates, which can be considered representative based on the results of Kosi Bay site. However, it remains uncertain if the MOD16 ETa data are capable of reflecting the large temporal variability of ET losses particularly if they are spatially averaged across a sub-catchment instead of using data from one point.

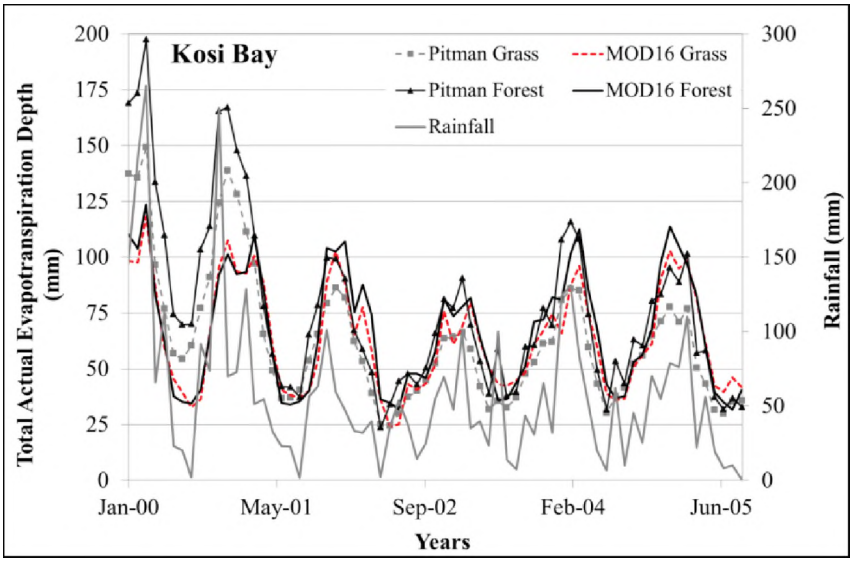

Figure 5.29: Comparison of MOD16 and Pitman model estimates of actual evapotranspiration time series for grassland and forested area. The grey solid line represents the WR2005 monthly rainfall data.

Figure 5.30 illustrates the comparison of the model simulated and MOD16 time series of actual evapotranspiration for grassland and the forested area at the Lake Sibaya site. The figure shows that the MOD16 data represents the anticipated patterns of evapotranspiration losses i.e. higher in the forested than the grassland area. Similar patterns, particularly during summer period, are observed from the model-simulated ETa. The time series (Pitman estimates) in the figure further suggests that the period before year 2002 hydrological year was wetter than the years after 2002. In some years, however, the model did not simulate distinguishable evapotranspiration losses between the grassland and the forested area. This could perhaps be attributed to the changes in forest growth (cutting of trees) which result in the reduction of ET losses. Given that the model-simulated ETa included the evapotranspiration losses from groundwater, which occurs mainly through deep-rooted forest, the previous statement could be true. It is striking, using the above assumption; that the MOD16 ETa

data for forested area did not capture these variations and makes it difficult to explain these differences.

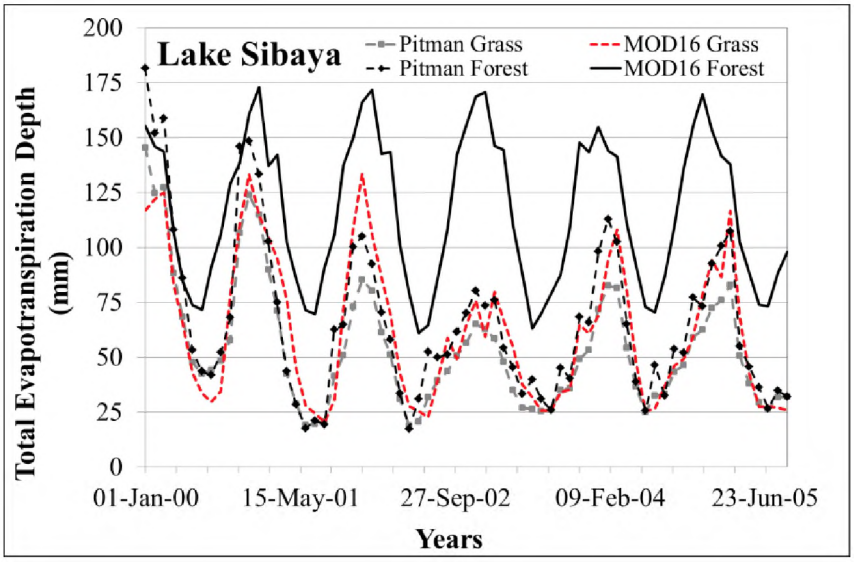

Figure 5.30: Lake Sibaya: Comparison of MOD16 and Pitman model estimates of actual evapotranspiration time series for grassland and forested area.

The results from the two sites suggested that it could be possible that the MOD16 data provides evapotranspiration estimates that can be considered representative of catchment water losses. For that reason, in this study, these data are used to constrain the model-simulated ETa despite some discrepancies in the data that are associated with the different landscapes reported by Hughes (2013).

5.6.2. Constraint Analysis of the Model-simulated Actual Evapotranspiration

The results of calibrating the model against actual evapotranspiration constraints using the MOD16 data are represented in this sub-section. It was demonstrated in the previous sub-section that the MOD16 ETa estimates could provide evapotranspiration losses dynamics that could be considered representative for different land cover types. However, the MOD16 ETa data used in the results presented in the previous sub-section were based point-based. The use of these data, as a catchment average, in comparing with the model-simulated ETa estimates remains a subject to be evaluated. Therefore, the results presented in this sub-section involved the use of catchment-averaged ETa estimates in constraining those simulated by the model at a catchment scale.

Before applying the MOD16 ETa data in the model, it has been a fundamental principle in water resources planning and management to start by evaluating if the data representing different components of a hydrological system result in the closure of catchment water balance. In this study, the estimated actual evapotranspiration from the water balance method, as a reference, was evaluated against those simulated by the model (using best ensemble of Mean {Pan} simulations) and estimated by the MOD16 algorithm. Despite the fact that the water balance method cannot reproduce the spatial patterns of ETa at a catchment scale, it has been widely used for at both basin and regional scales (e.g. Hobbins *et al.*, 2001). Catchment evapotranspiration losses (ETa) were determined using equation 5.1 which is given by:

$$ETa = P - Q \pm \Delta S \tag{5.1}$$

where P is precipitation, Q represents catchment runoff, and ΔS is change in sub-surface storage. All these components were expressed in volumetric units (m^3*10^6). While ETa and Q are influenced by the availability of moisture content in the sub-surface storage component (soil moisture and groundwater), changes in this component were ignored ($\Delta S \approx 0$) for this study owing to the assumption that it is the same at the start and end of a hydrological year (Everson, 2001). Neglecting the changes in the sub-surface storage was justified through the work of Graf *et al.* (2014) who concluded that this assumption would be valid only if the annual water balance calculations do not exceed the period of 3 years. Precipitation and MOD16 actual evapotranspiration data for study areas with multiple sub-catchments were averaged to represent one single hydrological unit that has a gauging station. The closure of the catchment water balance (equation 5.2) was calculated such that

$$P - Q - ETa = 0 \tag{5.2}$$

Table 5.17 lists the annual values of the measured and calculated water balance components. Precipitation (P) and observed flow (Q) are the measured, whereas actual evapotranspiration from water balance (P-Q), model simulation (*Pitman*), and MOD16 data (ET_{MOD}) are the calculated components. These components are also presented graphically, as annual variation comparison, in Figure 5.31. The figure illustrates that annual patterns of both model-simulated and water balance-based ETa are somewhat matching well in most catchments. An exceptional case is observed in catchment G10E where the model tends to under-estimate ETa before 2006 and after 2008 hydrological years. This could perhaps be attributed to the inability of the model to adequately

account for increased moisture in the soil storage, particularly in the wetter years. The figure also shows that there are two anomalies in the MOD16 ETa data (year 2008 and 2009) in most catchments apart from G10E. This inconsistency in the MOD16 data could be associated with the error either in the raw MOD16 data or in the processing of the data. Despite these data anomalies, in the forested catchments (K40A and X23A), MOD16 estimates tend to over-estimate evapotranspiration losses regardless of the wetness or dryness of the hydrological year. The MOD16 in other catchments, however, show a predominant trend of the under-estimation of ET losses with the exception of the Upper Buffalo River catchment which has, to some extent, matching patterns.

Table 5.17: Measured and calculated water balance components of the six selected catchments. All components are expressed in million cubic meters per year and the cover the period 2000 – 2010 with the exception of X23A, which ends in 2005

Catchments															
Time	Xhora (T11A-C) Water Balance Components					Klein Berg (G10E) Water Balance Components					Diep (K40A) Water Balance Components				
	P	*Q*	*P-Q*	*Pitman*	ET_{MOD}	*P*	*Q*	*P-Q*	*Pitman*	ET_{MOD}	*P*	*Q*	*P-Q*	*Pitman*	ET_{MOD}
2001	740	11	622	683	536	338	87	251	161	125	65	8	57	58	66
2002	1158	32	830	903	555	364	68	295	273	138	64	7	57	53	69
2003	637	51	586	618	461	240	27	214	200	121	65	12	53	51	68
2004	763	99	665	672	447	229	19	210	190	123	56	3	53	49	67
2005	828	98	731	710	513	294	43	252	204	131	61	5	56	51	68
2006	1072	20	866	812	485	229	47	182	197	123	82	19	64	56	59
2007	689	15	533	649	507	294	10	193	204	132	51	5	46	48	70
2008	912	15	758	770	1406	295	97	199	198	200	87	34	53	55	116
2009	624	45	579	581	1033	400	81	319	254	130	43	5	38	38	99
2010	731	96	635	670	490	396	74	322	241	132	42	3	39	39	56

Catchments															
Time	Upper Buffalo (R20A-C) Water Balance Components					Baviaans (Q60A-C) Water Balance Components					Noordkaap (X23A) Water Balance Components				
	P	*Q*	*P-Q*	*Pitman*	ET_{MOD}	*P*	*Q*	*P-Q*	*Pitman*	ET_{MOD}	*P*	*Q*	*P-Q*	*Pitman*	ET_{MOD}
2001	377	29	348	341	330	587	29	558	548	331	133	22	111	126	135
2002	463	46	417	386	329	566	5	561	531	322	118	17	101	107	135
2003	230	7	223	264	322	376	1	375	424	254	102	11	91	95	136
2004	306	12	293	249	313	580	2	578	523	229	133	10	123	108	132
2005	327	34	293	330	344	492	5	488	527	281	109	9	100	102	134
2006	507	41	466	398	324	661	8	652	620	318	-	-	-	-	-
2007	293	62	231	300	342	552	3	549	568	301	-	-	-	-	-
2008	302	21	282	284	557	381	7	374	367	1402	-	-	-	-	-
2009	276	7	269	261	449	406	2	404	401	1137	-	-	-	-	-
2010	220	7	213	222	298	332	2	330	328	265	-	-	-	-	-

Note: ***P****–Precipitation;* ***Q****–Observed Flow;* ***P-Q****–Water Balance ETa;* ***Pitman****–Simulated ETa;* $\boldsymbol{ET_{MOD}}$*–MOD16 ETa.*

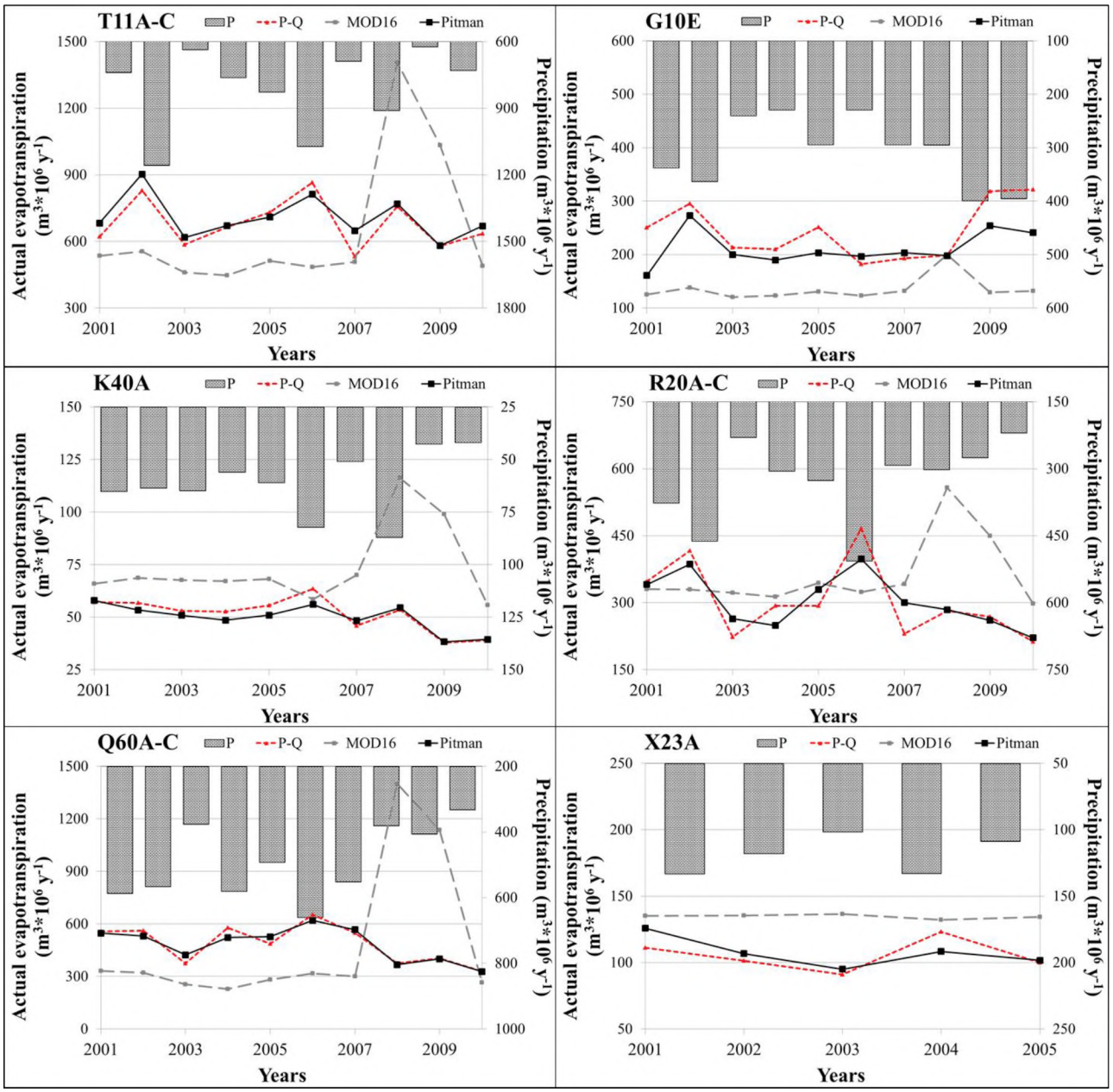

Figure 5.31: Comparison of the annual actual evapotranspiration from catchment water balance calculation (P-Q), MOD16 data, and model simulation (Pitman) as well as annual values of precipitation (P) on the secondary axes.

Table 5.18 provides a brief summary of the annual water balance closure, bias and statistical differences in the measured and estimated water balance components of the selected catchments. In the majority of the catchments, the MOD16 data does not result in the closure of the catchment water balance. This condition suggests that these data are inadequate to be used as a process constraint of the Pitman model simulated actual evapotranspiration.

Table 5.18: Water balance-based precipitation using MOD16 actual evapotranspiration estimates (P_{Q+MOD}), percentage differences in the measured and calculated precipitation (ΔP) water balance closure derived from both model-simulated (ET_P) and MOD16 (ET_{MOD}) estimates, and the percentage bias in actual evapotranspiration between model-simulated and MOD16 data

Catchments																		
	Xhora (T11A-C)						Klein Berg (G10E)						Diep (K40A)					
Time	*Water Balance*		*WB Closure*		*%BIAS*		*Water Balance*		*WB Closure*		*%BIAS*		*Water Balance*		*WB Closure*		*%BIAS*	
	P_{Q+MOD}	ΔP (%)	ET_P	ET_{MOD}	ET_P	ET_{MOD}	P_{Q+MOD}	ΔP (%)	ET_P	ET_{MOD}	ET_P	ET_{MOD}	P_{Q+MOD}	ΔP (%)	ET_P	ET_{MOD}	ET_P	ET_{MOD}
2001	654	-12	-61	86	10	-14	212	-37	90	125	-36	-50	74	14	-1	-9	2	16
2002	884	-24	-73	275	9	-33	206	-43	22	157	-8	-53	75	19	3	-12	-6	21
2003	513	-20	-33	125	6	-21	147	-39	14	93	-6	-43	79	23	2	-15	-4	28
2004	546	-28	-7	217	1	-33	142	-38	20	87	-10	-41	70	26	4	-14	-8	27
2005	611	-26	21	218	-3	-30	173	-41	48	121	-19	-48	74	21	5	-13	-8	23
2006	692	-35	53	381	-6	-44	170	-26	-14	59	8	-33	77	-6	8	5	-12	-8
2007	664	-4	-116	26	22	-5	234	-21	-11	61	6	-31	75	47	-2	-24	5	53
2008	1561	71	-11	-648	1	85	296	0	1	-1	0	1	150	72	-1	-63	2	117
2009	1078	73	-1	-454	0	78	211	-47	65	189	-20	-59	104	144	-1	-61	1	162
2010	586	-20	-35	145	6	-23	206	-48	81	190	-25	-59	59	40	0	-17	1	43

Catchments																		
	Upper Buffalo (R20A-C)						Baviaans (Q60A-C)						Noordkaap (X23A)					
Time	*Water Balance*		*WB Closure*		*%BIAS*		*Water Balance*		*WB Closure*		*%BIAS*		*Water Balance*		*WB Closure*		*%BIAS*	
	P_{Q+MOD}	ΔP (%)	ET_P	ET_{MOD}	ET_P	ET_{MOD}	P_{Q+MOD}	ΔP (%)	ET_P	ET_{MOD}	ET_P	ET_{MOD}	P_{Q+MOD}	ΔP (%)	ET_P	ET_{MOD}	ET_P	ET_{MOD}
2001	359	-5	7	17	-2	-5	361	-39	10	227	-2	-41	157	18	-15	-24	13	22
2002	376	-19	30	87	-7	-21	328	-42	30	239	-5	-43	152	29	-5	-34	5	34
2003	329	43	-41	-99	18	44	255	-32	-48	121	13	-32	147	45	-4	-45	4	50
2004	325	7	44	-20	-15	7	231	-60	55	349	-10	-60	142	7	15	-9	-12	7
2005	378	16	-37	-51	13	17	286	-42	-39	206	8	-42	143	32	-2	-34	2	34
2006	365	-28	68	142	-15	-30	326	-51	32	334	-5	-51	-	-	-	-	-	-
2007	404	38	-69	-111	30	48	304	-45	-19	248	3	-45	-	-	-	-	-	-
2008	578	91	-3	-276	1	98	1409	270	7	-1028	-2	275	-	-	-	-	-	-
2009	456	66	8	-181	-3	67	1139	181	3	-733	-1	181	-	-	-	-	-	-
2010	305	39	-9	-85	4	40	268	-19	2	65	0	-20	-	-	-	-	-	-

Note: P_{Q+MOD}–precipitation calculated using MOD16 ETa data; ΔP (%)–Percentage difference between the measured P and P_{Q+MOD}.

Despite the noted uncertainties in the MOD16 ETa data, limited attempts to constrain the model-simulated ETa with these data were made for few catchments (i.e. T11C, R20B, and X23A). Figure 5.32 illustrates the resulting time series of the model-simulated and MOD16-based actual evapotranspiration after the constraints attempts. Increasing (e.g. T11C) and reducing (e.g. X23A) the evapotranspiration losses in the model did not only result in the insignificant changes in the simulated ETa but also affected the generation of catchment runoff by resulting in poor *CE* and *CE (ln)* values.

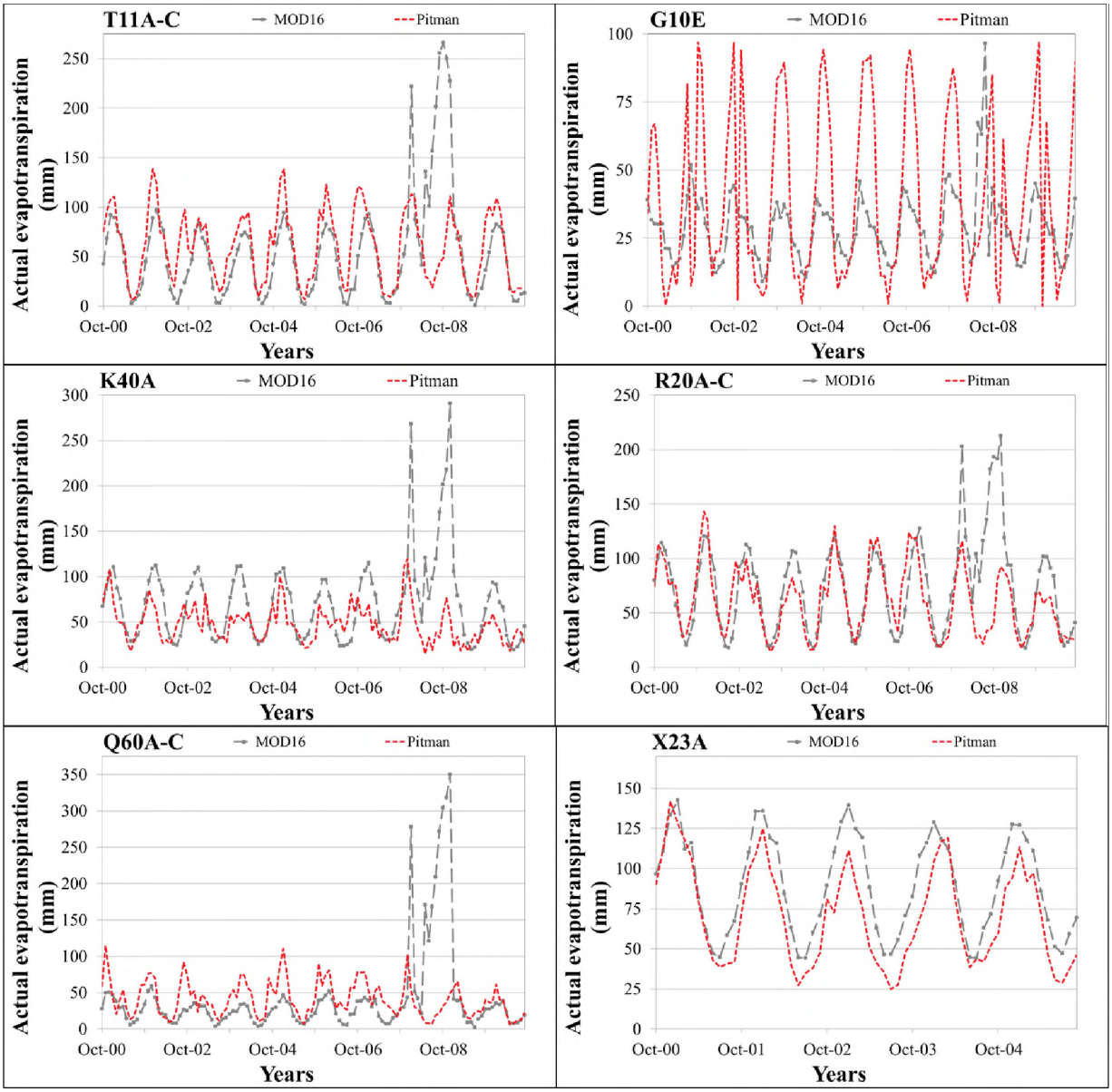

Figure 5.32: Comparison of time series of actual evapotranspiration derived from MOD16 data and model simulations for the selected catchments.

CHAPTER SIX

6. DISCUSSION, CONCLUSIONS AND RECOMMENDATIONS

6.1. INTRODUCTION

South Africa is located in a water-stressed region, which has high rainfall and evapotranspiration variability in both space and time because of different climatic conditions. Limited available observation data used to support model applications in this region are often characterised by many sources of uncertainties. It has been a common practice to conduct water resources evaluations with these highly uncertain data because there is no additional data to either define the uncertainties or reduce them. These uncertainties arise from inappropriate measurement of rainfall, stream flow with poor observation records, catchment water uses, and poor representation of catchment hydrological processes in models. All these factors therefore introduce uncertainties in the establishment of an understanding of hydrological processes through the model calibration process.

In South Africa model parameters used in standard water resource assessments (WR90 and WR2005) are derived from regionalisation methods. Because of the non-uniqueness of model parameter sets that generate acceptable hydrological response (equifinality), regionalised parameters used in the WR2005 study (Middleton and Bailey, 2008) may affect the evaluations of the impact of applying different climatic inputs in the model. This is simply because the fixed parameter set limits the ability to account for the changes in climatic forcing data inputs (Paturel *et al.*, 1995; Andréassian *et al.* 2001). Therefore, using the combination of both the single-run and the uncertainty version of the Pitman model was one of the effective methods of understanding the functioning of the model as well as exploring various parameter combinations that can be used to in the evaluation of the impacts of different climatic input data.

The discussion of the results follows the same sequence of steps used during the study which were guided by the questions that the study attempts to answer through the research aims and objectives.

6.2. THE CALIBRATION OF THE PITMAN MODEL

Developing an understanding of the catchment hydrological processes is crucial for conducting reliable water resources assessments and is usually achieved through the calibration of the model

parameters using hydrological response data to ensure satisfactory performance of the model. Because of the lack of observational data, calibrating a model in a dynamic hydrological system represents a serious challenge. Over the years, there have been many developments of the most effective methods to improve realism of the Pitman model for effective water resources assessments and management. These include various methods of estimating parameters (e.g. Kapangaziwiri *et al.*, 2010), developing guidelines for calibrating the model (e.g. Kapangaziwiri and Hughes, 2008), and establishing model output constraints (e.g. Tumbo and Hughes, 2015) using various sources of information (e.g. Hughes *et al.*, 2014a). A combination of some of these developments was used in this study.

6.2.1. Naturalised Hydrological Response Simulations

Before it was possible to investigate the benefits of different evapotranspiration forcing approaches to setting up the chosen model (Pitman), it was essential to make sure that the basic model setups for all of the selected catchments were able to represent both natural and developed conditions. It was decided to do this using the conventional approach to PET forcing and the regional PET data available within the South African Water Resources studies (mostly using the WR2005 data). The assessment of the model results for natural catchment response were similarly based on the naturalised flow data given in WR2005, while the present day (developed) simulations were based on the available observed flow data.

The single-run version of the Pitman model, together with manual adjustment of the parameters, was found to be a very useful way to learn about the structure of the model, but the uncertainty version is certainly a more efficient way of exploring various parameter combinations and their impacts on the outputs. However, the single-run version can be useful to guide the process of establishing the parameter ranges that are used as input to the uncertainty version. The relatively high degree of equifinality within the Pitman model parameters set can confuse a manual calibration process. Section 5.3.6 illustrated the equifinality issue using an assessment of the variability in the values of the interflow and groundwater recharge parameters determining moderate to low flow responses. This section identified a high degree of equifinality amongst these parameters and concluded that an index of total low flow response (FT/PW+GW/GPOW) is the best way to examine the 'best' parameter set. Available information on the physical catchment characteristics and groundwater recharge data were the 'best' information that was available for establishing the uncertain parameter

constraints and for accounting for hydrological process spatial heterogeneity within the sub-basins of some of the model setups.

Because of the relatively small size of the selected sub-catchments, some information used was not available at the appropriate scales to represent catchment characteristics. Therefore, the process of assigning parameter value constraints was not always straightforward. Some of the results presented in Section 5.3 suggest that there are uncertainties in the data or information used to guide the model calibration process. Overall, the study illustrated that the version of the model that was used (with the inclusion of the groundwater recharge and discharge functions given in Hughes, 2004) generated acceptable simulations when compared with those based on naturalised observed flows from the WR2005 study.

6.2.2. Present-day Simulations

The established behavioural parameter sets together with water resource developments impacts resulted in both good and poor simulations based on the ranges of the objective functions used. Some of the poor results are associated with the inability of the model to simulate both the very high and low flows (low CE and $CE\ \{ln\}$ values). Very little observed data or reliable information is available to resolve the uncertainties associated with water resources developments. This study illustrated that various sources of uncertainty often hinder a comprehensive assessment of the impacts of developments on present-day flows. The main uncertainties identified by this study are summarised as follows:

- ***Small farm dams:*** The main problems are the lack of established capacity-area relationships and the difficulties in determining the upstream catchment areas of the scattered dams. In the Klein Berg River catchment, for example, the majority of small farm dams are not located on the main river channel but distributed across the catchment in varying topography. Therefore, determining the aggregated sub-catchment area draining to the 'dummy' dam (used in the model) and using a generalised capacity-area relationship to estimate dam volumes introduced uncertainties. While Hughes and Mantel (2010a) have highlighted some of these issues, additional uncertainties associated with the estimation of small farm dam volumes are also exacerbated by the fact that the capacity of the dam's changes continuously due to sedimentation and other human activities in catchment (Peng

et al., 2006; Feng *et al.*, 2011). In other catchments (e.g. Baviaans and Xhora), it was challenging to identify small farm dams due to their small size and the lack of satellite images covering the wet season.

- ***Irrigation water:*** Distinguishing the sources of irrigation water (supplied from either run-off-river or small farm dam's abstractions), and the lack of records on actual abstraction patterns, caused substantial uncertainty in the quantification of irrigation abstraction effects. Moreover, contradicting information on irrigation water sources obtained from different agencies in different times (e.g. WR2005 database: Middleton and Bailey, 2008, WARMS database: DWS, 2014a and WCDA, 2015) made it difficult to quantify the water use parameters. For example, assuming that irrigated areas along the riverbanks are supplied directly from run-of-river abstractions could not be true in some cases. Some small farm dams (e.g. G10E) that are located along the riverbanks could be used as off-channel storage facilities supplied from the river. Water-diverting canals to the small dams (e.g. sub-catchment Q60C) also introduced confusion in the identification and the quantification of the sources of irrigation water.
- ***Large reservoirs*:** The limitations of the data on irrigation or environmental flow releases from large reservoirs affected the proper representation of present-day flows of sub-catchment R20B.
- ***Observed flows:*** The results indicated that short stream flow records make it difficult to understand the non-stationarity trends in some catchments (e.g. T11C). Furthermore, the inability of some of the gauging stations to accurately measure both extreme high and low flows due to the design capacity and infrequent calibration of their rating curves (low flows) may have also contributed to poor objective function statistics regardless of whether the model is representing the processes well or not.

The sources of uncertainties in the present-day simulations are not only limited to model parameter, water use and calibration data, others may be associated with the interpolated rainfall data that influence the estimation of some of the model parameters. This could be particularly true in the mountainous areas where large spatial variability in rainfall is expected but not measured by the available rainfall gauges. In the absence of additional data, it is very difficult to examine the rainfall uncertainty effects on the model parameter sets and results. Even if additional data were available, it would remain difficult to apportion total uncertainty to the different sources.

6.3. INITIAL EVALUATION OF THE MOD16 ET DATA

Most river basins in the developing world are ungauged, and even when they are gauged their observation networks are generally poor and do not provide the hydrometeorological variable data that are essential for water resources assessments. Hydrological response or input data are therefore often estimated using extrapolation from nearby gauged sites, which is not always straightforward. Extrapolating data from gauged to ungauged catchments requires statistical or process-based methods (or a combination of both). The methods are almost impossible to validate and rarely reflect the real heterogeneity of processes at catchment scale. This certainly true for South Africa where standard model applications are traditionally conducted with regionalised PET datasets that are often assumed to be the best representation of evapotranspiration demand at a catchment scale. The inherent uncertainties associated with this type of PET estimation method suggest that there are opportunities for the use of data derived using other methods, such as MODIS.

The results of the study demonstrated that the MODIS (MOD16) data generally over-estimate potential evapotranspiration in the catchments when compared with the regionalised pan-based estimates from the WR2005 database (Middleton and Bailey, 2008). As expected, the MOD16 PET data indicated that catchments located in arid to semi-arid areas (e.g. Baviaans River) have higher evapotranspiration demands than those in humid to sub-humid zones (e.g. Upper Buffalo, Noordkaap). This confirms that the components of potential evapotranspiration are strongly dependent on climatic conditions. For example, during the dry summer season, in the winter rainfall region of South Africa, high temperatures associated with low levels of relative humidity result in the increase of evapotranspiration demands. However, in the humid zones higher temperatures in combination with high levels of relative humidity limit the potential evapotranspiration demands. This is evident in PET time series of the Klein Berg and Noordkaap River catchments, which are located in semi-arid and humid climatic zones of the country, respectively. Nevertheless, the observed differences in PET estimates from the MOD16 product are consistent with the iso-reference evaporation maps produced by Savva and Frenken (2002) and were also reported in a study that evaluated MOD16 PET data across South Africa (Jovanovic *et al.*, 2015).

The fact that the MOD16 PET data, for the selected catchments, have different values to the regionalised pan-based data (Mean {Pan}) that are traditionally used with the Pitman model does not necessarily mean that they are not suitable for forcing the models evapotranspiration demands.

This is because different model parameter values could be appropriate when using different evapotranspiration forcing data in the same way that changes in model parameters can compensate for (some) changes in rainfall forcing data. The key point is that the most appropriate set of parameter values that achieves the most behavioural (compared with known patterns of stream flow) result is not independent of the climate data used to force the model. However, there is always a limit to the extent to which the model parameters can compensate for inappropriate climate data as the water balance must always close. Perhaps one of the main issues is that the basic long-term (i.e. ignoring any changes in storage) water balance components are rainfall, actual evapotranspiration and stream flow. Within South Africa, there are typically large differences between potential and actual evapotranspiration, which is often determined more by the available moisture in storage than the potential demand. It is therefore possible or even quite likely that a model such as the Pitman model could be relatively insensitive to the PET forcing data and that changes in some parameter values can accommodate differences in input PET data. In effect, this is a form of equifinality (getting the same answer for different reasons), but between forcing data and parameters rather than just within the parameter set.

6.4. EVALUATION OF THE MOD16 PET DATA IN THE EFFICIENCY OF THE MODEL

This part of the study demonstrated that using different forms of PET inputs to force and calibrate the Pitman model has different impacts on the simulated flows and the model parameters. The approaches used to evaluate the efficiency and the sensitivity of the Pitman model to change in PET inputs are static and dynamic methods. In static sensitivity analysis, the 'best' parameter set that was calibrated from the Mean (Pan) data remains fixed when the different forms of PET data are used to simulate the hydrological response. When the dynamic sensitivity approach is used, the model parameters are re-calibrated every time the PET inputs data are changed. This implies that each model re-calibration step generates different optimum parameter sets. The model simulations of the 'best' parameter set calibrated for the two sensitivity approaches were evaluated against the reference simulations obtained from the calibrated parameter set using the Mean (Pan) data inputs.

Static analysis: The results presented in sub-section 5.5.1 illustrated that there are insignificant effects on runoff generation when applying T/S (Pan) inputs in the model as the values of the model efficiency improved slightly or remained unchanged (see Table 5.14). Forcing the model with the

generally higher T/S (MOD16) inputs has substantial negative impacts, particularly on the low flow simulations (low *CE* values). The use of T/S (Pan) inputs suggests that increasing potential evapotranspiration demands in the model does not significantly change the evapotranspiration losses from the unsaturated soil storage since PET is not limited by soil moisture. This behaviour of the model was observed in the results for most catchments with the exception of the Noordkaap. In this catchment, it was noted that T/S (MOD16) inputs tend to increase ETa losses throughout the season. Part of this could be attributed to the dominance of the deep-rooted vegetation that transpires even at lower levels of moisture storage.

The overall conclusion is that incorporating time series variation (rather than have fixed seasonal distributions for every year) in evapotranspiration demand did not improve model efficiency when the same parameter values are used.

Dynamic analysis: The results of applying a dynamic approach in Section 5.5.2 indicated that the model is flexible enough to compensate for changes in PET input data, when re-calibrated. The results demonstrated that re-calibrating the model under uncertain conditions allows for a larger number of parameter combinations that can generate acceptable steam flow simulations. This pattern was observed mostly when the model is calibrated with T/S (Pan) data inputs. The results of T/S (Pan) re-calibrations illustrated that the efficiency of the model for the simulated high flows improved but with an insignificant margin, whereas the low flow simulations had reduced *CE (ln)* values. While the statistics of model efficiency are somewhat similar to those obtained using the static analysis, scatterplots of the variation of objective function with the ensembles of parameter R and ST demonstrated that the acceptable simulations can be obtained with a variety of parameter combinations.

Model re-calibration using T/S (MOD16) data show varying differences in model efficiency as well as the values of the behavioural parameter sets. The model generally under-simulates the flows (decrease in *CE* and *CE {ln}* values). However, in the cases where the model performance was improved, *CE* and *CE (ln)* values did not vary significantly to those of Mean (Pan) calibrations. It was reported in the static analysis results that the use of T/S (MOD16) data inputs in the model have an effect on the simulated low flows. However, the best parameter set from T/S (MOD16) re-calibrations did not have significant impact on the low flows expect for the Xhora River catchment. These intriguing results are simply showing that the model is flexible to account not only for

increased evapotranspiration demands but also for different parameter combinations that generate acceptable hydrological response. The variations between the coefficients of efficiency (*CE* and *CE {ln}*) and the values of parameter R and ST demonstrated that there is large equifinality and a parameter identifiability problem in the model (see Figure 5.24 to 2.27 of sub-section 5.5.2).

The general conclusion from the static and dynamic tests is that the Pitman model appears to be largely insensitive to the variability the PET data inputs, which is largely because ETa in some catchments is limited by water availability, rather than energy availability. The dynamic approach illustrated that the model is flexible enough to achieve parameter sets appropriate to changing evapotranspiration demand data. This has been observed in the other models used in different studies (e.g. Vázquez and Feyen 2003; and Andréassian *et al.* (2004). This therefore suggests that as long as PET estimates are broadly representative in terms of seasonality patterns (T/S {Pan} data), the model parameters calibrated on that PET data are likely to result in acceptable simulations. This study further demonstrated if the annual mean of potential evapotranspiration is increased (T/S {MOD16} data), the model results are adversely affected. However, when the increased mean annual PET data are used to re-calibrate the model, then model efficiency remains largely unchanged. This demonstrate that the PET input data and the most appropriate model parameter set are not independent of each other. While Fowler (2002) and Oudin *et al.* (2005b) also demonstrated this behaviour in various models, the results of the dynamic sensitivity approach proved to be useful in exploring various parameter combinations and identifying the impact of changing PET inputs on them. However, the issues of equifinality and parameter identifiability, a common phenomenon in over-parameterised models (Beven, 2006), was evident in the results of model re-calibrations with different PET data inputs.

In general, the results indicated that PET time series inputs to the Pitman model do not necessarily provide significantly better stream flow simulations than traditional Mean (Pan) values. These observations are similar to those of Fowler (2002), Andréassian *et al.* (2004), and Oudin *et al.* (2005a, b) who found that hydrological models perform well when calibrated with mean monthly estimates of PET rather than temporally varying estimates of PET based on Penman method. It was demonstrated that the modelling approach used to evaluate the impacts of different forms of PET input data to force and calibrate the model could lead to different results. However, besides that, it is intriguing that a more detailed PET input data proved not successful in improving the efficiency of

the mode. The following sub-sections discuss some of the uncertainty issues that might explain the results of this study.

6.4.1. Uncertainties in Potential Evapotranspiration Data

The MOD16 data tend to have higher estimates of potential evapotranspiration than the regionalised Mean (Pan) data. In the literature (e.g. McMahon *et al.*, 2013), there is a wide range of methods to derive PET estimates used in rainfall-runoff models. The most frequently adopted methods to represent PET inputs include Penman-Monteith, FAO reference crop and pan evaporation data. Ideally, to represent PET dynamics of a catchment the method adopted should adequately capture all the climatic, energy and aerodynamic components of the evapotranspiration process. Recent decreasing trends in pan evaporation data from A-pan measurements (Hoffman *et al.,* 2011) together with the observed increase in mean annual temperatures (Roderick *et al.*, 2009) show the potential danger of using equations that do not adequately represent all relevant processes that affect evapotranspiration. While the Penman-Monteith approach has been preferred for hydrological modelling studies (Donohue *et al.*, 2010b; Allen *et al.,* 2011b) based on its ability to best capture the dynamics of evapotranspiration demands, pan-derived PET are still used in hydrological model applications. However, pan-based methods do no capture the spatial variability of the ET dynamics and this could make the data derived from these approach uncertain. It is for this reason that this study attempted to explore remote sensing-based evapotranspiration data.

The majority of satellite-based products tend to provide different ET (both PET and ETa) estimates compared to field-based estimates and these disparities seem to be quite common, as reported by Hu *et al.* (2015). Discrepancies in the MOD16 ET data are associated with the uncertainties in the input data of the MOD16 ET algorithm and conceptualisation of the algorithm itself as well as the validation process as noted by Choi *et al.* (2011) and Mu *et al.* (2007a, 2011). The main inputs for the MOD16 ET algorithm are land use and land cover classification (MOD12Q1 product), surface albedo (MCD43B3 product), leaf area index and fraction of photosynthetic absorbed radiation (LAI and FPAR: MOD15A2 product) as well as a variety of meteorological data derived from the Global Modelling and Assimilation Office (GMAO). The uncertainties associated with the above-mentioned components are summarised as a follows:

- The MODIS ***global land use land cover*** (MOD12Q1 Collection 4 product: Friedl e*t al.*, 2002) provides annual classification estimates based on the International Geosphere-Biosphere Program (IGBP) in only 17 different classes globally (Belward *et al.*, 1999). Moreover, the relatively coarse scale (500 m) of the MOD12Q1 data could be inadequate to capture the heterogeneity of the different land cover types that have different impacts on the PET dynamics. Despite the reported 85% accuracy at the continental scale (Friedl e*t al.*, 2002), misclassification and the larger spatial scale at which the MOD12Q1 data are derived can introduce uncertainties in the parameterisation of the MOD16 algorithm as already noted in the result of the improved MODIS land cover by Friedl *et al.* (2010). In South Africa, Jovanovic *et al.* (2015) reported that the MOD12Q1 data generally classified the inland part of the country (central and western regions) as open grassland and shrubland while the northeast parts are categorized as savanna types. This misclassification of land cover types inevitably introduces uncertainties in other products derived from the MOD12Q1 data.
- The estimation of the ***LAI, surface albedo, and FPAR*** at a global scale also contributes to the MOD16 ET data uncertainties (Demarty *et al.*, 2007). Ramoelo *et al.* (2014) reported that the PROSAIL model used in the generation of global MODIS-based LAI data (MOD15A2: Myneni *et al.*, 2002) does not always provide plausible estimates because of the global parameterisation and the lack of validation data. Furthermore, Leuning *et al.* (2005) and Cohen *et al.* (2006) found that, quite often, ground-based measurements of LAI result in lower and relatively consistent values than those of the MOD15A2 data product. The results of Pandya *et al.* (2006) and Ruhoff *et al.* (2013) suggest that the uncertainties in the MOD15A2 and MOD12Q1 data probably explain why the MOD16 PET data are over-estimated.
- The GMAO ***meteorological input*** data (spatial resolution 1.00°x 1.25°) were interpolated to fit the 1 km^2 spectral resolution of the MODIS pixels. This scale is too coarse to be representative of local meteorological variables. The work of Zhao *et al.* (2006) demonstrated that the meteorological variable data from GMAO and field-based measurements have large differences in terms of accuracy. Estimating the relative humidity at a global scale cannot be considered adequate because of large spatio-temporal variability even at local scale. The results of Kazamias (2016) illustrated that the relative humidity data used in the MOD16 algorithm are under-estimated. This implies that the

MOD16 algorithm assumes that the relative humidity is predominantly low which subsequently result in the increase of potential evapotranspiration demands.

- The ***MOD16 ET algorithm (PET and ETa)***, generally, does not account for plant biophysics for site-specific species, landscape heterogeneity and microclimate influences to soil surface and transpiration processes (Mu *et al.*, 2011). Furthermore, different plant growth stages and their relative transpiration rates under different soil moisture levels are also not accounted for explicitly in the MOD16 ET algorithm. A typical example in this regard is the plant stomata closure that was assumed to occur only at night-time in all versions of the algorithm (Mu *et al.* 2007a, 2011). This assumption could also be contributing to the under-estimation of ET because a variety of vegetation types over a range of ecosystems have nocturnal stomata opening which contribute to the total actual evapotranspiration (Caird *et al.,* 2007). Another typical example is an implicit assumption that the GMAO-derived relative humidity patterns can represent the status of the soil moisture (Su-Chuang *et al.*, 2015). The fact that changing patterns of soil moisture content and relative humidity are different makes this assumption questionable. Soil moisture content, which has large variability due to factors such as differences in the soil types and vegetation cover, is relatively stable over a period of short time, but shows a decreasing trend between two rainfall events. In contrast, relative humidity is highly dependent on atmospheric conditions, such as solar radiation and air temperature that regularly change on the daily and seasonal scale. With these differences, it is likely that the MOD16 ET products are affected by uncertainties.

Mu *et al.* (2011) and Trambauer *et al.* (2014) have shown that validating and conducting sensitivity analysis is important in identifying the variables that influence the MOD16 ET product. However, some studies (e.g. Kim *et al.,* 2012; Ramoelo *et al.*, 2014) have shown that the validation of the MOD16 PET data, using flux tower measurements, is affected by uncertainties. These are mostly associated with the energy balance closure that is influenced by the local weather conditions at the sites where the measurements are conducted (Ramoelo *et al.*, 2014). These uncertainties inevitably affect the validation process and perhaps introduce further uncertainty into the MOD16 data.

6.4.2. Pitman Model Structure Uncertainties

The sensitivity analysis suggests that the simplification of the relationship between evapotranspiration losses and a single layer of soil moisture storage could have affected the simulation results. In practical terms, evapotranspiration losses from heterogeneous soil moisture storage are largely dependent on the structure, layering of the soils and the availability of moisture content. Therefore, the simplification of these processes in the structure of hydrological models could also make the Pitman model insensitive to changing PET inputs. It has often been suggested (e.g. Andréassian *et al.*, 2004, Oudin *et al.*, 2005b) that some of the insensitivity of the structure of the hydrological models could be related to the conceptualisation of soil moisture accounting and its related processes. These are amongst others: (i) conceptual representation of the soil moisture storage as a linear regulator to ET losses (Parmele, 1972), (ii) soil moisture storage accounting acting as a low-pass filter which smooths the PET variations (Oudin *et al.*, 2004), and (iii) the flexibility of the model structure to accommodate different forms of PET estimates and compensate for them in the model routines (Andréassian *et al.*, 2004). Given these observations, the question remains whether models with multiple layers of the unsaturated storage zone would be more sensitive to different forms of PET inputs. However, increasing model complexity by adding parameters would increase equifinality. Balancing structural complexity, model sensitivity and equifinality remains a major subject of interest within the field of hydrological modelling.

Because PET data inputs primarily affect the dynamics of soil moisture variations, basic concepts from soil hydrology can be used to explain some of the hypothesis applied in conceptualizing the temporal variability of soil moisture in the hydrological models. The low-frequency characteristic of soil moisture variability, which is linked to atmospheric forcing variables (Entin *et al.*, 2000) and seasonality (Wilson *et al.*, 2004) could also contribute to model insensitivity if it is not accounted for in the structure. While it was not part of the scope of this study to explore the soil moisture-evapotranspiration routines of the Pitman model, the conclusion reached by Oudin *et al.* (2004) is that even when comparing the sensitivities of models with very different structures to varying PET inputs, it is unlikely to achieve unique results. The results from this study are, therefore, not different to those found by Fowler (2002) and Oudin *et al.* (2005a, b) who attempted to answer the representation of time-varying PET demands in rainfall-runoff models. The results of this nature from different types of rainfall-runoff models suggest that it is necessary to investigate complex feedback mechanisms between the buffering effect of soil moisture and climatic variable influences.

This would further improve the understanding of soil moisture-evapotranspiration relationships at a catchment scale as well as improving the evapotranspiration routines in the model as substantiated by several theoretical and observational studies (Entin *et al.*, 2000). These studies have shown that the soil-moisture storage layer acts as an integrator of short time scale atmospheric anomalies resulting in the insensitivity of the model structure.

6.5. CONSTRAINING THE MODEL-SIMULATED ACTUAL EVAPOTRANSPIRATION

The MOD16 data generally presented varying estimates of actual evapotranspiration in the selected catchments. When using the residual of the catchment water balance as the basis of comparison, in arid to semi-arid areas (Xhora, Baviaans, and Klein Berg), the MOD16 data under-simulates ETa compared to those in the humid zones. This could be suggesting that the MOD16 data accounts for the shallow-rooted vegetation which does not extract moisture from deep storage. However, in the densely forested catchments (e.g. Noordkaap and Diep) the MOD16 data show the capability to capture higher evapotranspiration losses. Despite being regarded as one of the promising remote sensing-based ETa dataset, little research has been done in validating the MOD16 ETa product in different parts of South Africa. The results of the annual catchment water-balance analyses illustrated that the MOD16 data are either over–or under-estimating evapotranspiration losses at a catchment scale. While it was originally thought that some uncertainty in the input rainfall data might account for these results, the water balances errors based on using MOD16 ETa data are outside the likely bounds of any input rainfall errors. The results of these simple analyses render any attempts to constrain the model-simulated ETa, somewhat, superfluous.

6.6. CONCLUSIONS

The present study is aimed at evaluating the use of satellite-derived evapotranspiration estimates for improving the efficiency of rainfall-runoff model applications in a South African context. The use of MOD16 PET data was compared with traditional approaches using uncertain regionalised potential evapotranspiration inputs derived from pan-measurements, while the use of actual evapotranspiration data (MOD16 ETa) to constrain the Pitman model outputs was also examined in this study. The outcomes of the study are summarised below by relating them to the key research questions, on which the objectives of the study are based.

Is the GW-PITMAN version of the Pitman model capable of simulating the naturalised and present-day hydrological responses considering the uncertainties?

A two-step modelling approach was employed to establish model parameter sets for naturalised flow conditions using a single-run (first step) and uncertainty (second step) versions of the model. The first step assisted in developing an understanding of the model's functionality, establishing initial parameter sets, and setting the uncertain parameter ranges for use in the uncertainty version of the model. The second step identified a wider range of possible parameter sets that generated acceptable hydrological responses. While the outcomes were largely satisfactory, it was not always possible to reduce the uncertainty and equifinality within the model given the available input data.

The study identified that the largest degree of uncertainty in simulating the developed conditions seem to be from the quantification of the impacts of small farm dams and distinguishing sources of irrigation water. While these uncertainties significantly affected the simulation results in some catchments (e.g. G10E and Q60C), the methods used were assumed appropriate given the limitations of the data available to validate these water uses. An additional major source of uncertainty lies in the quality (problems with observations of extreme high and low flows) and non-stationarity of the observed stream flow data for some of the gauging stations. These uncertainties contribute to the difficulties of establishing representative (behavioural) parameter sets and of adequately validating the model setups.

Can remote sensing data be used to improve the application of hydrological models and assist in reducing uncertainties in the model input data?

Earth observation data can potentially address many model uncertainties. Their application includes, for example, relating vegetation types to soil moisture depth, estimating groundwater variations, as well as quantifying evapotranspiration dynamics. Frequently, however, these data are provided at large spatial and temporal scales which are not applicable in catchment-scale modelling studies. Furthermore, assimilating these data into standard modelling platforms requires the further development of tools to extract the data. The study focused on exploring the use of earth observation data in attempts to reduce uncertainty in the use of regionalised PET estimates in the Pitman model.

This study used static and dynamic sensitivity analysis approaches to evaluate the effects of forcing the Pitman model with temporally varying PET estimates derived from MOD16 data. The

conclusion reached is that there are no substantial improvements in the efficiency of the model when the same parameter values calibrated on one type of PET estimate are used to evaluate model sensitivity to changing PET data inputs (static approach). Part of the reason is that the static analysis approach neglects the adaptive capacity of the parameter sets of rainfall-runoff models. In some catchments, the model was relatively insensitive to PET changes, while in others the model performance deteriorated quite substantially.

The study also demonstrated that model re-calibration with different forms of PET data inputs (dynamic approach) have varying impacts on the simulated flows and on the number of behavioural parameter sets. This demonstrated the dependency of model parameter sets on climatic inputs due to a flexible parameter space which accounts for a variety of parameter/input data combinations. The T/S (Pan) re-calibrations had a large number of acceptable simulations but the model performance was not substantially different compared to Mean (Pan) simulations. The use of T/S (MOD16) to re-calibrate the model improved the low flow simulations in terms of the statistics. Is it difficult to conclude why the overall model efficiency did not improve when more detailed PET data inputs are used when a dynamic approach was used.

Discrepancies in the MOD16 PET data associated with the inadequate conceptualisation of the MOD16 algorithm and uncertainties within the input data used in the algorithm, could have contributed to an inadequate representation of evapotranspiration demands. Some of the components that affect evapotranspiration processes are not explicitly represented in the MOD16 algorithm whereas the input data to the algorithm are often estimated at large spatial scales and not deemed adequate to represent processes at a catchment scale. A further possibility is that the simplified linear relationships between soil moisture-evapotranspiration losses in the structure of the Pitman model are not complex enough to represent the heterogeneity of these processes across the catchment (as well as under changing moisture status conditions) and were assumed to have also contributed to the insensitivity of the model to changes in PET.

Can remote sensing-based actual evapotranspiration be used to constrain the Pitman model simulated ETa?

The MOD16 ETa data resulted in the non-closure of the annual catchment water balance. While it was considered possible that uncertainties in both the input rainfall and observed stream flow data could contribute to this result, the study concluded that the water balance errors that occur when

MOD16 ETa data are used could not be accounted for by likely uncertainties in the other water balance components. The patterns of over– and under-estimation of actual evapotranspiration by the MOD16 product could be related to the characteristics of the vegetation cover in the case study catchments with deep-rooted (over-estimated) and shallow-rooted vegetation (under-estimated) showing consistent differences. Initial evaluations of the MOD16 ETa data prior to their application in the model as process constraints identified large discrepancies in these datasets.

6.7. RECOMMENDATIONS

Addressing uncertainties associated with observation data such as evapotranspiration inputs is particularly important for improving water resource evaluations. The literature suggests that the use of evapotranspiration estimates from earth observation systems have a lot of potential to be used to better represent climatic forcing (PET) data and as process constraints (ETa) in the calibration of rainfall-runoff models. However, the conclusions of this study suggest that this potential was not realised within the relatively small sample of catchments included. Based on the conclusions of the study, the following recommendations are made:

i. While the parameter uncertainty bounds used in this study were based on somewhat subjective interpretations of catchment physical characteristics and uncertain climatic inputs, addressing observational data uncertainties and the collection of other hydrological data will greatly improve the establishment of behavioural parameters. It is recommended that hydrometeorological data uncertainties be reduced by ***improving the collection of data through both the improvement of existing measurement techniques and obtaining earth observation data with higher spatial resolution***. The Manubi Forest example (Hughes *et al.*, 2014a) that compared MOD16 ETa data with Eddy Covariance observations is quite rare and more studies of this type should contribute to an improved understanding of the relationships between different evapotranspiration estimates. Such studies could ultimately point to improved approaches for the use of remotely sensed data in hydrological modelling studies.

ii. One of the noted challenges that the study encountered in simulating present-day flow regimes was the availability, quality and length of the observation data that could provide credible information with which to represent hydrological processes. Observed stream flow data for the catchments located in relatively arid areas are markedly uncertain due to the inability of many gauge stations to capture low flows. ***It is recommended that the DWS re-calibrate the rating curves of stations located in arid and semi-arid areas, and that the upstream pools of the stations be surveyed on regular basis (once every 5 years) to improve the measurement of stream flow***. Furthermore, increasing water competition amongst users means ***there is a need for enforced legal compliance of water users on the volumes of water used***. The data on actual use should be updated in the WARMS database (DWS, 2014a) to assist in conducting efficient water resource evaluations.

iii. ***Sources of uncertainty need to be more explicitly identified, including forcing, process, and parameterisation errors, in the MOD16 ET data***. The identification and quantification of uncertainty sources will guide methods aimed at improving the MOD16 forcing data, conceptualisation of soil moisture-evapotranspiration dynamics, and remote sensing technology at large. The integration or building of hybrid methods that combine different evapotranspiration estimation techniques using remote sensing data will be valuable. ***It is further recommended that the spatial scales of the satellite-derived inputs to the MOD16 algorithm be improved in the future***. The current global MOD16 input data products suffer from coarse spatial resolution making it harder for MODIS to meet many of the practical needs of its data products. As availability of earth observation data grows, ***further improvement and publication of data process techniques will increase the easy usability of satellite-derived observation data***.

iv. It is recommended that ***hydrological modelling studies attempt to explore the potential use of other earth observation data for different aspects of modelling*** with the ultimate goal of improving the confidence of both standard water resource evaluation tools and satellite data.

v. Lastly, there is a need for an improved representation of soil moisture accounting used in the routines of the Pitman model. ***It is therefore recommended that the relationship between soil characteristics and evapotranspiration losses for different dominant vegetation types be investigated for further improvement in the model***.

REFERENCES

Abbott, M.B., Bathurst, J.C., Cunge, J.A., O'Connell, P.E. and Rasmussen, J., (1986). An introduction to the European Hydrological System. *Journal of Hydrology,* ***87***(1–2), 45-59.

Abtew, W.B. and Melesse, A.M., (2012). *Evaporation and Evapotranspiration: Measurements and Estimations,* 1st Edition. Springer: London, England, pp. 63-91.

Abtew, W.B., Obeysekera, J. and Iricanin, N., (2011). Pan evaporation and potential evapotranspiration trends in South Florida. *Hydrological Processes,* ***25***(6), 958-969.

Adam, J.C., Haddeland, I., Su, F. and Lettenmaier, D.P., (2007). Simulation of reservoir influences on annual and seasonal streamflow changes for the Lena, Yenisei, and Ob'rivers. *Journal of Geophysical Research: Atmospheres (1984–2012),* ***112***(D24), 1-22.

Adler, R.F., Huffman, G.J., Chang, A., Ferraro, R., Xie, P., Janowiak, J., Rudolf, B., Schneider, U., Curtis, S. and Bolvin, D., (2003). The version-2 Global Precipitation Climatology Project (GPCP) monthly precipitation analysis (1979-present). *Journal of Hydrometeorology,* ***4***(6), 1147-1167.

AGIS., (2013). *AGIS Comprehensive Atlas.* Agricultural Geo-Referenced Information System, available from: www.agis.agric.za, retrieved in November 2013.

Aird, R., Koekemoer, D., Timm, D. and Mallory, S., (2014). *Current and Future Water Requirements and Water Resources: Water Requirements and Availability Reconcilliation Strategy for the Mbombela Municipal Area.* DWA Report No. PWMA 05/X22/00/2012/3, Department of Water and Affairs, Pretoria.

Albergel, C., de Rosnay, P., Gruhier, C., Muñoz-Sabater, J., Hasenauer, S., Isaksen, L., Kerr, Y. and Wagner, W., (2012). Evaluation of remotely sensed and modelled soil moisture products using global ground-based in situ observations. *Remote Sensing of Environment,* ***118***, 215-226.

Aldous, J.G., Smithers, J.C. and van der Spuy, D., (2014). Assessment of the impact of gauging weir limitations on the estimation of runoff volumes and flood peaks. *Paper presented at the 17th SANCIAHS National Hydrology Symposium, hosted by the Institute of Water Studies, University of the Western Cape, Cape Town, September 2014,* pp. 1-10.

Allen, R.G., Pereira, L.S., Raes, D. and Smith, M., (1998). Crop evapotranspiration-Guidelines for computing crop water requirements-FAO Irrigation and drainage paper 56. *FAO, Rome,* ***300***, 1-15.

Allen, R.G., Pereira, L.S., Howell, T.A. and Jensen, M.E., (2011a). Evapotranspiration information reporting: I. Factors governing measurement accuracy. *Agricultural Water Management,* ***98***(6), 899-920.

Allen, R.G., Pereira, L.S., Howell, T.A. and Jensen, M.E., (2011b). Evapotranspiration information reporting: II. Recommended documentation. *Agricultural Water Management,* ***98***(6), 921-929.

Allen, R.G., Irmak, A., Trezza, R., Hendrickx, J.M.H., Bastiaanssen, W.G.M. and Kjaersgaard, J., (2011c). Satellite-based ET estimation in agriculture using SEBAL and METRIC. *Hydrological Processes,* ***25***(26), 4011-4027.

Andréassian, V., Perrin, C., Michel, C., Usart-Sanchez, I. and Lavabre, J., (2001). Impact of imperfect rainfall knowledge on the efficiency and the parameters of watershed models. *Journal of Hydrology,* ***250***(1–4), 206-223.

Andréassian, V., Perrin, C. and Michel, C., (2004). Impact of imperfect potential evapotranspiration knowledge on the efficiency and parameters of watershed models. *Journal of Hydrology,* ***286***(1–4), 19-35

Arnaud, P., Bouvier, C., Cisneros, L. and Dominguez, R., (2002). Influence of rainfall spatial variability on flood prediction. *Journal of Hydrology,* ***260***(1–4), 216-230.

Bailey, A.K. and Pitman, W.V., (2015). *Water Resources of South Africa 2012 Study (WR2012): Executive Summary Version 1.* WRC Report No. K5/2143/1, Water Research Commission, Gezina.

Bárdossy, A., (2007). Calibration of hydrological model parameters for ungauged catchments. *Hydrology and Earth System Sciences,* ***11***(2), 703-710.

Barnes, W.L., Pagano, T.S. and Salomonson, V.V., (1998). Prelaunch characteristics of the moderate resolution imaging spectroradiometer (MODIS) on EOS-AM1. *IEEE Transactions on Geoscience and Remote Sensing,* ***36***(4), 1088-1100.

Bastiaanssen, W.G.M., Menenti, M., Feddes, R.A. and Holtslag, A.A.M., (1998a). A remote sensing surface energy balance algorithm for land (SEBAL) – Part 1: Formulation. *Journal of Hydrology,* ***212-213***, 198-212.

Bastiaanssen, W.G.M., Pelgrum, H., Wang, J., Ma, Y., Moreno, J.F., Roerink, G.J. and van der Wal, T., (1998b). A remote sensing surface energy balance algorithm for land (SEBAL) – Part 2: Validation. *Journal of Hydrology,* ***212-213***, 213-229.

Becker, M.W., (2006). Potential for satellite remote sensing of ground water. *Ground Water,* ***44***(2), 306-318.

Belward, A.S., Estes, J.E. and Kline, K.D., (1999). The IGBP-DIS global 1-km land-cover data set DISCover: A project overview. *Photogrammetric Engineering and Remote Sensing*, ***65***(9), 1013-1020.

Bergström, S., (1995). The HBV model. In: Singh, V.P. (Ed.), *Computer models of watershed hydrology,* Water Resources Publications: Colorado, USA, pp. 443-476.

Beven, K.J., (1989). Changing ideas in hydrology–The case of physically-based models. *Journal of Hydrology,* ***105***(1–2), 157-172.

Beven, K.J., (2002). Towards an alternative blueprint for a physically based digitally simulated hydrologic response modelling system. *Hydrological Processes,* ***16***(2), 189-206.

Beven, K.J., (2006). A manifesto for the equifinality thesis. *Journal of Hydrology,* ***320***(1), 18-36.

Beven, K.J., (2012). *Rainfall-Runoff Modelling: The Primer,* 2nd Edition. Wiley: Blackwell, England.

Beven, K.J., (2016). Facets of uncertainty: epistemic uncertainty, nonstationarity, likelihood, hypothesis testing, and communication. *Hydrological Sciences Journal*, ***61***(9), 1652-1665.

Beven, K.J. and Freer, J., (2001). Equifinality, data assimilation, and uncertainty estimation in mechanistic modelling of complex environmental systems using the GLUE methodology. *Journal of Hydrology,* ***249***(1), 11-29.

Beven, K.J. and Westerberg, I., (2011). On red herrings and real herrings: disinformation and information in hydrological inference. *Hydrological Processes,* ***25***(10), 1676-1680.

Beven, K.J. and Young, P., (2013). A guide to good practice in modeling semantics for authors and referees. *Water Resources Research,* ***49***(8), 5092-5098.

Biondi, D., Freni, G., Iacobellis, V., Mascaro, G. and Montanari, A., (2012). Validation of hydrological models: Conceptual basis, methodological approaches and a proposal for a code of practice. *Physics and Chemistry of the Earth, Parts A/B/C,* ***42–44***(2012), 70-76.

Boyle, D.P., Gupta, H.V. and Sorooshian, S., (2000). Toward improved calibration of hydrologic models: Combining the strengths of manual and automatic methods. *Water Resources Research,* ***36***(12), 3663-3674.

Brocca, L., Moramarco, T., Melone, F., Wagner, W., Hasenauer, S. and Hahn, S., (2012). Assimilation of Surface-and Root-Zone ASCAT Soil Moisture Products Into Rainfall–Runoff Modeling. *IEEE Transactions on Geoscience and Remote Sensing,* ***50***(7), 2542-2555.

Brunner, P., Franssen, H.J.H., Kgotlhang, L., Bauer-Gottwein, P. and Kinzelbach, W., (2007). How can remote sensing contribute in groundwater modelling? *Hydrogeology Journal,* ***15***(1), 5-18.

Buffalo City Metropolitan Municipality, (BCMM)., (2014). *2014/2015 Integrated Development Plan Review:* 1st draft, Buffalo City Metropolitan Municipality, East London, South Africa.

Burman, R.D., (2008). Evapotranspiration: formulas. In: Trimble, S.W. (Ed.), *Encyclopedia of Water Science.* Taylor and Francis Group: Michigan, USA, pp. 253-257.

Butts, M.B., Payne, J.T., Kristensen, M. and Madsen, H., (2004). An evaluation of the impact of model structure on hydrological modelling uncertainty for streamflow simulation. *Journal of Hydrology,* ***298***(1), 242-266.

Caird, M.A., Richards, J.H. and Donovan, L.A., (2007). Nighttime stomatal conductance and transpiration in C3 and C4 plants. *Plant Physiology,* ***143***(1), 4-10.

Castellarin, A., Botter, G., Hughes, D.A., Liu, S., Ouarda, T.B.M.J., Parajka, J., Post, D.A., Sivapalan, M., Spence, C., Viglione, A. and Vogel, R.M., (2013). Prediction of flow duration curves in ungauged basins. In: Blöschl, G., Sivapalan, M., Wagener, T., Viglione, A. and

Savenije, H.H.G. (Eds.), *Runoff Prediction in Ungauged Basins: Synthesis across Processes, Places and Scales.* Cambridge University Press: Cambridge, England, pp. 135-162.

Chen, F., Crow, W.T., Starks, P.J. and Moriasi, D.N., (2011). Improving hydrologic predictions of a catchment model via assimilation of surface soil moisture. *Advances in Water Resources, **34***(4), 526-536.

Chevallier, L.P., Gibson, L.A., Nhleko, L.O., Woodford, A.C., Nomquphu, W. and Kippie, I., (2004). *Hydrogeology of Fractured-rock Aquifers and Related Ecosystems within the Qoqodala Dolerite Ring and Sill Complex, Great Kei catchment, Eastern Cape.* WRC Report No. 1238/1/04, Water Research Commission, Gezina.

Choi, M., Kim, T.W., Park, M. and Kim, S.J., (2011). Evapotranspiration estimation using the Landsat-5 Thematic Mapper image over the Gyungan watershed in Korea. *International Journal of Remote Sensing, **32***(15), 4327-4341.

Clark, M.P., Kavetski, D. and Fenicia, F., (2011). Pursuing the method of multiple working hypotheses for hydrological modeling. *Water Resources Research, **47***(9), W09301.

Clarke, R., Mendiondo, E. and Brusa, L., (2000). Uncertainties in mean discharges from two large South American rivers due to rating curve variability. *Hydrological Sciences Journal, **45***(2), 221-236.

Cleugh, H.A., Leuning, R., Mu, Q. and Running, S.W., (2007). Regional evaporation estimates from flux tower and MODIS satellite data. *Remote Sensing of Environment, **106***(3), 285-304.

Cohen, W.B., Maiersperger, T.K., Turner, D.P., Ritts, W.D., Pflugmacher, D., Kennedy, R.E., Kirschbaum, A., Running, S.W., Costa, M. and Gower, S.T., (2006). MODIS land cover and LAI collection 4 product quality across nine sites in the western hemisphere. *IEEE Transactions on Geoscience and Remote Sensing, **44***(7), 1843-1857.

Council for Geoscience., (1997). *Simplified Geology of South Africa.* South African Council for Geoscience, Bellville, South Africa.

De Groen, M.M., (2002). *Modelling interception and transpiration at monthly time steps; introducing daily variability through Markov chains.* Unpublished PhD Thesis, UNESCO-IHE, Delft, The Netherlands.

Demarty, J., Chevallier, F., Friend, A. D., Viovy, N., Piao, S., Ciais, P. (2007). Assimilation of global MODIS leaf area index retrievals within a terrestrial biosphere model. *Geophysical Research Letters*, ***34***(15), L15402.

Department of Water Affairs and Forestry, (DWAF)., (2004a). *Berg Water Management Area: Internal Strategic Perspective Perspective: Volume 1.* DWAF Report No. P WMA 19/000/00/0304, Department of Water Affairs and Forestry, Pretoria.

Department of Water Affairs and Forestry, (DWAF)., (2004b). *Mzimvubu to Keiskamma Water Management Area: Amatole – Kei Internal Strategic Perspective.* DWAF Report No. P WMA 12/000/00/0404, Department of Water Affairs and Forestry, Pretoria.

Department of Water Affairs and Forestry, (DWAF)., (2005a). *Mzimvubu to Keiskamma Water Management Area: Internal Strategic Perspective of the Mzimvubu to Mbashe ISP Area.* DWAF Report No. P WMA 12/000/00/0305, Department of Water Affairs and Forestry, Pretoria.

Department of Water Affairs and Forestry, (DWAF)., (2005b). *Fish to Tsitsikamma Water Management Area: Fish to Sundays Internal Strategic Perspective.* DWAF Report No. P WMA 15/000/00/0405, Department of Water Affairs, Pretoria.

Department of Water Affairs and Forestry, (DWAF)., (2005c). *Groundwater Resource Assessment, Phase II.* Tender No. 2003-150, Department of Water Affairs and Forestry, Pretoria.

Department of Water Affairs and Forestry, (DWAF)., (2006). *Guidelines for Water Supply Systems Operation and Management Plans During Normal and Drought Conditions, Volume 1: Main Report.* DWAF Report No. RSA C000/00/2305, Department of Water Affairs and Forestry, Pretoria.

Department of Water Affairs, (DWA)., (2010a). *Reconciliation Strategy for Tulbagh.* DWA Report submitted by Umvoto Africa (Pty) Ltd. to the Department of Water Affairs, Bellville.

Department of Water Affairs, (DWA)., (2010b). *Reconciliation Strategy for Elliot.* DWA Report submitted by Umvoto Africa (Pty) Ltd. to the Department of Water Affairs, Bellville.

Department of Water Affairs, (DWA),. (2010c). *Amatole Water Supply System Reconciliation Strategy: Status Report.* DWA Report submitted by Umvoto Africa (Pty) Ltd. to the Department of Water Affairs, Bellville.

Department of Water Affairs, (DWA)., (2011a). *Development of Reconciliation Strategies for all Towns in the Southern Planning Region: Summary Report–Cape Winelands District Municipality.* DWA Report No. P RSA 000/00/15411, Department of Water Affairs, Bellville.

Department of Water Affairs, (DWA)., (2011b). *Amatole System Annual Operational Analysis.* DWA Report submitted by IWR Water Resources (Pty) Ltd. in association with Clear Pure to the Department of Water Affairs, King Williams Town.

Department of Water and Sanitation, (DWS)., (2014a). *Water Use Authorisation and Registration Management System.* Department of Water and Sanitation, available from: https://www.dwa.gov.za/Projects/WARMS/, retrieved in April 2015.

Department of Water and Sanitation, (DWS)., (2014b). *Annual Performance Evaluation Report for Amathole District Municipality - Xhora Bulk Water Supply Scheme.* Chief Directorate: Bulk Infrastructure Programme, King Williams Town.

Department of Water and Sanitation, (DWS)., (2015). *National Groundwater Archive.* Department of Water and Sanitation, available from: https:// www3.dwa.gov.za/NGANet/HomeForm.aspx/, retrieved in May 2015.

Di Baldassarre, G. and Montanari, A., (2009). Uncertainty in river discharge observations: a quantitative analysis. *Hydrology and Earth System Sciences, **13***(6), 913-921.

Dondo, C., Chevallier, L., Woodford, A.C., Murray, R., Nhleko, L.O., Nomnganga, A. and Gqiba, D., (2010). *Flow conceptualisation, recharge and storativity determination in Karoo Aquifer, with special emphasis on Mzimvubu Keiskamma and Mvoti - Umzimkhulu water management areas in the Eastern Cape and KwaZulu-Natal provinces of South Africa.* WRC Report No. 1565/1/10, Water Research Commission, Gezina.

Donohue, R.J., McVicar, T.R. and Roderick, M.L., (2010b). Assessing the ability of potential evaporation formulations to capture the dynamics in evaporative demand within a changing climate. *Journal of Hydrology, **386***(1), 186-197.

Donohue, R.J., Roderick, M.L. and McVicar, T.R., (2010a). Can dynamic vegetation information improve the accuracy of Budyko's hydrological model? *Journal of Hydrology, **390***(1), 23-34.

Dottori, F., Martina, M. and Todini, E., (2009). A dynamic rating curve approach to indirect discharge measurement. *Hydrology and Earth System Sciences, **13***(6), 847-863.

Dye, P.J. and Croke, B.F.W., (2003). Evaluation of streamflow predictions by the IHACRES rainfall-runoff model in two South African catchments. *Environmental Modelling and Software, **18***(8), 705-712.

Engman, E.T., (1993). Remote sensing: A developing technology for hydrology. *Hydrological Processes, **7***(2), 119-119.

Engman, E.T., (1996). Remote sensing applications to hydrology: future impact. *Hydrological Sciences Journal, **41***(4), 637-647.

Entin, J.K., Robock, A., Vinnikov, K.Y., Hollinger, E.S., Liu, S. and Namkhai, A., (2000). Temporal and spatial scales of observed soil moisture variations in the extratropics. *Journal of Geophysics Research, **105***(D-9), 11865-11877.

Everson, C., (2001). The water balance of a first order catchment in the montane grasslands of South Africa. *Journal of Hydrology, **241***(1), 110-123.

Farah, H.O. and Bastiaanssen, W.G.M., (2001). Impact of spatial variations of land surface parameters on regional evaporation: a case study with remote sensing data. *Hydrological Processes, **15***(9), 1585-1607.

Faurès, J., Goodrich, D., Woolhiser, D.A. and Sorooshian, S., (1995). Impact of small-scale spatial rainfall variability on runoff modeling. *Journal of Hydrology, **173***(1), 309-326.

Feng, L., Hu, C.M., Chen, X.L., Li, R.F., Tian, L.Q. and Murch, B., (2011). MODIS observations of the bottom topography and its inter-annual variability of Poyang Lake. *Remote Sensing of Environment, **115***, 2729-2741.

Fenicia, F., McDonnell, J.J. and Savenije, H.H.G., (2008). Learning from model improvement: On the contribution of complementary data to process understanding. *Water Resources Research, **44***(6), W06419.

Ferguson, C.R. and Wood, E.F., (2010). An Evaluation of Satellite Remote Sensing Data Products for Land Surface Hydrology: Atmospheric Infrared Sounder. *Journal of Hydrometeorology, **11***(6), 1234-1262.

Foody, G.M., (2002). Status of land cover classification accuracy assessment. *Remote Sensing of Environment, **80***(1), 185-201.

Fowler, A., (2002). Assessment of the validity of using mean potential evaporation in computations of the long-term soil water balance. *Journal of Hydrology, **256***(3), 248-263.

Friedl, M.A., (2002). Forward and inverse modeling of land surface energy balance using surface temperature measurements. *Remote Sensing of Environment, **79***(2–3), 344-354.

Friedl, M.A., McIver, D.K., Hodges, J.C.F., Zhang, X.Y., Muchoney, D., Strahler, A.H., Woodcock, C.E., Gopal, S., Schneider, A. and Cooper, A., (2002). Global land cover mapping from MODIS: Algorithms and early results. *Remote Sensing of Environment, **83***(1–2), 287-302.

Friedl, M.A., Sulla-Menashe, D., Tan, B., Schneider, A., Ramankutty, N., Sibley, A. and Huang, X., (2010). MODIS Collection 5 global land cover: Algorithm refinements and characterization of new datasets. *Remote Sensing of Environment, **114***(1), 168-182.

Fu, G., Charles, S.P. and Yu, J., (2009). A critical overview of pan evaporation trends over the last 50 years. *Climatic Change, **97***(1), 193-214.

Gao, H., Hrachowitz, M., Fenicia, F., Gharari, S. and Savenije, H., (2014). Testing the realism of a topography-driven model (flex-topo) in the nested catchments of the Upper Heihe, China. *Hydrology and Earth System Sciences*, ***18***(5), 1895-1915.

Gharari, S., Hrachowitz, M., Fenicia, F. and Savenije, H.H.G., (2013a). An approach to identify time consistent model parameters: sub-period calibration. *Hydrology and Earth System Sciences, **17***(1), 149-161.

Gharari, S., Hrachowitz, M., Fenicia, F., Gao, H. and Savenije, H.H.G., (2014). Using expert knowledge to increase realism in environmental system models can dramatically reduce the need for calibration. *Hydrology and Earth System Sciences, **18***(12), 4839-4859.

Gharari, S., Shafiei, M., Hrachowitz, M., Fenicia, F., Gupta, H.V. and Savenije, H.H.G., (2013b). A strategy for "constraint-based" parameter specification for environmental models. *Hydrology and Earth System Sciences Discussions, **10***(2013), 14857-14871.

Gibson, L.A., Münch, Z., Engelbrecht, J., Petersen, N. and Conrad, J.E., (2010). *Remote sensing as a tool for resource assessment towards the determination of the legal compliance of surface and groundwater use.* WRC Report No. 1690/1/09, Water Research Commission, Gezina.

Gibson, L.A., Münch, Z., Carstens, M. and Conrand, J.E., (2011). *Remote Sensing Evapotranspiration (SEBS) Evaluation using Water Balance.* WRC Report No. KV 272/11, Water Research Commission, Gezina.

Global Modeling and Assimilation Office, (GMAO)., (2004). *File Specification for GEOS-DAS Gridded Output.* NASA Goddard Space Flight Center, available from: https://gmao.gsfc.nasa.gov/operations/GMAO-1001v5.3.pdf, retrieved in September 2012.

Google Earth., 2013. *Google Earth Imagery.* 2013th Edition, AfriGIS (Pty) Ltd., South Africa.

Görgens, A.H.M. and De Clercq, W.P., (2006). *Water quality information systems for integrated water resource management: The Riviersonderend-Berg River system.* WRC Report No. TT 262/06, Water Research Commission, Pretoria.

Götzinger, J. and Bárdossy, A., (2008). Generic error model for calibration and uncertainty estimation of hydrological models. *Water Resources Research, **44***(12), W00B07.

Gourley, J.J., Hong, Y., Flamig, Z.L., Wang, J., Vergara, H. and Anagnostou, E.N., (2011). Hydrologic evaluation of rainfall estimates from radar, satellite, gauge, and combinations on Ft. Cobb basin, Oklahoma. *Journal of Hydrometeorology, **12***(5), 973-988.

Graf, A., Bogena, H.R., Drüe, C., Hardelauf, H., Pütz, T.P., Heinemann, G. and Vereecken, H., (2014). Spatiotemporal relations between water budget components and soil water content in a forested tributary catchment. *Water Resources Research*, ***50***, 4837–4857.

Grimes, D.I.F. and Diop, M., (2003). Satellite-based rainfall estimation for river flow forecasting in Africa. I: Rainfall estimates and hydrological forecasts. *Hydrological Sciences Journal, **48***(4), 567-584.

Grismer, M.E., Orang, M., Snyder, R. and Matyac, R., (2002). Pan evaporation to reference evapotranspiration conversion methods. *Journal of Irrigation and Drainage Engineering, **128***(3), 180-184.

Gupta, H.V., Beven, K.J. and Wagener, T., (2005). Model calibration and uncertainty estimation. In: Anderson, M.G. (Ed.), *Encyclopedia of Hydrological Sciences.* John Wiley and Sons (Pty) Ltd.: Chichester, England, pp. 1-17.

Gupta, H.V., Blöschl, G., McDonnell, J.J., Savenije, H.H.G., Sivapalan, M., Viglione, A. and Wagener, T., (2013). Outcomes of synthesis. In: Blöschl, G., Sivapalan, M., Wagener, T., Viglione, A. and Savenije, H.H.G. (Eds.), *Runoff Prediction in Ungauged Basins: Synthesis Across Processes, Places and Scales*, Cambridge University Press: Cambridge, England, pp. 361- 382.

Gupta, H.V., Kling, H., Yilmaz, K.K. and Martinez, G.F., (2009). Decomposition of the mean squared error and NSE performance criteria: implications for improving hydrological modelling. *Journal of Hydrology*, ***377***(1), 80-91.

Gupta, H.V., Sorooshian, S., Hogue, T.S. and Boyle, D.P., (2003). Advances in automatic calibration of watershed models. In: Duan, Q., Gupta, H.V., Sorooshian, S., Rousseau, A.N. and Turcotte, R. (Eds.), *Calibration of Watershed Models: Water and Applications, Volume 6.* American Geophysical Union: Washington DC, USA, pp. 9-28.

Gupta, H.V., Wagener, T. and Liu, Y., (2008). Reconciling theory with observations: elements of a diagnostic approach to model evaluation. *Hydrological Processes, **22***(18), 3802-3813.

Habib, E. and Krajewski, W.F., (2002). Uncertainty analysis of the TRMM ground-validation radar-rainfall products: Application to the TEFLUN-B field campaign. *Journal of Applied Meteorology, **41***(5), 558-572.

Hamel, P. and Guswa, A., (2015). Uncertainty analysis of a spatially explicit annual water-balance model: case study of the Cape Fear basin, North Carolina. *Hydrology and Earth System Sciences, **19***(2), 839-853.

Hancox, P. and Rubidge, B., (2001). Breakthroughs in the biodiversity, biogeography, biostratigraphy, and basin analysis of the Beaufort Group. *Journal of African Earth Sciences, **33***(3), 563-577.

Hellegers, P.J.G.J., Soppe, R., Perry, C.J. and Bastiaanssen, W.G.M., (2009). Combining remote sensing and economic analysis to support decisions that affect water productivity. *Irrigation Science, **27***(3), 243-251.

Hobbins, M.T., Ramírez, J.A. and Brown, T.C., (2001). The complementary relationship in estimation of regional evapotranspiration: An enhanced advection-aridity model. *Water Resources Research, **37***(5), 1389-1403.

Hoffman, M.T., Cramer, M.D., Gillson, L. and Wallace, M., (2011). Pan evaporation and wind run decline in the Cape Floristic Region of South Africa (1974–2005): implications for vegetation responses to climate change. *Climatic Change, **109***(3–4), 437-452.

Hortgro., (2015). *Key Deciuous Fruit Statistics.* Hortgro, available from: http://www.hortgro.co.za/market-intelligence-statistics/key-deciduous-fruit-statistics/, retrieved in May 2015.

Hossain, F. and Huffman, G.J., (2008). Investigating error metrics for satellite rainfall data at hydrologically relevant scales. *Journal of Hydrometeorology, **9***(3), 563-575.

Hostache, R., Lai, X., Monnier, J. and Puech, C., (2010). Assimilation of spatially distributed water levels into a shallow-water flood model. Part II: Use of a remote sensing image of Mosel River. *Journal of Hydrology, **390***(3–4), 257-268.

Hrachowitz, M., Fovet, O., Ruiz, L., Euser, T., Gharari, S., Nijzink, R., Freer, J., Savenije, H. and Gascuel-Odoux, C., (2014). Process consistency in models: The importance of system signatures, expert knowledge, and process complexity. *Water Resources Research*, ***50***(9), 7445-7469.

Hrachowitz, M., Savenije, H.H.G., Blöschl, G., McDonnell, J.J., Sivapalan, M., Pomeroy, J.W., Arheimer, B., Blume, T., Clark, M.P., Ehret, U., Fenicia, F., Freer, J.E., Gelfan, A., Gupta, H.V., Hughes, D.A., Hut, R.W., Montanari, A., Pande, S., Tetzlaff, D., Troch, P.A., Uhlenbrook, S., Wagener, T., Winsemius, H.C., Woods, R.A., Zehe, E. and Cudennec, C., (2013a). A decade of Predictions in Ungauged Basins (PUB)—a review. *Hydrological Sciences Journal, **58***(8), 1198-1255.

Hrachowitz, M., Savenije, H.H.G., Bogaard, T.A., Tetzlaff, D. and Soulsby, C., (2013b). What can flux tracking teach us about water age distribution patterns and their temporal dynamics? *Hydrology and Earth System Sciences, **17**(2), 533-564.

Huffman, G.J., Bolvin, D.T., Nelkin, E.J., Wolff, D.B., Adler, R.F., Gu, G., Hong, Y., Bowman, K.P. and Stocker, E.F., (2007). The TRMM Multisatellite Precipitation Analysis (TMPA): Quasi-global, multiyear, combined-sensor precipitation estimates at fine scales. *Journal of Hydrometeorology, **8**(1), 38-55.

Hughes, D.A., (1992). A monthly time step, multiple reservoir water balance simulation model. *Water SA, **18**(4), 279-286.

Hughes, D.A., (1995). Monthly rainfall-runoff models applied to arid and semiarid catchments for water resource estimation purposes. *Hydrological Sciences Journal, **40**(6), 751-769.

Hughes, D.A., (2004). Incorporating groundwater recharge and discharge functions into an existing monthly rainfall-runoff model. *Hydrological Sciences Journal, **49**(2), 297-311.

Hughes, D.A., (2006). Comparison of satellite rainfall data with observations from gauging station networks. *Journal of Hydrology, **327**(3), 399-410.

Hughes, D.A., (2008). Modelling semi-arid and arid hydrology and water resources–the southern Africa experience. In: Wheater, H., Sorooshian, S. and Sharma, K.D. (Eds.), *Hydrological Modelling in the Arid and the Semi-arid Areas.* Cambridge University Press: Cambridge, England, pp. 29-40.

Hughes, D.A., (2010). Hydrological models: mathematics or science? *Hydrological Processes, **24**(15), 2199-2201.

Hughes, D.A., (2013). A review of 40 years of hydrological science and practice in southern Africa using the Pitman rainfall-runoff model. *Journal of Hydrology, **501***, 111-124.

Hughes, D.A., (2015). Simulating temporal variability in catchment response using a monthly rainfall–runoff model. *Hydrological Sciences Journal, **60**(7–8), 1286-1298.

Hughes, D.A., Andersson, L., Wilk, J. and Savenije, H.H.G., (2006). Regional calibration of the Pitman model for the Okavango River. *Journal of Hydrology, **331**(1–2), 30-42.

Hughes, D.A. and Forsyth, D.A., (2006). A generic database and spatial interface for the application of hydrological and water resource models. *Computers and Geosciences, **32**(9), 1389-1402.

Hughes, D.A., Gush, M., Tanner, J. and Dye, P., (2014a). Using targeted short-term field investigations to calibrate and evaluate the structure of a hydrological model. *Hydrological Processes, **28**(5), 2794-2809.

Hughes, D.A., Kapangaziwiri, E. and Sawunyama, T., (2010a). Hydrological model uncertainty assessment in southern Africa. *Journal of Hydrology, **387**(3–4), 221-232.

Hughes, D.A., Kapangaziwiri, E. and Baker, K., (2010b). Initial evaluation of a simple coupled surface and ground water hydrological model to assess sustainable ground water abstractions at the regional scale. *Hydrology Research,* ***41***(1), 1-12.

Hughes, D.A., Kapangaziwiri, E., Mallory, S.J.L., Wagener, T. and Smithers, J., (2011). *Incorporating Uncertainty in Water Resources Simulation and Assessment Tools in South Africa.* WRC Report No. 1838/1/11, Water Research Commission, Pretoria.

Hughes, D.A. and Mantel, S.K., (2010a). Estimating uncertainties in simulations of natural and modified streamflow regimes in South Africa. *Global Change: Facing Risks and Threats to Water Resources: Proceedings of the Sixth World FRIEND Conference, 25-29 October 2010, Fez, Morocco, Wallingford, United Kingdom, IAHS-AISH Publication No. 340,* pp. 358-364.

Hughes, D.A. and Mantel, S.K., (2010b). Estimating the uncertainty in simulating the impacts of small farm dams on streamflow regimes in South Africa. *Hydrological Sciences Journal,* ***55***(4), 578-592.

Hughes, D.A., Mwelwa, E., Andersson, L. and Wilks, J., (2004). Southern Africa FRIEND phase II – regional water resources and river flow modelling. In: Meigh, J. and Fry, M. (Eds). *IHP-VI Technical Document in Hydrology No. 69.* International Hydrological Programme (IHP) of the United Nations Educational, UNESCO: Paris, France, pp. 5-30.

Hughes, D.A. and Palmer, C.G., (2005). *SPATSIM, an integrating framework for ecological reserve determination and implementation: incorporating water quality and quantity components for rivers.* WRC Report No. TT245/04, Water Research Commission, Pretoria.

Hughes, D.A., Tshimanga, R.M., Tirivarombo, S. and Tanner, J., (2014b). Simulating wetland impacts on stream flow in southern Africa using a monthly hydrological model. *Hydrological Processes,* ***28***(4), 1775-1786.

Jarmain, C., Everson, C.S., Savage, M.J., Clulow, A.D., Walker, S. and Gush, M.B., (2009a). *Refining tools for evaporation monitoring in support of water resources management.* WRC No. 1567/1/08, Water Research Commission, Gezina, South Africa.

Jarmain, C., Mengitsu, M., Jewitt, G., Kongo, V. and Bastiaanssen, W., (2009b). *A methodology for near-real time spatial estimation of evaporation.* WRC Report No. 1751/1/01, Water Research Commission, Gezina.

Jewitt, G.P.W., (2006). Integrating blue and green water flows for water resources management and planning. *Physics and Chemistry of the Earth, Parts A/B/C,* ***31***(15), 753-762.

Jewitt, G.P.W., Garratt, J.A., Calder, I.R. and Fuller, L., (2004). Water resources planning and modelling tools for the assessment of land use change in the Luvuvhu Catchment, South Africa. *Physics and Chemistry of the Earth, Parts A/B/C,* ***29***(15), 1233-1241.

Jones, M.O., Jones, L.A., Kimball, J.S. and McDonald, K.C., (2011). Satellite passive microwave remote sensing for monitoring global land surface phenology. *Remote Sensing of Environment,* ***115***(4), 1102-1114.

Jovanovic, B., Jones, D.A. and Collins, D., (2008). A high-quality monthly pan evaporation dataset for Australia. *Climatic Change, **87***(3–4), 517-535.

Jovanovic, N.Z. and Israel, S., (2012). *Critical review of methods for the estimation of actual evapotranspiration in hydrological models.* Report No. Workflow 8310, InTechOpen, Council for Scientific and Industrial Research, Stellenbosch.

Jovanovic, N.Z., Masiyandima, M., Naiken, V., Dzikiti, S. and Gush, M.B., (2012). *Remote Sensing Applications in Water Resources Management—Desktop Validation and Draft Paper.* CSIR Report No. CSIR/NRE/ECOS/IR/2011/0097/A, Council for Scientific and Industrial Research, Pretoria.

Jovanovic, N.Z., Mu, Q., Bugan, R.D.H. and Zhao, M., (2015). Dynamics of MODIS evapotranspiration in South Africa. *Water SA, **41***(1), 79-90.

Kalma, J.D., McVicar, T.R. and McCabe, M.F., (2008). Estimating land surface evaporation: A review of methods using remotely sensed surface temperature data. *Surveys in Geophysics, **29***(4–5), 421-469.

Kapangaziwiri, E., (2010). *Regional application of the Pitman monthly rainfall-runoff model in southern Africa incorporating uncertainty.* Unpublished PhD Thesis, Rhodes University, Grahamstown, South Africa.

Kapangaziwiri, E. and Hughes, D.A., (2008). Towards revised physically based parameter estimation methods for the Pitman monthly rainfall-runoff model. *Water SA, **34***(2), 183-192.

Kapangaziwiri, E., Hughes, D.A. and Wagener, T., (2012). Incorporating uncertainty in hydrological predictions for gauged and ungauged basins in southern Africa. *Hydrological Sciences Journal, **57***(5), 1000-1019.

Kauffeldt, A., Halldin, S., Rodhe, A., Xu, C.-Y. and Westerberg, I. K., (2013). Disinformative data in large-scale hydrological modelling. *Hydrology and Earth System Sciences*, ***17***(7), 2845-2857.

Kavetski, D., Fenicia, F. and Clark, M.P., (2011). Impact of temporal data resolution on parameter inference and model identification in conceptual hydrological modeling: Insights from an experimental catchment. *Water Resources Research, **47***(5), W05501.

Kazamias, A.P., (2016). *Validation of MODIS evapotranspiration product (MOD16) for an agricultural region in Austria.* Unpublished Master's Thesis, University of Natural Resources and Life Sciences, Vienna, Austria. Available on: http://permalink.obvsg.at/bok/AC13091971

Kendall, M.G., (1975). *Rank Correlation Methods,* 4th Edition. Charles Griffin: London, England.

Khu, S.T. and Madsen, H., (2005). Multiobjective calibration with Pareto preference ordering: An application to rainfall-runoff model calibration. *Water Resources Research, **41***(3), W03004.

Kim, H.W., Hwang, K., Mu, Q., Lee, S.O. and Choi, M., (2012). Validation of MODIS 16 global terrestrial evapotranspiration products in various climates and land cover types in Asia. *KSCE Journal of Civil Engineering,* ***16***(2), 229-238.

Kim, S.J., Kwon, H.J., Park, G. and Lee, M.S., (2005). Assessment of land-use impact on streamflow via a grid-based modelling approach including paddy fields. *Hydrological Processes,* ***19***(19), 3801-3817.

Kongo, M.V., (2011). Personal Communication via e-mail.

Kongo, M.V., Jewitt, G.W.P. and Lorentz, S.A., (2011). Evaporative water use of different land uses in the upper-Thukela river basin assessed from satellite imagery. *Agricultural Water Management,* ***98***(11), 1727-1739.

Krause, P., Boyle, D.P. and Bäse, F., (2005). Comparison of different efficiency criteria for hydrological model assessment. *Advances in Geosciences,* ***5***(5), 89-97.

Kundzewicz, Z.W. and Robson, A.J., (2004). Change detection in hydrological records—a review of the methodology. *Hydrological Sciences Journal,* ***49***(1), 7-19.

Kustas, W.P. and Anderson, M., (2009). Advances in thermal infrared remote sensing for land surface modeling. *Agricultural and Forest Meteorology,* ***149***(12), 2071-2081.

Kustas, W.P., Agam, N., Anderson, M.C., Li, F. and Colaizzi, P.D., (2007). Potential errors in the application of thermal-based energy balance models with coarse resolution data. In: Neale, C.M.U., Owe, M. and D'Urso, G. (Eds.), *Proceedings of SPIE Volume 6742, Remote Sensing for Agriculture, Ecosystems, and Hydrology IX,* Florence, Italy, pp. 674208-1 - 674208-2.

Lettenmaier, D. P., Alsdorf, D., Dozier, J., Huffman, G. J., Pan, M. and Wood, E. F., (2015). Inroads of remote sensing into hydrologic science during the WRR era. *Water Resources Research*, ***51***(9), 7309-7342.

Leuning, R., Cleugh, H., Zegelin, S. and Hughes, D., (2005). Carbon and water fluxes over a temperate Eucalyptus forest and a tropical wet/dry savanna in Australia: measurements and comparison with MODIS remote sensing estimates. *Agricultural and Forest Meteorology*, ***129***, 151-173.

Lindström, G., Johansson, B., Persson, M., Gardelin, M. and Bergstrom, S., (1997). Development and test of the distributed HBV-96 hydrological model. *Journal of Hydrology*, ***201***(1-4), 272-288.

Liu, T., Willems, P., Feng, X.W., Li, Q., Huang, Y., Bao, A.M., Chen, X., Veroustraete, F. and Dong, Q.H., (2012). On the usefulness of remote sensing input data for spatially distributed hydrological modelling: case of the Tarim River basin in China. *Hydrological Processes,* ***26***(3), 335-344.

Lu, J., Sun, G., McNulty, S.G. and Amatya, D.M., (2005). A comparison of six potential evapotranspiration methods for regional use in the southeastern United States. *Journal of the American Water Resources Association,* ***41***(3), 621-633.

Lubke, R. and De Moor, I.J., (1998). *Field guide to the Eastern and Southern Cape coasts,* 2nd Edition. University of Cape Town Press: Rondebosch, South Africa.

Lucht, W., Schaaf, C.B. and Strahler, A.H., (2000). An algorithm for the retrieval of albedo from space using semi-empirical BRDF models. *IEEE Transactions on Geoscience and Remote Sensing,* ***38***(2), 977-998.

Madi, K., (2010). *Neotectonics and its Applications for the Exploration of Groundwater in the Fractured Karoo Aquifers in the Eastern Cape, South Africa.* Unpublished MSc Thesis, University of Fort Hare, Alice, South Africa.

Madsen, H., Wilson, G. and Ammentorp, H.C., (2002). Comparison of different automated strategies for calibration of rainfall-runoff models. *Journal of Hydrology,* ***261***(1–4), 48-59.

Mann, H.B., (1945). Nonparametric tests against trend. *Econometrica: Journal of the Econometric Society,* ***13***(3), 245-259.

Martinez, G.F. and Gupta, H.V., (2011). Hydrologic Consistency as a basis for assessing complexity of monthly water balance models for continental United States. *Water Resources Research,* ***47***(12), W12540.

McCabe, M.F., Rodell, M., Alsdorf, D.E., Miralles, D.G., Uijlenhoet, R., Wagner, W., Lucieer, A., Houborg, R., Verhoest, N.E.C., Franz, T.E., Shi, J., Gao, H. and Wood, E.F., (2017). The future of earth observation in hydrology. *Hydrologic and Earth Science Systems Discussion,* ***54***, doi:10.5194/hess-2017-54..

McCuen, R.H., Knight, Z. and Cutter, A.G., (2006). Evaluation of the Nash–Sutcliffe efficiency index. *Journal of Hydrologic Engineering,* ***11***(6), 597-602.

McDonnell, J.J., Sivapalan, M., Vaché, K., Dunn, S., Grant, G., Haggerty, R., Hinz, C., Hooper, R., Vaché, K.B. and Roderick, M.L., (2007). Moving beyond heterogeneity and process complexity: A new vision for watershed hydrology. *Water Resources Research,* ***43***(7), W07301.

McMahon, T.A., Finlayson, B.L. and Peel, M.C., (2016), Historical developments of models for estimating evaporation using standard meteorological data. *Wiley Interdisciplinary Reviews: Water*, ***3***(6), 788-818.

McMahon, T.A., Peel, M.C., Lowe, L., Srikanthan, R. and McVicar, T.R., (2013). Estimating actual, potential, reference crop and pan evaporation using standard meteorological data: A pragmatic synthesis. *Hydrology and Earth System Sciences,* ***17***(4), 1331-1363.

McMillan, H.K., Clark, M.P., Bowden, W.B., Duncan, M. and Woods, R.A., (2011). Hydrological field data from a modeller's perspective: Part 1. Diagnostic tests for model structure. *Hydrological Processes,* ***25***(4), 511-522.

McMillan, H.K., Freer, J., Pappenberger, F., Krueger, T. and Clark, M., (2010). Impacts of uncertain river flow data on rainfall-runoff model calibration and discharge predictions. *Hydrological Processes,* ***24***(10), 1270-1284.

Meigh, J., (1995). The impact of small farm reservoirs on urban water supplies in Botswana. *Natural Resources Forum,* ***19***(1), 71-83.

Meijerink, A.M.J., Barnet, D., Batelaan, O., Lubczynsky, M.W. and Pointet, T., (2007). *Remote Sensing Applications to Groundwater,* IHP-VI Series on Groundwater No.16, UNESCO: Paris, France.

Menenti, M. and Choudhury, B.J., (1993). Parameterization of land surface evaporation by means of location dependent potential evaporation and surface temperature range. In: Bolle, H.J., Feeds, R.A. and Kalma, J.D. (Eds.), *Exchange Process at the Land Surface for the Range of Space and Time scales.* IAHS Press: Wallingford, England, pp. 561-568.

Middleton, B.J. and Bailey, A.K., (2008). *Water Resources of South Africa, 2005 Study (WR2005).* WRC Report No's. TT380 to 382/08, Water Research Commission, Gezina.

Midgley, D.C., Pitman, W.V. and Middleton, B.J., (1994). *Surface Water Resources of South Africa 1990, Volume I to IV.* WRC Report No's 298/1.1/94 to 298/6.2/94, Water Research Commission, Pretoria.

Milly, P., Julio, B., Malin, F., Robert, M., Zbigniew, W., Dennis, P. and Ronald, J., (2007). Stationarity is dead. *Ground Water News and Views,* ***4***(1), 6-8.

Milzow, C., Krogh, P.E. and Bauer-Gottwein, P., (2011). Combining satellite radar altimetry, SAR surface soil moisture and GRACE total storage changes for hydrological model calibration in a large poorly gauged catchment. *Hydrological and Earth System Sciences,* ***15***(6), 1729-1743.

MODIS Reprojecting Tool (MRT)., (2011). *MODIS Preprojecting Tool User's Manual.* Release 4.1, Land Processes DAAC,USGS Earth Resources Observation and Science (EROS) Center, Sioux Falls, USA.

Montanari, A., (2007). What do we mean by 'uncertainty'? The need for a consistent wording about uncertainty assessment in hydrology. *Hydrological Processes,* ***21***(6), 841-845.

Montanari, A., Young, G., Savenije, H.H.G., Hughes, D.A., Wagener, T., Ren, L.L., Koutsoyiannis, D., Cudennec, C., Toth, E., Grimaldi, S., Blöschl, G., Sivapalan, M., Beven, K., Gupta, H., Hipsey, R., Schaefli, B., Arheimer, B., Boegh, E., Schymanski, S.J., Di Baldassarre, G., Yu, B., Hubert, P., Huang, P., Schumann, A., Post, D.A., Srinivasan, V., Harman, C., Thompson, S., Rogger, M., Viglione, A., McMillan, H., Characklis, G., Pang, Z. and Belyaev, V., (2013). "Panta Rhei–Everything Flows": Change in hydrology and society–The IAHS Scientific Decade 2013–2022. *Hydrological Sciences Journal,* ***58***(6), 1256-1275.

Monteith, J.L., (1965). Evaporation and environment. *Symposia of the Society of Experimental Biology,* ***19***, 205-234.

Monteith, J.L., (1981). Evaporation and surface temperature. *Quarterly Journal, Royal Meterological Society,* ***107***(451), 1-27.

Moriasi, D.N., Arnold, J.G., van Liew, M.W., Bingner, R.L., Harmel, R.D. and Veith, T.L., (2007). Model evaluation guidelines for systematic quantification of accuracy in watershed simulations. *Transactions of the ASABE,* ***50***(3), 885-900.

Morrison, G., Fatoki, O.S., Zinn, E. and Jacobsson, D., (2001). Sustainable development indicators for urban water systems: A case study evaluation of King William's Town, South Africa, and the applied indicators. *Water SA,* ***27***(2), 219-232.

Mu, Q., Heinsch, F.A., Zhao, M. and Running, S.W., (2007a). Development of a global evapotranspiration algorithm based on MODIS and global meteorology data. *Remote Sensing of Environment,* ***111***(4), 519-536.

Mu, X., Zhang, L., McVicar, T.R., Chille, B. and Gau, P., (2007b). Analysis of the impact of conservation measures on stream flow regime in catchments of the Loess Plateau, China. *Hydrological Processes,* ***21***(16), 2124-2134.

Mu, Q., Zhao, M. and Running, S.W., (2011). Improvements to a MODIS global terrestrial evapotranspiration algorithm. *Remote Sensing of Environment,* ***115***(8), 1781-1800.

Mu, Q., Zhao, M. and Running, S.W., (2012). *Brief Introduction to MODIS Evapotranspiration Data Set (MOD16).* Numeric Terradynamic Simulation Group, available from: http://www.ntsg.umt.edu/project/mod16#data-product, retrieved in May 2012.

Mucina, L. and Rutherford, M.C., (2006). *The Vegetation of South Africa, Lesotho and Swaziland,* South African National Biodiversity Institute: Pretoria.

Mul, M., Savenije, H.H.G. and Uhlenbrook, S., (2009). Spatial rainfall variability and runoff response during an extreme event in a semi-arid, meso-scale catchment in the South Pare Mountains, Tanzania. *Hydrology and Earth System Sciences*, ***13***(9),1659-1670.

Mussá, F.E.F., Zhou, Y., Maskey, S., Masih, I. and Uhlenbrook, S., (2015). Groundwater as an emergency source for drought mitigation in the Crocodile River catchment, South Africa. *Hydrology and Earth System Sciences,* ***19***(2), 1093-1106.

Müller, M.F., Dralle, D.N. and Thompson, S.E., (2014). Analytical model for flow duration curves in seasonally dry climates. *Water Resources Research,* ***50***(7), 5510-5531.

Műnch, Z., Conrad, J.E., Gibson, L.A., Palmer, A.R. and Hughes, D.A., (2013). Satellite earth observation as a tool to conceptualize hydrogeological fluxes in the Sandveld, South Africa. *Hydrogeology Journal,* ***21***(5), 1053-1070.

Myneni, R.B., Hoffman, S., Knyazikhin, Y.U., Privette, J.L., Glassy, J., Tian, Y., Wang, Y., Song, X., Zhang, Y. and Smith, G.R., (2002). Global products of vegetation leaf area and fraction absorbed PAR from year one of MODIS data. *Remote Sensing of Environment,* ***83***(1), 214-231.

Nandakumar, N. and Mein, R.G., (1997). Uncertainty in rainfall—runoff model simulations and the implications for predicting the hydrologic effects of land-use change. *Journal of Hydrology,* ***192***, 211-232.

National Aeronautics and Space Administration, (NASA)., (2006). *Earth Science Reference Handbook: A Guide to NASA's Earth Science Program and Earth Observing Satellite Missions,* National Aeronautics and Space Administration: Washingtod D.C., USA.

National Aeronautics and Space Administration, (NASA)., (2012). *MODIS Web.* The National Aeronautics and Space Administration, available from: http://modis.gsfc.nasa.gov/, retrieved in June 2012.

National Land Cover, (NLC)., (2014). *South African National Land-cover.* South African National Biodiversity Institute: Biodiversity GIS available from: bgis.sanbi.org/DEA_Landcover/project.asp, retrieved in November 2016.

Nash, J.E. and Sutcliffe, J.V., (1970). River flow forecasting through conceptual models: Part I—A discussion of principles. *Journal of Hydrology,* ***10***(3), 282-290.

Ndiritu, J.G., (2009). A comparison of automatic and manual calibration using the Pitman model. *Physics and Chemistry of the Earth, Parts A/B/C,* ***34***(13–16), 729-740.

Njoku, E.G., Jackson, T.J., Lakshmi, V., Chan, T.K. and Nghiem, S.V., (2003). Soil moisture retrieval from AMSR-E. *IEEE Transactions on Geoscience and Remote Sensing,* ***41***(2), 215-229.

Nouri, H., Beecham, S., Kazemi, F. and Hassanli, A.M., (2013). A review of ET measurement techniques for estimating the water requirements of urban landscape vegetation. *Urban Water Journal,* ***10***(4), 247-259.

O'Keeffe, J.H., Van Ginkel, C.E., Hughes, D.A., Hill, T.R. and Ashton, P.J., (1996). *A situation analysis of water quality in the catchment of the Buffalo River, Eastern Cape, with special emphasis on the impacts of low cost, high-density urban development on water quality.* WRC Report No. 405/1/96, Water Research Commission, Pretoria.

Oudin, L., Andréassian, V., Perrin, C. and Anctil, F., (2004). Locating the sources of low-pass behavior within rainfall-runoff models. *Water Resources Research,* ***40***(11), W1110.

Oudin, L., Hervieu, F., Michel, C., Perrin, C., Andréassian, V., Anctil, F. and Loumagne, C., (2005b). Which potential evapotranspiration input for a lumped rainfall–runoff model?: Part 2—Towards a simple and efficient potential evapotranspiration model for rainfall–runoff modelling. *Journal of Hydrology,* ***303***(1), 290-306.

Oudin, L., Michel, C. and Anctil, F., (2005a). Which potential evapotranspiration input for a lumped rainfall-runoff model? Part 1—Can rainfall-runoff models effectively handle detailed potential evapotranspiration inputs? *Journal of Hydrology,* ***303***(1), 275-289.

Oudin, L., Perrin, C., Mathevet, T., Andréassian, V. and Michel, C., (2006). Impact of biased and randomly corrupted inputs on the efficiency and the parameters of watershed models. *Journal of Hydrology,* ***320***(1), 62-83.

Öztürk, M., Copty, N.K. and Saysel, A.K., (2013). Modeling the impact of land use change on the hydrology of a rural watershed. *Journal of Hydrology,* ***497***, 97-109.

Pandya, M.R., Singh, R.P., Chaudhari, K.N., Bairagi, G.D., Sharma, R., Dadhwal, V.K. and Parihar, J.S., (2006). Leaf area index retrieval using IRS LISS-III sensor data and validation of the MODIS LAI product over central India. *IEEE Transactions on Geoscience and Remote Sensing*, ***44***(7), 1858-1865.

Pappenberger, F. and Beven, K.J., (2006). Ignorance is bliss: Or seven reasons not to use uncertainty analysis. *Water Resources Research,* ***42***(5), W05302.

Parajka, J., Naeimi, V., Blöschl, G., Wagner, W., Merz, R. and Scipal, K., (2006). Assimilating scatterometer soil moisture data into conceptual hydrologic models at the regional scale. *Hydrology and Earth System Sciences,* ***10***(3), 353-368.

Parkinson, C.L. and Greenstone, R., (2000). *Earth Observation Systems Data Products Handbook: Volume 2.* NASA Goddard Space Flight Center: Greenbelt, USA.

Parmele, L.H., (1972). Errors in output of hydrologic models due to errors in input potential evapotranspiration. *Water Resources Research,* ***8***(2), 348-359.

Paturel, J.E., Servat, E. and Vassiliadis, A., (1995). Sensitivity of conceptual rainfall-runoff algorithms to errors in input data — case of the GR2M model. *Journal of Hydrology,* ***168***(1–4), 111-125.

Pechlivanidis, I.G., Jackson, B.M., Mcintyre, N.R. and Wheater, H.S., (2011). Catchment scale hydrological modelling: a review of model types, calibration approaches and uncertainty analysis methods in the context of recent developments in technology and applications. *Global Nest Journal,* ***13***(3), 193-214.

Peel, M.C. and Blöschl, G., (2011). Hydrological modelling in a changing world. *Progress in Physical Geography,* ***35***(2), 249-261.

Peng, D.Z., Guo, S.L., Liu, P. and Liu, T., (2006). Reservoir storage curve estimation based on remote sensing data. *Journal of Hydrologic Engineering,* ***11***, 165-172.

Penman, H.L., (1948). Natural evaporation from open water, bare soil and grass. *Proceedings of the Royal Society of London: Series A. Mathematical and Physical Sciences,* ***193***(1032), 120-145.

Perrin, C., Michel, C. and Andréassian, V., (2010). A set of hydrological models. In: Tanguy, J.M. (Ed.), *Environmental Hydraulics: Mathematical Models.* Wiley Online Library: New York, USA, pp. 493-509.

Pettitt, A.N., (1979). A non-parametric approach to the change-point problem. *Journal of the Royal Statistical Society. Series C (Applied Statistics),* ***28***(2), 126-135.

Pitman, W.V., (1973). *A mathematical model for generating monthly river flows from meteorological data in South Africa.* Report No 2/73, Hydrological Research Unit, University of the Witwatersrand, Johannesburg

Porat, N. and Botha, G.A., (2008). The chronology of dune development on the Maputaland coastal plain, southeast Africa. *Quaternary Sciences Reviews,* ***27***(9–10), 1024-1046.

Porter, J.W. and McMahon, T.A., (1976). *The Monash model: user manual for daily program HYDROLOG*. Civil Engineering Research Report 2/76, Monash University.

Qin, C., Jia, Y., Su, Z., Zhou, Z., Qiu, Y. and Suhui, S., (2008). Integrating Remote Sensing Information Into A Distributed Hydrological Model for Improving Water Budget Predictions in Large-scale Basins through Data Assimilation. *Sensors, **8***(7), 4441-4465.

Ramoelo, A., Majozi, N., Mathieu, R., Jovanovic, N., Nickless, A. and Dzikiti, S., (2014). Validation of Global Evapotranspiration Product (MOD16) using Flux Tower Data in the African Savanna, South Africa. *Remote Sensing, **6***(8), 7406-7423.

Rana, G. and Katerji, N., (2000). Measurement and estimation of actual evapotranspiration in the field under Mediterranean climate: a review. *European Journal of Agronomy, **13***(2–3), 125-153.

Refsgaard, J.C. and Hansen, J.R., (2010). A good-looking catchment can turn into a modeller's nightmare. *Hydrological Sciences Journal, **55***(6), 899-912.

Refsgaard, J.C., Van der Sluijs, Jeroen P, Brown, J. and Van der Keur, P., (2006). A framework for dealing with uncertainty due to model structure error. *Advances in Water Resources, **29***(11), 1586-1597.

Refsgaard, J.C., Van der Sluijs, Jeroen P, Højberg, A.L. and Vanrolleghem, P.A., (2007). Uncertainty in the environmental modelling process–a framework and guidance. *Environmental Modelling and Software, **22***(11), 1543-1556.

Renard, B., Kavetski, D., Kuczera, G., Thyer, M. and Franks, S.W., (2010). Understanding predictive uncertainty in hydrologic modeling: The challenge of identifying input and structural errors. *Water Resources Research, **46***(5), W05521.

River Health Programme, (2004). *State-of-Rivers Report: Berg River System.* ISBN No: 0-620-32075-3, Department of Water Affairs and Forestry, Pretoria.

Roderick, M. L., Hobbins, M. T. and Farquhar, G.D. (2009). Pan evaporation trends and the 15 terrestrial water balance. I. Principles and Observations. *Geography Compass*, ***3***(2), 746-760.

Rodrigues, L.N., Sano, E.E., Steenhuis, T.S. and Passo, D.P., (2012). Estimation of small reservoir storage capacities with remote sensing in the Brazilian Savannah Region. *Water Resources Management, **26***(4), 873-882.

Ruhoff, A.L., Paz, A.R., Aragao, L.E.O.C., Mu, Q., Malhi, Y., Collischonn, W., Rocha, H.R. and Running, S.W., (2013). Assessment of the MODIS global evapotranspiration algorithm using eddy covariance measurements and hydrological modelling in the Rio Grande basin. *Hydrological Sciences Journal, **58***(8), 1658-1676.

Rwasoka, D., Gumindoga, W. and Gwenzi, J., (2011). Estimation of actual evapotranspiration using the Surface Energy Balance System (SEBS) algorithm in the Upper Manyame catchment in Zimbabwe. *Physics and Chemistry of the Earth, Parts A/B/C, **36***(14), 736-746.

Saraiva-Okello, A.M.L., Masih, I., Uhlenbrook, S., Jewitt, G.P.W., Van der Zaag, P. and Riddell, E., (2015). Drivers of spatial and temporal variability of streamflow in the Incomati River basin. *Hydrology and Earth System Sciences,* ***19***(2), 657-673

Savenije, H.H.G., (2001). Equifinality, a blessing in disguise? *Hydrological Processes,* ***15***(14), 2835-2838.

Savva, A.P. and Frenken, K., (2002). *Crop water requirements and irrigation scheduling. Irrigation Manual Module 4.* Water Resources Development and Management Office, FAO Sub-Regional office for East and Southern Africa. Fontline Electronic Publishing, Harare, pp. 122.

Sawunyama, T. and Hughes, D.A., (2008). Application of satellite-derived rainfall estimates to extend water resource simulation modelling in South Africa. *Water SA,* ***34***(1), 1-9.

Schaaf, C.B., Gao, F., Strahler, A.H., Lucht, W., Li, X., Tsang, T., Strugnell, N.C., Zhang, X., Jin, Y. and Muller, J., (2002). First operational BRDF, albedo nadir reflectance products from MODIS. *Remote Sensing of Environment,* ***83***(1), 135-148.

Schreider, S.Y., Jakeman, A., Letcher, R., Nathan, R., Neal, B. and Beavis, S., (2002). Detecting changes in streamflow response to changes in non-climatic catchment conditions: farm dam development in the Murray–Darling basin, Australia. *Journal of Hydrology,* ***262***(1), 84-98.

Schultz, G.A., (1988). Remote sensing in hydrology. *Journal of Hydrology,* ***100***(1), 239-265.

Schultz, G.A. and Engman, E.T., (2000). *Remote Sensing in Hydrology and Water Management,* 1st Edition. Springer: Berlin, Germany.

Schulze, R.E., (1997). *South African Atlas of Agrohydrology and Climatology.* Report TT85/96, Water Research Commission, Pretoria.

Schulze, R.E. and Maharaj, M., (2004). *Development of a Database of Gridded Daily Temperatures for Southern Africa.* WRC Report No. 1156/02/04, Water Research Commission, Pretoria.

Schulze, R.E. and Maharaj, M., (2006). Temeperature Database. In: Schulze, R.E. (Ed.), *South African Atlas of Climatology and Agrohydrology.* WRC Report No. 1489/1/06, Water Research Commission, Pretoria.

Scipal, K., Scheffler, C. and Wagner, W., (2005). Soil moisture-runoff relation at the catchment scale as observed with coarse resolution microwave remote sensing. *Hydrology and Earth System Sciences,* ***9***(3), 173-183.

Segond, M., Wheater, H. and Onof, C., (2007). The significance of spatial rainfall representation for flood runoff estimation: A numerical evaluation based on the Lee catchment, UK, *Journal of Hydrology.* ***347***(1–2), 116-131.

Seibert, J. and Beven, K.J., (2009). Gauging the ungauged basin: how many discharge measurements are needed? *Hydrology and Earth System Sciences,* ***13***(6), 883-892.

Seibert, J. and McDonnell, J.J., (2002). On the dialog between experimentalist and modeler in catchment hydrology: Use of soft data for multicriteria model calibration. *Water Resources Research,* ***38***(11), 1241.

Shrestha, R., Tachikawa, Y. and Takara, K., (2006). Input data resolution analysis for distributed hydrological modeling. *Journal of Hydrology,* ***319***(1–4), 36-50.

Shuttleworth, W.J., (1993). Evaporation. In: Maidment, D.R. (Ed.), *Handbook of Hydrology.* McGraw-Hill: Michigan, USA, pp. 4.1-4.53.

Shuttleworth, W.J., Serrat-Capdevila, A., Roderick, M.L. and Scott, R.L., (2009). On the theory relating changes in area-average and pan evaporation. *Quarterly Journal of the Royal Meteorological Society,* ***135***(642), 1230-1247.

Sieber, A. and Uhlenbrook, S., (2005). Sensitivity analyses of a distributed catchment model to verify the model structure. *Journal of Hydrology,* ***310***(1–4), 216-235.

Singh, V.P. and Xu, C.Y., (1997). Evaluation and generalization of 13 mass-transfer equations for determining free water evaporation. *Hydrological Processes,* ***11***(3), 311-323.

Sivapalan, M., (2003). Prediction in ungauged basins: a grand challenge for theoretical hydrology. *Hydrological Processes,* ***17***(15), 3163-3170.

Sivapalan, M., Takeuchi, K., Franks, S.W., Gupta, V.K., Karambiri, H., Lakshmi, V., Liang, X., McDonnell, J.J., Mendiondo, E.M. and O'connell, P.E., (2003). IAHS Decade on Predictions in Ungauged Basins (PUB), 2003–2012: Shaping an exciting future for the hydrological sciences. *Hydrological Sciences Journal,* ***48***(6), 857-880.

Stisen, S., McCabe, M.F., Refsgaard, J.C., Lerer, S. and Butts, M.B., (2011). Model parameter analysis using remotely sensed pattern information in a multi-constraint framework. *Journal of Hydrology,* ***409***(1–2), 337-349.

Su, Z., (2000). Remote sensing of land use and vegetation for mesoscale hydrological studies. *International Journal of Remote Sensing,* ***21***(2), 213-233.

Su, Z., (2002). The Surface Energy Balance System (SEBS) for estimation of turbulent heat fluxes. *Hydrology and Earth System Sciences,* ***6***(1), 85-100.

Su, Z., Schmugge, T., Kustas, W. and Massman, W., (2001). An evaluation of two models for estimation of the roughness height for heat transfer between the land surface and the atmosphere. *Journal of Applied Meteorology,* ***40***(11), 1933-1951.

Su-Chuang, D., Zhao-Liang, L., Ronglin, T., Hua, W., Bo-Hui, T. and Jing, L., (2015). Integrating two layers of soil moisture parameters into the MOD16 algorithm to improve evapotranspiration estimations. *International Journal of Remote Sensing,* ***36***(19–20), 4953-4971.

Tada, T. and Beven, K.J., (2012). Hydrological model calibration using a short period of observations. *Hydrological Processes,* ***26***(6), 883-892.

Tang, Y., Reed, P. and Wagener, T., (2006). How effective and efficient are multiobjective evolutionary algorithms at hydrologic model calibration? *Hydrology and Earth System Sciences,* ***10***(2), 289-307.

Tanner, J.L., (2015). Personal Communication via interview.

Tanner, J.L. and Hughes, D.A., (2013). Assessing uncertainties in surface-water and groundwater interaction modelling—a case study from South Africa using the Pitman model. In: Cobbing, J., Adams, S., Dennis, I. and Riemann, K. (Eds.), *Assessing and Managing Groundwater in Different Environments.* International Association of Hydrogeologists: Selected Papers. CRC Press, Taylor and Francis Group: London, England, pp. 121-134.

Tanner, J.L. and Hughes, D.A., (2015). Surface water–groundwater interactions in catchment scale water resources assessments—understanding and hypothesis testing with a hydrological model. *Hydrological Sciences Journal,* ***60***(11), 1880-1895.

Tapley, B.D., Bettadpur, S., Watkins, M. and Reigber, C., (2004). The gravity recovery and climate experiment: Mission overview and early results. *Geophysical Research Letters,* ***31***(9), L09607.

Taylor, N.J. and Gush, M.B., (2014). *The water use of selected fruit tree orchards (Volume 1): Review of available knowledge.* WRC Report No. 1770/1/14, Water Research Commission, Gezina.

Thompson, S.E., Sivapalan, M., Harman, C.J., Srinivasan, V., Hipsey, M.R., Reed, P., Montanari, A. and Blöschl, G., (2013). Developing predictive insight into changing water systems: use-inspired hydrologic science for the Anthropocene. *Hydrology and Earth System Sciences,* ***17***(12), 5013-5039.

Thorne, V., Coakeley, P., Grimes, D. and Dugdale, G., (2001). Comparison of TAMSAT and CPC rainfall estimates with raingauges, for southern Africa. *International Journal of Remote Sensing,* ***22***(10), 1951-1974.

Todini, E., (1988). Rainfall-runoff modelling—past, present and future. *Journal of Hydrology,* ***100***(1–3), 341-352.

Trambauer, P., Dutra, E., Maskey, S., Werner, M., Pappenberger, F., van Beek, L. and Uhlenbrook, S., (2014). Comparison of different evaporation estimates over the African continent. *Hydrology and Earth System Sciences,* ***18(1),*** 193-212.

Tshimanga, R.M. and Hughes, D.A., (2014). Basin-scale performance of a semi-distributed rainfall-runoff model for hydrological predictions and water resources assessment of large rivers: The Congo River. *Water Resources Research,* ***50***(2), 1174-1188.

Tumbo, M. and Hughes, D.A., (2015). Uncertain hydrological modelling: application of the Pitman model in the Great Ruaha River basin, Tanzania. *Hydrological Sciences Journal,* ***60***(11), 2047-2061.

Uhlenbrook, S. and Sieber, A., (2005). On the value of experimental data to reduce the prediction uncertainty of a process-oriented catchment model. *Environmental Modelling and Software,* ***20***(1), 19-32.

Van Emmerik, T.H.M., Mulder, G., Eilander, D., Piet, M. and Savenije, H.H.G., (2015). Predicting the ungauged basin: model validation and realism assessment. *Frontiers in Earth Science,* ***3***(62), doi: 10.3389/feart.2015.00062.

Van den Berg, E.C., Plarre, C., van den Berg, H.M. and Thompson, M.W., (2008). *The South African National Land-Cover 2000.* Unpublished Report No. GW/A/2008/86, Agricultural Research Council-Institute for Soil, Climate and Water, South Africa.

Van Ginkel, C.E., O'Okeeffe, J.H., Hughes, D.A., Herald, J.R. and Ashton, P.J., (1993). *A Situation Analysis of Water Quality in the Catchment of the Buffalo River, Eastern Cape, with Special Emphasis on the Impacts of Low Cost, High-Density Urban Development on Water Quality. Volume II: Appendices.* WRC Report No 405/2/96, Water Research Commission, South Africa.

Van Heerden, P.S., Crosby, C.T., Grové, B., Benadé, N., Theron, E., Schulze, R.E. and Tewolde, M.H., (2009). *Integrating and Upgrading of SAPWAT and PLANWAT to Create a Powerful and User-friendly Irrigation Water Planning Tool: Program Version 1.0.* WRC Report No. TT391/08, Water Research Commission, Gezina.

Vázquez, R.F. and Feyen, J., (2003). Effect of potential evapotranspiration estimates on effective parameters and performance of the MIKE SHE-code applied to a medium-size catchment. *Journal of Hydrology*, ***270***(3–4), 309-327.

Verhoef, A. and Campbell, C.L., (2005). Evaporation Measurement. In: Anderson, M.G. (Ed.), *Encyclopedia of Hydrological Sciences.* John Wiley and Sons (Pty) Ltd.: Chichester, England, pp. 589-600.

Verstraeten, W.W., Veroustraete, F. and Feyen, J., (2008). Assessment of evapotranspiration and soil moisture content across different scales of observation. *Sensors,* ***8***(1), 70-117.

Wagener, T., (2003). Evaluation of catchment models. *Hydrological Processes,* ***17***(16), 3375-3378.

Wagener, T., Blöschl, G., .Goodrich, D.C., Gupta, H., Sivapalan, M., Tachikawa, Y., Troch, P.A. and Weiler, M., (2013). A synthesis framework for runoff prediction in ungauged basins. In: Blöschl, G., Sivapalan, M., Wagener, T., Viglione, A. and Savenije, H.H.G. (Eds.), *Runoff Prediction in Ungauged Basins: Synthesis Across Processes, Places and Scales*, Cambridge University Press: Cambridge, England, pp. 11-28.

Wagener, T. and Gupta, H.V., (2005). Model identification for hydrological forecasting under uncertainty. *Stochastic Environmental Research and Risk Assessment,* ***19***(6), 378-387.

Wagener, T., Gupta, H., Yatheendradas, S., Goodrich, D., Unkrich, C. and Schaffner, M., (2007). Understanding sources of uncertainty in flash-flood forecasting for semi-arid regions. *Proceedings of Symposium of HS2004 held during International Union of Geodesy and Geophysics 2007 at Perugia, Italy, July 2007, IAHS-AISH Publication No. 313,* pp. 204-212.

Wagener, T., McIntyre, N., Lees, M., Wheater, H. and Gupta, H., (2003). Towards reduced uncertainty in conceptual rainfall-runoff modelling: Dynamic identifiability analysis. *Hydrological Processes,* ***17***(2), 455-476.

Wagener, T. and Montanari, A., (2011). Convergence of approaches toward reducing uncertainty in predictions in ungauged basins. *Water Resources Research,* ***47***(6), W06301.

Wagener, T., Sivapalan, M., Troch, P.A., McGlynn, B.L., Harman, C.J., Gupta, H.V., Kumar, P., Rao, P.S.C., Basu, N.B. and Wilson, J.S., (2010). The future of hydrology: An evolving science for a changing world. *Water Resources Research,* ***46***(5), W05301.

Wagner, W., Verhoest, N., Ludwig, R. and Tedesco, M., (2009). Editorial: 'Remote sensing in hydrological sciences'. *Hydrology and Earth System Sciences,* ***13***(6), 813-817.

Warmink, J., Janssen, J., Booij, M.J. and Krol, M.S., (2010). Identification and classification of uncertainties in the application of environmental models. *Environmental Modelling and Software,* ***25***(12), 1518-1527.

WaterWatch., (2011). *SEBAL Projects.* WaterWatch, available from: http://www.waterwatch.nl/index.php?id=140, retrieved in October 2011.

Wessels, P. and Rooseboom, A., (2009a). Flow-gauging structures in South African rivers part 1: An overview. *Water SA,* ***35***(1), 1-9.

Wessels, P. and Rooseboom, A., (2009b). Flow-gauging structures in South African rivers part 2: calibration. *Water SA,* ***35***(1), 11-19.

Westerberg, I., Guerrero, J., Younger, P., Beven, K., Seibert, J., Halldin, S., Freer, J. and Xu, C., (2011). Calibration of hydrological models using flow-duration curves. *Hydrology and Earth System Sciences,* ***15***(7), 2205-2227.

Western Cape Department of Agriculture, (WCDA)., (2015). *CapeFarmMapper: Version 1.3.9.0.* Research and Technology Development Services, Western Cape Department of Agriculture, available from: http://gis.elsenburg.com/apps/cfm/.

Western, A.W., Zhou, S., Grayson, R.B., McMahon, T.A., Blöschl, G. and Wilson, D.J., (2004). Spatial correlation of soil moisture in small catchments and its relationship to dominant spatial hydrological processes. *Journal of Hydrology,* ***286***(1), 113-134.

Wheater, H.S., (2008). Modelling hydrological processes in arid and semi-arid areas: An introduction to the workshop. In: Wheater, H.S., Sorooshian, S. and Sharma, K.D. (Eds.), *Hydrological Modelling in Arid and Semi-Arid Areas.* Cambridge University Press: Cambridge, England, pp. 1-20.

Wheater, H.S., McIntyre, N. and Wagener, T., (2008). Calibration, uncertainty and regional analysis of conceptual rainfall-runoff models. In: Wheater, H.S., Sorooshian, S. and Sharma, K.D. (Eds.), *Hydrological Modelling in Arid and Semi-arid Areas.* Cambridge University Press: Cambridge, England, pp. 99-112.

Wilk, J., Kniveton, D., Andersson, L., Layberry, R., Todd, M.C., Hughes, D., Ringrose, S. and Vanderpost, C., (2006). Estimating rainfall and water balance over the Okavango River Basin for hydrological applications. *Journal of Hydrology,* ***331***(1–2), 18-29.

Wilson, D.J., Western, A.W. and Grayson, R.B., (2004). Identifying and quantifying sources of variability in temporal and spatial soil moisture observations. *Water Resources Research,* ***40***(2), W02507.

Winsemius, H.C., Savenije, H.H.G. and Bastiaanssen, W.G.M., (2008). Constraining model parameters on remotely sensed evaporation: justification for distribution in ungauged basins. *Hydrological and Earth System Sciences,* ***12***(6), 1403-1413.

Winsemius, H.C., Schaefli, B., Montanari, A. and Savenije, H.H.G., (2009). On the calibration of hydrological models in ungauged basins: A framework for integrating hard and soft hydrological information. *Water Resources Research,* ***45***(12), W12422.

Woodford, A.C. and Chevallier, L.P., (2002). *Hydrogeology of the main Karoo Basin: Current knowledge and future research needs.* WRC Report No. TT 179/02, Water Research Commission, Gezina.

Wotling, G., Bouvier, C., Danloux, J. and Fritsch, J., (2000). Regionalization of extreme precipitation distribution using the principal components of the topographical environment. *Journal of Hydrology,* ***233***(1), 86-101.

Xu, C. and Singh, V., (2000). Evaluation and generalization of radiation-based methods for calculating evaporation. *Hydrological Processes,* ***14***(2), 339-349.

Yapo, P.O., Gupta, H.V. and Sorooshian, S., (1996). Automatic calibration of conceptual rainfall-runoff models: sensitivity to calibration data. *Journal of Hydrology,* ***181***(1–4), 23-48.

Zhao, M., Running, S.W. and Nemani, R.R., (2006). Sensitivity of Moderate Resolution Imaging Spectroradiometer (MODIS) terrestrial primary production to the accuracy of meteorological reanalyses. *Journal of Geophysical Research: Biogeosciences,* ***111***(G1), G01002.

Zwart, S.J. and Bastiaanssen, W.G.M., (2007). SEBAL for detecting spatial variation of water productivity and scope for improvement in eight irrigated wheat systems. *Agricultural Water Management,* ***89***(3), 287-296.

APPENDICES

Appendix 1: MOD16 Data Processing Steps

1. Importing MOD16 data into HDFView

All the downloaded *hdf files were manually converted to *txt files with the HDFView software. The first step involved the importation of *hdf data into HDFView software, using the import function. The generic steps are as follows:

- Click File, Open File or use the short cut Ctrl-O. Browse the location where files are saved. Select an *hdf file to be converted and click open. Figure A shows the open file functionality in HDFView.

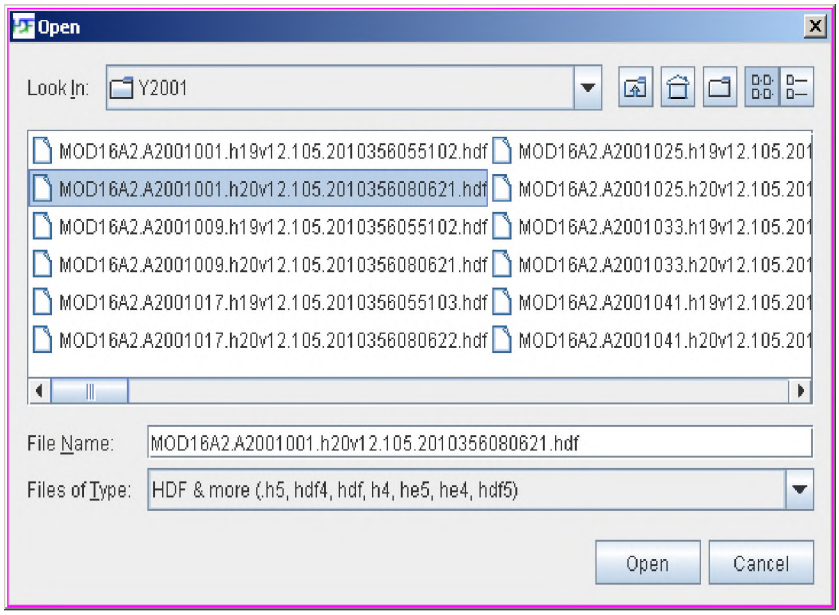

Figure A: Open window of the import function of the HDFView software.

- In the navigation pane, double-click tile name, then double-click the "Data Fields" subfolder that has tile data content as:

  i. Actual evapotranspiration (ETa) labelled as "ET_1km",

  ii. Latent heat flux labelled as "LE_1km",

iii. Potential evapotranspiration (PET) labelled as “PET_1km”,

iv. Potential latent heat flux labelled as “PLE_1km”, and

v. Annual quality control labelled as ‘ET_QC_1km”.

A sample in Figure B shows the table of data content (pixel values) of the latent heat flux on the display pane, whereas the metadata pane shows the attributes of the data which include number of pixel, valid pixel range, scale factor, and units.

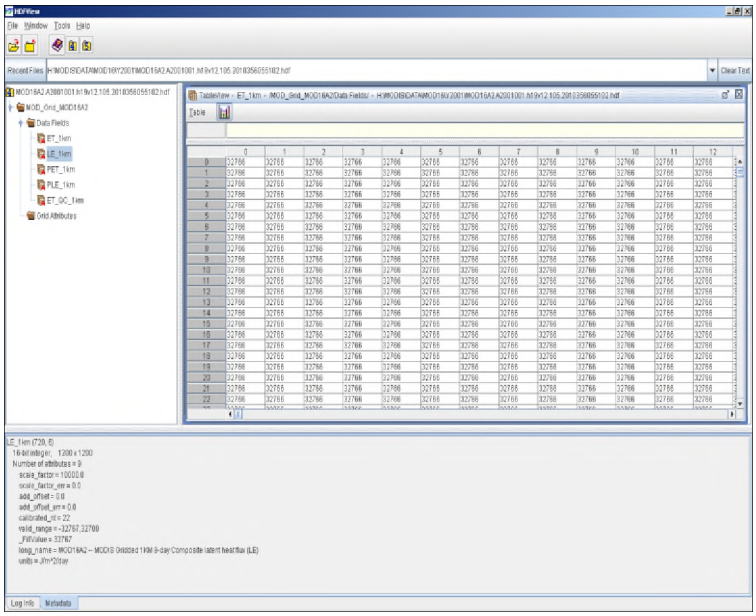

Figure B: Display of data content in HDFView software.

- Double-click or right-click and open data file of interest. The default settings of the HDFView will open the pixel table. To view file options, right-click on the file of interest and select “Open As” options. This functionality has options to display data content as “Spreadsheet” or “Image” (with different palettes available from the dropdown arrow) as shown in Figure C.

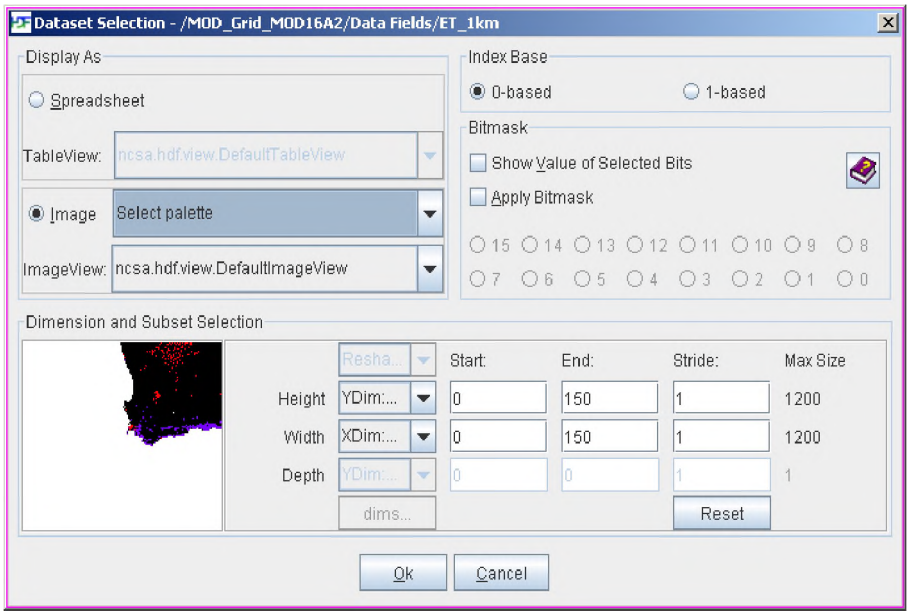

Figure C: MOD16 tile data display options and settings.

- To convert the MOD16 pixel data, select "Spreadsheet option" under display as pane and in the table view pane, left-click text "Table" in the top-left corner of the table view pane, then select "Export Data to Text File". The new "Save window" will pop up; then navigate to a suitable directory to save the converted data.

- For file identification purposes, keep the file name the same and only change the file extension to *txt, then click save. After saving, the MOD16 tile data will be in text format and this will ease the process of manipulating its content.

Steps 1 to 6 were repeated to convert all downloaded MOD16 tile data. The next step (in 3.5.2) of MOD16 data preparation was to select catchment pixels within h19v12 and h20v12 tiles used in the development of the algorithm.

2. Selection of pixel of interest within catchments

The MOD16 tile data are in sinusoidal projection systems, which are incompatible with the projection systems and geographic coordinate system of catchment shape files, MOD16 tiles had to be transformed to the projection and geographic coordinate system compatible with selected catchments shape files. Two MOD16 tile data samples, in *hdf format from h19v12 and h20v12 positions, were used in the reprojection and setting of a compatible geographic coordinate system.

This study intended to use the MODIS Reprojection Tool (MRT) from NASA, but because of its limitations, the transformation and projection steps of MOD16 tiles were conducted in ArcGIS, using reprojection tools.

In the first step, the MOD16 tile data were transformed to Universal Transverse Mercator (UTM) projections with a World Geodetic Systems 1984 (WGS84) datum. After this step, MOD16 sample tile data had both the geographic coordinate system and the projected coordinate system defined in terms of the WGS84 ellipsoid. In the second step, MOD16 tile data were set to the Hartebeesthoek_1994 geographic coordinate system to make them compatible with the catchments shape files. The MOD16 tile data were used to identify and select pixels that belonged to the selected catchments. Thus, the two reprojected MOD16 sample tile data were used in the pixel selection, but they had to be converted from raster format (*hdf) to point data format. This conversion was aimed at isolating pixels from a clustered raster data which makes it impossible to manipulate pixels individually.

3. Converting MOD16 raster to point data

ArcGIS was used to convert two tiles of MOD16 data from raster format to point data using the following steps:

- In ArcMap, add South African quaternary catchment shape files into the map display.
- Open ArcToolbox, select "Conversion Tools", then select "From Raster to Point", and double click or right-click and open. Figure D shows the raster conversion tools in ArcToolbox of the ArcGIS.
- Browse to select the raster file to be converted; in this case, the two MOD16 tiles were converted separately. Select a suitable file destination and a filename of the new file, and then click the "OK button" after populating the field data. The ArcGIS will convert the data and the pop-up window will ask if the user wants to add the converted file into display or not. Since the converted data was of particular interest for this study, both tiles were added into the map display overlapping the quaternary catchment shape files. Figure E illustrates the h20v12 and h19v12 MOD16 tiles point data superimposed over the South African quaternary catchment

map. The tile depicted in black is h19v20, whereas the tile depicted in green represents h20v20 tile point data.

The converted MOD16 point data were used in the identification of the catchment-selected pixels. The following section describes the methodology used to select pixels of interest.

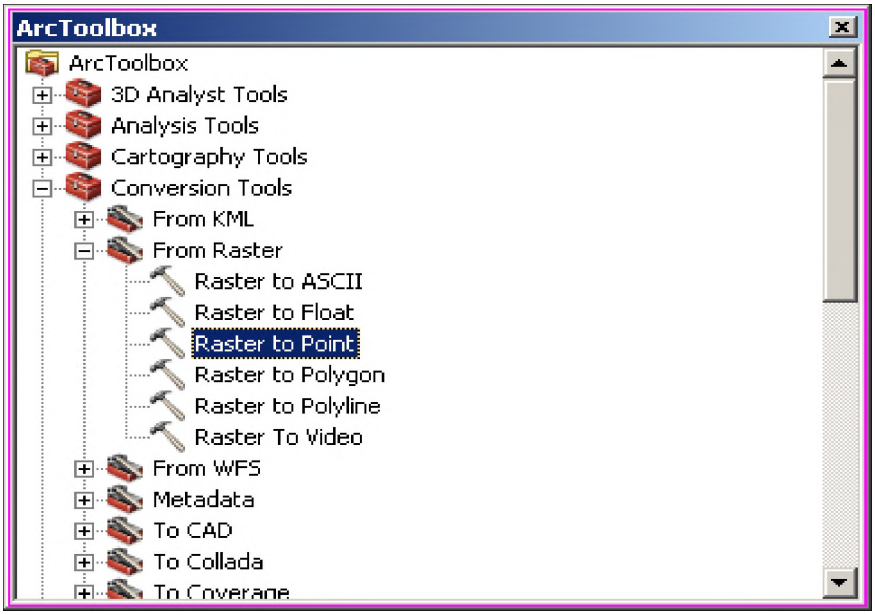

Figure D: Raster conversion tools in ArcToolbox.

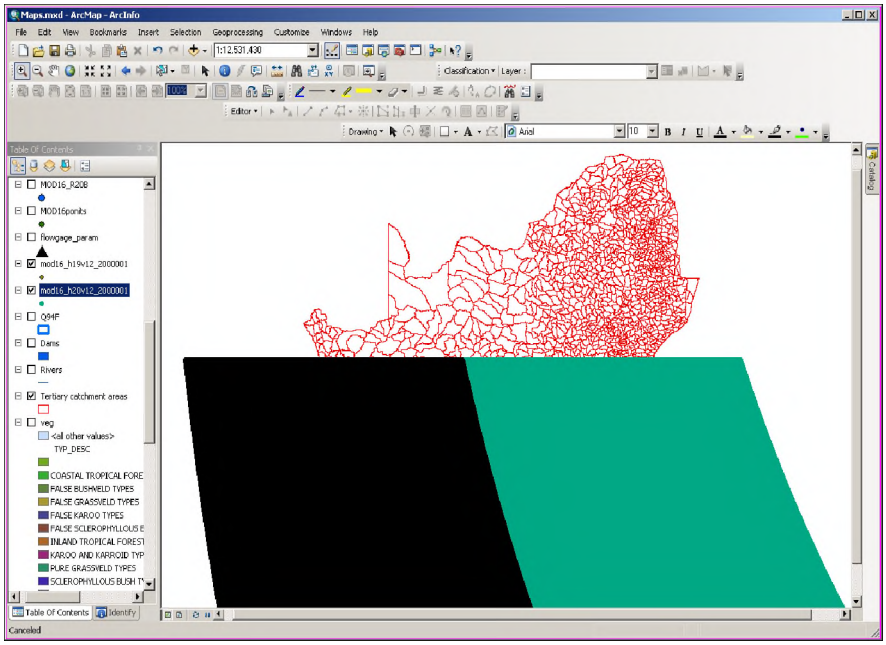

Figure E: Two MOD16 tile mapped over South African quaternary catchments map.

4. MOD16 pixel selection

The ArcGIS selection tool was used to select pixels within the selected quaternary catchments shape files. Figure F and G provide snapshot examples of the catchment-selected pixels. New layers of catchment-selected pixels were created for all selected quaternary catchments and were given file names that corresponded with their catchment name. After creating these layers, the next step was to determine the pixel positions (row and column number) in relation to the original MOD16 tile data. This step is discussed in the next subsection.

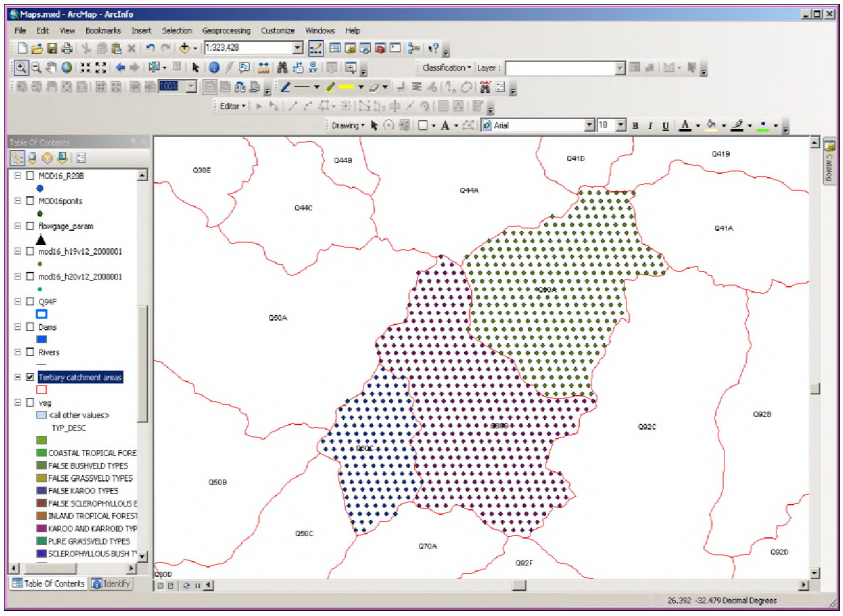

Figure F: Sample of the selected pixels in three interlinked quaternary catchments.

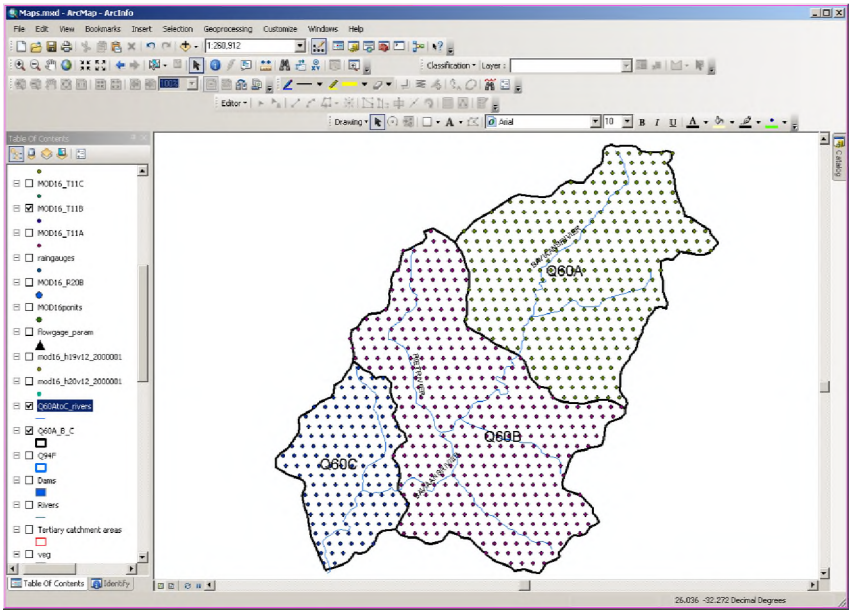

Figure G: Clipped MOD16 pixels over three quaternary catchments.

5. Determination of selected pixel position

Since all downloaded MOD16 tile data are gridded and large, it was necessary to conceptualise a method that would disaggregate and combine all the data to extract the time series of the specific selected catchments at once. Therefore, identifying the position of the selected pixel positions in reference to the original MOD16 tile was essential to develop the algorithm to extract the data. Table A illustrates an example of MOD16 tile data in a table format as they depict the pixel values. This table format was used to determine the position of catchment-selected pixels in reference to the MOD16 tile and the following steps were taken:

- In ArcGIS, add and display the catchment-selected pixel layer and the quaternary catchment shape file as shown in Figure H. MOD16 tile pixels has a unique "Point ID" number, denoting position starting from row 1 column 1 given Point ID as 1, with increments of 1 along all 1200 rows and columns. The Point IDs of MOD16 catchment-selected pixels did not change; they resemble the original MOD16 tile data. These IDs needed to be identified for each catchment-selected pixel in order to determine their position in reference to the original MOD16 tile.

- The "Identify" tool of ArcGIS was used to identify the Point ID of the first leftmost pixels for all rows in the catchment-selected MOD16 pixels. When clicking point data using the "Identify" function, the attribute data content is displayed in the left window pane (Figure I).

This attribute data consists of Field ID, shape, Point ID, and Grid code. Field ID is a unique primary key in a counting sequence used by ArcGIS to identify point data, shape represents the type of data, which is point data, Point ID provides a pixel position number in reference to MOD16 original tile, and Grid code stores the value of pixel content.

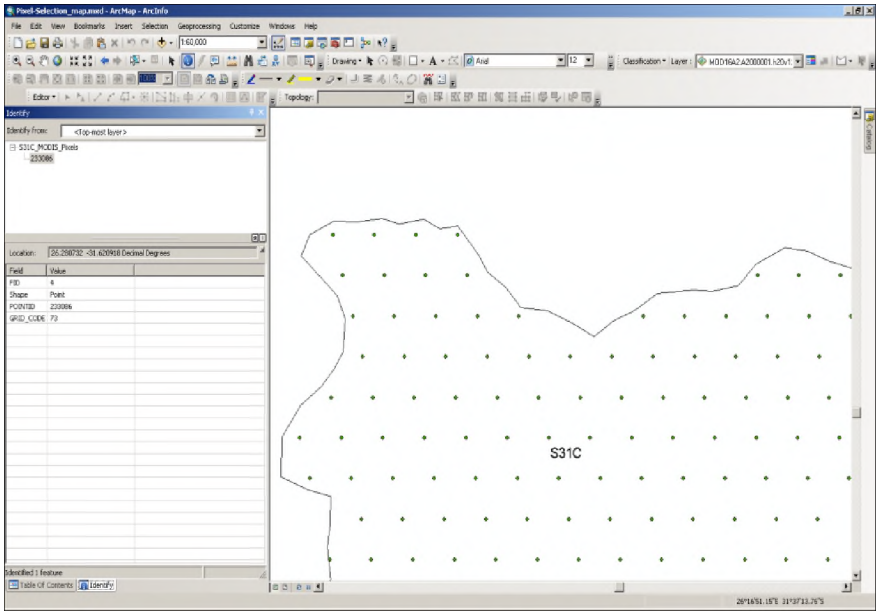

Figure I: Screenshot sample of MOD16 selected pixels in a quaternary catchment.

Table A: MOD16 tile data sample.

	Column 1	Column 2	Column 3	Column 4	*	*	*	.Coulmn 1200
Row 1	0	1	2	3	*	*	*	1199
Row 2	1200	1201	1202	1203	*	*	*	2399
Row 3	2400	2401	2402	2403	*	*	*	3599
Row 4	3600							*
Row 5	4800							*
*	*							*
*	*							*
*	*							*
Row 1198	1436400	*	*	*	*	*	*	1437599
Row 1199	1437600	*	*	*	*	*	*	1438799
Row 1200	1438800	*	*	*	*	*	*	1439999

A new Excel table with 1200 labelled columns and 1200 labelled rows (see Table A) was created using the Microsoft Excel Spreadsheet program. This Excel table was used to mimic the MOD16 tile frame. Within this table, sub-tables of each of the selected catchments were created to determine the catchment-selected pixel row and column number using Point ID values. Table shows the sample of the sub-table that was created and used in the determination procedures, which were as follows:

- Identify Point ID of the first pixel starting with the upper-left by clicking the pixel and record its value in a Microsoft Excel worksheet under a column labelled as "catchment start pixel".

- Count the number of pixels after the first pixel and record its value under a column labelled "number of pixels after the first pixel in a row". In a case where pixels were not continuous (see the second row in Figure above), the Point ID of the first pixel of the separated pixels was identified, recorded, and the pixels on the right were counted and recorded as well.

- Identify and record the Point ID of the last pixel in a row under a column labelled "catchment last pixel".

- Repeat (i), (ii), and (iii) if necessary for all catchment-selected pixels in each row for the selected catchments.

The identified catchment-selected starting pixel, the number of pixels after the first pixel in a row, and the last pixel values of the catchment were used to determine the actual row and column number position of pixels on MOD16 tile data. Two columns were added in an Excel worksheet, namely "tile pixel start column" and "tile pixel end column" (see Table B). Before determining column positions, "start row" and "end row" had to be identified. The procedure for row number determination was conducted using the following steps:

MOD16 tile pixel start and end row determination:

- "Start row" numbers were determined using the Point ID value of the first catchment-selected pixel and the start pixel (column 1) values of MOD16 tile. Catchment-selected start pixel Point ID values were manually checked to determine the range where it belonged within the MOD16 tile data rows. To use the catchment data shown in Table B as an example: MOD16 tile start pixel in row one has a Point ID value of 213601, and an end pixel value of 214811,

whereas the catchment-selected start pixel has a Point ID value of 213906. The start pixel value of the catchment-selected pixels falls within a range of 1200 pixels that are between 213601 and 214811. This procedure was only done for the first rows of the catchment-selected pixels for all selected catchments.

- The "end row" numbers were determined by counting the number of pixel rows of the catchment-selected pixel data.

MOD16 tile pixel start and last column identification:

- To get the "tile pixel start column", the difference between the Point ID of the first catchment-selected pixels and the Point ID of the first pixel of MOD16 tile was calculated.

- The "tile pixel last column" numbers were determined by adding the value of the "number of pixels after the first in a row".

The procedure used in the above two sets of steps (for row and column determination) were repeated for all catchment-selected pixels of all selected catchments.

Table B: The determination of row and column numbers of the selected catchment pixels.

S31B Quaternary Catchment						
Tile row number	Tile first POINTID number in a row	Catchment Start Pixel (POINTID)	Catchment Last Pixel (POINTID)	No. of pixels after the first in a row	Tile Pixel Start Column	Tile Pixel Last Column
Row 179	213601	213906	213909	3	305	308
Row 180	214801	215105	215109	4	304	308
Row 181	216001	216305	216312	7	304	311
Row 182	217201	217504	217513	9	303	312
Row 183	218401	218704	218713	9	303	312
Row 184	219601	219904	219913	9	303	312
Row 185	220801	221103	221113	10	302	312
Row 186	222001	222302	222312	10	301	311
Row 187	223201	223500	223511	11	299	310
Row 188	224401	224696	224697	1	295	296
Row 189	225601	225895	225911	16	294	310
Row 190	226801	227095	227112	17	294	311
Row 191	228001	228294	228313	19	293	312
Row 192	229201	229492	229514	22	291	313
Row 193	230401	230691	230714	23	290	313
Row 194	231601	231890	231914	24	289	313
Row 195	232801	233090	233095	5	289	294

After determining all the rows and columns positions for all selected catchments, a text file was created to store the values of "row number", "tile pixel start column", and "tile pixel last column" for respective selected catchments. In this file, a text denoting catchment name and tile number was used to identify data to be read by an algorithm. Figure J shows the screenshot of the final text file used by an algorithm to read and process MOD16 data.

A text file for all selected catchment that was needed for data extraction and processing was compiled; the next step was the development of an algorithm.

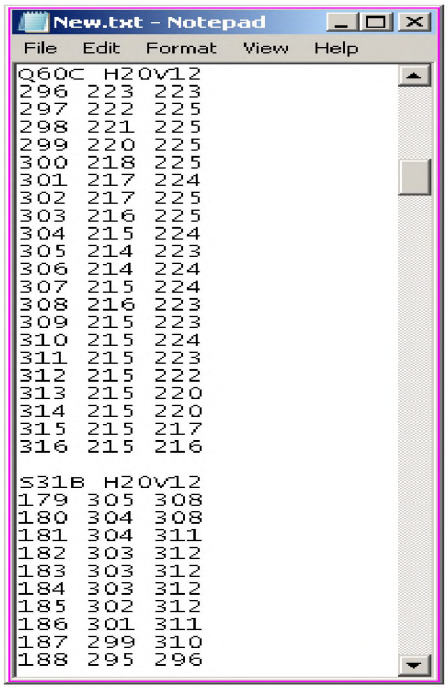

Figure J: Text file sample of data used in the algorithm to extract and process MOD16 data.

Appendix 2: Final Optimum Parameter Sets

Parameters	'Best' Parameter Sets											
	T11A	**T11B**	**T11C**	**G10E**	**K40A**	**R20A**	**R20B**	**R20C**	**Q60A**	**Q60B**	**Q60C**	**X23A**
PI1	1.4	1.4	1.4	1.4	1.6	1.6	1.5	1.6	1.4	1.4	1.4	1.8
PI2	4	4	4	4	5	5	5	5	4	4	4	5
AFOR	16.0	5.0	2.0	2.2	60	2	2	3	0	0	0	70
FF	1.3	1.3	1.3	1.3	1.4	1.3	1.3	1.4	1	1	1	1.4
PEVAP	1500	1450	1400	1635	1400	1450	1450	1450	1700	1700	1700	1425
ZMIN	84	20	18	32	10	25	33	47	44	42	51	144
ZAVE	218	265	199	368	162	332	233	389	307	258	222	565
ZMAX	412	513	404	428	201	672	786	920	558	627	534	987
ST	128	152	84	464	195	159	265	262	155	155	162	720
POW	3.4	3.2	3.2	2.9	2.1	3.5	3.8	3.3	3.2	3.2	3.1	2.2
FT	25	9	13	43	37	20	7	7	0	0	0	38
GW	4.0	2.0	2.2	3.1	2.1	4.5	2.2	1.9	0.7	1.3	0.9	13.0
R	0.5	0.4	0.4	0.7	0.2	0.3	0.3	0.3	0.5	0.5	0.5	0.1
GPOW	2.8	3.4	3.0	2.1	2.9	3.6	3.7	3.7	2.5	2.6	2.5	3.5
RIP	0.1	0.2	0.2	0.3	0.1	0.3	0.3	0.3	0.1	0.2	0.2	0.3

Appendix 3: Scatterplots of the variations of the coefficients of efficiency based on untransformed (*CE*) and log-transformed (*CE {ln}*) flows with ensemble values of parameter R and ST for the some of the selected catchments

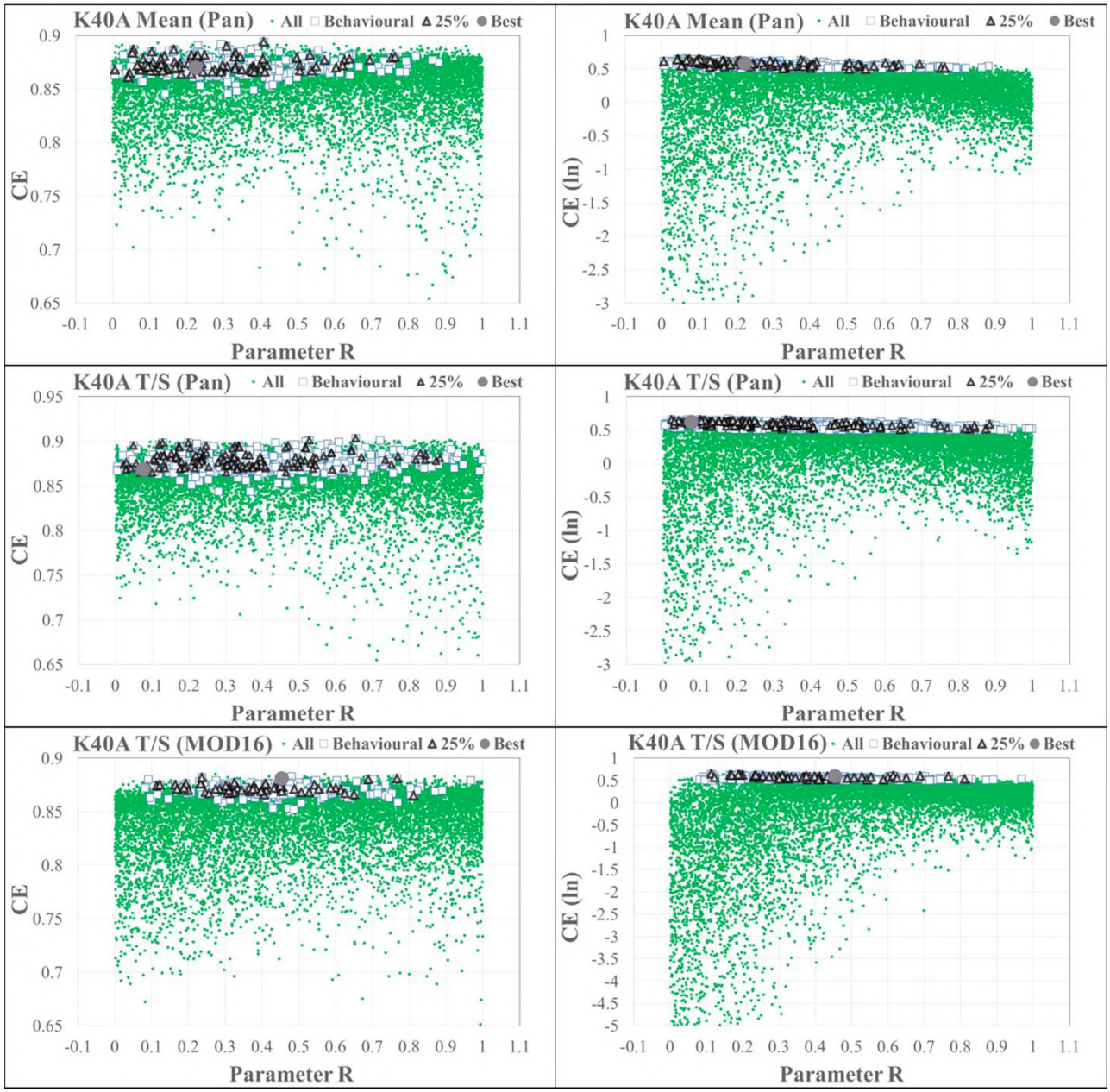

Appendix 3 continued…

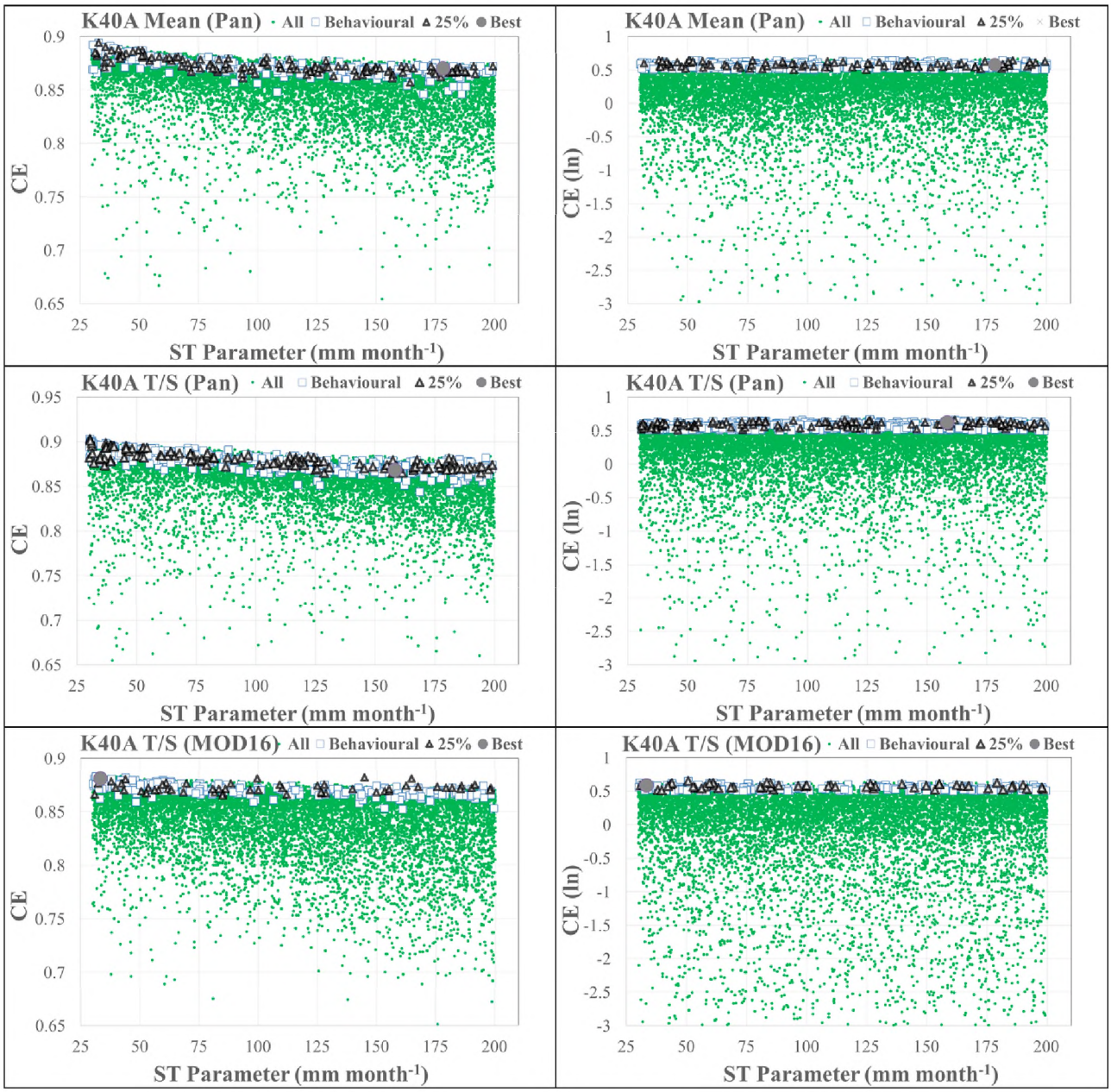

Appendix 3 continued…

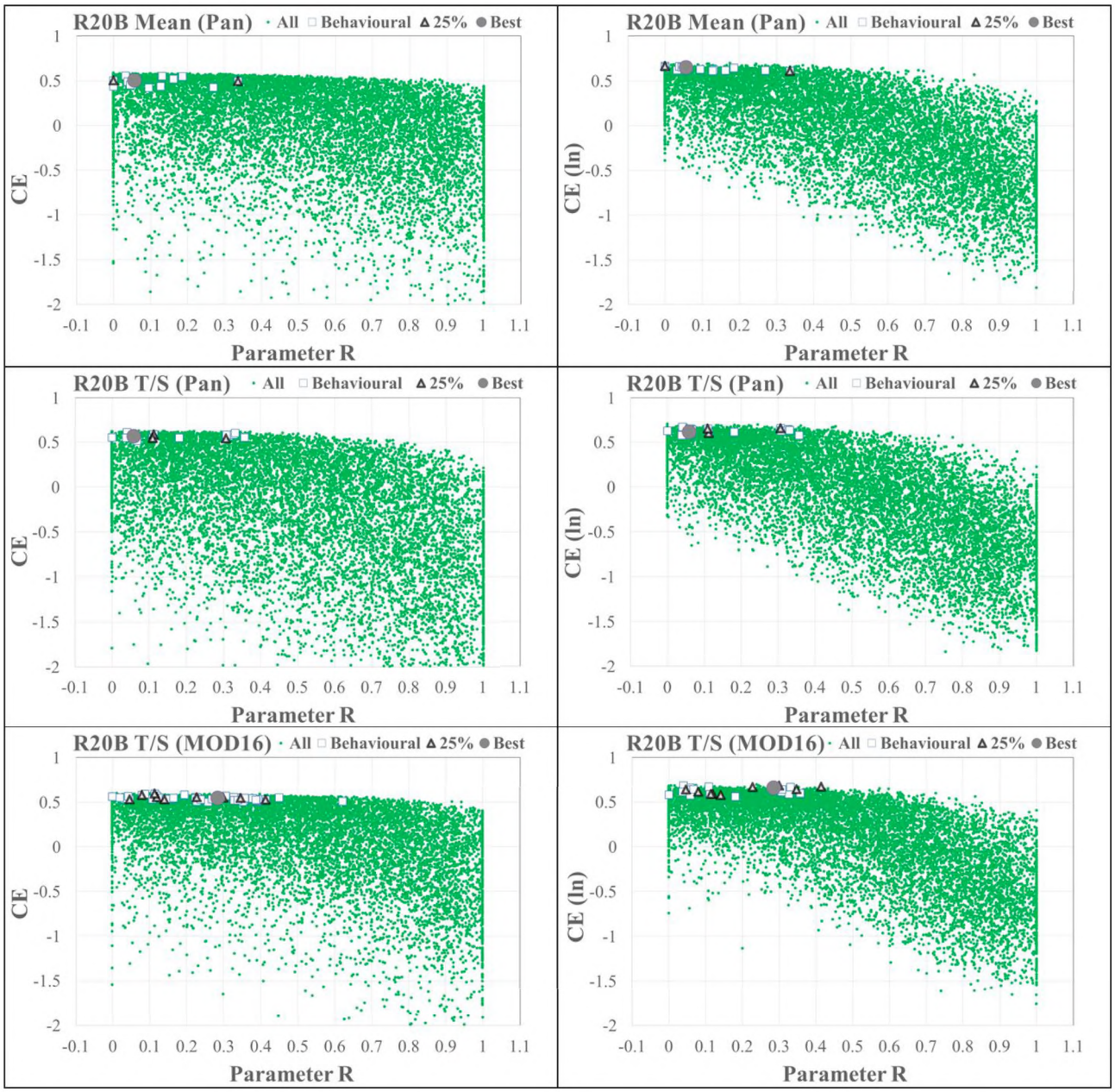

Appendix 3 continued…

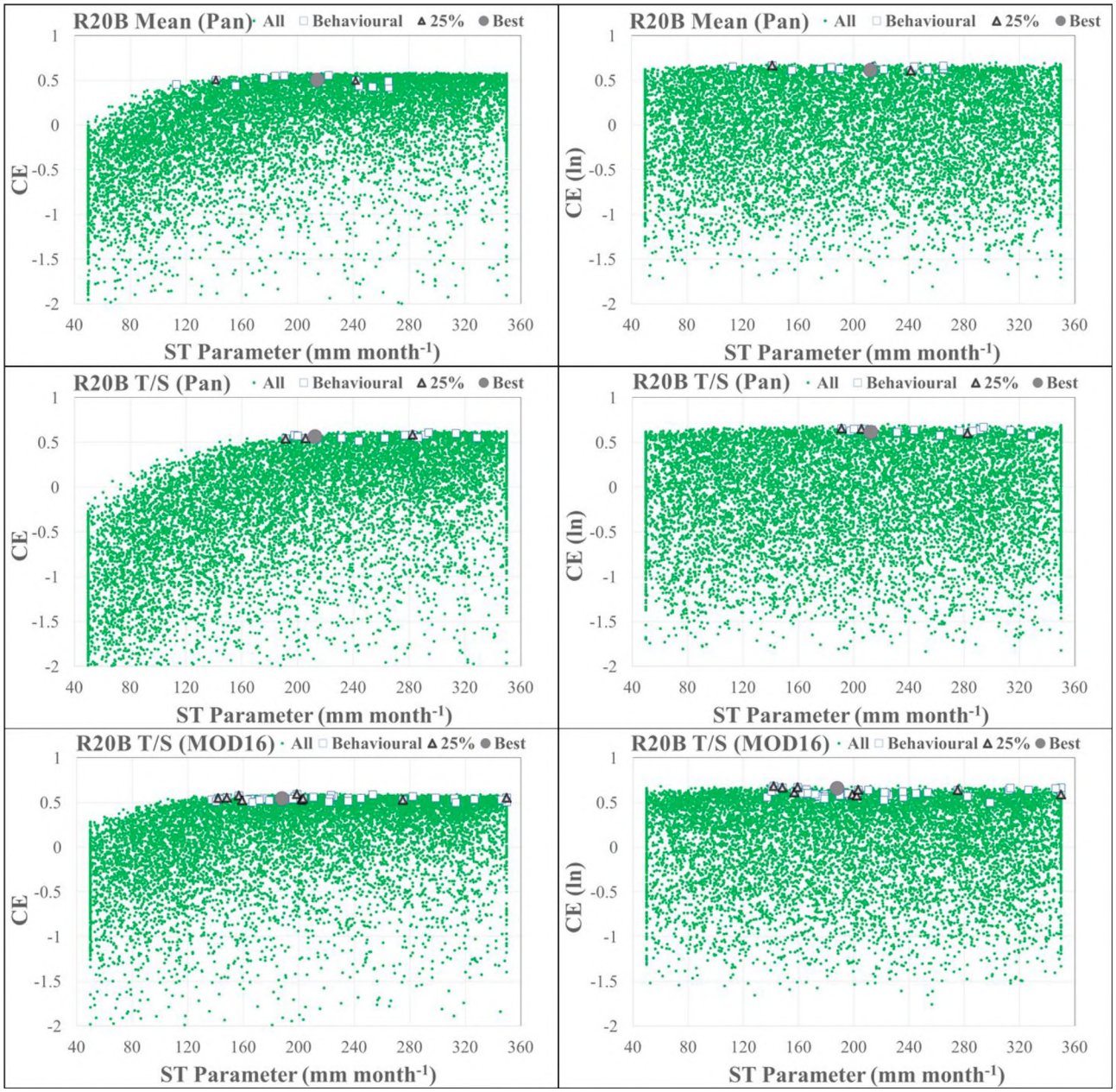

Appendix 3 continued…

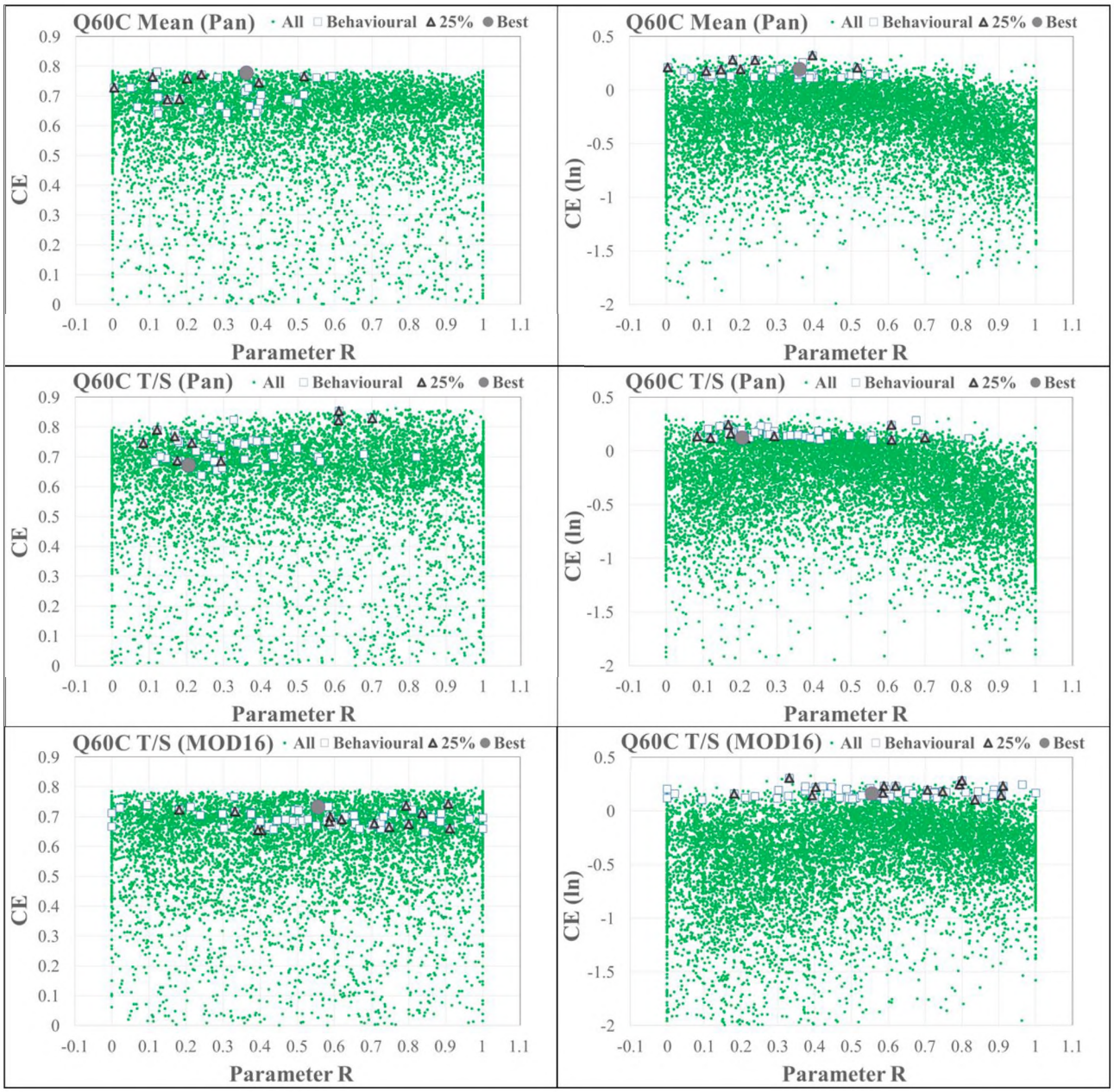

Appendix 3 continued…

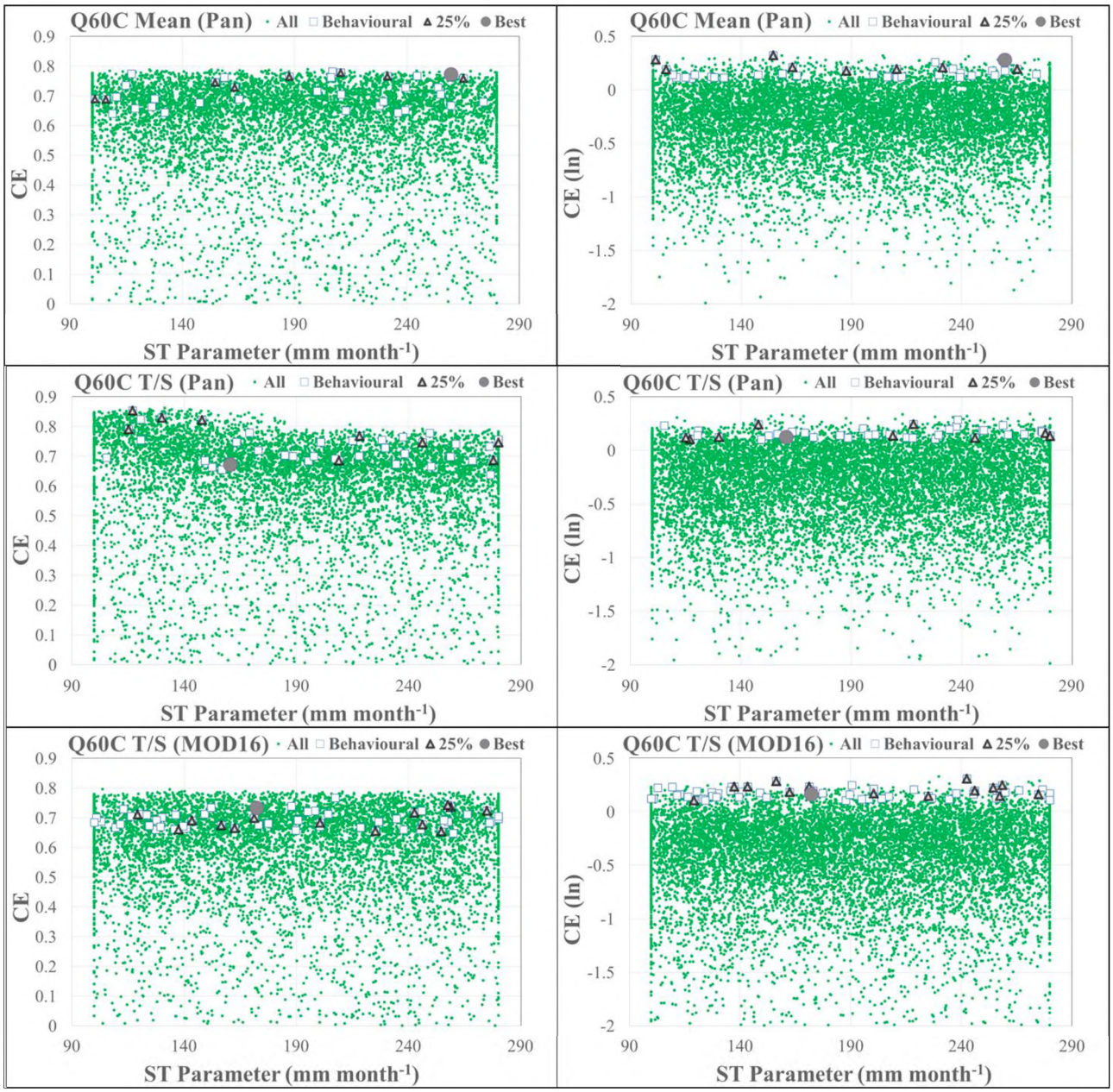

Appendix 3 continued…

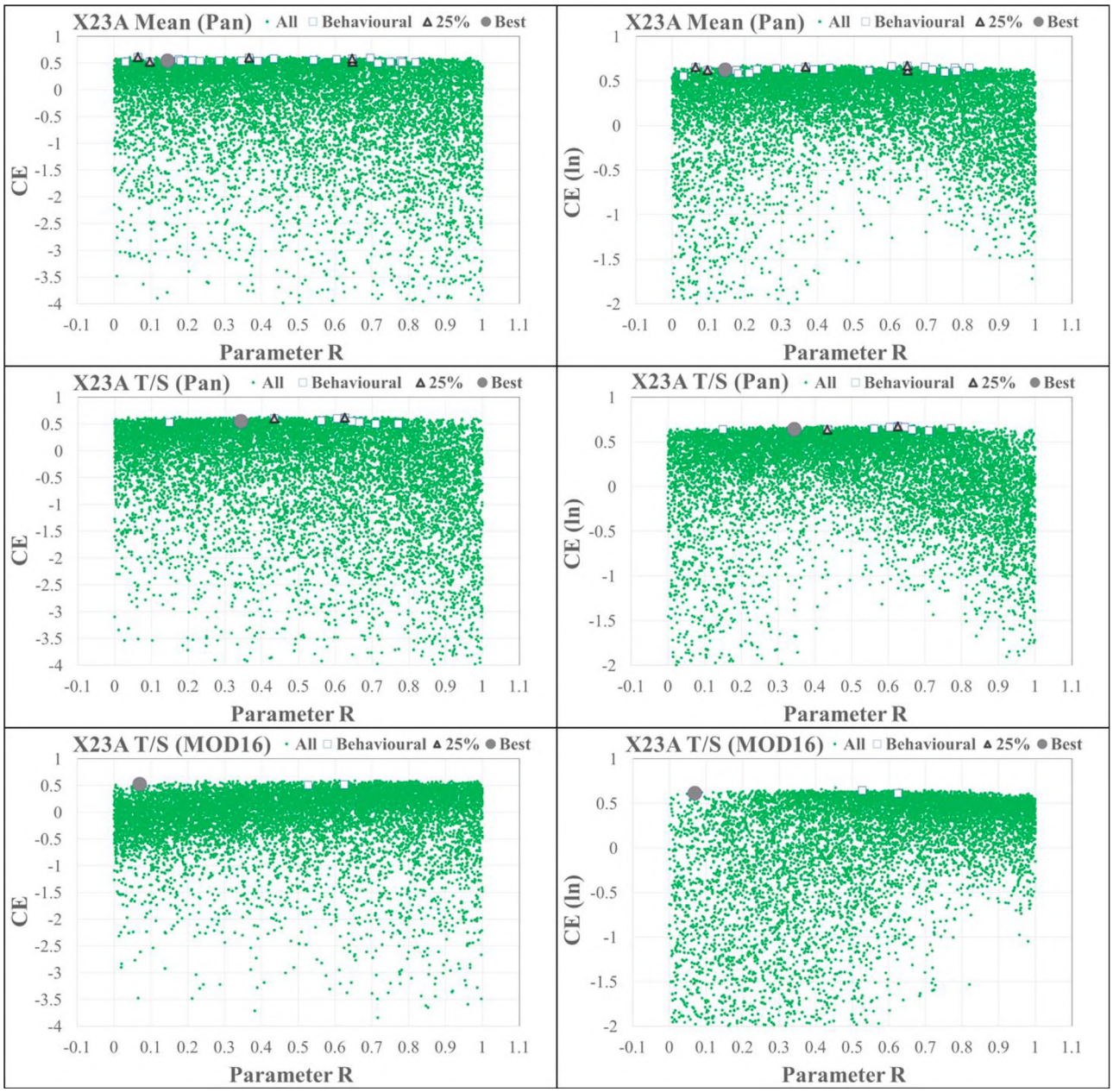

Appendix 3 continued…